Optimizing and Simulating Evacuation in Urban Areas

Von der Mercator School of Management, Fakultät für Betriebswirtschaftslehre der

Universität Duisburg-Essen

zur Erlangung des akademischen Grades

eines Doktors der Wirtschaftswissenschaft (Dr. rer. oec.)

genehmigte Dissertation

von

Klaus-Christian Maassen

aus

Düsseldorf.

Referent: Prof. Dr. Alf Kimms
Korreferent: Prof. Dr. Peter Chamoni
Tag der mündlichen Prüfung: 18.01.2012

Preface

The present work evolves from my research activities as a research assistant at the University of Duisburg-Essen, Chair of Logistics and Operations Research. The research process was financially supported by the West LB Stiftung Zukunft NRW over a period of three years.
During the orientation phase at the beginning of this work, it became apparent that evacuation planning for urban areas can be regarded only as a peripheral field of interest. Moreover, extensions of evacuation planning problems – e.g. integrating rescue teams or diverse traffic participants – are even more rare. Another incentive to address the topic of evacuation planning arose from the fact that the residential and working areas – i.e. mainly the Ruhr-Area and the Rhineland – of involved persons are densely populated regions that are endangered by flooding, bomb disposals and chemical facilities. These observations motivate to contribute to this low frequented field of research.

This work would not have been finished without the major support and assistance of many persons. At first, I would like to thank Professor Dr. Alf Kimms for his belief in my person, his understanding and inspiring discussions. Moreover, I thank Professor Dr. Peter Chamoni for reviewing this thesis.
A big thank you also goes to my dear colleagues Sarah Bretschneider, Demet Çetiner, Julia Drechsel and Michaela Graf as well as Waldemar Grauberger, Igor Kozeletskyi, Christoph Reiners and Rianne Rovers. You warmly welcomed me to the team and all of you contribute to a very pleasant working environment. You helped me passing work- and non-work related struggling times and to cope with the peculiarities of teaching and research at a university.
Moreover, I thank Çağdaş Özgür, Christian Kästner and Volodymyr Volodko for their IT- and programming support as well as Stefanie Kockerols and Vera Riesenweber for their help in literature research.

For priceless support, always being there in tough times, their trust, their love and affection, I am deeply indebted to my parents, Dagmar and Dieter Maassen, to my sister Barbara and her husband Peter and to my very special friend Katharina Tkaczick. You made it all possible and for that reason, I would like to dedicate this work to you.

Duisburg, September 2011 Klaus-Christian Maassen

Vorwort

Die vorliegende Arbeit entstand im Rahmen meiner Forschungstätigkeit als wissenschaftlicher Mitarbeiter an der Universität Duisburg-Essen, Lehrstuhl für Logistik und Operations Research. Der Forschungsprozess wurde finanziell durch die West LB Stiftung Zukunft NRW über einen Zeitraum von drei Jahren unterstützt.
In der Orientierungsphase dieser Arbeit wurde klar, dass die Evakuierungsplanung für städtische Gebiete lediglich als ein Randgebiet der Forschung angesehen werden kann. Zudem sind Erweiterungen des Evakuierungsplanungsproblems – z.B. die Integration von Rettungskräften oder unterschiedlichen Verkehrsteilnehmern – noch seltener zu finden. Ein weiterer Anreiz das Themengebiet der Evakuierungsplanung zu behandeln ergab sich aus der Tatsache, dass die Wohn- und Arbeitsgegenden – hauptsächlich das Ruhrgebiet und das Rheinland – der an dieser Arbeit mitwirkenden Personen stark besiedelte Regionen sind, die durch Hochwasser, Bombenentschärfungen und Anlagen der Chemieindustrie gefärdet sind. Diese Beobachtungen haben dazu motiviert einen Beitrag in diesem Forschungsgebiet zu leisten.

Diese Arbeit hätte nicht ohne die große Unterstützung und Mitwirkung einiger Personen fertiggestellt werden können. Zu Beginn möchte ich Professor Dr. Alf Kimms für sein Vertrauen in mich, sein Verständnis und für inspirierende Diskussionen danken. Zudem danke ich Professor Dr. Peter Chamoni für die Begutachtung dieser Arbeit.
Ein großes Danke geht außerdem an meine geschätzten Kollegen Sarah Bretschneider, Demet Çetiner, Julia Drechsel und Michaela Graf sowie Waldemar Grauberger, Igor Kozeletskyi, Christoph Reiners und Rianne Rovers. Ihr habt mich herzlich in das Team aufgenommen und zu einem sehr angenehmen Arbeitsklima beigetragen. Ihr habt mir durch beruflich und privat schwierige Zeiten sowie durch die Eigentümlichkeiten der Lehre und Forschung an einer Universität geholfen.
Außerdem möchte ich Çağdaş Özgür, Christian Kästner und Volodymyr Volodko für ihre IT- und Programmierunterstützung sowie Stefanie Kockerols und Vera Riesenweber für ihre Hilfe bei der Literaturbeschaffung danken.

Für unbezahlbaren Rückhalt, da sein in schweren Zeiten, ihr Vertrauen, ihre Liebe und Zuneigung stehe ich in tiefer Schuld zu meinen Eltern, Dagmar und Dieter Maassen, meiner Schwester Barbara und ihrem Ehemann Peter und zu meiner ganz besonderen Freundin Katharina Tkaczick. Ihr habt dies alles ermöglicht und aus diesem Grund möchte ich euch diese Arbeit widmen.

Duisburg, September 2011 Klaus-Christian Maassen

Contents

List of Figures

List of Tables

Chapter 1

Introduction

If people are in danger due to threats like a large forest fire, volcanic eruption, flooding or chemical accident, the dislocation (evacuation) of people from their current position (e.g. their homes, workplaces) to a more secure location outside the endangered area may be the only option to ensure safety. In this context, several decisions about how to prepare and how to organize the movement of possibly thousands of people have to be made. For example, safe destinations have to be defined and equipped with basic needs, people have to be assigned to safe destinations and routes to safe destinations have to be defined and signposted. Depending on the car ownership in the affected region, people may evacuate by vehicle, by foot or by public transit (if still operating). However, some people may not be able to evacuate on their own (e.g. patients in hospitals or residents of nursing homes) so that special services in terms of shuttle buses or ambulances are needed to take those people out of the endangered area.
In the case of emergency situations in urban areas, it can be assumed that the car ownership allows everyone to evacuate by vehicle. Available storage room within vehicles also allows the evacuees to take valuables with them so that the evacuation by car will be the first choice of the evacuees. Unfortunately, the existing street network in urban areas is often overloaded even by everyday traffic, but the network load during an evacuation can be assumed to be even higher. Thus, the efficient usage of sparse road capacities during an evacuation is of major importance to ensure a fast and secure evacuation process. This work focuses on the question, how traffic should be routed through a street network in order to minimize danger for evacuees during an evacuation. We make use of methods of combinatorial optimization as well as simulation to handle this problem.

1.1 Evacuation Planning

The "Centre for Research on the Epidemiology of Disasters" (CRED) maintain the "Emergency Events Database" (EM-DAT) that contains information about the occurance and the effects of reported natural and technological (i.e. anthropogenic) disasters worldwide from 1900 to today, see http://www.emdat.be/. The CRED is a World Health Organization (WHO) collaborating centre with international status under Belgian law.
Long-range trends adapted from the EM-DAT database clearly show that the number of natural and technological disasters during the last decades massively increased, affecting more and more people. The most frequently reported natural disasters are storms (e.g. hurricane "Katrina" in the Gulf coast region, USA, 2005), floods (e.g. flooding in the state of Queensland, Australia, 2010/2011), epidemics (e.g. bacterial infectious diseases,

Zimbabwe, 2008) and earthquakes (e.g. Haiti, 2010). Most of technological disasters are caused by fires or explosions. More detailed information can be obtained from the histograms of the CRED in Appendix A.
Suchlike disasters represent potential danger for people which may require protective arrangements in order to ensure safety for affected people. Depending on the disaster itself, the United States Federal Emergency Management Agency (FEMA) differentiates in the "Guide for All-Hazard Emergency Operations Planning" between two basic protective alternatives, namely evacuation and in-place protection (sheltering in-place), see FEMA (1996). For selecting the most advisable alternative, the FEMA suggests to take potential health risks due to exposure, speed of onset and persistence as well as the potential usage of barriers (e.g. closed windows and doors) into consideration. Thus, in the case of a threat by hazardous materials, it may beneficial to let people shelter in place instead of evacuating them, because the received exposure might be higher, when people are located outside (in a vehicle) compared to stay in place with closed windows/doors and using a wet towel for respiratory protection. The same holds also for some natural disasters (e.g. tornadoes), where sheltering in the basement (if available) would be a better choice than to evacuate in most cases. On the other side, for a large number of disasters like flooding, hurricanes (with flooding), volcanic eruptions or large (forest) fires an evacuation would be the preferable option to ensure safety, since primarily safe places to shelter may be destroyed during the disaster.
According to Stepanov and MacGregor Smith (2009), the process of evacuation can be divided into seven consecutive phases, see Figure 1.1.

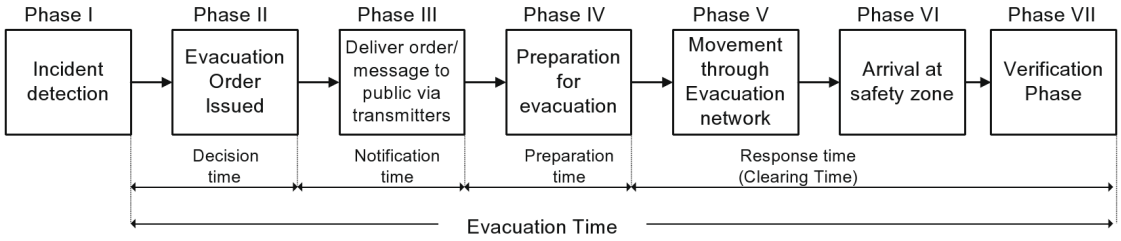

Figure 1.1: Evacuation Phases (Stepanov and MacGregor Smith (2009))

The first phase deals with the detection of an (unforeseeable) threat that causes the evacuation. Phase II and Phase III can be regarded as the official decision to evacuate and the delivery of the evacuation order to the population. Afterwards, both potential evacuees as well as officials prepare for the actual evacuation (e.g. preparing the journey to a shelter or positioning traffic guidances) in Phase IV. The last three phases (Phase V – Phase VII) consists of the evacuation itself as well as the arrival and registration of the evacuees at a safe destination.
In this work, we will focus on Phase V (and partially on Phase VI). We assume the existence of a threat that requires the evacuation of the endangered area in order to protect the population. Moreover, we assume that the decision to evacuate has been made and that the entire population already has been informed to prepare for the imminent evacuation. The next phase contains the movement of evacuees through the network. For evacuation scenarios with only few evacuees and sufficient road capacities, it may be relatively simple to route traffic efficiently through the network. However, for large-scale evacuation scenarios with thousands of evacuees as well as large and complex street networks, an efficient traffic routing through the network can not be obtained easily. Taking into consideration that urban road networks are even overloaded by everyday

traffic, it should be the major objective for evacuation planners to utilize the existing road network capacities as efficient as possible, since the traffic load caused by an evacuation can be expected to be even higher.
Southworth (1991) postulates that (among other information about traffic routing, leaving behavior and car ownership) the knowledge about the transportation infrastructure and the spatial distribution of the population is of major interest in the context of evacuation planning. Additionally, information about the locations and capacities of shelters must be present. On the basis of these information, a sequential evacuation planning procedure can be defined, see Figure 1.2.

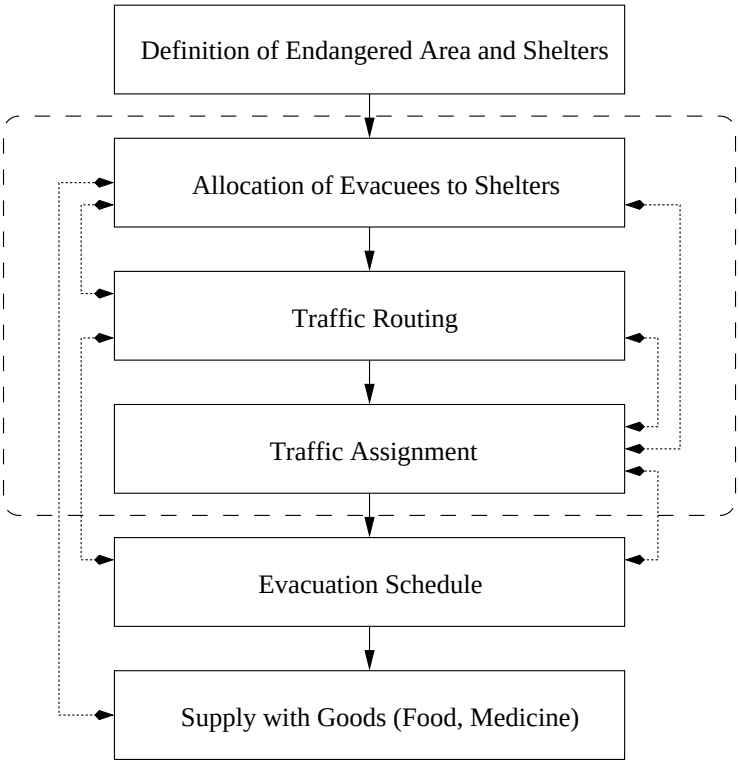

Figure 1.2: Sequential Evacuation Planning Procedure (based on Lahmar et al. (2006))

At the beginning, the endangered area and possible locations and capacities of shelters must be determined. This must be carried out under consideration of space requirements, access to basic needs (e.g. water, food, housing) and danger, see Saadatseresht et al. (2009). Afterwards, the next step of the sequential planning procedure contains the assignment of evacuees to shelters. As we will discuss in the literature review (Chapter 2), one possible solution for this problem is to assign evacuees to their nearest safe destination. If the assignment of evacuees to shelters is fixed, the traffic routing determines the driving direction of each road. In the case of an evacuation, the original road network functionality may be reorganized by so-called "'contraflow"' operations that reverse the driving direction of lanes in order to increase road network capacities, see Wolshon (2001). This method is well approved in the United States, thus practiced by states frequently endangered by hurricanes, see Urbina and Wolshon (2003). In the next step, the traffic assignment performs the allocation of evacuees/traffic flows to evacuation routes within the scope of the previously fixed traffic routing. At this point, each household knows, which shelter should be approached and which route (to the assigned shelter) should be taken.

Nevertheless, there is still some planning potential left open since the departure time of each household can be varied. If departure times are taken into account during evacuation planning, a (unique) departure time can be assigned to each household. The motivation to perform scheduled/staged evacuations (in contrast to simultaneous evacuations) is the potential reduction of total evacuation time, see Chen and Zhan (2008). The last step of the sequential planning procedure for evacuation planning involves the supply of evacuees in shelters with basic needs (e.g. food, housing, medicine).
It is apparent, that a large amount of interdependencies between the presented planning steps exist (indicated by dashed lines with arrows in Figure 1.2). Primarily, the assignment of evacuees to shelters, traffic routing and traffic assignment strongly affect each other. For example, an assignment that allocates evacuees to their nearest shelter massively constrains the traffic routing (and traffic assignment) since a large number of possible traffic routings following different assignment strategies are not applicable any more. Moreover, Han et al. (2006) demonstrated that suchlike assignments can be suboptimal since effects that will be apparent in succeeding planning steps (i.e. traffic routing/assignment) are neglected. As a second example, if the traffic routing is fixed, the traffic assignment must be performed within narrow confines since the driving directions are fixed and turning movements are mostly specified. Already these two examples illustrate that the problem of assigning evacuees to shelters, routing traffic as well as assigning traffic should be solved within an integrated approach to cover the existing interdependencies and to provide an evacuation plan that efficiently uses road capacities.

1.2 Chapter Synopsis

This thesis is built upon the preceding work of Kimms and Maassen (2011b, 2009, 2010a,b, 2011a). We focus on mathematical optimization models for assigning evacuees to shelters, routing traffic and assigning traffic (tasks in the dashed box in Figure 1.2) in one step. Thus, tasks for planning and equipping emergency shelters are neglected. Moreover, heuristic solution procedures and extensions for covering rescue teams and pedestrians will be presented. Our approaches should be regarded as pre-incident planning approaches since time is needed for preparation (collecting data, building networks, etc.) and solving the optimization problems. Thus, several evacuation plans for different scenarios should be prepared in advance so that the implementation of a chosen plan can be carried out right after the incident detection. Additionally, we assume that the entire population will be informed simultaneously and that the car ownership allows everyone to evacuate by car (except if pedestrian traffic will be taken into account, see Chapter 7).
The text is structured as follows: Chapter 2 contains a comprehensive literature review, covering aspects of evacuation planning with vehicles, evacuation planning with pedestrians and simulation-based optimization approaches. Afterwards, a basic cell-transmission based evacuation planning model (CTEPM) will be introduced in Chapter 3. Additionally, this chapter includes the application of the presented model to a real-world case study as well as a sensitivity analysis on the basis of a microscopic traffic simulation. In the following Chapter 4, several weaknesses of the previously introduced model will be addressed. Moreover, a simulation-based optimization approach will be developed and tested for a real-world example. To allow the applicability of our evacuation planning models to larger instances, two heuristic solution procedures will be introduced and evaluated in Chapter 5. Chapter 6 and Chapter 7 extend the evacuation planning models by integrating rescue team traffic (Chapter 6) and pedestrian traffic (Chapter 7). Finally, Chapter 8 contains some summarizing conclusions and an outlook on future research.

Chapter 2

Literature Review

The need for evacuation planning exists in environments of different size, e.g. large scale evacuations in urban or rural areas by vehicles, medium scale evacuations of pedestrians from buildings, ships and stadiums or small scale evacuations of pedestrians from single rooms, e.g. restaurants. Although a large amount of literature can be found regarding these topics, a large portion rely either on optimization approaches, simulation approaches or combined simulation-based optimization approaches for traffic routing and/or traffic assignment in emergency situations. Extensive reviews of evacuation planning approaches can be found in Bretschneider (2011) and Hamacher and Tjandra (2001). To give a brief overview in this work, we will also discuss literature dealing with evacuation planning and simulation-based optimization approaches. Since a large part of the presented work bases on the Cell-Transmission approach by Daganzo (1994) and Daganzo (1995), we will also focus on this approach in the literature review.

2.1 Evacuation Planning

Independent of the diversity of considered traffic participants (e.g. vehicles, pedestrians,...), we roughly classify methods of evacuation planning as displayed in Figure 2.1.

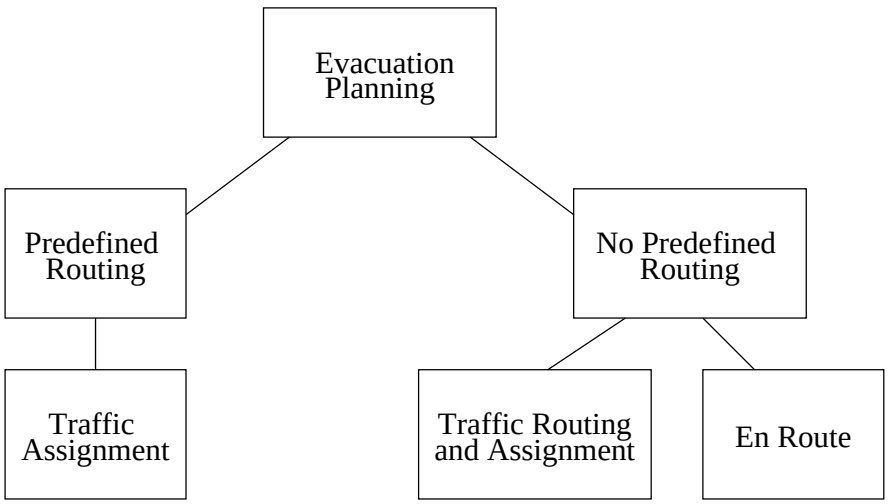

Figure 2.1: Classification of Evacuation Planning Approaches

At the first level, we divide by the existence of a predefined evacuation routing. If the evacuation routing is already predetermined (e.g. by a preceding procedure or simply using a non-emergency everyday life traffic routing with the possibility of lane-reversals), the remaining problem consists of assigning traffic within the given routing possibilities. This can be done under consideration of a given objective function (e.g. minimization of total evacuation time).
If the evacuation routing is not fixed in advance, we differentiate between the simultaneous determination of evacuation routing and the assignment of traffic to the evacuation routing as well as making routing decisions by the evacuees en route. In comparison to the traffic assignment problem with a fixed evacuation routing, the problem of defining an evacuation routing and assigning traffic simultaneously can be regarded as more integrated approach since meaningful interdependencies exist, see Figure 1.2 and the discussion in Section 1. If routing decisions are made en route by evacuees, no planning in terms of fixing an evacuation routing and assigning traffic has to be made. Thus, suchlike approaches can be regarded as the illustration of evacuations without planning.
If evacuation planning in the narrower sense takes place (i.e. in terms of traffic routing and/or traffic assignment), optimization approaches (partially supplemented by simulations) are often applied. For the case of en route decisions by evacuees, usually traffic simulations are used since there is no need for optimization.
As we will see in the following, there are several works in literature that are not fitting into this classification perfectly, for example, if traffic routing and traffic assignment are carried out separately, but within an integrated framework. On other hand, there are e.g. traffic assignment models that predetermine the predecessors and successors of street segments (i.e. defining the traffic routing), but also allow lane-reversals which also has an impact on traffic routing.

2.1.1 Evacuation Planning with Vehicles

En Route
Sheffi et al. (1982) were one of the first to cope with evacuation planning in a broader sense. They propose the macroscopic simulation model NETVACI to estimate the total evacuation time for a given region taking network topology, intersection design and control as well as dynamic route selection behavior of evacuees into account. The network is modeled as a graph with links (representing one-way roads) and nodes (representing intersections). The authors apply the model to the network of a 10-mile evacuation zone around a nuclear power plant with approximately 10,000 affected vehicles.
Later, Sinuany-Stern and Stern (1993) investigate the influence of traffic factors (e.g. “friction” between vehicles and pedestrians or car ownership), route choice mechanisms (shortest paths vs. myopic behavior) and evacuation circumstances (population size) on the microscopic traffic simulation SNEM. The concept of the simulation model is similar to Sheffi et al. (1982) although the level of detail has been increased and different traffic participants are considered in SNEM. The model is applied to a real world network (Dimona, Isreal) and all results refer to this case study. The authors find out that the usage of a myopic route selection behavior leads to more realistic results than assigning vehicles to shortest paths to safe destinations. In addition, increase of population results in disproportionate longer evacuation times. The consideration of “friction” between pedestrians and vehicles also increases the evacuation time. To the best of our knowledge, only Sinuany-Stern and Stern (1993) discuss the problem of evacuation planning with vehicles and pedestrians simultaneously.

Georgiadou et al. (2007) examine the evacuation from a major industrial site, also accounting for health consequences, e.g. in terms of received doses of contaminated air. The simulation is modeled as a discrete state stochastic Markov process and the considered evacuation network is built up of nodes and connecting links between them. The movement of evacuees from one node to another node is simulated as a random process en route, while the transition probability to proceed from one node to another depends on current traffic conditions. For an artificial network, the authors perform a sensitivity analysis to investigate the effects of different population sizes, node capacities and vehicle speeds on the total evacuation time. For a real-world case study in a densely populated area in West Attica (Greece), the authors study the sensitivity of the expected number of fatalities as a function of warning time for different road capacities.
Chen and Zhan (2008) focus on examining the effects of staged evacuations using the traffic simulation software Paramics. Again, the authors assume that routing decisions are made by the drivers en route under consideration of traffic conditions. Moreover, the simulation allows one to consider different types of driver behavior, ranging from conservative to aggressive. In their study, the authors consider an artificial grid road network, an artificial ring road network as well as real world network based on the city of San Marcos, Texas (USA). The results of simulations indicate that the simultaneous evacuation start (i.e. a non-staged evacuation) leads to the shortest total evacuation time, if no congestion occurs. However, if the population density is higher (leading to a greater risk of congestion), the staged evacuation time is superior for the grid road network and for the real world network. In contrast, a staged evacuation shows no advantage for the ring road network.

Traffic Routing and Assignment
A general framework for evacuation planning in the narrower sense is proposed by Yamada (1996). The author defines the major problem of evacuation planning to be the assignment of traffic participants to exits. The evacuation network is modeled as a graph with nodes and arcs. The first model assigns evacuees to safe destinations by shortest paths using the algorithm from Dijkstra (1959), thus leading to an evacuation plan with the minimum traveling distance. The second model is a simple network flow optimization model with capacity restrictions of safe destinations that also minimizes the total traveling distance.
In evacuation planning, often several safe destinations exist. However, it is not clear, to which destination evacuees should travel. As discussed, one possible solution is to assign evacuees to their closest exit. However, Han et al. (2006) demonstrate that the assignment of evacuees to the nearest exit can be suboptimal. The authors integrate the destination choice into the optimization problem by adding an artificial super sink that is connected to all possible destinations with dummy links with zero cost and travel time. In a case study for Knox County, Tennessee (USA) with a population of approximately 382,000, Han et al. (2006) illustrate the benefits of their one-destination-approach for different routing strategies. They take advantage of the internal path-processing methodologies of the simulation software Dynasmart-P to perform the traffic assignment. It turns out that the assignment of evacuees to one "super-destination" is superior to the assignment to the nearest exits. Moreover, Han et al. (2006) show that the dynamic route choice taking real-time traffic conditions into account outperforms the static route choice that fixes the paths of evacuees at the very beginning of the evacuation.
In the case of an evacuation, evacuees may desire to consolidate with other family members before evacuating together. Murray-Tuite and Mahmassani (2003) and Murray-Tuite and Mahmassani (2004) address this circumstance by integrating this behavior into the traffic routing approach. The authors propose to successively solve two linear optimiza-

tion models to determine the location of the meeting point for the family members of each household and to generate a so called trip chain for the vehicle of each household. The results from these models (i.e. set of origins, trip chain and destination for each household) are then loaded as inputs for traffic simulation into Dynasmart-P. Murray-Tuite and Mahmassani (2004) apply their framework to the south-central portion of Fort Worth, Texas (USA) with approximately 20,000 households and 30,000 vehicles.
Kim and Shekhar (2008) present an evacuation planning model based on graph theory. The evacuation network is defined as a directed graph with nodes and edges. Each node has an initial occupancy (population in this node) and a given capacity. Each edge also has a given capacity, travel time and an initial direction. Now, the problem consists of constructing a network configuration (including contraflow) by assigning a desired driving direction to each edge. The authors prove NP-completeness for their problem and develop a greedy as well as a bottleneck relief heuristic. A case study for the region of Monticello, Minnesota (USA) with approximately 42,000 evacuees is conducted.
Similar to the work of Kim and Shekhar (2008), Andreas and Smith (2009) also consider a directed graph with nodes and edges for formulating an evacuation planning problem as the problem of finding an evacuation tree. By using the tree concept, very simple evacuation plans are generated since no diverging processes are allowed. Moreover, the authors consider a discrete set of possible evacuation scenarios in their optimization problem that differ e.g. in terms of population, travel times and capacities. Thus, assuming penalty costs for usage of edges in the evacuation tree in the objective function, the optimization problem minimizes the expected penalty costs for a given set of scenarios. To solve this optimization problem, the authors introduced a solution algorithm based on Benders decomposition.
Stepanov and MacGregor Smith (2009) present a framework for evacuation planning under multiple objectives (i.e. minimization of excess total traveling distance and excess total evacuation time) that separates traffic routing and traffic assignment. Possible evacuation routes for each origin-destination pair are computed by the k shortest paths algorithm from Eppstein (1999). Afterwards, an IP model – supplemented by time delay functions from a $M/G/c/c$ queuing model – assigns evacuees from each origin to one of the k shortest paths to a destination. Afterwards, the obtained evacuation plan is evaluated in a simulation by crucial values, e.g. total traveling distance, total evacuation time and congestion levels. For a sample case study with 4,500 households, the authors compare their solution framework with the assignment of traffic to shortest paths. It turns out that the total evacuation time and blocking effects can be significantly reduced in return to a moderately increase of total traveling distance.
Evacuation planning may not only consist of traffic planning for evacuating vehicles. Instead, rescue teams (e.g. bomb disposal experts, fire fighters) have to be considered to curtail the origin of danger in the case of large fires or chemical accidents. Xie and Turnquist (2009) present an integrated approach for evacuation planning with rescue teams. In a first step, routes for rescue teams are determined by a simple shortest path algorithm. Afterwards, their optimization model – structured as a bi-level problem – for determining the traffic routing and assignment is solved. The upper level problem is formulated as a lane-based discrete network design model that minimizes the total evacuation time taking lane-reversals and the avoidance of crossing conflicts into account. The lower level problem assigns traffic to the network based on a stochastic traffic flow equilibrium framework. They propose a combination of a Lagrangian relaxation and a tabu search based approach to solve this (non-convex) optimization problem. They apply their framework to the same network as Kim and Shekhar (2008), i.e. Monticello, Minnesota (USA) with

approximately 42,000 evacuees.
Later, Xie et al. (2010) and Xie and Turnquist (2011) consider the simpler case of evacuation planning without rescue teams. In both works, a bi-level network design optimization problem is introduced. Similar to a previous work, the authors again consider lane-reversals as well as the avoidance of crossing conflicts and the upper level problem again minimizes the total evacuation time. Subsequently, the lower level problems in both models solve the traffic assignment problem reaching a user-equilibrium. In Xie et al. (2010), the lower level problem is built on the cell-transmission theory by Daganzo (1994) and Daganzo (1995), while the lower level problem in Xie and Turnquist (2011) is designed as a mixed integer network flow problem. In both works, the authors propose a combined Lagrangian relaxation tabu search based solution procedure to solve the bi-level optimization problems. Case studies for Monticello, Minnesota (USA) are conducted.
Bretschneider and Kimms (2012) and Bretschneider and Kimms (2011) present lane-based dynamic network flow models for evacuation planning. The network modeling shows some similarities to the works of Cova and Johnson (2003), Xie et al. (2010) and Xie and Turnquist (2011). The authors also allow lane-reversals and avoid crossing conflicts in both works. Bretschneider and Kimms (2011) propose a relaxation based heuristic followed by an additional adjustment heuristic to ensure feasibility of the solution. Bretschneider and Kimms (2012) modify the dynamic network flow model into a pattern-based dynamic network flow model. The basic idea of using patterns is to use a discrete set of possible traffic flow patterns for intersections and roads (between intersections) and to assign exactly one pattern to each intersection and road so that a feasible evacuation plan is defined. The authors develop a two-stage heuristic that determines traffic routing and vehicle flows on a less detailed network in the first step. Afterwards, the results from the first step (i.e. the driving direction and capacities of roads) are used as inputs for the second step where the evacuation plan for the original network is determined. Their solution procedures show very promising performance in large computational studies. More detailed information can be found in Bretschneider (2011).

Traffic Assignment
Although not considering the case of an evacuation, the seminal work of Ziliaskopoulos (2000) should be mentioned here since it builds the basis for numerous publications. The model presented by Ziliaskopoulos (2000) is a single destination system optimum dynamic traffic assignment problem based on the cell-transmission model (CTM) by Daganzo (1994). The basic idea of the CTM is to model a given network with cells of equal size. The size of a cell corresponds to the distance that can be traveled by a vehicle under light traffic in one period of time. Hence, the planning horizon is divided into a discrete set of periods of equal length. Under consideration of traffic flow capacities, vehicles move from one cell to another representing the traffic flow.
Ukkusuri and Waller (2008) also consider traffic assignment problems built upon the CTM approach. They compare a single destination dynamic user equilibrium network design problem to a dynamic system optimal network design problem similar to the traffic assignment model by Ziliaskopoulos (2000). Moreover, they extend their model to cover demand uncertainties within a stochastic programming approach.
A common attribute of traffic assignment models based on the CTM approach is the knowledge of the evacuation routing in advance in terms of knowledge about predecessors and successors of a street segment. In some works, the general driving direction of a street is defined in advance and in other works, a standard traffic routing (as applied in (non-emergency) everyday life situations) with lane-reversal possibilities is assumed.

Thus, if contraflow operations are considered within traffic assignment models, the traffic routing can also be affected since the driving direction on lanes can be changed. In order to illustrate the knowledge about predecessors and successors of a street segment, suchlike approaches are discussed at this point.
Cova and Johnson (2003) introduce a lane-based network flow optimization model for evacuation planning. The increase of detail due to the explicit consideration of lanes allows one to avoid crossing conflicts and to limit the number of merging traffic streams at nodes. Similar to Yamada (1996), Cova and Johnson (2003) also minimize the total traveling distance. The authors apply their mixed-integer optimization model to a nine-intersection sample network and compare the obtained solution to other routing strategies via microscopic traffic simulations (Paramics). Moreover, they demonstrate real-world applicability of their model by calculating a lane-based evacuation plan for an area of Salt Lake City, Utah (USA).
The work of Tuydes and Ziliaskopoulos (2004) extend the dynamic traffic assignment model by Ziliaskopoulos (2000) to be applicable to evacuation planning problems. Moreover, they incorporate lane reversibility into their optimization model so that higher flow and storage capacities of cells are possible. In a subsequent work, Tuydes and Ziliaskopoulos (2006) present a tabu search heuristic to solve the traffic assignment problem with lane reversibility for real-world instances. In a case study of evacuating approximately 33,000 vehicles from the city of Evanston, Illinois (USA), the authors compare evacuation times with and without contraflow possibilities. On the basis that evacuees were assigned to their nearest safe destination, total system traveling time can be reduced by 20%.
A simulation-based optimization approach for a traffic assignment problem with evacuation scheduling is presented by Sbayti and Mahmassani (2006). The authors distinguish between two user classes, those who have to be evacuated and those who have not to be evacuated but follow their everyday activities. The model assigns departure times, safe destinations and the path to a safe destination to evacuees. It has to be noticed, that the set of available paths must be known in advance. The aim of the presented model is to minimize the total evacuation time for evacuees. The presented simulation-based optimization procedure utilizes Dynasmart-P to evaluate evacuation plans (i.e. departure times and paths assignments). As long as the stopping criterion is not met, the iterative procedure reassigns departure times, destinations and paths to destinations to evacuees. Sbayti and Mahmassani (2006) demonstrate the real-world applicability of their model in a case study in Fort Worth, Texas (USA) with a total vehicle demand of approximately 47,000 vehicles and different demands for evacuating vehicles.
The work of Chiu et al. (2007) is also based on the seminal work of Ziliaskopoulos (2000). The presented traffic assignment model is transformed into a single destination traffic assignment model for evacuation purposes. The transformation to a single destination problem is performed similar to Han et al. (2006) by adding a super sink to a given network, that is linked with all "regular" safe destinations. This procedure allows one to include the assignment of evacuees to safe destinations into the optimization process. However, the evacuation routing must still be known in advance.
Liu et al. (2008) introduced a comprehensive framework for evacuation planning. The embedded optimization module utilizes a revised formulation of the CTM approach by Daganzo (1994) to assign network flows. In a first step, major corridors/arterials for evacuation are selected. The second step assigns vehicles to (predetermined) access streets of corridors. Afterwards, traffic signals will be optimized in order to maximize traffic throughput on arterials. The last step evaluates the generated evacuation plan and identifies potential bottlenecks. For a case study in Washington D.C. (USA), the authors find

out that the preassignment of evacuees to access streets – provided by the local department of transportation – is suboptimal, since evacuation times on major arterials differ significantly.
Kalafatas and Peeta (2009) provide a cell-transmission based optimization model for evacuation planning with lane reversibility on a detailed network representation. Lane reversals are covered by incorporating a set of so-called network design options. Depending on the selection of certain network design options, lane-reversals are applied in the evacuation network. For an artificial test network, the authors investigate the effects of different numbers of reversed lanes, population size and population distribution.

2.1.2 Evacuation Planning with Pedestrians

The movement of pedestrians is different compared to the movement of vehicles. For example, there are no "lanes" when people evacuate from an area (although lane formations by pedestrians themselves can be observed when pedestrians evacuate from a long corridor, see Burstedde et al. (2001)), people can almost instantly accelerate and decelerate and people show some unique behavioral patterns, e.g. "faster-is-slower" effect due to increased blocking clusters (Parisi and Dorso (2005)), self-organization-effects due to interactions between pedestrians called "social force" (Guo and Huang (2008)), herding behavior in panic situations (Kirchner and Schadschneider (2002)) or the tendency to escape chaotically or ordered (Song et al. (2006)).
As we will see in the following, large portions of the literature focus on the simulation of pedestrian evacuations from a single room, so that no evacuation planning in the narrower sense takes place. Instead, pedestrians made decisions on where to go en route, taking their direct environment into consideration. If evacuations of pedestrians from larger areas are of interest, methods of optimization are also often used to determine the evacuation routing.
Due to the diversity of unique characteristics of pedestrian movements, various approaches for the microscopic simulation of pedestrians in emergency situations have been developed to cover important effects simultaneously. Reviews of evacuation planning for pedestrians can be found in Gwynne et al. (1999) and Lee et al. (2003). The work of Hamacher and Tjandra (2001) contains a more general review of frameworks for evacuation planning which can also be applied to pedestrian evacuation planning. As can be seen in the review of Zheng et al. (2009), the most commonly used models for simulating pedestrian movements are cellular automata models, lattice gas models, social force models, fluid-dynamic models, agent-based models and game theoretic models. The last three approaches are rarely used compared to the first three approaches. Since the agent-based models are also often combined with the cellular automata and social force model, we will focus on the cellular automata model, lattice gas model and the social force model in the following.
The cellular automata approach by Nagel and Schreckenberg (1992) was originally intended to describe vehicle traffic on a microscopic level of detail. The basic idea of this model is to divide a given street into cells of the size of a vehicle. Each cell can either be empty or occupied by a vehicle. The simulation updates periodically with a fixed period length. Thus, vehicle movements through a street are generated by vehicles moving from cell to cell during the planning horizon. Although this approach shows some similarities to the CTM by Daganzo (1994), major differences exist in terms of cell size, flow propagation and the level of detail. Large-scale applicability of this approach for traffic illustration has been demonstrated, see Nagel and Rickert (2001).
This approach can be applied to pedestrian traffic with slight pedestrian-specific adjust-

ments of cell size, movement speed and period length. A major difference between the simulation of evacuating vehicles and the simulation of evacuating pedestrians is the number of possible moving directions. On a single lane, cells are ordered in a row. Thus, vehicles on a single lane have only one alternative to proceed (i.e. the driving direction). In terms of pedestrian evacuation, a grid of cells is assumed, where pedestrians have eight possible moving directions, because each cell is surrounded by eight neighboring cells.
Burstedde et al. (2001) make use of the cellular automata model to simulate pedestrian movements within a single room with one exit and without obstacles. In order to consider social interactions between pedestrians, the authors add a so called "static floor field" and a "dynamic floor field". These floor fields can be interpreted as additional layers above the original grid. The static floor field represents a constant level of attractiveness for cells, e.g. high attractiveness for the exit and low attractiveness for cells far away from the exit. Thus, it can be regarded as the knowledge of the pedestrians about the surrounding. The dynamic floor field also represents the attractiveness of a cell, but in this field, the attractiveness is not constant over time. In detail, the attractiveness increases with an increasing number of pedestrians passing this cell. Thus, the dynamic floor field dynamically affects the transition probability, because more attractive cells (in terms of the floor field) have a higher probability to be visited. Hence, this modification of the cellular automata approach allows to consider herding behavior in groups of pedestrians. The authors also incorporate diffusion and decay of the dynamic floor field in their simulation model to limit the temporal interaction range of the dynamic floor field.
Kirchner and Schadschneider (2002) adopt the approach from Burstedde et al. (2001) and investigate the sensitivity of the model parameters for the case of pedestrians evacuating from a large room with two exits. They find out that both, the knowledge about the location and a certain degree of herding behavior in combination results in the shortest evacuation times.
Varas et al. (2007) also use the cellular automata model with a static floor field to simulate pedestrian evacuations. They consider several aspects to make the model more realistic, e.g. using a random process to choose between two possible destination cells of the same attractiveness. On the basis of this model, they study the effect of obstacles as well as door sizes and door positions in the case of evacuating a large classroom. It turns out that larger and well-positioned doors help to reduce the evacuation time.
Zheng et al. (2010) also employ the cellular automata model as the basic concept for their pedestrian simulation. Additionally, they also take a static floor field and social forces (as described above) into account. The authors also consider obstacles during the evacuation of pedestrians from a large room, but they regard the obstacle in terms of a partition wall as an instrument to lower evacuation time instead of a handicap for pedestrians. They find out that too short partition walls have less coordination effects on pedestrian flows, but if the partition wall is too long, increased jamming of pedestrians in front of the bottleneck between the wall of the room and the partition wall can be observed.
The basic concept of using a grid to divide a given area into cells that can be passed in one time step is also used by Yue et al. (2011). They enhance this concept by introducing a direction-parameter and an empty-parameter to take effects of pedestrian jams into account. Moreover, they apply a cognition coefficient to consider the ability of pedestrians to recognize jams around exits. The resulting "Dynamic Parameter Model" is then used for investigating the effects of asymmetrical exit layouts.
An other approach to simulate the movement of pedestrians is the lattice gas model. These models are a special case of cellular automata, see Zheng et al. (2009). Often, lattice gas models are combined with social force models to incorporate interactions between pedes-

trians and other pedestrians as well as obstacles or walls.
Song et al. (2006) introduce the so-called "multi-grid model" using the basic ideas of the lattice gas model. Additionally, they refine the lattice so that a pedestrian does not occupy only one grid, but nine (3×3) grids with a "center" located in the middle. By doing so, Song et al. (2006) are able to incorporate more detailed rules for simulating extrusion, repulsion and friction between pedestrians. They also consider a variable which represents the tendency to evacuate ordered or chaotically, called drift. They found out that a more chaotic behavior of pedestrians leads to increasing evacuation times compared to an ordered evacuation, where pedestrians were forming queues in front of an exit that reduce blocking clusters.
Guo and Huang (2008) also use the basic concept of the lattice gas model to simulate pedestrian movements, but they address the problem of inexactly computation of the moving distance and evacuation time when pedestrians move diagonally through the lattice. They overcome this weakness by introducing the "mobile lattice gas model" that allows mobile positions for the surrounding lattices. Similar to Song et al. (2006), they also integrate social forces into their model in terms of repulsion and friction. Both works are applied to the evacuation of single rooms, where realistic results with typical pedestrian behavior patterns – e.g. blocking clusters – can be observed.
The social force model for the simulation of pedestrian dynamics is introduced by Helbing and Molnár (1995). The authors assume that the movement of pedestrians is basically influenced by three major forces. They propose that pedestrians would like to reach a given destination, that pedestrians are keeping distance to other pedestrians and obstacles (e.g. walls) and that pedestrians are attracted by other pedestrians. In order to integrate a certain degree of randomness, the authors also add a fluctuation term which represents random variations of the pedestrians' behavior.
Parisi and Dorso (2005) adopt the social force model by Helbing and Molnár (1995). Among other things, they investigate the relationship between the door size and the existence of blocking clusters. It turns out that the probability of finding blocking clusters only goes to zero for very wide doors and that the stability of blocking clusters decrease with increasing door size. These effects finally result in reduced evacuation times, when exit doors become larger.

The previously presented approaches for evacuation planning with pedestrians focuses on microscopic simulation of pedestrians evacuating from a single room. Hence, these approaches work well, when the realistic predictions of pedestrians behavior are needed. Nevertheless, when larger areas (e.g. large buildings or ships) need to be evacuated, egress routes first have to be determined. This task is usually carried out by optimization approaches on a lower level of detail.
Karbowicz and Macgregor Smith (1984) present a mathematical optimization model for evacuation planning in buildings. The model assigns pedestrians to egress routes in a way that total evacuation time and total traveling distance will be minimized. The authors also propose a simulation-based optimization procedure based on a k shortest path algorithm that reassigns evacuees to alternative egress routes if significant queuing appears. This iterative procedure stops, if the actual level of queuing is below a prespecified level of queuing.
The work of Sinuany-Stern and Stern (1993) dealing with the simultaneous evacuation of vehicles and pedestrians has already been discussed in Section 2.1.1.
Yamada (1996) develop two approaches for evacuation planning, namely the allocation of evacuees to their nearest exits and a simple network flow model taking capacity restrictions

of shelters into account. Originally designed for evacuation planning with pedestrians only, these approaches can be applied to evacuation planning with pedestrians as well as evacuation planning with vehicles due to its highly aggregated formulation.
Fang et al. (2011) define a multi-objective evacuation routing problem on the basis of a hierarchical directed network. The optimization problem minimizes the total evacuation time, total evacuation distance and the cumulative congestion during evacuation. They develop a modified ant colony optimization approach that shows promising performance for the evacuation of a stadium.

2.1.3 Further Related Problems

As discussed above, large portions of literature focus on traffic routing and/or traffic assignment in the context of evacuation planning. However, other tasks in evacuation planning have also to be solved, see Figure 1.2. In the following, we will present several approaches covering the problem of shelter planning, the supply with medical services and how public transport can be integrated into evacuation planning.
Sherali et al. (1991) present a location-allocation model for selecting a set of shelters out of potential locations and routing traffic in order to minimize the total evacuation time. The authors assume that each possible shelter has a limited capacity for evacuees and that each shelter requires a predetermined amount of (limited) staff to be operated. The resulting optimization model is a network flow model considering limited capacities for shelters.
Kongsomsaksakul et al. (2005) also consider the shelter choice in their evacuation planning approach. They present a bi-level optimization framework. Similar, to Sherali et al. (1991), the upper level chooses a set of shelters from a given set of possible safe destinations. Subsequently, the lower level determines the assignment of evacuees to shelters and the traffic routing simultaneously. To solve this optimization problem, the authors develop a genetic algorithm based heuristic procedure.
Saadatseresht et al. (2009) suggest the extensive use of a geographical information system (GIS) for evacuation planning within a three-stage planning approach. The first step determines safe destinations taking available space, basic living requirements and danger into account. The second step allocates potential candidate (safe) destinations to each building block. The paths between each building block and potential destinations are computed by a shortest path algorithm. The last step contains a multiobjective optimization problem that assigns each building block to a safe destination. A case study for an area of Tehran (Iran) with approximately 22,000 evacuees is conducted.
A two-stage stochastic programming model for shelter planning within an evacuation is presented in Li et al. (2011). The authors differentiate between existing permanent shelters, new permanent shelters and temporary shelters as well as distribution centers supplying the shelters. The first stage of their approach assigns locations and capacities (in terms of staff and commodities) and held resources to new permanent shelters. Here, fix and variable costs for building new shelters and holding inventory are minimized. In the second stage, evacuees are assigned to all type of shelters so that transportation costs for evacuees and resource distribution as well as surplus/shortage costs for resources will be minimized. A heuristic procedure for solving the two-stage stochastic programming model is proposed and tested in a case study in the Gulf coast region (USA).

If a disaster strikes an unprepared populated region, many casualties may need medical services. In suchlike situations, medical capacities (e.g. ambulances and health personnel)

must be utilized efficiently to keep the number of fatalities low.
Jia et al. (2007) model the problem of allocating medical resources (medical facilities) to so-called "demand points" as a maximal covering facility location problem. They assume that each demand point can be covered at a certain service level depending on the distance between the medical facility and the demand point. Moreover, the maximum number of facilities is limited and possible locations for medical facilities must be known in advance so that only a subset of these locations will be used as facilities. The authors proposed several heuristic solution procedures which are tested for a large case study in Los Angeles County, California (USA).
An approach for the localization and distribution of medical supply under consideration of multiple scenarios is presented in Mete and Zabinsky (2010). The authors propose a two-stage stochastic programming model that selects warehouses (for storing medical supply) and determines inventory levels for each medical supply type in each warehouse in the first stage. The objective is to minimize the warehouse operating costs plus the expected value of the objective of the second stage problem. The second stage contains the distribution of medical supply from warehouses to hospitals so that the total transportation duration and penalties of unfulfilled demand will be minimized. A real-world case study for the city of Seattle, Washington (USA) is presented.

Most of the presented literature only considers the evacuation by vehicle and/or by foot out of an endangered area. However, in urban areas, the public transportation system (e.g. metro, bus) represents a mass transit with the potential to get a large number of persons out of an endangered area quickly.
Sayyady and Eksioglu (2010) consider the evacuation via public transport only. They formulate a static network flow problem as a mixed-integer linear optimization problem to determine the routing of public transport vehicles under consideration of limited capacities (evacuees per vehicle, total number of available vehicles). Moreover, the authors suggest to use a tabu search based heuristic procedure to solve large instances of the optimization problem. A case study for Fort Worth, Texas (USA) is performed to prove real-world applicability.
Bish (2011) introduces a bus-based evacuation planning approach in terms of two mathematical programming formulations. The author assumes that buses (initially located at yards) transport evacuees from pickup locations to shelters with limited capacities so that the total evacuation time will be minimized. The presented models are classified within the known literature of vehicle routing problems and two heuristic solution procedures are developed and tested for artificial scenarios.
In Bretschneider (2011), shuttle buses are considered within an evacuation planning approach. The presented model differentiates between public lanes (i.e. for evacuation traffic and shuttle buses) and emergency lanes (i.e. only for shuttle buses). Since the existence of a feasible solutions can not be guaranteed if all crossing avoidance constraints within intersections will be kept, penalty costs are introduced to rate the existence of crossing conflicts within intersections. The author propose a four-staged heuristic solution procedure that shows promising performance in a computational study.

2.2 Simulation-based Optimization

Real-world optimization problems are often difficult to solve due to complex interactions which can not be handled analytically in a closed form and due to stochastic influences, see Mayer (2011). Here, simulations are the method of choice to evaluate the objective value and to check the feasibility of a solution. If (optimum) solutions for such kind of problems are desired, simulation-based optimization procedures should be applied. These methods often take the outcome of a simulation into account to improve the solution in an iterative process. In the following, we will present frequently applied simulation-based optimization methods and give examples for applications.
In general, we assume the following optimization (minimization) problem, see Fu et al. (2008). Maximization problems can be treated similar.

$$\min_{\theta \in \Theta} J(\theta) \tag{2.1}$$

Here, θ is a p-dimensional solution vector within the feasible solution space Θ. For complex optimization problems, we usually have no knowledge about the convexity or linearity of $J(\theta)$ and Θ. Instead, in the context of simulation-based optimization, we assume that $J(\theta)$ can be represented by the expected value of the sample performances $L(\theta, \omega)$, themselves depending on the solution vector θ and the simulation replication ω, see equation (2.2).

$$J(\theta) = E[L(\theta, \omega)] \tag{2.2}$$

The simulation replication ω represents the uncertainty/randomness in the model. It can also be interpreted as a certain scenario, i.e. a feasible (deterministic) realization of uncertain parameters. We will use this notation in the following when simulation-based optimization methods will be discussed. In detail, we will focus on the response surface method, sample path optimization, stochastic approximation, ranking and selection, random search and metaheuristic approaches. The following explanations of these methods are mainly taken from Fu (2002), Fu et al. (2008) and Mayer (2011).

Response Surface Method
The basic principle of the response surface method (RSM) is to obtain a functional relationship – i.e. the response surface – between the input and the output (response) of the simulation. If two variables are considered, the response surface will look like a hilly landscape, where the height of the landscape denotes the response for given values for the variables. If the complete domain is relevant, neural networks or regression methods are often used to determine the entire response surface. However, if this is not possible, an (iterative) sequential response surface method can be applied instead. The basic idea is to construct a response surface for a small part of the entire domain and to use the information gained from this local area to select a new promising local area that can be investigated in the next iteration. Suchlike procedures often make use of gradient estimation/steepest descent method to determine in which area the response surface should be investigated next. The procedure closes with a detailed search in the last response surface, if no more promising local areas exist.
Jaluria (2009) proposes the response surface method for the application in thermal systems since relationships in chemical processes are often non-linear, but steady-going. Thus, a well-approximating response surface can be constructed with a relatively low number of measuring points.

Sample Path Optimization
The sample path optimization (SPO) deals with the application of deterministic optimization methods to originally non-deterministic problems. This is possible because of the transition from stochastic optimization model to a deterministic optimization model. Let us assume that a total of m different scenarios exist and that we consider the first n of them, i.e. $\omega = (\omega_1, \ldots, \omega_n, \ldots, \omega_m)$, then we can compute the mean of $L(\theta, \omega_i)$ (i.e. $E[L(\theta, \omega_i)]$) for the first n scenarios (i.e. the sample path) by equation (2.3).

$$\overline{L}_n(\theta) = \frac{1}{n} \sum_{i=1}^{n} L(\theta, \omega_i) \tag{2.3}$$

If each $L(\theta, \omega_i)$ is an independent and unbiased estimator of $J(\theta)$, then $\overline{L}_n(\theta)$ will converge to $J(\theta)$ for a sufficiently large n, see Fu (2002).
In other words, we use a finite set of different scenarios with deterministic realizations of originally non-deterministic parameters and compute the mean value of all scenarios for a given solution θ. This approach allows one to take advantage of the methods for deterministic optimization.
Sample Path Optimization methods are often used in supply chain planning. Jung et al. (2004) develop an simulation-based optimization approach on the basis of sample path optimization to cope with the problem of determining safety stock levels under uncertain demand so that a given customer satisfaction level will be met.

Stochastic Approximation
The stochastic approximation can be regarded as a gradient based search method for non-deterministic/non-linear optimization problems. Taking the current solution as a reference, the stochastic approximation iteratively computes a new solution θ_{n+1} according to equation (2.4), see Fu (2002).

$$\theta_{n+1} = \prod_{\Theta} (\theta_n - a_n \widehat{\nabla} J(\theta_n)) \tag{2.4}$$

Here, $\prod_{\Theta}$ denotes the projection of the new solution θ_{n+1} back in the constraint set, if θ_{n+1} would be located outside the feasible region. Moreover, a_n denotes the step size and $\hat{\nabla} J(\theta_n)$ represents the estimated gradient of the objective function of the current solution. The i-th gradient of the objective function can be estimated by the one-sided finite difference (FD) (eqn. (2.5)), the two-sided symmetric difference (SD) (eqn. (2.6)) and by the method of simultaneous perturbations (SP) (eqn. (2.7)), see Fu (2002).

$$(\widehat{\nabla} J(\theta))_i = \frac{\widehat{J}(\theta + c_i e_i) - \widehat{J}(\theta)}{c_i} \tag{2.5}$$

$$(\widehat{\nabla} J(\theta))_i = \frac{\widehat{J}(\theta + c_i e_i) - \widehat{J}(\theta - c_i e_i)}{2c_i} \tag{2.6}$$

$$(\widehat{\nabla} J(\theta))_i = \frac{\widehat{J}(\theta + \Delta) - \widehat{J}(\theta - \Delta)}{2\Delta_i} \tag{2.7}$$

Here, $\widehat{J}(\theta)$ is the estimation of the objective function considering solution θ. In the equations (2.5) and (2.6), c_i is a positive scalar and e_i is the unit vector. $\Delta = [\Delta_1, \ldots, \Delta_p]$ denotes a p-dimensional perturbation vector, e.g. the symmetric Bernoulli Distribution, see equation (2.7). It should be noticed that the number of required simulation runs to

compute the estimation of the gradient differ significantly with $p + 1$ for the FD, $2p$ for the SD and 2 for the SP, see Fu (2002).
The stochastic approximation is used for problems in different applications. Schwartz et al. (2006) consider a supply chain planning problem with supply and demand uncertainties. They use the stochastic approximation in combination with the method of simultaneous perturbations (SPSA) to manage inventory levels. Graf and Kimms (2011) apply the simultaneous perturbation stochastic approximation to the problem of determining booking limits for capacity control in the context of revenue management for strategic airline alliances.

Ranking and Selection
In contrast to previously discussed simulation-based optimization methods, ranking and selection contains no search for improved solutions, but an – usually exhaustive – evaluation of a given set of alternative solutions. Hence, ranking and selection methods are methods of comparison rather than of optimization. Gosavi (2003) suggests to consider not more than 20 solution alternatives.
Similar to the sample path optimization where a given number of scenarios is taken into account, we can estimate the objective function for a given solution under consideration of S scenarios by equation (2.8).

$$\overline{L}_S(\theta) = \frac{1}{S} \sum_{i=1}^{S} L(\theta, \omega_i) \tag{2.8}$$

The difference to the sample path optimization is the absence of any optimization process. Instead, the ranking and selection method simply computes the estimation of the objective function of all solution alternatives – each considering S scenarios – and selects the best solution. A variant of this approach additionally requires the definition of an indifference zone and a confidence interval to assist the selection of the best solution.
Ahmed and Alkhamis (2002) combined the ranking and selection method with a simulated annealing algorithm to solve a general discrete stochastic optimization problem and an inventory optimization problem with uncertain demands.

Random Search
The random search can be regarded as the counterpart of a local search for deterministic problems. Starting with an initial solution $\hat{\theta} \in \Theta$, the neighborhood of this solution $N(\hat{\theta})$ can be obtained by modifying the original solution $\hat{\theta}$ according to predetermined rules. In order to guarantee the convergence of this method to a global optimum, Andradóttir (1996) proposed to define the neighborhood of $\hat{\theta}$ ($N(\hat{\theta})$) to contain all $\theta \in \Theta \backslash \{\hat{\theta}\}$ so that, in fact, a global search would be performed.
A possible random search for minimization problems works as follows, see Fu (2002): Starting with $\hat{\theta}$ as an initial (and currently best) solution, the random search now iteratively selects a new solution $\theta_i \in N(\hat{\theta})$ and evaluates this new solution by the estimation of the objective function $\widehat{J}(\theta_i)$. If the estimation of the objective function of the new solution $\widehat{J}(\theta_i)$ outperforms the estimation of the objective function of the currently best solution $\widehat{J}(\hat{\theta})$ (i.e. $\widehat{J}(\theta_i) < \widehat{J}(\hat{\theta})$ for minimization problems), then $\hat{\theta} \leftarrow \theta_i$ and a new neighborhood of θ_i as the new best solution will be defined. Now, the next iteration starts with the selection and evaluation of a new solution out of the new neighborhood $N(\hat{\theta})$. The procedure stops, if the stopping criterion (e.g. a given number of iterations or a given number of iterations without improvements) is reached and the best solution $\hat{\theta}$ will be returned.

A framework for choosing high quality solutions for discrete stochastic optimization problems using the random search method can be found in Alrefaei and Alawneh (2005). The authors combine their approach with a simulated annealing algorithm to solve a discrete stochastic optimization problem containing a $M/M/1$ queuing model.

Metaheuristic Approaches
Procedures belonging to the class of metaheuristic solution approaches are characterized by general search techniques that can be applied to a large number of different problems. Typical examples of metaheuristic approaches are genetic algorithms (GA), simulated annealing (SA) and tabu search (TS), see Domschke and Drexl (2005). Usually, these approaches construct new solutions (or a population of solutions) by given rules (e.g. mutation and crossover in GA or definition of neighborhoods in SA and TS) and evaluate these solutions. Depending on the type of problem, the evaluation of a solution can be done by calculating the objective function value in case of a deterministic optimization problem or by estimating the objective function via simulation, if non-deterministic (stochastic) optimization problems have to be solved. In the latter case, the simulation can be regarded as a black box that only evaluates solutions, see April et al. (2003).
Li (2009) combines a genetic algorithm with a circuit simulator for the optimization of low noise amplifier designs. The author uses the weighted deviation of the simulation results of a given circuit design from a target specification as the fitness score.

2.3 Summary

The number of cited works dealing with evacuation planning illustrate, that this type of problem represents an interesting field of research. Taking the basic thoughts about evacuation planning for urban areas from Section 1 into account, the following advantages and disadvantages can be derived.
As inherent to their functional principle, traffic simulation approaches are not capable of any optimization process. On the other hand, traffic simulation approaches allow a much more realistic illustration of traffic, especially when microscopic simulations are used. Hence, these approaches are the method of choice to evaluate a given evacuation plan and to provide helpful information within a simulation-based optimization approach.
Traffic assignment optimization models allows one to assign traffic within a given traffic routing framework in a way that minimizes/maximizes an objective function (e.g. total evacuation time). A large portion of the presented work considering traffic assignment problems is built upon the CTM approach from Daganzo (1994). This approach – that was originally intended to be used as a macroscopic traffic simulation model – integrates basic traffic dynamics into an optimization approach. Hence, the CTM seems to be a good compromise between computational complexity (the CTM can be embedded into an optimizational approach) and reasonable traffic illustration.
Some works taking traffic routing and traffic assignment into consideration lack of an adequate traffic representation. In the beginning, static network flow problems were proposed (see e.g. Yamada (1996) or Cova and Johnson (2003)). Later, combinations of optimization and simulation methods were partially combined (see e.g. Murray-Tuite and Mahmassani (2003), Murray-Tuite and Mahmassani (2004) or Stepanov and MacGregor Smith (2009)) to allow a more realistic illustration of traffic and to evaluate the solutions generated by optimization approaches by a traffic simulation.
These observances motivates us to utilize the basic ideas of the CTM approach by Daganzo (1994) to formulate evacuation planning models that simultaneously determines the

traffic routing and traffic assignment in the case of an evacuation in one step. Since the traffic representation of the CTM approach is clearly outperformed by microscopic traffic simulations, we will combine a CTM based evacuation planning model with a microscopic traffic simulation to benefit from the advantages of both approaches. The basic idea of our CTM based evacuation planning model has also been adapted to a related problem, see Kimms et al. (2011) for traffic guiding in the case of big events.

Chapter 3

Cell-Transmission-Based Evacuation Planning

In this chapter, a basic evacuation planning model based on the cell-transmission approach by Daganzo (1994) will be presented, compare Kimms and Maassen (2011b). First, we introduce the reader to the basic ideas behind the Cell-Transmission-Model (CTM). Afterwards, the Cell-Transmission-Based Evacuation Planning Model (CTEPM) will be formulated and discussed. In a first step, we use the CTEPM to compute the evacuation routing as well as the traffic assignment and in a second step, a microscopic traffic simulation will be applied to obtain a more realistic illustration of traffic flows during an evacuation. To demonstrate real-world applicability of our approach, we will compute and simulate an evacuation plan for a neighborhood in the city of Duisburg, Germany. A sensitivity analysis is performed to investigate the effects of changing evacuation circumstances (i.e. departure pattern, population size, initial traffic loading).

3.1 Cell-Transmission Basics

Daganzo (1994) studied the evolution of traffic over a one–way highway without any intermediate entrances or exits and proposed the cell transmission model in this context. This model bases on the hydrodynamic traffic flow model by Lighthill and Whitham (1955) and Richards (1956). Since we will use the cell transmission model as a basis for our work, we will briefly review the underlying ideas of Daganzo's cell transmission model: The highway to be studied is to be divided into sections (cells) and I is the set of section numbers. These sections are inspected in snapshots which are taken every tick of a clock. The length of the sections are set equal to the distances traveled in light traffic by a vehicle in one clock tick which means that a vehicle can advance from one section to the next with each tick if the traffic is light. Let clock tick t be the end of the time window $]t-1;t]$ which is referred to as period t, and let x_{it} be the number of vehicles in section i at clock tick t. Under light traffic and unidirectional flow we observe a flow of vehicles $y_{i,i+1,t}$ which leave from section i in period t which reach section $i+1$ during period $t+1$. Due to our application, all values x_{it} and $y_{i,i+1,t}$ must fulfill the non–negativity condition. To model queuing Daganzo introduced two parameters: N_{it}, the maximum number of vehicles that can be present in section i at the same time, and Q_{it}, the maximum number of vehicles that can flow into section i during a period. Using this notation the flows must fulfill the following three conditions: (i) $y_{i,i+1,t} \leq x_{it}$, (ii) $y_{i,i+1,t} \leq Q_{i+1,t}$, and (iii) $y_{i,i+1,t} \leq N_{i+1,t} - x_{i+1,t}$. Boundary conditions for the first and the last section can be specified easily. With these

recursive relations between sections, Daganzo run a simulation of the traffic along a one–way highway without intermediate entrances and exits. In a sequel to the above cited paper, Daganzo (1995) studied an extension of the cell transmission model that can be used to simulate traffic in road networks, but we will not review the details here. As discussed in Chapter 2, several authors presented optimization methods based on Daganzo's cell transmission model, e.g. Ziliaskopoulos (2000), Tuydes and Ziliaskopoulos (2004), Tuydes and Ziliaskopoulos (2006) or Chiu et al. (2007). Ziliaskopoulos (2000) considers a dynamic traffic assignment problem which is confined to one single destination and where the integrality condition of the traffic flows (number of vehicles) is relaxed. Tuydes and Ziliaskopoulos (2004) and Tuydes and Ziliaskopoulos (2006) use the dynamic traffic assignment problem formulation and allow lane reversals, i.e. the redirection of lanes. Chiu et al. (2007) present a linear programming model with multiple destinations (leading to a super sink) and solved a small example. In contrast to the optimization model that we will define in this chapter, the work of Chiu et al. (2007) is more restrictive with regard to the following aspects: It is not taken into account that the level of danger differs within the considered area. The orientation of traffic flow is predefined (cells have successors and predecessors), but the orientation is not a result of the computation. Departure times are only indirectly considered by observing the vehicle outflow from source cells.
The contribution of the following approach is twofold:

- Daganzo's idea of considering road sections and flows between these sections is modified to formulate an optimization problem for evacuation that is more general than previous work for computing possible traffic routes in complex street networks as well as assignments to safe destinations. So, the cell transmission approach is used for optimization and not for simulation in our model.

- Given the possible traffic routes from the previous step, a simulation which is more detailed than Daganzo's work is done to predict the traffic's evolution in complex street networks. Thus, the traffic simulation is based on an optimized network design.

3.2 Cell-Transmission-Based Evacuation Planning Model

3.2.1 Notation

Assume that a street network is given so that the endangered zone is a subnetwork of the given network and safe destinations are part of the given network as well. A real–world street network is modeled as a graph where nodes of the graph represent equal–sized sections of a street and edges in the graph indicate that two sections are close to each other in reality (see Figure 3.1 for an illustration). The nodes in the graph, i.e. the sections of the streets, are numbered. Let $I = \{1, ..., |I|\}$ be the index set of the cells where $|I|$ denotes the super sink. A parameter $\beta_{ij} = 1$ indicates that sections $i \in I$ and $j \in I$ are adjacent to each other (the order of indices is irrelevant and hence $\beta_{ij} = \beta_{ji}$). If two sections $i \in I$ and $k \in I$ are not adjacent the value β_{ik} is 0.
Similar to Daganzo's cell transmission model we assume a clock and take a snapshot of the situation at every clock tick. The time interval between two consecutive clock ticks is one period by definition. The size of the sections represented by a node in the graph is chosen such that a vehicle can pass this distance within one period if the traffic is light. If, for instance, the speed of a vehicle under light traffic is 13.89 meters per second (= 50 kilometers per hour) and the time interval between two consecutive clock ticks is assumed to be 9 seconds then a graph node represents a section of length 125 meters. If we further

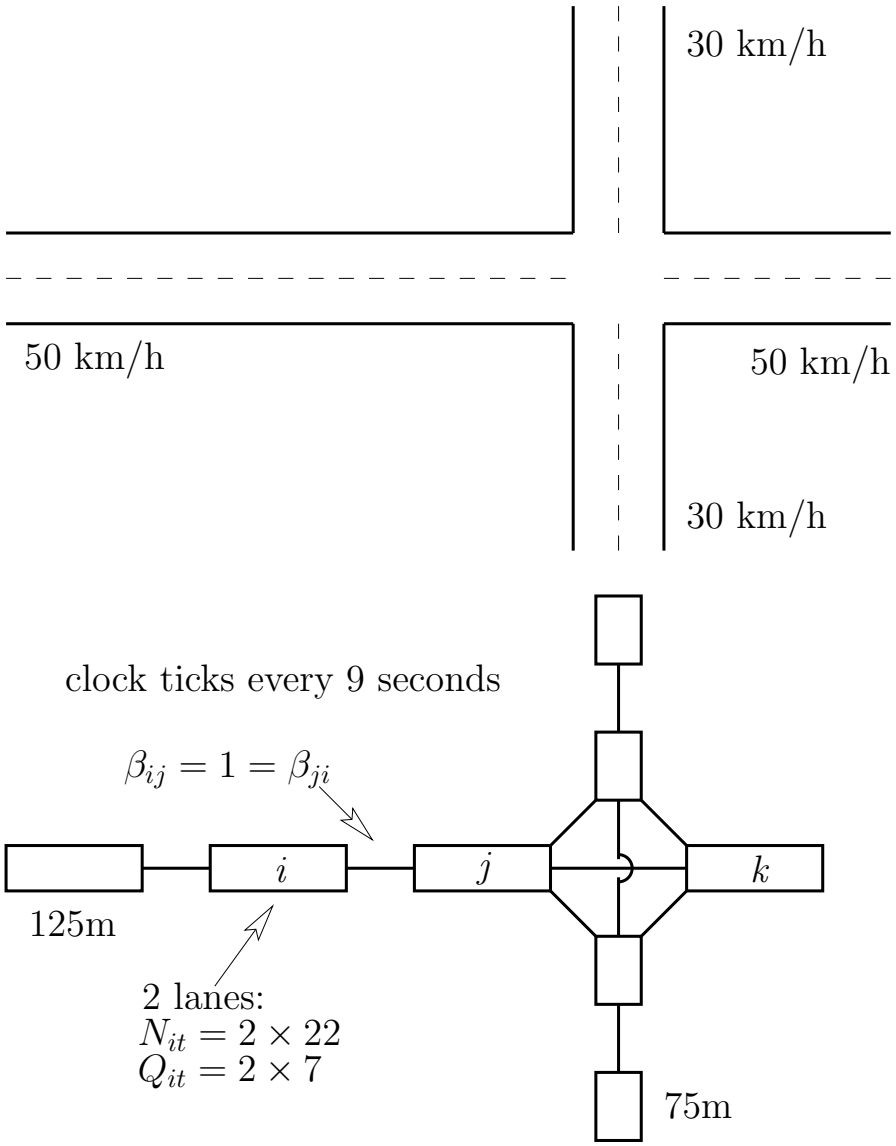

Figure 3.1: An Illustration of the Graph Representation of a Street Network

assume that the street section consists of a single lane and an average vehicle has a length of 4.5 meters and the distance between two consecutive vehicles with speed 13.89 meters per second is, say, 13.3 meters, the maximum number of vehicles traveling with normal speed on one lane in the same section is about 7 ($\approx 125/(4.5 + 13.3)$) which means that no more than 7 vehicles can enter this section within one period. In a traffic jam where vehicles move slowly or not at all we may observe a distance between two vehicles of just one meter on average which means that about 22 vehicles ($= \lfloor 125/5.5 \rfloor$) at most can be on one lane inside the same section. Likewise, if we consider a street where the light traffic speed is 30 kilometers per hour, one section represents 75 meters of the street (again, the clock ticks every 9 seconds). Given the number of lanes for each section, we have parameters N_{it} for the maximum number of vehicles in section i, Q_{it} for the maximum number of vehicles which can enter section i in one period or which can leave section i in one period. See again Figure 3.1 for an illustration. These parameters have an index t, because the

capacity of a section may vary over time (e.g. streets may be unusable after some time). In the following, we assume that storage and flow capacities will be constant over time.

Further notation is necessary to formulate a mathematical programming formulation of the evacuation problem. Let $T = \{1, ...\}$ be the index set of the clock ticks taken into account where $|T|$ is an upper bound for the time needed to evacuate all. E_i is the number of vehicles to be evacuated from section $i \in I$. We can assume $E_{|I|} = 0$, because nobody is located within the super sink. Since the danger for being in different sections may be different, a weight $c_{it} \geq 0$ is used to specify the danger in section i in period t (the higher the weight, the greater the danger). Of course, even if the danger in section i is constant over time one may choose values $c_{it} = c_i \cdot t$ which increase with t to avoid unnecessary waiting. We can assume $c_{|I|,t} = 0$, because there is no danger at a safe place (= super sink).
The decision variables of the evacuation problem are z_{it} the number of residing, leaving or waiting vehicles which use section i in period t, x_{it} the number of residing vehicles in section i at clock tick t (the end of period t) — assume x_{i1} to be the given number of vehicles on street segment i before the evacuation starts —, y_{ijt} the number of vehicles which leave section i in period t and reach section j in period $t + 1$ — please note that it is sufficient to consider only those flow variables y_{ijt} where $\beta_{ij} = 1$ holds —, and b_{it} the number of vehicles out of E_i which start to move in period t.

3.2.2 Model Formulation

The mathematical programming formulation of a cell-transmission-based evacuation planning model (CTEPM) which determines the traffic routing, which (indirectly) assigns traffic to the existing lanes, which assigns vehicles from parts of the network to safe destinations, and which determines when vehicles start to move reads as follows:

$$\min \sum_{i \in I} \sum_{t \in T} c_{it} z_{it} \tag{3.1}$$

subject to

$$z_{it} = x_{it} + \sum_{j \in I} y_{ijt} + (E_i - \sum_{\tau=1}^{t} b_{i\tau}) \qquad i \in I; t \in T \tag{3.2}$$

$$x_{it} = b_{it} + x_{i,t-1} + \sum_{j \in I} y_{ji,t-1} - \sum_{j \in I} y_{ijt} \qquad i \in I; t = 2, \ldots, |T| \tag{3.3}$$

$$z_{it} \leq N_{it} + (E_i - \sum_{\tau=1}^{t} b_{i\tau}) \qquad i \in I; t \in T \tag{3.4}$$

$$\sum_{t \in T} b_{it} = E_i \qquad i \in I \tag{3.5}$$

$$x_{|I|,|T|} = \sum_{i \in I} E_i + \sum_{i \in I} x_{i1} \tag{3.6}$$

$$y_{ijt} \leq N_{it} \beta_{ij} \qquad i, j \in I; t \in T \tag{3.7}$$

$$\sum_{j \in I} y_{jit} \leq N_{it} - x_{it} \qquad i \in I; t \in T \tag{3.8}$$

$$\sum_{j \in I} y_{jit} \leq Q_{it} \qquad i \in I; t \in T \tag{3.9}$$

$$\sum_{j \in I} y_{ijt} \leq Q_{it} \qquad i \in I; t \in T \qquad (3.10)$$

$$z_{it} \geq 0 \qquad i \in I; t \in T \qquad (3.11)$$

$$x_{it} \geq 0 \qquad i \in I; t \in T \qquad (3.12)$$

$$y_{ijt} \geq 0 \qquad i, j \in I; t \in T \qquad (3.13)$$

$$b_{it} \geq 0 \qquad i \in I; t \in T \qquad (3.14)$$

$$x_{i1} = 0 \qquad i \in I \qquad (3.15)$$

$$y_{ij1} = 0 \qquad i, j \in I \qquad (3.16)$$

$$b_{i1} = 0 \qquad i \in I \qquad (3.17)$$

The objective (3.1) is to minimize the weighted number of residing, leaving or waiting vehicles in all sections over time. The weights for the sections take into account the danger in a section (sections with low danger (i.e. low c_i-values) are preferred) and the time of use (early flow (i.e. low values for t) is preferred). The number of vehicles which use a section in a period is defined to be the sum of those which remain in the section at the end of a period, the number of those which leave the section in that period, and those which wait for departure — see (3.2). The number of vehicles which remain in section i at the end of a period — see (3.3) — equals the number of vehicles which start to move in the period plus the number which were in the section the previous period plus the number of vehicles which enter from other sections minus the number of vehicles which leave the section in that period. Because of (3.4) the number of vehicles which use a section must not exceed the capacity limit of the section where vehicles waiting for departure are assumed to occupy no street capacity. All vehicles within the endangered network must start to move (3.5). Due to (3.6) all vehicles reach a safe destination. Traffic can flow from one section to another only if these two sections are linked (3.7). The restrictions (3.8) make sure that the inflow into a section does not lead to an excessive capacity usage in the section, i.e. empty space must be available. Inflow (3.9) and outflow (3.10) capacity limits are taken into account as well. The domains of the decision variables are defined by (3.11)–(3.14). Boundary conditions to avoid any vehicle movement before the evacuation starts are stated in (3.15)–(3.17).

Please note that we define all decision variables as non-integer so that the optimization problem becomes an LP. In fact, it may happen that some variables take non-integer values but for our example with only integer parameters, all variables – which are relevant for the simulation – were set to integer values automatically. These variables are mainly the cumulated number of vehicles traveling from cell i to j, because these variables determine how many vehicles will travel on given street connections. We use $\eta_{ij} = \sum_{t \in T} y_{ijt}$ to denote the total number of vehicles traveling from cell i to cell j during the complete planning horizon. Moreover, driving directions and lane allocations have to be determined for the simulation. Let $\varphi_{ij} = 1$ ($\varphi_{ij} \in \{0, 1\}$) if vehicles travel from cell to i to cell j ($\eta_{ij} > 0$) and let ϵ_{ij} ($\epsilon_{ij} \in \mathbb{N}_0$) denote the number of lanes used between two cells. We compute ϵ_{ij} with $\epsilon_{ij} = \left\lceil \frac{y_{ij}^{\max}}{(Q_i/l_i)} \right\rceil$ where $y_{ij}^{\max}$ is the maximum amount of vehicles traveling from cell i to cell j (on all lanes) considering all periods and (Q_i/l_i) is the maximum vehicle flow capacity per lane where l_i is the number of lanes in cell i. Please note that we assume that vehicle flow capacities are not changing within the planning horizon so that using Q_i (instead of Q_{it}) is sufficient. Moreover, we assume that the vehicle flow capacity per lane (Q_i/l_i) is the same for all cells $i \in I$.
A possible heuristic postprocessing approach to overcome issues caused by non-integrality

of η_{ij} (φ_{ij} and ϵ_{ij} are set automatically to integer values) consists of a simple static network flow model which uses the (integer and/or non-integer) η_{ij} values from the CTEPM as a starting point to generate a less as possible modified solution consisting only of integer values for the cumulated number of vehicles traveling between two cells, see Chapter 4.2.2. Since suchlike adjustments were not necessary for our instances, we took the original η_{ij} values from the CTEPM. We have used the commercial software package GUROBI to solve instances of this model formulation optimally.
Please note that the model allows feasible solutions with traffic flows in opposite directions between two street segments, i.e. $y_{ijt} > 0$ for some period t does not imply $y_{jit'} = 0$ for all periods t'. Also, typical solutions let the traffic from a particular street section flow to a limited number of exits. Please note that the model allows that vehicles from one street section flow to different exists which means that at some intersections we observe a divergent traffic flow. Hence, if such a solution is implemented, one needs to control the traffic in a proper way (such rules may be that vehicles on some lanes must make a left turn while vehicles on other lanes must make a right turn or a policeman directs some vehicles to the left and some others to the right).
The described optimization model assumes deterministic data and many aspects that are due to the dynamic nature of traffic are considered roughly at best. The creation of traffic jam, for instance, is taken into account by means of capacity constraints, i.e. street sections cannot contain more than a limited number of cars and the number of cars which move from one section to another within one period is limited as well, but this is a very rough description of real behavior. Also, capacity restrictions at junctions are not explicitly modeled by street sections, because the size of a junctions is relatively small compared to the street segments. Hence, most of the congested traffic will be observed on the lanes that are taken into account in the model. In reality there are many dynamic aspects which have an impact on the observed traffic. For example, the speed of the vehicles depends on the traffic density and lane-changing movements are performed under consideration of free space in the destination lane. Such aspects are not fully covered by the proposed optimization model. Hence, we use parts of the output of the optimization as an input for a second phase where traffic is simulated to get a better picture of what will happen if the evacuation begins. How this works is described in detail in the next section.

3.3 Microscopic Traffic Simulation

To perform the traffic simulation, we use the open source SUMO (Simulation of Urban MObility) microscopic road traffic simulation package by the Institute of Transportation Systems at the German Aerospace Center. SUMO takes advantage of the car-following behavior model by Krauß et al. (1997)/Krauß (1998) and the lane changing model by Krajzewicz (2009). As already explained in the previous section, three categories of values from the optimization part are passed to the traffic simulation, namely η_{ij} to denote the total number of vehicles traveling from cell i to cell j, φ_{ij} values indicating whether a connection from cell i to cell j is used by escaping vehicles and ϵ_{ij} values assigning an integer number of lanes to two cells where a traffic flow exists. The information contained in the values of the z_{it}, x_{it} and b_{it} variables from the optimization part is ignored. Thus, the optimization model described in the previous section can be seen as a heuristic for finding a directed street network for which traffic simulation is performed.
The road network in the SUMO simulation can be described by the terms edges and nodes. Each street segment can be represented by at least one edge and every intersection represents one node in the network. A close up of the simulation visualization is illustrated

in Figure 3.2. Vehicles are represented by triangles moving across street segments and junctions. Dots at one side of a triangle indicate forthcoming turning movements.

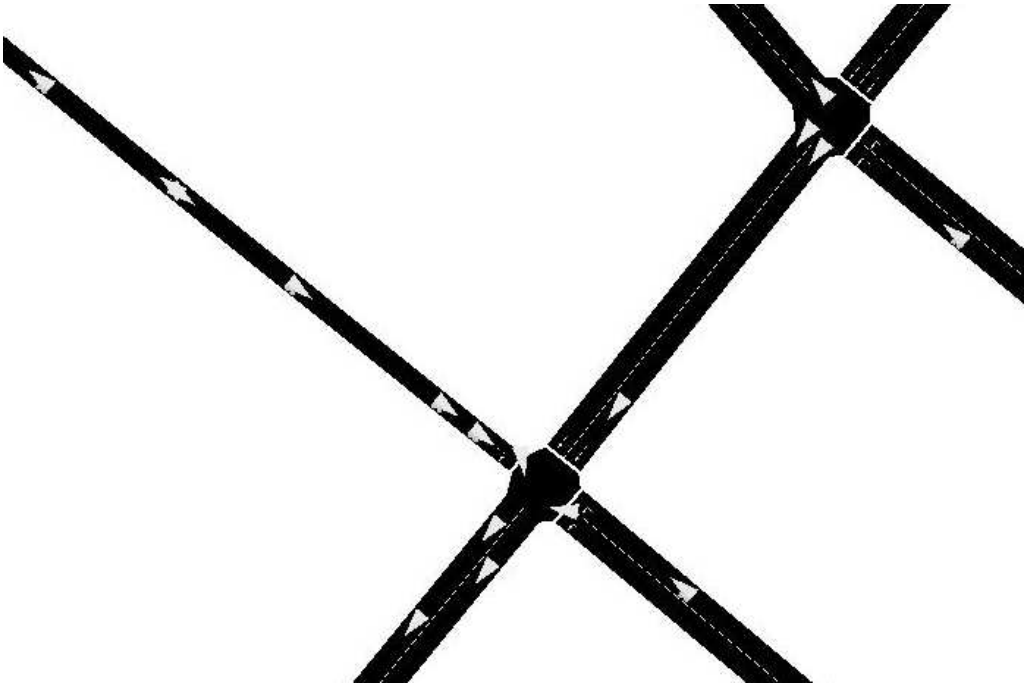

Figure 3.2: Detail View of Sumo Visualization

Each street segment is characterized by a given number of available lanes and a starting as well as an ending node, i.e. two junctions. However, it has to be noticed that the length of a street segment in the simulation is not the same as in the optimization part because the simulation allows to model street segments in much smaller steps (and thus better matching the effective length of a street segment) than a standard cell size in the optimization part. According to the optimization part, we assume that vehicles travel with a driving speed of 50 km/h (≈13.89 m/s) and 30 km/h (≈8.33 m/s) depending on the street segment itself and that all vehicles have the same length of 4.5m. Of course, other values for driving speeds and vehicle length can also be applied, if desired.
The car following model Krauß et al. (1997)/Krauß (1998) belongs to the class of so-called "safe-distance models" which are characterized by the assumption that a driver adjusts his driving speed in due consideration to the distance to the vehicle ahead. Thereby the model allows to include assumptions regarding driving behavior, e.g. acceleration, deceleration (braking), response time before acting and target driving speed.
The lane allocation is performed by a relatively simple rule. If vehicles turn right (left) at the end of the street, all right-turning (left-turning) lanes have to be located as far as possible to the right (left) side of the street. The allocation of lanes with vehicles driving straight ahead is located in the center of the street trying to interfere with left- or right turning lanes as few as possible. It also has to be mentioned that vehicle flows may cross each other at junctions which would be a huge risk in real world situations, because no traffic lights exist in our approach. The traffic simulation rules in SUMO ensure a smooth traffic flow throughout the complete simulation so that no accidents occur. However, we are not aware of any publications which deal with traffic flow simulation where accidents play a key role. In practice, if two vehicle flows cross each other at a junction, one vehicle

flow will wait until there is enough free space to enter the previously blocked junction. These relations are also displayed in Figure 3.3.

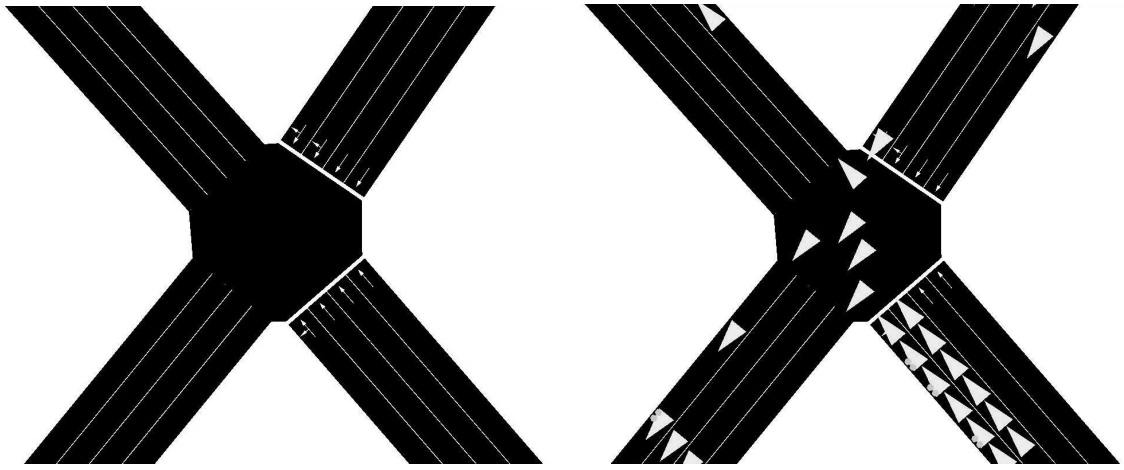

(a) Junction with Allocation of Driving Directions (b) Junction with Blocked Traffic Flows

Figure 3.3: Lane Allocation and Blocking at Junctions

Figure 3.3 (a) displays a junction before the evacuation starts. It can be easily seen that the allocation of driving directions to lanes is performed in the previously introduced manner. Moreover, the solution from the optimization part leads to a huge risk due to crossing traffic streams. In Figure 3.3 (b), it can be recognized that one traffic stream is blocked as long as vehicles from the crossing traffic stream pass the junction. If enough free space is available, the waiting vehicles enter the junction so that the vehicles from other traffic stream have to wait.
The starting time of vehicles is part of the optimization process. However, for the SUMO simulation, we assume that the number of evacuees which have left their homes till a certain point of time can be modeled by means of a gamma distribution with parameters α and β. For $\alpha = 3$ and $\beta = 3$ the peak of the density function is $(\alpha - 1)\beta = 6$, i.e. that during the sixth minute most evacuees will leave their homes. Of course, all resulting numbers are considered to be minutes. When high traffic density in certain areas of the endangered network exist, residents may have to wait to start the evacuation due to not enough space to enter the network. Suchlike observations mainly occur for very fast leaving behaviors, e.g. setting $\alpha = 3$ and $\beta = 1$ resulting in slower departure patterns as originally computed by the gamma distribution.

3.4 Case Study: Duisburg (Neudorf), Germany

3.4.1 Basic Information and Assumptions

To test the proposed optimization and simulation procedures, we have implemented the models with commercial and open source software. For the optimization part we have used GUROBI 3.0.1 and the simulation was done with SUMO 0.11.1. All computational tests were done on an Intel X9100 (3.06 Ghz) with 8 GB RAM running Windows Vista (64-bit).
We tested a hypothetical evacuation scenario with data of a real–world–sized problem. The neighborhood around the University of Duisburg–Essen was used as an example. We

know that approx. 26,000 people live in the Duisburg–Neudorf neighborhood and we assumed that on average three persons share one vehicle which means that 8,801 vehicles are simulated. The distribution of these people was given to us by the city administration, see Figure 3.4. In total, there are eight exits where evacuees can escape from the endangered network. An illustration of the simulation model for the Duisburg–Neudorf case can be found in Appendix B.

Figure 3.4: Population Density in Duisburg–Neudorf

In the cell transmission model based mathematical program the network of Duisburg–Neudorf turned out to require $|I| = 256$ sections including the super sink $|I|$ and we set $|T| = 76$. Moreover, we assume a uniformly distribution of danger of $c_{it} = c_i \cdot (t-1)$ with $c_i = 100$ for all cells within the endangered network and $c_{|I|,t} = 0$ for the super sink $|I|$. The objective function has been extended by two additional terms to ensure a "straight-forward" solution and to avoid "unpractical" vehicle flows. If two adjacent cells share the same level of danger, unnecessary vehicle movements between these cells may occur. This would not correspond to a desired "straight-forward" solution so that the term

$$+10^{-6} \cdot \sum_{i \in I} \sum_{j \in I} \sum_{t \in T} y_{ijt} \tag{3.18}$$

has been added to the objective function to avoid unnecessary vehicle movements. In order to avoid odd situations where vehicle use adjacent cells as short cuts to bypass bottlenecks we also added the following term to the objective function.

$$+10^{-6} \cdot \sum_{i \in I} \sum_{\substack{j \in I: \\ \beta_{ij}=1}} \sum_{\substack{k \in I: \\ \beta_{ik}= \\ \beta_{jk}=1}} \sum_{t \in T} (y_{ijt} + y_{jkt}) \tag{3.19}$$

As an example, imagine a t-junction with three cells, see Figure 3.5. The model formulation allows traffic flows, where vehicles first move from cell i and cell j and then move from cell j to cell k. To reduce suchlike situations, the term has been added to the objective function.

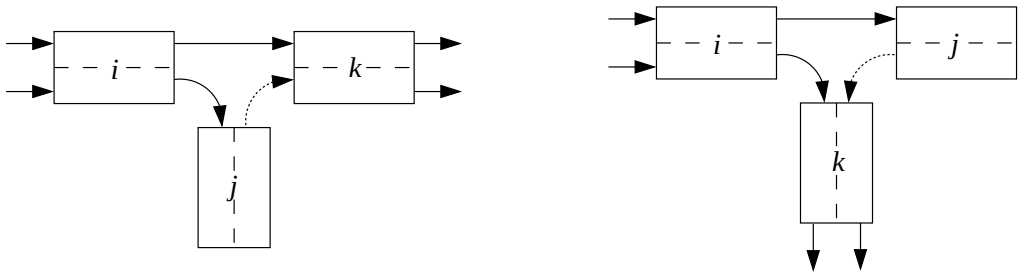

Figure 3.5: Undesired Situations in Evacuation Plans

Using these extensions to the objective function, the GUROBI solver found an optimal solution in about 67 seconds.

In the optimization model, it makes no difference whether vehicles are waiting at home or if these vehicles are waiting within the cell if streets are congested since we assume that all cells share the same level of danger at each time. Therefore, there exist a large number of different (optimal) solutions with different leaving patterns. In order to display extreme situations with extremely fast and extremely slow departures, we added an additional term

$$+/- 10^{-6} \cdot \sum_{i \in I} \sum_{t \in T} (E_i - \sum_{\tau=1}^{t} b_{i,\tau}) \tag{3.20}$$

to the objective function in order to "push" the optimum solution into the desired direction of generating very fast or very slow departures without degrading the original objective function value. As can bee seen in Figure 3.6, departure times generated by the cell transmission based model (i.e. the b_{it} variables) differ significantly from the departure times which are expected in the gamma distribution for $\alpha = 3$ and $\beta = 1$.

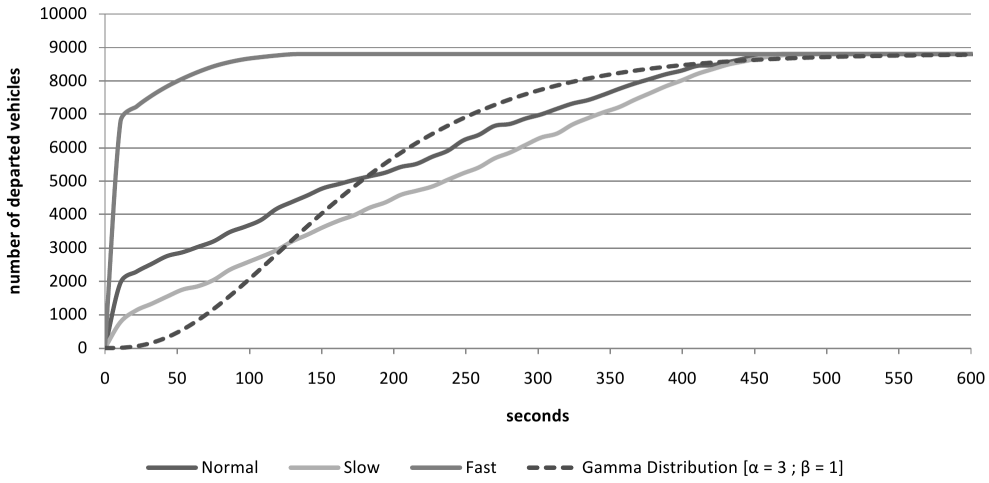

Figure 3.6: CTEPM Based versus Gamma Distributed Embarkation

In all cases, the cell transmission based model loads the road network very fast, especially at the very beginning of the evacuation. In contrast, the gamma distribution assumes that at the very beginning of the evacuation process almost no vehicles enter the network which is a more realistic assumption since some time is needed for preparation. In the following, the CTEPM with fast departures loads approximately 75% of the total population into the network within the first seconds. In the case of very slow departures and for the case without influencing the departure pattern by (3.20) significantly less vehicles depart in the same time horizon. In detail, only about 10% (20%) of the total population departs within the first seconds. After this first initial traffic loading, all departure patterns show a comparable behavior since all departure patterns are characterized by an almost linear rising until all vehicles are departed. In comparison to the gamma distribution using $\alpha = 3$ and $\beta = 1$ the slow departure pattern and the uninfluenced departure pattern show the strongest accordance with relatively large deviations at the very beginning of the evacuation. Of course, the difference between the departure pattern from the CTEPM and the gamma distribution using $\alpha = 3$ and $\beta = 3$ would be even larger. The slow departure pattern also demonstrates the point in time, where all vehicles should have left their homes at the latest (after approximately 500 seconds) so that the evacuation lasts not longer than necessary because of late vehicles traveling on empty roads. However, the departure times of the CTEPM are not expected to be observed in reality, so that the more established gamma distribution (see Lindell (2008)/Yazici and Ozbay (2008)) will be used in all simulation runs.

3.4.2 Sensitivity Analysis

A part of the result of the optimization problem is now used as input for the second phase, the simulation. From the optimization phase we get the information what street segment can be used in what direction and in which directions turns can be made at intersections. With this input we start phase two, the simulation, to integrate more realistic traffic dynamics which are included in the SUMO traffic simulation. A simulation run for the Duisburg–Neudorf example took approx. 20 seconds.
We have simulated the evacuation problem in Duisburg–Neudorf with three different

departure time scenarios (the underlying gamma distribution has parameters $(\alpha, \beta) \in \{(3,1),(3,3),(3,5)\}$. Figure 3.7 illustrates the effect of these parameter settings by giving the probability distribution and the density function.

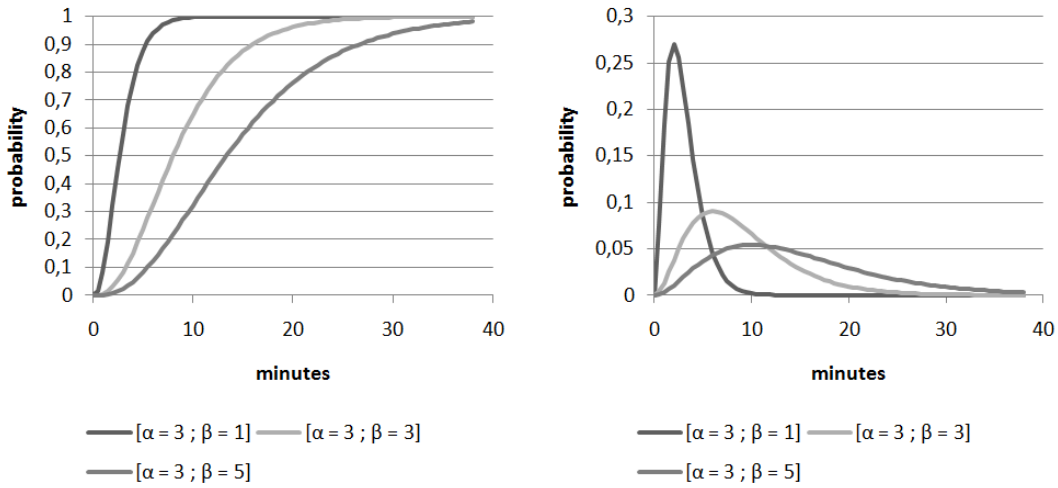

Figure 3.7: Different Departure Time Scenarios

Furthermore, we have varied the population size $\Pi \in \{100\%, 90\%, 70\%\}$, i.e. the number of vehicles to be considered (for $\Pi = 100\%$ we evacuate the aforementioned 8,801 vehicles). In addition to that, we study the impact of the number of vehicles already on the road when evacuation starts (the initial occupation on major street segments is varied with $\Sigma \in \{0\%, 15\%, 40\%\}$ of the street capacity).

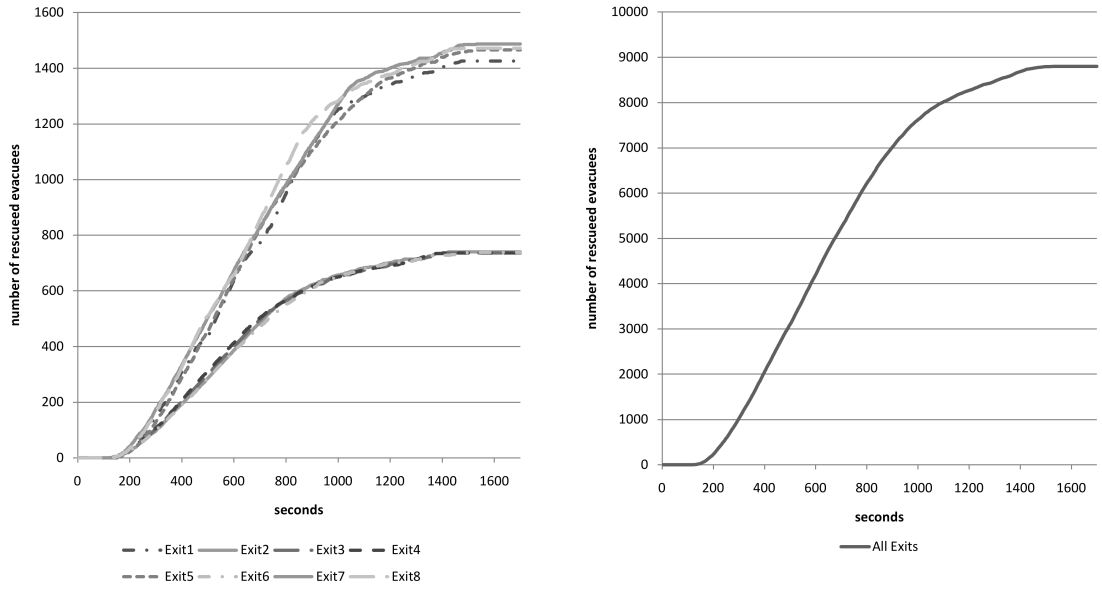

(a) Exit 1–8

(b) Cumulated

Figure 3.8: Number of Evacuated Vehicles for $(\alpha, \beta) = (3,3)$,$\Pi = 100\%$ and $\Sigma = 0\%$

Figure 3.8 shows the increase of the number of evacuated vehicles over time when $(\alpha, \beta) =$

$(3,3)$, $\Pi = 100\%$ and $\Sigma = 0\%$ as a point of reference. Under these circumstances, the simulation reveals that all vehicles are evacuated after approx. 25.5 minutes (after a bit more than 10 minutes about 50% of the vehicles escaped from the endangered zone). The vehicle load of the destinations differs mainly because of different capacities (different number of lanes) at these exits.
If we vary the departure behavior, i.e. the parameters (α, β), we can observe if and how the vehicle arrivals over time changes. Figure 3.9 provides our findings. The most interesting observation is that if the departure of the vehicles is sped up ($(\alpha, \beta) = (3,1)$ versus $(\alpha, \beta) = (3,3)$), the total time to evacuate all decreases from 25.5 minutes to 20.5 minutes although the difference in the departure pattern is much higher. The almost parallel evolution of the corresponding curves in the arrival pattern suggests that the maximum traffic flow is achieved in both cases so that the theoretical advantage of faster departing times could not be transfered to the arrivals. However, if the delay is too long ($(\alpha, \beta) = (3,5)$) then the total evacuation time increases again because of the late vehicles.

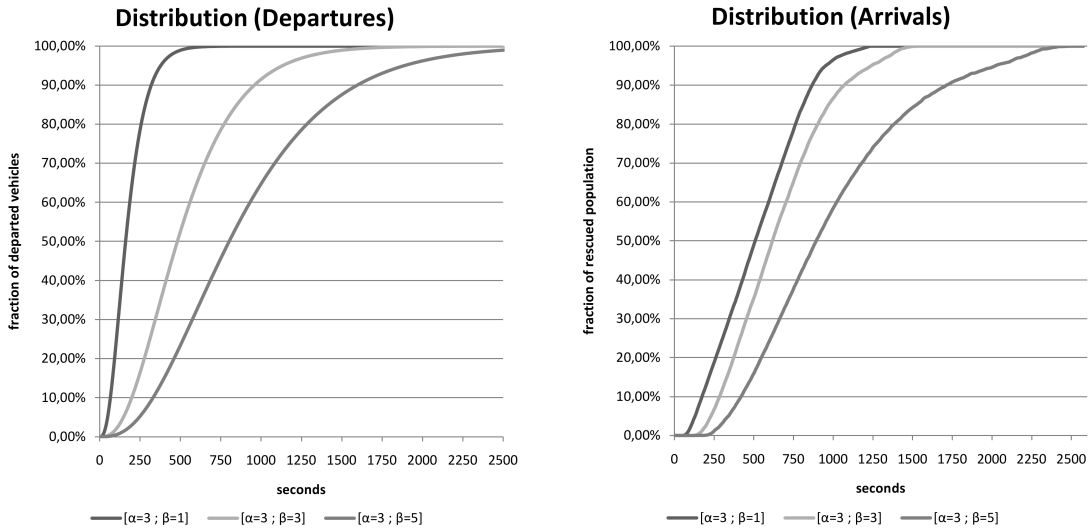

(a) Departure (b) Arrival

Figure 3.9: Impact of Different Departure Patterns for $\Pi = 100\%$ and $\Sigma = 0\%$

Figure 3.10 shows what happens if we vary the size of the population to be evacuated given the parameters $(\alpha, \beta) = (3,3)$. As we see, the population size does not affect the evolution of the relative number of evacuated vehicles over time much. This may be, because the street capacity is not a bottleneck in this scenario (given the underlying population size). Therefore, we also tested the impact of the population size for the parameters $(\alpha, \beta) = (3,1)$ where we have learned from Figure 3.9 already that street capacity is a problem. Figure 3.11 shows the results for this study. Now we see what was expected: If the street capacity is scarce then a lower number of vehicles results in shorter total evacuation times. It is interesting to note, however, that 70% of the vehicles is evacuated after approx. 11 minutes if 8,801 vehicles ($\Pi = 100\%$) is assumed, but evacuating a total of approx. 6,160 vehicles ($\Pi = 70\%$) takes approx. 13 minutes (both cases with $(\alpha, \beta) = (3,1)$). Thus, the best delay with which vehicles depart not only depends on the street capacity (as suggested by Figure 3.9), but also on the total number of vehicles. Hence, finding a good departure schedule depends on the infrastructure as well as on the capacity load.
All computational tests so far have assumed that all streets are empty if the evacuation

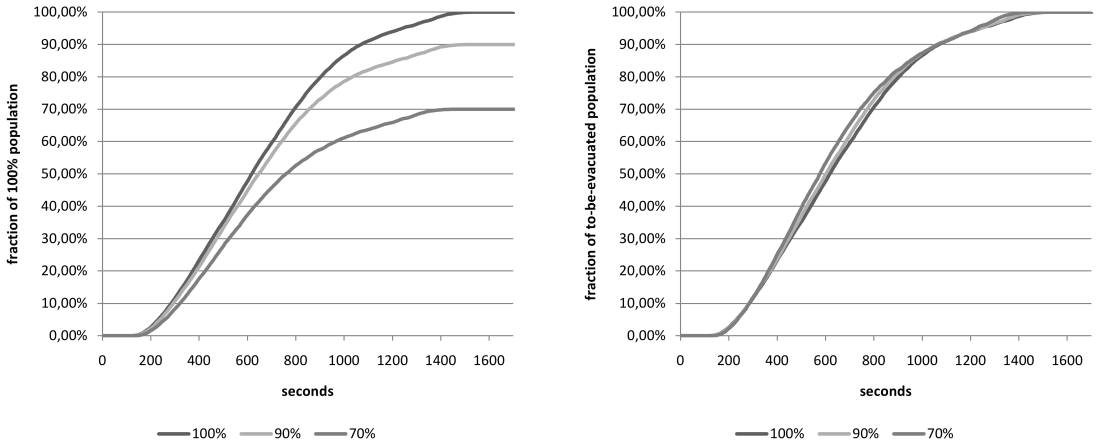

(a) 100% Population (b) To-Be-Evacuated Population

Figure 3.10: Impact of the Population Size for $(\alpha, \beta) = (3, 3)$ and $\Sigma = 0\%$

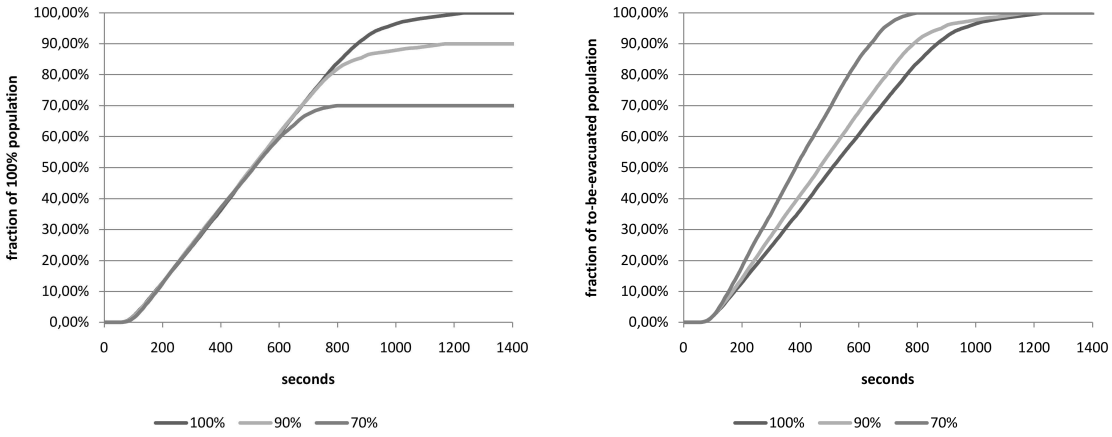

(a) 100% Population (b) To-Be-Evacuated Population

Figure 3.11: Impact of the Population Size for $(\alpha, \beta) = (3, 1)$ and $\Sigma = 0\%$

starts ($\Sigma = 0\%$). This, of course, is not very realistic, but we can easily take an initial occupation of the streets into account. Figure 3.12 provides some insights into the impact of traffic already on the streets when the evacuation begins.
For $\Sigma = 15\%$ we have 462 additional vehicles and for $\Sigma = 40\%$ we have 1294 additional vehicles to evacuate (these numbers depend on the available capacities on the lane segments and due to rounding we get $1294 \neq 462 \cdot (40/15)$). We observe no differences in total evacuation time. The reason is that due to some delayed departure of the residents ($(\alpha, \beta) = 3, 3$)) the time shortly after start of the evacuation is mainly used to clear the streets from the initial traffic.
To investigate this further, we used a departure pattern $(\alpha, \beta) = (3, 1)$ as well. Figure 3.13 shows the outcome of our tests. Now, small differences are existent leading to a slightly increased evacuation time (+2 minutes) in the case of a large initial traffic load compared to no initial traffic. However, the initial traffic again uses mostly the time short after the evacuation start to escape.

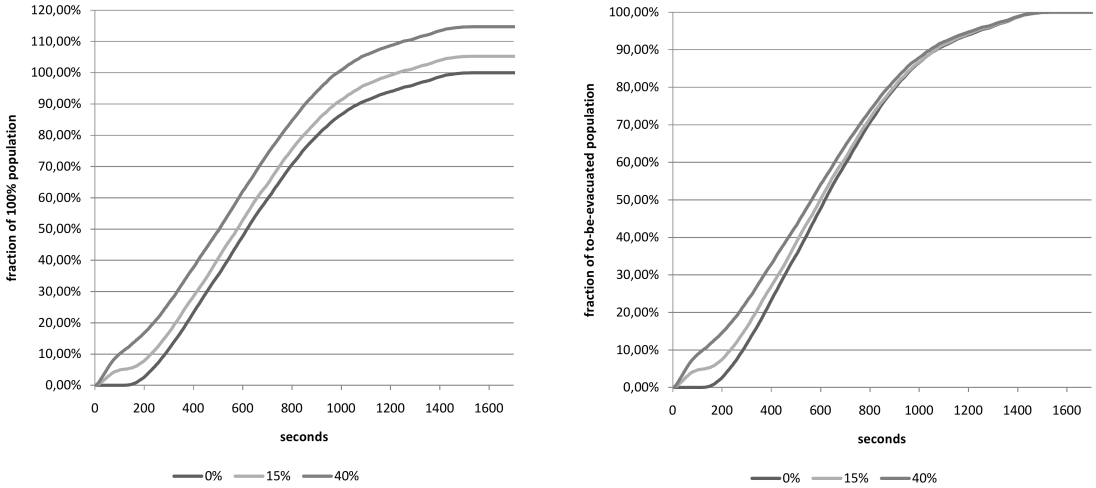

(a) 100% Population (b) To-Be-Evacuated Population

Figure 3.12: Impact of the Initial Street Occupation for $(\alpha, \beta) = (3, 3)$ and $\Pi = 100\%$

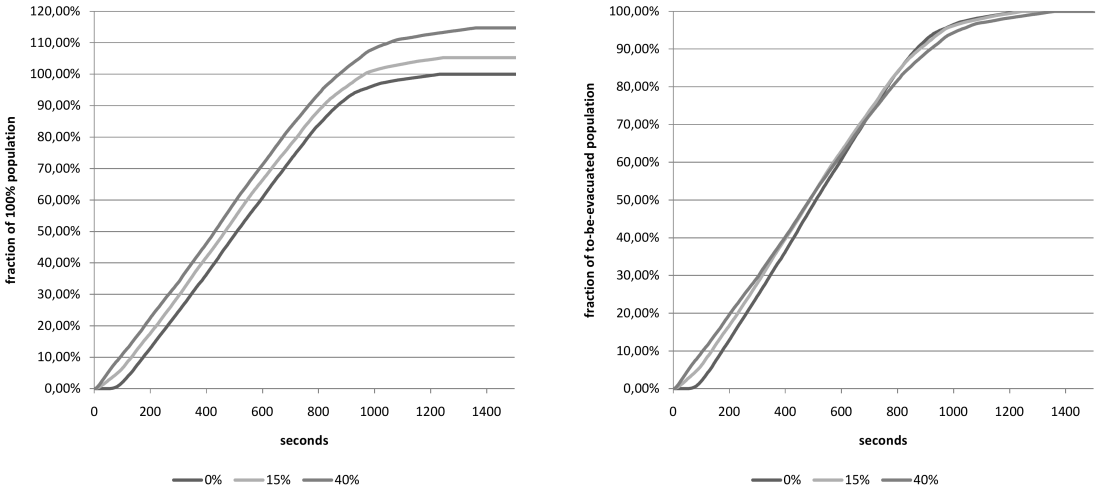

(a) 100% Population (b) To-Be-Evacuated Population

Figure 3.13: Impact of the Initial Street Occupation for $(\alpha, \beta) = (3, 1)$ and $\Pi = 100\%$

Chapter 4

Extended Cell-Transmission-Based Evacuation Planning Model

This chapter addresses four major weaknesses of the CTEPM, namely (i) the usage of a fixed single cell size, (ii) missing consideration of lanes, (iii) missing limitations for traffic flows and (iv) possible traffic flow redirections during the evacuation and shows how to overcome them. Stimulated by this, we formulate the extended Cell-Transmission-Based Evacuation Planning Model (ExCTEPM) and a new optimization model to facilitate this model in terms of choosing the optimum cell size. Additionally, we will present an iterative simulation-based optimization approach in order to evaluate and to enhance results in a more realistic environment. This approach takes advantage of a standalone vehicle reallocation optimization model, additional traffic flow limitations as well as the microscopic traffic simulation known from Chapter 3. A heuristic postprocessing approach to ensure usability of computed solutions in the traffic simulation will be presented as well. We will demonstrate the effectiveness of this approach in a real-world example. The content of this chapter can also be found in Kimms and Maassen (2009).

4.1 Extending the CTEPM

The CTEPM has some major weaknesses. On the one hand, the use of cells with a fixed single size may lead to several disadvantages in terms of an unnecessary high number of (relatively small) cells to meet a predetermined accuracy level in network representation and to excessive amounts of constraints and variables in the optimization model caused by the very high number of required cells, respectively. On the other hand, missing consideration of lanes, limitations for merging and diverging traffic flows as well as traffic flow redirections during the planning horizon may result in solutions that may be optimal regarding the optimization model, but may also be inappropriate or even infeasible in real-world applications. We will discuss these issues in detail in Section 4.1.2. In the following text we will first show how to implement multiple cell sizes into the model and demonstrate the benefits of this approach. Subsequently, explicit consideration of lanes as well as traffic flow limitations will be discussed and implemented to formulate the ExCTEPM.

4.1.1 Multiple Cell Sizes

In order to represent a given network with the CTEPM, it is necessary to choose a cell size which matches the length of the network arcs adequately. As can easily imagined, this will lead to a tradeoff between the number of cells (which immensely affects the number

of side constraints and variables) and the accuracy of the network representation. In this chapter, we will extend the CTEPM by the usage of multiple cell sizes whereas larger cell sizes will be integer multiples of the reference (standard) cell size due to the discrete nature of the Cell-Transmission approach.

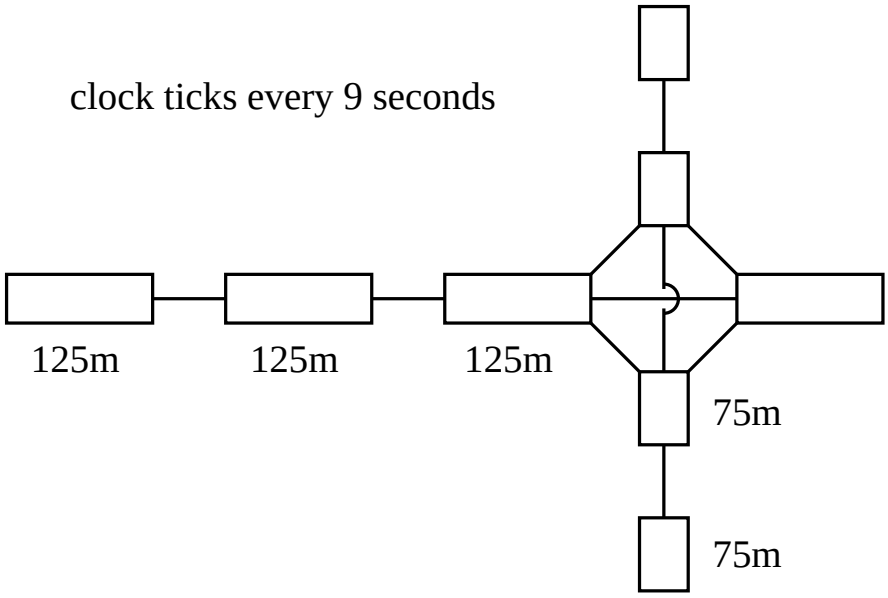

Figure 4.1: Network Representation Using One Cell Size

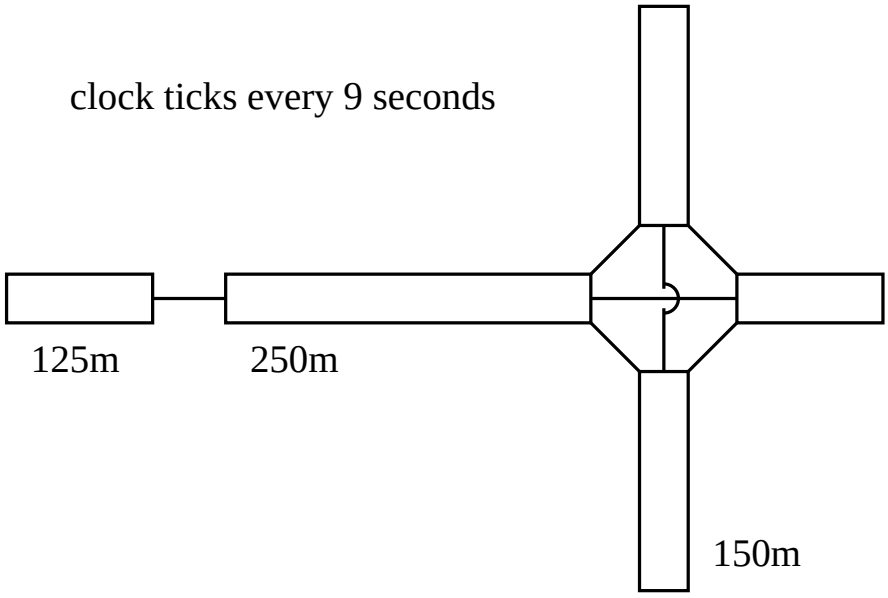

Figure 4.2: Network Representation Using Two Cell Sizes

Figures 4.1 and 4.2 illustrate this idea in the case of a very small network. There, we model four street sections at 50 km/h and 30 km/h driving speed, respectively. As can be seen easily, the number of required cells can be lowered from eight to five cells. In this example, vehicles need two periods to pass large cells, of course.

In the mathematical formulation, we assume to use $|N|$ different cell sizes, where a certain cell size n is n-times larger than cell size *1*. For example, $|N| = 3$ leads to three different cell sizes (and three set of cells, namely I_1, I_2, I_3), where all cells $i \in I_2$ (I_3) will be two-times (three-times) larger than cells $i \in I_1$, if the same driving speed is assumed. As can be seen in Figure 4.1 and 4.2 several cells can be combined to a larger cell without any loss in network representation accuracy.
This approach results in the following advantages: firstly, the accuracy of the network representation using the same number of cells can be improved since a smaller standard cell size (and integer multiples of this cell size) tends to match the underlying arc lengths more accurate, if the same number of cells is used as before. Moreover, the same accuracy in network representation can be achieved with less cells since standard sized cells can be merged into one larger cell. Secondly, the computational effort can be reduced due to a usually smaller number of required cells. Admittedly, the mathematical formulation of the (extended) CTEPM will get more complex, but the advantages of the reduced number of cells still prevail as can be seen later in this section and in Section 4.1.5.
We will first recapitulate the CTEPM as written in Section 3.2. Afterwards, we will introduce two different approaches to capture multiple cell sizes in the CTEPM.

Parameters:

$T = \{1, \dots, \|T\|\}$	index set of periods (where $\|T\|$ is the index of the last period of the planning horizon)
$N = \{1, \dots, \|N\|\}$	index set of different cell size multipliers (where $\|N\|$ denotes the maximum cell size)
$I = \{1, \dots, \|I\|\}$	index set of cells
I_n	index set of cells of cell size n ($\bigcup_{n \in N} I_n = I$)
$\|I\|$	index of super sink
I_S	index set of sink cells ($I_S = \{i \in I : \beta_{i,\|I\|} = 1\}$)
c_{it}	danger of being at cell i in period t ($c_{it} \geq 0$)
β_{ij}	$= \beta_{ji} = 1$, if a traffic flow from cell i to cell j (and vice versa) can be established (0, otherwise)
N_{it}	maximum vehicle capacity of cell i (on all lanes) in period t
E_i	number of vehicles starting their evacuation in cell i (derived from population in cell i)
Q_{it}	maximum number of in- and outflowing vehicles (on all lanes) per period into / from cell i in period t
x_{i1}	number of vehicles en route at cell i at the end of period 1, i.e. before the evacuation starts

Decision Variables:

z_{it}	number of vehicles residing, leaving or waiting in cell i in period t
x_{it}	number of residing vehicles at cell i at the end of period t
y_{ijt}	number of vehicles leaving section i in period t and reaching section j in period $t + 1$
b_{it}	number of vehicles starting their evacuation at cell i in period t

Given this notation, the CTEPM can be formulated as follows:

$$\min \sum_{i \in I} \sum_{t \in T} z_{it} \cdot c_{it} \tag{4.1}$$

subject to

$$z_{it} = x_{it} + \sum_{j \in I} y_{ijt} + (E_i - \sum_{\tau=1}^{t} b_{i\tau}) \qquad i \in I\,;\ t \in T \tag{4.2}$$

$$x_{it} = b_{it} + x_{i,t-1} + \sum_{j \in I} y_{ji,t-1} - \sum_{j \in I} y_{ijt} \qquad i \in I\,;\ t = 2, \ldots, |T| \tag{4.3}$$

$$z_{it} \leq N_{it} + (E_i - \sum_{\tau=1}^{t} b_{i\tau}) \qquad i \in I\,;\ t \in T \tag{4.4}$$

$$x_{it} \leq N_{it} \qquad i \in I\,;\ t \in T \tag{4.5}$$

$$\sum_{t \in T} b_{it} = E_i \qquad i \in I \tag{4.6}$$

$$x_{|I|,|T|} = \sum_{i \in I} (E_i + x_{i1}) \tag{4.7}$$

$$\sum_{i \in I} y_{ijt} \leq (N_{jt} - x_{jt}) \qquad j \in I\,;\ t \in T \tag{4.8}$$

$$\sum_{i \in I} y_{ijt} \leq Q_{jt} \qquad j \in I\,;\ t \in T \tag{4.9}$$

$$\sum_{j \in I} y_{ijt} \leq Q_{it} \qquad i \in I\,;\ t \in T \tag{4.10}$$

$$y_{ijt} \leq N_{it} \cdot \beta_{ij} \qquad i,j \in I\,;\ t \in T \tag{4.11}$$

$$z_{it}, x_{it}, b_{it} \geq 0 \qquad i \in I\,;\ t \in T \tag{4.12}$$

$$y_{ijt} \geq 0 \qquad i,j \in I\,;\ t \in T \tag{4.13}$$

$$x_{i1} = 0 \qquad i \in I \tag{4.14}$$

$$b_{i1} = 0 \qquad i \in I \tag{4.15}$$

$$y_{ij1} = 0 \qquad i \in I\,;\ j \in I \tag{4.16}$$

The objective function (4.1) minimizes total danger for all vehicles during the complete planning horizon. Here, the parameter c_{it} might be related to some key figures, e.g. the probability that an area will be reached by a tsunami wave or the concentration of hazardous material at a certain point of the planning horizon, see Chakraborty and Armstrong (1995) and Zhang et al. (2000). The case of $c_{it} = c_i \cdot t$ may be used for scenarios with no movement of danger during the planning horizon, e.g. a preventive evacuation. However, using general values for c_{it} is more flexible since it allows to capture movement of danger during in the planning horizon, e.g. movement of a hazardous plume over time. The calculation of all vehicles residing, leaving or waiting in cell i is done in equation (4.2). Vehicle-flow-constraints have to be defined with respect to the cell size n. For $n = 1$, the standard vehicle flow constraint from the single cell size CTEPM can be adopted (see (4.3)), whereas the number of residing vehicles at the end of period t equals the number of vehicles starting their evacuation in period t plus the number of residing vehicles in cell i at the end of period *t-1* plus the number of inflowing vehicles reaching cell i in period t minus the number of outflowing vehicles leaving cell i till the end of period t, respectively. This vehicle flow equation also allows vehicle holding, if this would

be beneficial with regards to the objective value. Moreover, (4.4) ensures that the number of vehicles (incl. all vehicles that have not left their homes, yet) in a cell i during a period t does not exceed the maximum capacity of this cell plus the number of vehicles which have not entered the network so far. Similar to (4.4), constraint (4.5) forces the number of vehicles in cell i at the end of period t to be lower than the maximum capacity of this cell. (4.6) determines the departure schedule for each cell and that all residents will leave their homes. Furthermore, equation (4.7) assures that each vehicle (residents in vehicles in terms of E_i and initial traffic (e.g. due to rush hour traffic) in terms of x_{i1}) will be evacuated. Here, it is important that $|T|$ is sufficiently large so that all vehicles can escape within the planning horizon. In (4.8), the maximum number of cell-changing vehicles is limited to the remaining capacity (=maximum vehicle capacity minus the number of vehicles at the end of a period) of the corresponding cells. As stated in (4.9) and (4.10) the maximum number of in- and outflowing vehicles additionally must be limited by the in- and outflow capabilities of a cell. In the following, we assume that flow capacities are constant over time so that using Q_i (instead of Q_{it}) is sufficient. Furthermore, traffic flows can stream from a cell i to cell j, if and only if, a physical connection between these cells exist, i.e. these cells are adjacent – see (4.11). (4.12) and (4.13) finally determine the domains of the decision variables. Please note that it is sufficient to consider only those flow variables y_{ijt} where $\beta_{ij} = 1$ holds. In order to assure that no vehicle movements occur in the first period – where the evacuation has not started yet –, boundary conditions (4.14)–(4.16) fix the decision variables x_{it}, b_{it} and y_{ijt} to zero in the first period. However, if initial traffic is existent, (4.14) has to be specified for all affected cells.

Although z_{it}, x_{it}, b_{it} and y_{ijt} can be defined to take only integer values, we decided to relax integrality. Firstly, this relaxation helps to reduce computational effort due to less integer variables. Secondly, in all computational tests throughout this chapter – all parameters of the ExCTEPM are set to integer values – all variables which will be used in the succeeding simulation runs take only integer values automatically, so that there was no need to restore integrality constraints of the decision variables. In detail, three variables are passed to the simulation, see Chapter 3. First, let η_{ij} denote the total number of vehicles traveling from cell i to cell j during the complete planning horizon, i.e. $\eta_{ij} = \sum_{t \in T} y_{ijt}$. Secondly, the driving direction is expressed by φ_{ij} ($\varphi_{ij} \in \{0, 1\}$) indicating if a connection from cell i to cell j is used ($\varphi_{ij} = 1$). Thirdly, assigned lanes between cell i and cell j are denoted by ϵ_{ij} ($\epsilon_{ij} \in \mathbb{N}_0$). The variables z_{it}, x_{it}, b_{it} from the optimization part will be ignored in the simulation. Since φ_{ij} and ϵ_{ij} are set to integer values by definition, only η_{ij} may take non-integer values. In such cases, we developed a simple postprocessing approach (see Section 4.2.2) which uses the (integer and / or non-integer) η_{ij} values from the optimized solution as a starting point to construct a slightly modified (feasible) solution only consisting of integer values for η_{ij}.

The CTEPM (and later the ExCTEPM) also optimizes departures times (in terms of b_{it}) for each cell. However, in evacuation scenarios evacuees may not attend orders, especially those affecting their own safety. Hence, departure times shall be regarded as parameters following a prespecified departure distribution. Those circumstances can be easily adopted in the ExCTEPM by adding further constraints, e.g. $b_{it}^{min} \leq b_{it} \leq b_{it}^{max}$ for all $i \in I; t \in T$ to the model formulation. Another problem may cover the fact that the capacities of exit cells (i.e. safety zones) are limited. Suchlike aspects can be implemented by adding a new constraint, e.g. $\sum_{t \in T} y_{i,|I|,t} \leq K_i$ for all $i \in I_S$ to the model formulation where K_i is the maximum capacity of the safe area behind exit cell $i \in I_S$ ($I_S = \{i \in I : \beta_{i,|I|} = 1\}$). Notwithstanding, people have to leave houses which is a problem that is covered by building evacuation literature. However, suchlike problems will not be modeled in detail in our

approach.
In order to obtain feasible solutions, $|T|$ must be chosen sufficiently large so that all evacuees have the ability to escape within the planning horizon. A lower bound for $|T|$ can be computed by $|T|_{LB} = \sum_{i \in I} E_i / \sum_{i \in I_S} Q_i$. However, for our computational tests we set $|T| = 1.5 \cdot |T|_{LB}$. However, larger values for $|T|$ will not lead to any computational issues.

4.1.1.1 Multiple Cell Sizes – Approach 1

The basic idea of this approach is to divide a cell into subcells, whereas the number of subcells corresponds to the cell size of the cell $(1, \ldots, n)$. A vehicle needs at least one period to pass a subcell so that n subcells lead to a minimum travel time of n periods. In order to capture vehicle movement from subcell to subcell, a new decision variable y^k_{iit} must be introduced. This variable is an auxiliary flow variable which displays the number of vehicles moving from subcell k to subcell $k+1$ in cell i in period t. Thus, there must be $n-1$ additional flow variables for a cell of cell size n. Now, the CTEPM with multiple cell sizes using this approach can be formulated by replacing equation (4.2) by (4.17), (4.3) by (4.18) and adding three more constraints (4.19) – (4.21):

$$z_{it} = x_{it} + \sum_{j \in I} y_{ijt} + \sum_{n \in N} y^n_{iit} + (E_i - \sum_{\tau=1}^{t} b_{i\tau}) \qquad i \in I\ ;\ t \in T \tag{4.17}$$

$$x_{it} = b_{it} + x_{i,t-1} + \sum_{j \in I} y_{ji,t-1} - \sum_{j \in I} y_{ijt} \qquad i \in I_1\ ;\ t = 2, \ldots, |T| \tag{4.18}$$

$$\begin{aligned} x_{it} &= b_{it} + x_{i,t-1} + \sum_{j \in I} y_{ji,t-1} \\ &- \sum_{k=1}^{n-1} y^k_{iit} + \sum_{k=1}^{n-1} y^k_{ii,t-1} - \sum_{j \in I} y_{ijt} \end{aligned} \qquad \begin{aligned} &n \in N : n \geq 2\ ;\ i \in I_n\ ; \\ &t = 2, \ldots, |T| \end{aligned} \tag{4.19}$$

$$y^k_{ii,t-1} = y^{k+1}_{iit} \qquad \begin{aligned} &n \in N : n \geq 3\ ;\ k = 1, \ldots, n-2\ ; \\ &i \in I_n\ ;\ t = 2, \ldots, |T| \end{aligned} \tag{4.20}$$

$$y^{n-1}_{ii,t-1} = \sum_{j \in I} y_{ijt} \qquad \begin{aligned} &n \in N : n \geq 2\ ;\ i \in I_n\ ; \\ &t = 2, \ldots, |T| \end{aligned} \tag{4.21}$$

$$y^n_{iit} \geq 0 \qquad n \in N\ ;\ i \in I\ ;\ t \in T \tag{4.22}$$

Equation (4.2) must by replaced by (4.17) in order to cover the vehicle movements from subcell to subcell in the objective value. The standard vehicle flow equation (4.3) now only holds for cells of size 1, see (4.18). For larger cells, an extended vehicle flow equation (4.19) must be introduced. Vehicle flows from subcell to subcell are captured by (4.20) and (4.21). However, this approach has some disadvantages in terms of traffic flow representation. First, traffic holding is only possible in the first subcell, because of (4.20) and (4.21) forcing traffic to flow from one subcell to the next subcell in successive periods. Secondly, all evacuees starting their evacuation in a cell of cell size $|N| \geq 2$ also have to pass all subcells before they can leave the cell.

4.1.1.2 Multiple Cell Sizes – Approach 2

The concept of the second approach to capture multiple cell sizes is to limit traffic outflow with respect to traffic inflow of a cell so that a minimum travel time of n periods for a cell of size n can be ensured. Because of (4.3), this assumption automatically holds for cells with size 1. For cells of size $n \geq 2$, we introduce constraint (4.23) to ensure a minimum travel time of n_i periods for a cell i of size n_i. The CTEPM with multiple cell sizes using the seconds approach can be formulated by adding the following constraint to the model formulation (4.1)–(4.16):

$$\sum_{j \in I} \sum_{\tau=1}^{t} y_{ij\tau} \leq \sum_{j \in I} \sum_{\tau=1}^{\max(t-n_i,1)} y_{ji\tau} + \sum_{\tau=1}^{\max(t-\lceil n_i/2 \rceil+1,1)} b_{i\tau} + x_{i1} \quad i \in I : n_i \geq 2 \; ; \; t = 2, \ldots, |T| \tag{4.23}$$

This constraint limits the cumulated number of vehicles leaving a cell i between period 1 and period t to the cumulated number of vehicles entering the cell between period 1 and period $t - n_i$ plus the vehicles starting their evacuation between period 1 and period $t - \lceil n_i/2 \rceil + 1$ plus the initial street occupation in terms of x_{i1}, where n_i is the size of cell i. This approach has several advantages compared to the first approach. First, no new variables have to be introduced and less constraints are needed when cells of size $|N| \geq 3$ are used. Secondly, waiting vehicles can escape from a cell immediately after the minimum travel time has passed. Thirdly, evacuees start their evacuation in the "center" of a cell if the term $t - \lceil n_i/2 \rceil + 1$ is used. However, this approach allows to modify the "starting point" as desired by the decision maker.

4.1.1.3 Impact of Multiple Cell Sizes on Problem Size

To illustrate the effectiveness of both approaches, we calculate the optimum number of cells for $|N| \in \{1, 2, 3, 4, 5, 10\}$ in the case of three randomly generated networks of different size applying the cell size optimization model (4.37)–(4.47) that will be described in detail in Section 4.1.4. On the basis of this number we also compute the number of constraints and variables that would emerge in model (4.1)–(4.11) plus the corresponding additional constraints to cover multiple cell sizes. The networks consist of 50, 100 and 150 street sections representing a total network length of 15.852m, 30.978m and 47.691m, respectively. In addition, we assume 70% (30%) of the street sections allow a driving speed of 50 km/h (30 km/h) and that the length of 50 km/h (30 km/h) sections can take all integer values within the interval [100m, 700m] ([50m, 200m]). Furthermore, we force the absolute deviation between the street sections lengths and the lengths of the corresponding cells to be lower than 15% of the street sections length.
In the following, the number of constraints as well as the number of variables are calculated assuming a planning horizon of 600 seconds. The results for the first approach are shown in Tables 4.1 – 4.3 and for the second approach in Tables 4.4 – 4.6. Bracketed percentages display the relative reduction in comparison to the application of only one cell size ($|N| = 1$), which equates the (standard) CTEPM defined before.

Two major findings can be derived from these tables: firstly, massive improvements in terms of problem size reduction can be achieved, whereas the additional benefit decreases with increasing values for $|N|$. Secondly, relative benefit is almost the same for all networks and cell sizes $|N|$. Thirdly, relative reduction in problem size is much larger than the relative reduction of cells in all cases.

#Cell Sizes	#Cells	Period Length	#Constraints	#Variables
$\|N\| = 1$	283	4.0 sec.	12,310,501	12,140,700
$\|N\| = 2$	153 (-45.9%)	4.0 sec.	3,692,861 (-70.0%)	3,601,200 (-70.3%)
$\|N\| = 3$	107 (-62.2%)	4.0 sec.	1,857,117 (-84.9%)	1,793,100 (-85.2%)
$\|N\| = 4$	94 (-66.8%)	4.0 sec.	1,454,348 (-88.2%)	1,398,150 (-88.5%)
$\|N\| = 5$	76 (-73.1%)	4.0 sec.	978,683 (-92.1%)	933,300 (-92.3%)
$\|N\| = 10$	53 (-81.3%)	4.0 sec.	513,208 (-95.8%)	481,650 (-96.0%)

Table 4.1: Size of Model Formulation (4.1), (4.4) – (4.11), (4.17) – (4.21) for a 50-Street-Network

#Cell Sizes	#Cells	Period Length	#Constraints	#Variables
$\|N\| = 1$	798	2.7 sec.	143,252,971	142,541,154
$\|N\| = 2$	425 (-46.7%)	2.7 sec.	41,032,045 (-71.4%)	40,653,346 (-71.5%)
$\|N\| = 3$	292 (-63.4%)	2.7 sec.	19,590,453 (-86.3%)	19,330,532 (-86.4%)
$\|N\| = 4$	233 (-70.8%)	2.7 sec.	12,607,357 (-91.2%)	12,400,138 (-91.3%)
$\|N\| = 5$	197 (-75.3%)	2.7 sec.	9,109,333 (-93.6%)	8,934,272 (-93.7%)
$\|N\| = 10$	131 (-83.6%)	2.7 sec.	4,198,561 (-97.1%)	4,082,461 (-97.1%)

Table 4.2: Size of Model Formulation (4.1), (4.4) – (4.11), (4.17) – (4.21) for a 100-Street-Network

#Cell Sizes	#Cells	Period Length	#Constraints	#Variables
$\|N\| = 1$	1,432	2.3 sec.	537,829,129	536,334,120
$\|N\| = 2$	758 (-47.1%)	2.3 sec.	151,537,691 (-71.8%)	150,747,075 (-71.9%)
$\|N\| = 3$	528 (-63.1%)	2.3 sec.	73,985,981 (-86.2%)	73,435,743 (-86.3%)
$\|N\| = 4$	416 (-70.9%)	2.3 sec.	46,223,009 (-91.4%)	45,789,840 (-91.5%)
$\|N\| = 5$	345 (-75.9%)	2.3 sec.	32,015,121 (-94.0%)	31,656,168 (-94.1%)
$\|N\| = 10$	204 (-85.8%)	2.3 sec.	11,596,405 (-97.8%)	11,384,820 (-97.9%)

Table 4.3: Size of Model Formulation (4.1), (4.4) – (4.11), (4.17) – (4.21) for a 150-Street-Network

#Cell Sizes	#Cells	Period Length	#Constraints	#Variables
$\|N\| = 1$	283	4.0 sec.	12,310,501	12,140,700
$\|N\| = 2$	153 (-45.9%)	4.0 sec.	3,692,861 (-70.0%)	3,580,200 (-70.5%)
$\|N\| = 3$	107 (-62.2%)	4.0 sec.	1,845,495 (-85.0%)	1,765,500 (-85.5%)
$\|N\| = 4$	94 (-66.8%)	4.0 sec.	1,437,362 (-88.3%)	1,367,700 (-88.7%)
$\|N\| = 5$	76 (-73.1%)	4.0 sec.	957,227 (-92.2%)	900,600 (-92.6%)
$\|N\| = 10$	53 (-81.3%)	4.0 sec.	484,898(-96.1%)	445,200 (-96.3%)

Table 4.4: Size of Model Formulation (4.1) – (4.11), (4.23) for a 50-Street-Network

#Cell Sizes	#Cells	Period Length	#Constraints	#Variables
$\|N\| = 1$	798	2.7 sec.	143,252,971	142,541,154
$\|N\| = 2$	425 (-46.7%)	2.7 sec.	41,032,045 (-71.4%)	40,563,700 (-71.5%)
$\|N\| = 3$	292 (-63.4%)	2.7 sec.	19,533,177 (-86.4%)	19,209,220 (-86.5%)
$\|N\| = 4$	233 (-70.8%)	2.7 sec.	12,521,443 (-91.3%)	12,262,324 (-91.4%)
$\|N\| = 5$	197 (-75.3%)	2.7 sec.	9,005,215 (-93.7%)	8,786,200 (-93.8%)
$\|N\| = 10$	131 (-83.6%)	2.7 sec.	4,060,477 (-97.2%)	3,914,542 (-97.3%)

Table 4.5: Size of Model Formulation (4.1) – (4.11), (4.23) for a 100-Street-Network

#Cell Sizes	#Cells	Period Length	#Constraints	#Variables
$\|N\| = 1$	1,432	2.3 sec.	537,829,129	536,334,120
$\|N\| = 2$	758 (-47.1%)	2.3 sec.	151,537,691 (-71.8%)	150,554,718 (-71.9%)
$\|N\| = 3$	528 (-63.1%)	2.3 sec.	73,862,481 (-86.3%)	73,176,048 (-86.4%)
$\|N\| = 4$	416 (-70.9%)	2.3 sec.	46,035,549 (-91.4%)	45,493,344 (-91.5%)
$\|N\| = 5$	345 (-75.9%)	2.3 sec.	31,784,241 (-94.1%)	31,335,660 (-94.2%)
$\|N\| = 10$	204 (-85.8%)	2.3 sec.	11,287,525 (-97.9%)	11,021,508 (-97.9%)

Table 4.6: Size of Model Formulation (4.1) – (4.11), (4.23) for a 150-Street-Network

The results for the second approach shows great similarity to the first one. However, for $|N| \geq 3$ the number of constraints and variables is always lower.

4.1.2 Consideration of Lanes and Limiting Traffic Flows

Another major weakness of the CTEPM is related to the lack of explicit consideration of lanes. In its standard form, flow capacity of a cell is determined by the flow capacity per lane multiplied by the number of lanes. This might lead to problems, see Figure 4.3.

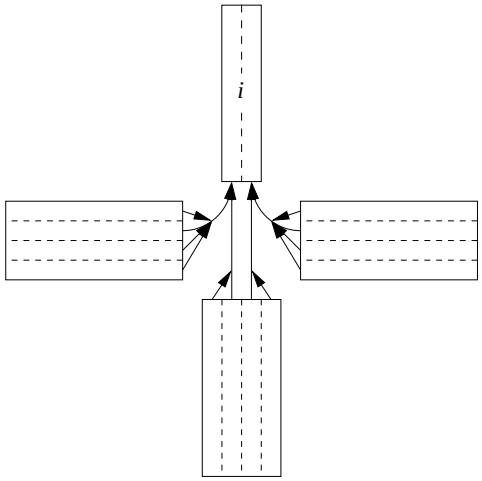

Figure 4.3: Consideration of Lanes and Traffic Flow Limitations - Example

Imagine that the total vehicle flow capacity (using all lanes) for cell i (see Figure 4.3) will be 16 vehicles per period. The CTEPM without explicit consideration of lanes allows that the total vehicle flow capacity per period can be divided into fractions, e.g. 6, 5 and 5 vehicles per period (6+5+5 = 16). When lanes are explicitly considered in the model,

vehicle flow capacity per lane would be 16 / 2 = 8 vehicles per period per lane for cell i. Thus, vehicle flows of 6,5 and 5 vehicles per period result in 6/8 = 0.75, 5/8 = 0.625 and 0.625 lanes which will of course not be viable in real world problems. Therefore it is important to express the vehicle flow capacity per period of a cell i as integer multiples of the vehicle flow capacity per lane.
Another important aspect of safe traffic routing covers the limitation of traffic flows. Traffic flow limitation contains two essential aspects, namely merging / diverging of traffic flows as well as time-dependent traffic flow redirection. The CTEPM has no such limitations whereby solutions may be obtained where traffic flows merge and diverge very often or even will be repeatedly redirected over time. As an illustrative example, imagine a four-way junction with three four-lane streets and one two-lane street as the only available exit, see Figure 4.3. If a total of 12 lanes (4 lanes from each different direction) will be merged into two lanes at a junction, merging processes have to take place at the junction. Of course, this would result in a traffic chaos. However, such solutions may be optimal in a given optimization model if no corresponding constrains exist, but not in real world applications. In detail, we limit traffic routing due to three major reasons: firstly, it is not advantageous to allow an unlimited number of cells to be merged into just one cell (e.g. directly in front of a sink cell as mentioned above). Secondly, conflicting traffic flows in general as well as crossing traffic flows at junctions often exists due to multi-diverging traffic flows and thirdly, the organization of an evacuation (e.g. positioning safety fences for traffic flow routing) will be much simpler, if traffic flows are merged and diverged only when necessary and if traffic flows are not redirected over time, respectively. Such limitations will be implemented in the CTEPM in the following section.

4.1.3 ExCTEPM Model Formulation

Further parameters and variables are needed to consider lanes and restrict traffic flows:

Additional Parameters:

- l_i number of lanes in cell i
- p maximum number of outflowing traffic streams

Additional Decision Variables:

- φ_{ij} = 1, if traffic flows from cell i to cell j, 0 otherwise
- ϵ_{ij} number of used lanes between cell i and cell j

Given this notation the ExCTEPM with multiple cell sizes on the basis of Approach 2 can be formulated in the following manner:

$$\min \sum_{i \in I} \sum_{t \in T} z_{it} \cdot c_{it} \tag{4.24}$$

subject to (4.2) – (4.8), (4.11) – (4.16), (4.23) and

$$y_{ijt} \leq \frac{Q_{jt}}{l_j} \cdot \epsilon_{ij} \qquad i,j \in I \ ; \ t \in T \tag{4.25}$$

$$y_{ijt} \leq \frac{Q_{it}}{l_i} \cdot \epsilon_{ij} \qquad i,j \in I \ ; \ t \in T \tag{4.26}$$

$$\sum_{i \in I} \varphi_{ij} \leq l_j \qquad j \in I \tag{4.27}$$

$$\sum_{j \in I} \varphi_{ij} \leq p \qquad i \in I \tag{4.28}$$

$$\varphi_{ij} + \varphi_{jk} \leq 1 \qquad i,j,k \in I \ : \beta_{ij} = 1 \ ; \beta_{ik} = 1 \tag{4.29}$$

$$\varphi_{ij} \leq \beta_{ij} \qquad i,j \in I \tag{4.30}$$

$$\epsilon_{ij} \leq \varphi_{ij} \cdot \min\{l_i, l_j\} \qquad i,j \in I \tag{4.31}$$

$$\sum_{i \in I} \epsilon_{ij} \leq l_j \qquad j \in I \tag{4.32}$$

$$\sum_{j \in I} \epsilon_{ij} \leq l_i \qquad i \in I \tag{4.33}$$

$$\epsilon_{ij} \in \mathbb{N}_0 \qquad i,j \in I \tag{4.34}$$

$$\varphi_{ij} \in \{0, 1\} \qquad i,j \in I \tag{4.35}$$

Due to the consideration of lanes in the ExCTEPM, constraints (4.9) and (4.10) are replaced by (4.25) and (4.26). These constraints limit the number of cell-changing vehicles to the vehicle flow capabilities of the corresponding cells under consideration of allocated lanes. Furthermore, the constraints (4.27)–(4.29) limit the traffic routing in multiple ways. (4.27) ensures that the number of traffic flows streaming into cell j is not exceeding the number of available lanes in cell j. Hence merging processes at junctions due to traffic flows from different directions are not allowed any more. Constraint (4.28) bounds the number of outgoing traffic streams from cell i to a fixed value p. A discussion of possible values for p can be found in Section 4.3.2.

So far, the ExCTEPM may deliver solutions that are not feasible in real world applications, but in the optimization model as can be illustrated in a little example. Imagine an intersections with three entrances / exits as shown in Figure 3.5. If vehicle streams exist from cell i to cell k as well as from cell j to cell k, cell k represents a bottleneck for cell i and j. If we further assume that the cell j (or cell i) has no ingoing traffic flows, the ExCTEPM may generate a traffic stream from cell i to cell j that finally reaches cell k to circumvent the emerging bottleneck in cell k, see Figure 3.5. Such infeasibilities can be avoided by constraint (4.29) since it allows a traffic stream from cell i to cell j to cell k to be created, if and only if no direct connection between cell i and cell k exist. In addition, this constraint simplifies traffic routing by forcing every street section to be used only in one direction, except cells with no external traffic inflow. In addition, (4.30) and (4.31) assure that a traffic stream using a certain number of lanes from a cell i to a cell j only can be established, if a connection (in terms of β_{ij} and φ_{ij}, respectively) between these cells exists. Finally, constraints (4.32) and (4.33) limit the number of used lanes between a cell i and a cell j to the number of available lanes regarding both cells. Constraints (4.34) and (4.35) determine the domain of the additional decision variables. A graphical illustration of parameters and decision variables used in the extended Cell-Transmission-Based Evacuation Planning Model can be found in Figure 4.4.

These additional constraints help to guide traffic through the network in a safer and less conflictual way. However, there might exist some situations where these constraints, especially constraint (4.27) and (4.32) might result in no feasible solution if the number of lanes is relatively low and many junctions exist. As an example, imagine a t-junction with three one-lane streets whereas two of these streets are deadlocks. Now, these two (deadlock) streets have to use the (non-deadlock) street in order to be evacuated, but suchlike situations are forbidden by (4.27) and (4.32). In such cases, these constraints have to be relaxed and a new constraint $\sum_{i \in I} y_{ijt} \leq Q_{jt}$ for all cells $j \in I$ and periods $t \in T$ must be added in order to ensure that traffic flow capacities are not exceeded.

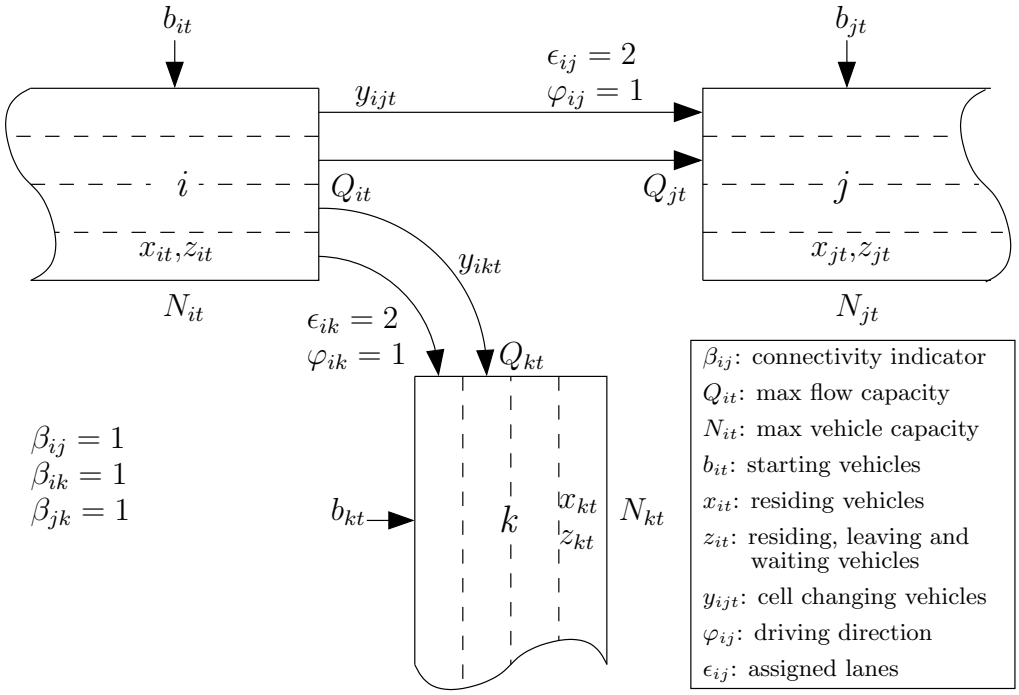

Figure 4.4: Graphical Illustration of Parameters and Decision Variables

Moreover, φ_{ij} allows the avoidance of traffic crossing and traffic touching conflicts at junctions as shown in Figure 4.5 by formulating (4.36). If a traffic stream from cell i to cell j is established (solid line), no other crossing or touching traffic stream (dashed lines) is allowed at this junction.

$$\varphi_{ij} + \varphi_{ji} + \varphi_{uv} + \varphi_{vu} \leq 1 \qquad i,j,u,v \in I \tag{4.36}$$

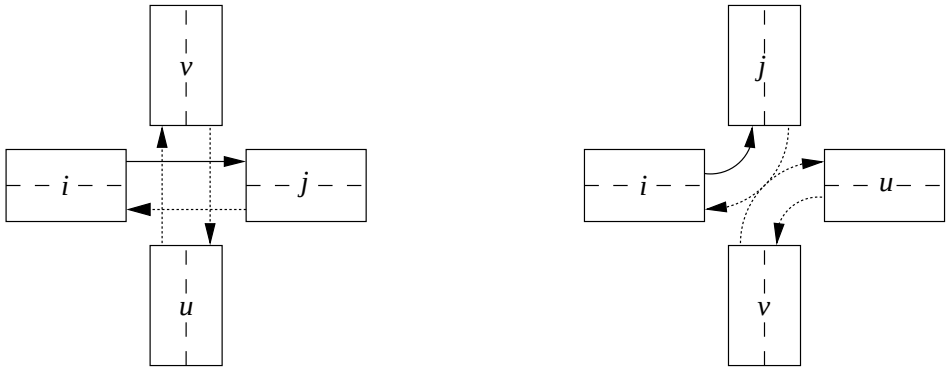

Figure 4.5: Traffic Crossing and Traffic Touching Conflicts at Junctions

Here, we assume that the cells i,j,u,v adjoin to the same junction, so that $\beta_{ij} = \beta_{iu} = \beta_{iv} = \beta_{ju} = \beta_{jv} = \beta_{uv} = 1$ holds. Please note that this constraint also holds for different values of p and for junctions with more than four entrances/exits since i, j and u, v pairs of cells always exist, independent of the number of entrances/exits of a junction.

4.1.4 Cell Size Optimization

Cell sizes have to be chosen adequately when a road network must be modeled as a cell network. In this section, we will introduce a simple optimization model which determines the optimum cell size(s) and the corresponding number of cells for a given road network. Assuming a given driving speed s, a certain cell size always corresponds to a certain cycle time (period length) with index k. Thus, a cell may represent different distances depending on the chosen cycle time k. Table 4.7 shows five examples for $s = 50$ km/h $= 13.89$ m/s and $s = 30$ km/h $= 8.33$ m/s.

k cycle time		1 1.8 sec.	2 3.6 sec.	3 7.2 sec.	4 10.8 sec.	5 14.4 sec.
cell size	$s = 50$ km/h	25m	50m	100m	150m	200m
cell size	$s = 30$ km/h	15m	30m	60m	90m	120m

Table 4.7: Relation between Cell Size and Cycle Time ($|N| = 1$)

As can be easily derived from Table 4.7, smaller cycle times are leading to smaller cell sizes, which enable us to represent a given network very accurate, by trend, but usually a larger number of (small) cells is required due to the lower cell size.
If we are using multiple cell sizes as explained in Section 4.1.1, every cycle time k corresponds to $|N|$ different cell sizes for a given driving speed s. Moreover, we assume every cell size of a given cycle time k to be a corresponding "version" l of this certain cycle time k with a length of g_{kl} so that, for example, a cycle time k leads to (for $|N| = 3$ and two different driving speeds) six versions with a length of $(g_{k1}, g_{k2}, g_{k3}, g_{k4}, g_{k5}, g_{k6})$. This notation has to be interpreted in the following manner:

$$\Big(\overbrace{\underbrace{g_{k1}}_{\text{single size}}, \underbrace{g_{k2}}_{\text{double size}}, \underbrace{g_{k3}}_{\text{triple size}}}^{\text{Cells at 50 km/h driving speed}}, \overbrace{\underbrace{g_{k4}}_{\text{single size}}, \underbrace{g_{k5}}_{\text{double size}}, \underbrace{g_{k6}}_{\text{triple size}}}^{\text{Cells at 30 km/h driving speed}}\Big)$$

Due to the discrete nature of the ExCTEPM, the assumption that vehicles drive at 50 km/h and 30 km/h and taking g_{k1} (single cell size, 50 km/h driving speed) as a point of reference, the following relations between these six versions exist:

$$\begin{aligned} g_{k2} &= 2 \cdot g_{k1} \\ g_{k3} &= 3 \cdot g_{k1} \\ g_{k4} &= 0.6 \cdot g_{k1} \\ g_{k5} &= 0.6 \cdot g_{k2} = 1.2 \cdot g_{k1} \\ g_{k6} &= 0.6 \cdot g_{k3} = 1.8 \cdot g_{k1} \end{aligned}$$

Given these considerations, Table 4.7 can be complemented as shown in Table 4.8.
It is now clear that the optimization of cell sizes is equivalent to the selection of the optimum cycle time, whereas conflicting objectives must be handled: on the one hand, cell sizes of a cycle time k should be as small as necessary to match the corresponding arc length perfectly, but on the other hand, cell sizes of this cycle time k should be as big as possible so that only few cells are needed and that the number of variables and constraints in the CTEPM and ExCTEPM model formulation can be kept low. In order to represent a given network adequately, it is useful to determine a certain level of accuracy, i.e. for example the maximum deviation between the length of a street section and the cumulated

k cycle time		1 1.8 sec.	2 3.6 sec.	3 7.2 sec.	4 10.8 sec.	5 14.4 sec.	l
cell size (I_1)	$s = 50$ km/h	25m	50m	100m	150m	200m	1
cell size (I_2)	$s = 50$ km/h	50m	100m	200m	300m	400m	2
cell size (I_3)	$s = 50$ km/h	75m	150m	300m	450m	600m	3
cell size (I_1)	$s = 30$ km/h	15m	30m	60m	90m	120m	4
cell size (I_2)	$s = 30$ km/h	30m	60m	120m	180m	240m	5
cell size (I_3)	$s = 30$ km/h	45m	90m	180m	270m	360m	6

Table 4.8: Relation between Cell Size and Cycle Time ($|N| = 3$)

length(s) of cell(s) assigned to this street section. Hence, the following MIP model selects the optimum cycle time in order to minimize the number of cells which are required to represent the network under consideration of the predetermined level of accuracy.
Please note that the standard CTEPM is a special case of the ExCTEPM, if traffic flow limitations are not considered. As such, the presented model can be used for the CTEPM as well. We use the following notation for the optimization model:

Parameters:

$K = \{1, \ldots, \lvert K \rvert\}$	Index set of cycle times
$S = \{1, \ldots, \lvert S \rvert\}$	Index set of driving speeds
J_s	Index set of street sections at driving speed s
$J = \bigcup_{s \in S} J_s$	Index set of street sections
P_s	Index set of available versions which can be used at street sections at driving speed s
$P = \bigcup_{s \in S} P_s$	Index set of available versions
g_{kl}	length [m] of version l of cycle time k
d_j	length [m] of street section j
o_j	maximum relative deviation between the length of street section j and the (cumulated) length(s) of the corresponding cells
C	maximum number of cells

Decision Variables:

β_{kjl}	number of used cells of version l and cell type k at street section j
γ_k	$= 1$, if cell type (cycle time) k is used, 0 otherwise
Z_j	difference [m] between the length of street section j and the intended cell(s)

$$\min \sum_{k \in K} \sum_{j \in J} \sum_{l \in P} \beta_{kjl} \tag{4.37}$$

subject to

$$\sum_{j \in J} \sum_{l \in P} \beta_{kjl} \leq \gamma_k \cdot C \qquad k \in K \tag{4.38}$$

$$\sum_{k \in K} \sum_{l \in P} \beta_{kjl} \geq 1 \qquad j \in J \tag{4.39}$$

$$\sum_{k \in K} \gamma_k = 1 \tag{4.40}$$

$$\sum_{k \in K} \beta_{kjl} = 0 \qquad s \in S \ ; \ j \in J_s \ ; \ l \in P_{h:h \neq s} \tag{4.41}$$

$$d_j - \sum_{k \in K} \sum_{l \in P} g_{kl} \cdot \beta_{kjl} \leq Z_j \qquad j \in J \tag{4.42}$$

$$d_j - \sum_{k \in K} \sum_{l \in P} g_{kl} \cdot \beta_{kjl} \geq -Z_j \qquad j \in J \tag{4.43}$$

$$Z_j \leq o_j \cdot d_j \qquad j \in J \tag{4.44}$$

$$\beta_{kjl} \in \mathbb{N}_0 \qquad k \in K \ ; \ j \in J \ ; \ l \in P \tag{4.45}$$

$$\gamma_k \in \{0, 1\} \qquad k \in K \tag{4.46}$$

$$Z_j \geq 0 \qquad j \in J \tag{4.47}$$

The objective (4.37) is to minimize the total number of required cells. Constraint (4.38) ensures that a version l of cycle time k only can be used, if the corresponding cycle time is chosen to be used. To avoid infeasible solutions for a given set of cycle times due to too small values for C ((4.39) forces every street section to be covered at least by one cell), a lower bound for C can be calculated by (4.48):

$$C \geq \sum_{s=1}^{|S|} \sum_{j \in J_s} \left\lceil \frac{d_j}{\max_{k \in K, l \in P_s} g_{kl}} \right\rceil \tag{4.48}$$

(4.40) fixes the number of used cycle times to one and equation (4.41) assures that no inappropriate versions of cycle times are used. (4.42) as well as (4.43) calculate the actual difference between the length of street section j and the length(s) of the corresponding cells. An upper bound for this deviation is stated in (4.44). Finally, the domains of the decision variables are stated in (4.45), (4.46) and (4.47).
Beside the objective stated in (4.37), other objectives are also implementable. For example, the minimization of total deviation for a given C can be integrated by dropping (4.44) and replacing the objective function (4.37) with (4.49)

$$\min \sum_{j \in J} Z_j \tag{4.49}$$

For a given maximum number of cells this objective function will minimize the sum of all deviations between the length of street section j and the cell(s) intended to model this street section. The lowest possible objective value is $\sum_{j \in J} Z_j = 0$, i.e. all cells match perfectly the given street sections.
Another objective may cover the minimization of the largest deviation between a certain street section j and the corresponding cells. This objective can be implemented by replacing (4.49) with (4.50)

$$\min \quad W \tag{4.50}$$

and adding constraint (4.51):

$$W \geq Z_j \qquad j \in J \tag{4.51}$$

In this case, W will be set to the largest Z_j value whereas Z_j denotes the deviation between the length of street section j and the cell(s) intended to model this street section in the ExCTEPM.

If the (total/largest) deviation is minimized, additional constraints for automatic selection of large cell sizes (where possible) can eliminate redundancy, see (4.52):

$$\sum_{k\in K}\sum_{L\in\mathcal{P}(L_s)}\sum_{l\in L}\beta_{kjl}\leq 1 \qquad s\in S\ ;\ j\in J_s\ ;\ L_s=\{1,\ldots,|P_s|-1\} \tag{4.52}$$

4.1.5 Numerical Example

In order to illustrate the effect of multiple cell sizes as well as the explicit consideration of lanes and traffic flow limitations, we will present a numerical example in this section. In particular, four different cases will be computed:

1. Case: CTEPM with single cell size: (4.1) – (4.16).
2. Case: CTEPM with multiple cell sizes (Approach 1): (4.1), (4.4) – (4.16), (4.17) – (4.22)
3. Case: CTEPM with multiple cell sizes (Approach 2): (4.1) – (4.16), (4.23)
4. Case: CTEPM with single cell size and consideration of lanes and traffic flow limitations: (4.1) – (4.8), (4.11) – (4.16) and (4.25) – (4.36)
5. Case: CTEPM with multiple cell sizes (Approach 1), consideration of lanes and traffic flow limitations: (4.1), (4.4) – (4.8), (4.11) – (4.16), (4.17) – (4.22) and (4.25) – (4.36)
6. Case: CTEPM with multiple cell sizes (Approach 2), consideration of lanes and traffic flow limitations (=ExCTEPM):(4.1) – (4.8), (4.11) – (4.16), (4.23) and (4.25) – (4.36)

The considered test network consists of straight street sections of different lengths as displayed in Figure 4.6. The driving speed is 13.89 m/s on all 50m/100m sections and 8.33m/s on all 30m/60m sections. Using a period length of 3.6 seconds, the resulting cell sizes are $13.89\text{m/s}\cdot 3.6\text{s} = 50\text{m}$ and $8.33\text{m/s}\cdot 3.6\text{s} = 30\text{m}$. All cells are two- or four-laned. This network can be modeled in the single cell size CTEPM with 51 cells (including super sink), see Figure 4.7. If we assume that multiple cell sizes can be used, larger cells of 60m / 100m can be defined, so that two adjacent cells on a street section can be replaced by one larger cell. Now, the same network can be modeled with 35 cells (cell 1–18 single sized, cell 19–34 double sized and a super sink), see Figure 4.8. In this case, cell sizes of 50m/100m and 30m/60m match the street section lengths of the given road network perfectly. We set $c_{it} = c_i \cdot t$ with $c_i = 100$ for all cells except the super sink ($c_i = 0$ for the super sink) and $|T|$ is set to $|T| = 1.5 \cdot \sum_{i\in I} E_i / \sum_{i\in I_S} Q_i = 1.5 \cdot 2422/54 \approx 67$.
The computation times for solving the LPs (Case 1,2,3) optimally and MIPs (Case 4,5,6) to a maximum mipgap of 0.1% are shown in Table 4.9.
The CTEPM and the CTEPM with multiple cell sizes are linear programs (LP) which can be solved very fast using by GUROBI's (see *http://www.gurobi.com*) simplex algorithm (Case 1,2,3). Implementing lanes and traffic flow limitations into the model formulation results in a mixed integer problem (MIP) due to the introduction of φ_{ij} and ϵ_{ij}, so that GUROBI's branch & bound algorithm must be applied (Case 4,5,6). This leads to much larger computation times compared to the LPs. For all MIPs, GUROBI finds good (mipgap $\leq 0.1\%$) feasible solutions very fast. Using multiple cell sizes helps to reduce the computation time significantly. In particular, computation time drops by 41.5% / 54.7%

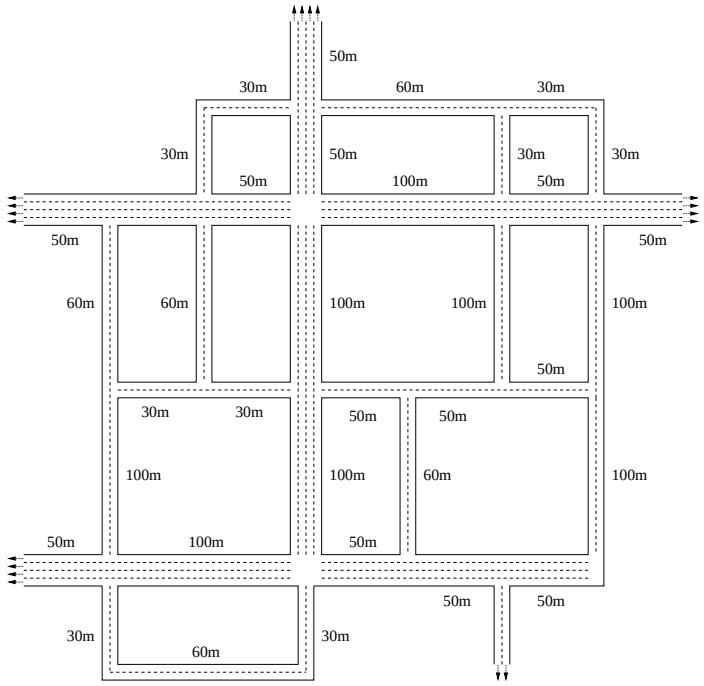

Figure 4.6: Random Street Network

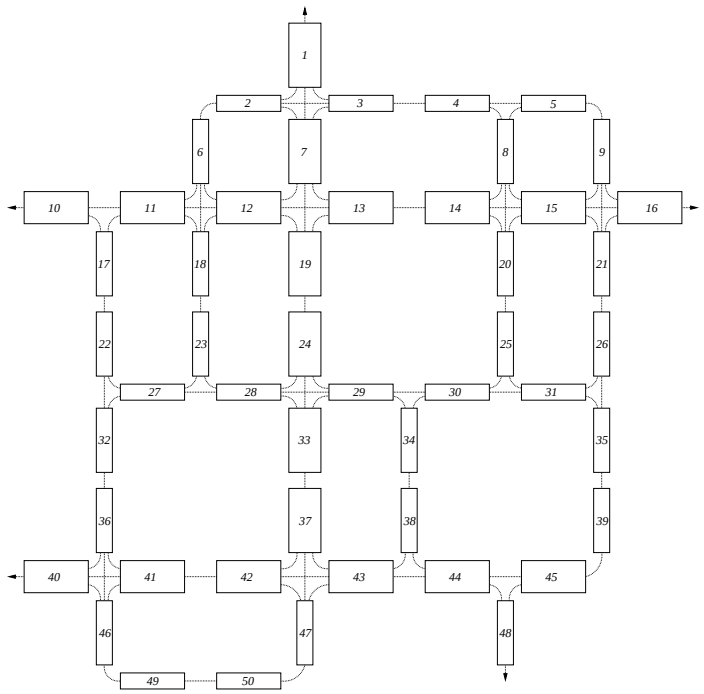

Figure 4.7: Random Street Network Representation with One Cell Size

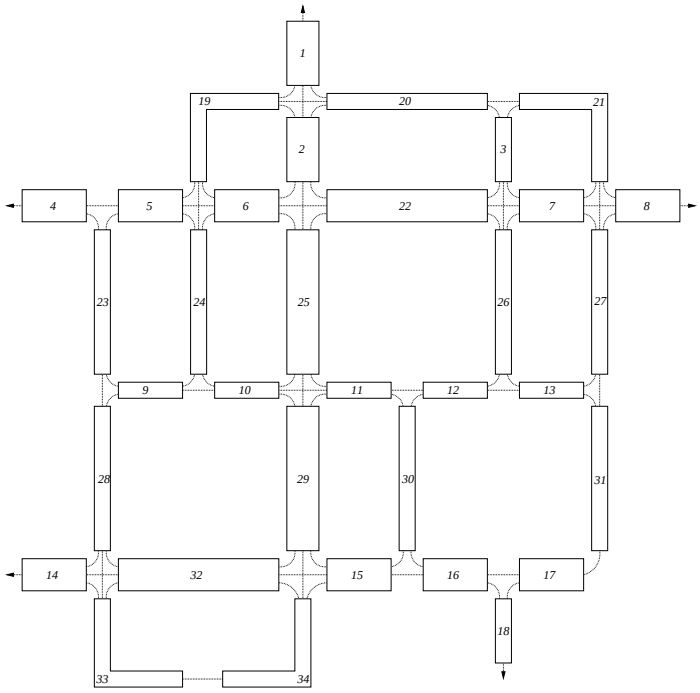

Figure 4.8: Random Street Network Representation with Two Cell Sizes

Model	Computation Time [sec.]	#Constraints (after AMPL's Presolve)	#Variables (after AMPL's Presolve)
1. Case	5.3	19,914	22,960
2. Case	3.1	14,699	18,834
3. Case	2.4	14,683	17,746
4. Case	1919.6	40,056	23,352
5. Case	876.1	32,668	19,096
6. Case	505.8	32,652	18,008

Table 4.9: Computation Times for Random Network with One and Two Cell Sizes

for the LPs and 54.4% / 73.6% for the MIPs. It should be mentioned that the application of multiple cell sizes reduces the number of cells by 31% in this case. For other instances (with larger reduction of cells due to multiple cell sizes), results may vary.
Another important aspect is the implementation of different driving speeds into the model. Of course, any number of different driving speeds can be modeled in all model formulations. Let us consider the random street network (Figure 4.6) again. For the sake of simplicity, we may assume that the driving speed corresponds to the length of the street section, so that street section lengths of 30m / 50m / 60m / 100m lead to driving speeds of 30km/h / 50km/h / 60km/h / 100km/h. The corresponding cell network will look identical to the case of using two cell sizes in Figure 4.8, but there are significant differences in the model formulation since now only single cell sizes with doubled driving speed (instead of doubled cell sizes with standard driving speed) are used. Therefore, all larger cells can be passed by one period instead of two periods. However, subsequent adjustments of driving speeds may require different cell sizes which need to be defined in a way to match the given street lengths adequately. In summary, any number of driving speeds can be combined with any number of different cell sizes. We will present a framework to determine the "optimum" cell sizes in the Section 4.3.2.

4.2 Simulation-Based Optimization Approach

When it comes to evacuation planning problems or traffic assignment problems in general, complex and dynamic traffic behavior is very hard to capture in an optimizational environment so that traffic simulations are the method of choice to evaluate solutions, see Han et al. (2006), Liu et al. (2008), Sbayti and Mahmassani (2006), Stepanov and MacGregor Smith (2009). Since there might exist a gap between the solution of the ExCTEPM and its implementation in a microscopic traffic simulation, we will use the observations gathered from the traffic simulation to modify the the evacuation routing in such a way that the outcome of the traffic simulation approximates the outcome of the optimization model in terms of exit occupation times.
We choose the exit occupation time as the key figure since for our real world example the ExCTEPM tends to generate solutions where the exit occupation times are well balanced. This result indicates that unused flow capacities at exits due to unbalanced exit occupation times have to be avoided. It has to be mentioned that similar exit occupation times may lead to different number of vehicles escaping through these exits because of different flow capacities, e.g. different number of lanes. Admittedly, the optimal solution of the ExCTEPM for extremely sparse networks may not result in perfectly balanced exit occupation times since traffic flow limitations may force some exits to be used only by a small number of vehicles. However, we assume that such affects will not appear in urban areas since urban street networks are often strongly connected.
We will discuss the components (reallocation of vehicles and traffic flow limitations) as well as the simulation-based optimization procedure itself in the following:

4.2.1 Components and Procedure

Vehicle Reallocation Model

The ExCTEPM allows to optimize traffic routing in road networks under consideration of queuing effects on a mesoscopic level of detail. We will now introduce a reallocation optimization model which will use data provided by our microscopic traffic simulation (SUMO). In particular, we assume a district i to be defined as the set of cells escaping

to exit i so that the number of districts is equal to the number of exits. We imply that all districts are part of a connected network, i.e. there are no insurmountable obstacles between districts, e.g. no options to cross a river by bridges or ferry boats. It has to be made clear that the reallocation model does not determine the shape of the districts themself, because the shape of the districts is the outcome of the ExCTEPM. We formulate the model using the following notation:

Parameters:

D	Index set of district / exits
s_i	number of vehicles using exit i (before reallocation)
p_i	largest index of period where exit i is still occupied (before reallocation)

Decision Variables:

w_{ij}	number of vehicles reallocated from exit i to exit j
e_i	number of vehicles using exit i (after reallocation)
t_i	largest index of period where exit i is still occupied (after reallocation)
Z	auxiliary variable

Based on this notation, the reallocation model can be formulated as a MIP model by:

$$\min Z \tag{4.53}$$

subject to

$$Z \geq t_i \qquad i \in D \tag{4.54}$$

$$e_i = s_i + \sum_{j \in I} w_{ji} - \sum_{j \in I} w_{ij} \qquad i \in D \tag{4.55}$$

$$\frac{s_i}{p_i} = \frac{e_i}{t_i} \qquad i \in D \tag{4.56}$$

$$w_{ij} \in \mathbb{N}_0 \qquad i,j \in D \tag{4.57}$$

$$e_i \in \mathbb{N}_0 \qquad i \in D \tag{4.58}$$

$$t_i \geq 0 \qquad i \in D \tag{4.59}$$

$$Z \geq 0 \tag{4.60}$$

The objective function (4.53) in combination with (4.54) minimizes the largest occupation time of all exits. Thus, the reallocation model determines the number of vehicles escaping through a certain exit in such a way that the overall occupation time for all exits will be balanced. In equation (4.55), the number of vehicles allocated to exit i (after reallocation) is calculated by the number of vehicles using exit i before reallocation plus the number of vehicles using exit i instead of exit j minus the number of vehicles using exit j instead of exit i. In addition, equation (4.56) approximates the index of period where exit i is not occupied any more after reallocation. Here, we assume that the throughput is constant over time so that the relation between escaped vehicles and the number of occupied periods is linear. Lastly, (4.57) – (4.60) determine the domains of the decision variables.

Additional Traffic Flow Limitations

It may happen that junctions are too small so that a large number of different traffic flows

may affect each other in terms of traffic blocking. Figure 4.9 displays such a case for a four way junction where traffic from cell i to cell u may be blocked due to not enough space on the junction.

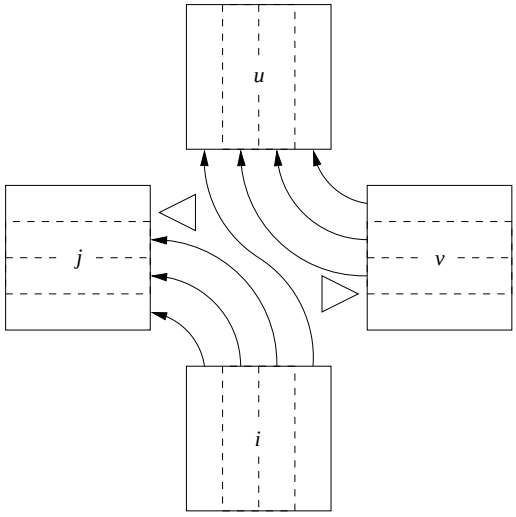

Figure 4.9: Possible Routing at a Junction

Suchlike situations are forbidden by (4.36) so that these effects will not take place when the ExCTEPM is solved. However, (4.36) makes the ExCTEPM also very hard to solve so that a relaxation of this constraint is likely to be used within a heuristic procedure. As will be seen later in this section, we will solve the ExCTEPM with a relaxed version of (4.36) that only covers traffic crossing, but not traffic touching conflicts like shown in Figure 4.9. If it comes to solutions where traffic is blocked due to missing space on a junction, the original constraint (4.36) will be restored for this junction.

Simulation-Based Optimization Procedure
We can use the vehicle reallocation model and additional traffic flow limitations to create an iterative solution heuristic composed of the these approaches, the ExCTEPM and the microscopic traffic simulation. The procedure works in the following manner:

1. Solve the ExCTEPM ((4.1) – (4.8), (4.11) – (4.16), (4.23), (4.25) – (4.36)).

2. Evaluation of this solution using the simulation model.
   (Result: Occupation time for each exit, number of vehicles at each exit and traffic blocking if so).

3. Stop, if stopping criterion is reached. (Given number of iterations without improvements.)

4. If total evacuation time is elongated due to blocked traffic streams on a junction, restore the original version of (4.36) for this junction and go back to Step 1.

5. Solve the vehicle reallocation model ((4.53)–(4.60)) with the data from Step 2. Stop, if relative reallocation is lower than a given percentage on all exit cells.

6. Set for all $i \in I_S$: $\sum_{t \in T} y_{i,|I|,t} \leq \lceil (1+\mu) \cdot e_i \rceil$.

7. Fix routing decisions (number of lanes (ϵ_{ij}) between two cells) for all cells $i \in I \backslash I_S$ representing more than 1% of total traffic (disregarding traffic to the super sink).

8. Return to Step 1.

Rounding in Step 6 is introduced to limit traffic flow of exit cells by an integer number of vehicles. Otherwise, the optimization model tends create solutions with non-integer values for y_{ijt} which are not suitable in the SUMO traffic simulation. Step 7 is inserted to ensure that the most relevant traffic routing decisions stay the same when the reallocation model is applied. Otherwise, other traffic routing decisions may lead to different traffic throughput in highly frequented cells which are not covered in the reallocation model. Fixing these decisions also results in less computation time as will be seen later in this section. In addition, $\mu \geq 0$ is required to allow a certain degree of freedom in traffic routing. We set $\mu = 0.025$ in our computational study.

4.2.2 Postprocessing Model

In case of non-integer vales for η_{ij} in the optimization of the (Ex)CTEPM, this postprocessing optimization model generates a modified solution only consisting of integer values for η_{ij}. We introduce two new decision variables, namely η'_{ij} and A_{ij}. Let η'_{ij} be the total number of vehicles traveling from cell i to cell j after the postprocessing and let A_{ij} be the absolute difference between the number of vehicles traveling from cell i to cell j before and after the postprocessing. On the basis of this notation, we can formulate the postprocessing optimization model as follows:

$$\min \sum_{i \in I} \sum_{j \in I} A_{ij} \tag{4.61}$$

subject to

$$\eta_{ij} - \eta'_{ij} \leq A_{ij} \qquad i,j \in I \tag{4.62}$$

$$\eta_{ij} - \eta'_{ij} \geq -A_{ij} \qquad i,j \in I \tag{4.63}$$

$$\sum_{i \in I} \eta'_{ij} + E_j = \sum_{k \in I} \eta'_{jk} \qquad j = 1, \ldots, |I| - 1 \tag{4.64}$$

$$\sum_{i \in I} E_i = \sum_{i \in I} \eta'_{i,|I|} \tag{4.65}$$

$$\eta'_{ij} \leq \eta_{ij} \cdot Y \qquad i,j \in I \tag{4.66}$$

$$\eta'_{ij} \in \mathbb{N}_0 \qquad i,j \in I \tag{4.67}$$

$$A_{ij} \geq 0 \qquad i,j \in I \tag{4.68}$$

The objective function (4.61) minimizes the total deviation between assigned vehicles before and after the postprocessing, whereas the deviation is calculated by (4.62) and (4.63). A simple static vehicle flow equation is stated in (4.64) and equation (4.65) takes care that all vehicles will be evacuated. To ensure that no new routes will be used after the postprocessing, (4.66) limits vehicle flows to those cell pairs where traffic occurs before the postprocessing. Here, Y is a large number, e.g. $Y = \sum_{i \in I} E_i$. The domain of the decision variables is defined in (4.67) and (4.68).
We will demonstrate the functionality of this approach for a simple network consisting of six cells where cell 6 is the super sink, see Figure 4.10. There are 10 vehicles starting in

cell 1–5 each. A possible solution with non-integer values for η_{ij} is displayed in Figure 4.11. The non-integer partitioning of the vehicles leaving cell 1 affects all vehicle flows, although only integer numbers of vehicles leave from cell 2–5. After the postprocessing, the number of vehicles traveling between cells are only integer values, see Figure 4.12. The objective value for this instance is 1.2.

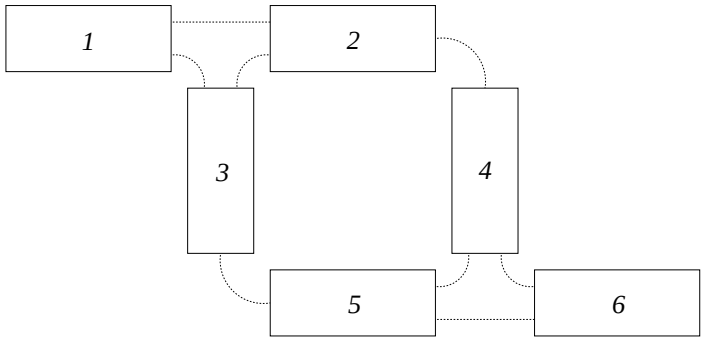

Figure 4.10: Sample Network for Postprocessing

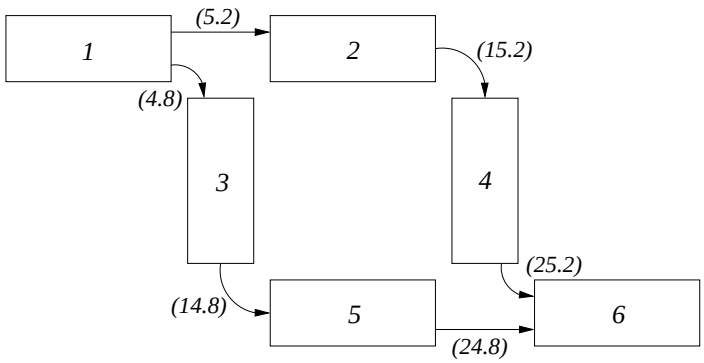

Figure 4.11: Cumulated Vehicle Flows before Postprocessing

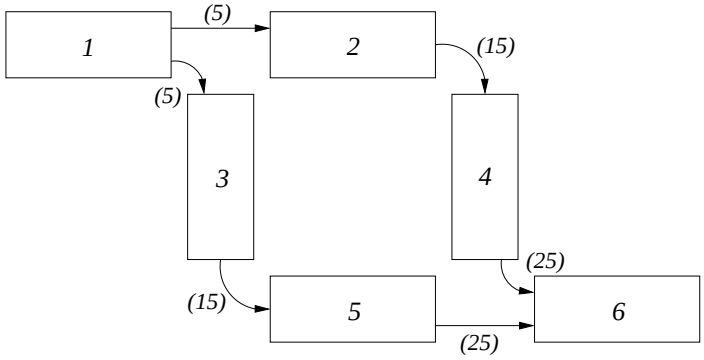

Figure 4.12: Cumulated Vehicle Flows after Postprocessing

4.3 Computational Study

For our computational study, the ExCTEPM and the vehicle reallocation model were coded in AMPL (see *http://www.ampl.com*) and solved with GUROBI 3.0.1 on a computer using an Intel X9100 (3.06 Ghz), 8 GB memory and Windows Vista (64-bit).

4.3.1 Scenario Basics

We tested our simulation-based optimization procedure using data from the neighborhood Neudorf in Duisburg, Germany, with a population of around 26,000 residents leading to 8,750 vehicles. The road network consists of one-, two- and four-lane streets at 50 km/h and 30 km/h. In addition, eight exits can be used for evacuation purposes. Figure 3.4 in the preceding chapter shows an aerophoto of Neudorf including population density and available exits.

We decided that it is not effective to include every small side- and dead-end street in the ExCTEPM. As such we disregard small and sparsely populated street sections so that the considered street network consists of 98 street sections with a total length of 23km plus eight exit street sections (and a super sink). For all tests, we use an evacuation scenario where 100% of residents have to be evacuated. Addionally, we assume that there is no initial network traffic (e.g. due to rush hour traffic) and that departure times of all residents can be described by a gamma distribution, see (4.69).

$$F(\tilde{x}) = 1 - e^{-\tilde{x}/\beta} \sum_{j=0}^{\alpha-1} \frac{(\tilde{x}/\beta)^j}{j!} \qquad \forall\ \tilde{x} \geq 0\ ;\ \alpha \in \mathbb{N} \tag{4.69}$$

Although the departure pattern in the case of an evacuation is not very well explored in literature, we decided to use a gamma distribution since two pertinent works by Lindell (2008) and Yazici and Ozbay (2008) confirm our assumption. Moreover, we decided to use $\alpha = 3$ and $\beta = 1$ since these parameter settings are reasonable to show the benefits of improved traffic routing which may be diluted, if vehicles are departing too slow, e.g. $\alpha = 3\ ;\ \beta = 3$ or $\alpha = 3\ ;\ \beta = 5$.

4.3.2 Optimization Basics

To calculate the optimum cell size, we first have to determine what an optimum cell size is. We will discuss three ideas in the following:

1. Minimum number of cells: In this case, each street section has to be modeled by exactly one cell, where cells can have different sizes.
2. Maximum accuracy in network representation: Here, the standard cell size has to be very small in order to match the lengths of the street sections adequately. Again, multiple cell sizes can be used.
3. Shortest computation time: Number of cells and cell sizes have to be chosen in way that minimizes computation time.

The minimum number of cells is determined by the number of street sections. Here, the standard cell size negatively correlates with the accuracy in network representation, i.e. higher accuracy leads to smaller standard cell sizes by trend. Smaller cells result in shorter

periods so that the number of periods to cover a certain planning horizon increases. The maximum accuracy in network representation is achieved, when all cells (of different size) match the corresponding street sections perfectly ($o_j = 0\%$ for all $j \in J$). However, in extreme situations this may lead to cell sizes of about 1m which results in very high number of periods due to short periods. These considerations should demonstrate that the problem size depends on the number of cells and the size of the cells which directly affects the number of periods. However, it is very hard to determine the effects to an increasing number of cells and periods so that the minimization of computation time by finding an "optimal" trade-off between number of cells, size of cells and accuracy in network representation is very difficult.
For our computational tests, we decide to minimize the number of cells. The number of different cell sizes directly corresponds to the accuracy in network representation. We run a short sensitivity analysis to capture these effects, see Table 4.10.

o_j values	Cell size (50km/h)	$\|N\|$	Period length	Mean Deviation	Total Deviation
10%	30m	25	2.2s	6.7m	661m
15%	44m	16	3.2s	10.8m	1060.2m
20%	52m	13	3.7s	10.8m	1061.4m
25%	70m	9	5.0s	15.8m	1547m
30%	82m	7	5.9s	19.4m	1898.2m
35%	106m	5	7.6s	27.2m	2669.4m
40%	122m	4	8.8s	32.5m	3185m

Table 4.10: Sensitivity Analysis for Different Levels of Accuracy

We use the model (4.37) – (4.47) presented in Section 4.1.4 with a slightly modified objective function. In detail, we added $+0.0001 \cdot \sum_{j \in J} Z_j$ to the objective function. By doing so, the gap between the length of a street section and the corresponding cell(s) will be minimized, as long as no further cells are needed. This modification helps to reduce total deviation when multiple cell sizes are used, because it may be beneficial to model a certain street by a cell of size $n = 5$ instead of size $n = 4$, whereas both cell sizes may be feasible in terms of (4.44). We set the accuracy level $o_j = 0.1, 0.15, \ldots, 0.35, 0.4$, $|K| = 100$ and $|S| = 2$ (50km/h and 30km/h). First, we calculate the number of cells with a single cell size for every driving speed for a given accuracy. By doing so, we can derive the minimum (multiple) cell size desired to describe every street section by one cell by $\max_{k \in K, j \in J, l \in P} \beta_{kjl}$. In a second run, we use the (minimum) multiple cell sizes for each level of accuracy to model each street section by exactly one cell. Table 4.10 contains some key figures of the sensitivity analysis.

The problem size of the ExCTEPM mainly depends on the number of cells and the number of periods. As the number of cells is the same for all accuracy levels in Table 4.10, problem size is only up the number of periods which correlates the standard cell size. We have computed solutions for the case of $o_j = 0.25, 0.3, 0.35, 0.4$ using the heuristic procedure later in this section to demonstrate the effect of increased problem size (due to more periods). The computation times are stated in Table 4.11.
On the basis that the ExCTEPM must be solved several times in the simulation-based optimization approach in Section 4.2, we decided to set $o_j = 0.35$ since this level of accu-

o_j values	Computation Time [sec.]
25%	11,554
30%	15,578
35%	4,318
40%	2,885

Table 4.11: Computation Times for Different Levels of Accuracy

racy seems to be a good compromise between computation time and level of accuracy.
For adjacent cells i and j with equal level of danger ($c_{it} = c_{jt}$), the ExCTEPM (and CTEPM) tends to generate solutions, where vehicles commute between these cells. This phenomenon does not correspond to a desired "straight-forward" solution. Therefore, the term $+10^{-5} \cdot \sum_{i \in I} \sum_{j \in I} \sum_{t \in T} y_{ijt}$ has been added to the objective function (4.24) to avoid unnecessary vehicle movements. Moreover, a second term $-10^{-6} \cdot \sum_{t \in T} x_{|I|,t}$ has been added to the objective in order to ensure that evacuating vehicles starting in sink cells are not evacuating later than necessary. This may happen when sink cells and the super sink share the same level of danger (c_{it}) so that there is no difference between residing in a sink cell or the super sink. During our computational tests, we also found out that the second term helps to reduce computation time significantly, so that it will be kept for our computational study. Furthermore, we assume that $c_{it} = c_i \cdot t$ holds and that danger is distributed uniformly within the actual network, setting $c_i = 100$ for all "regular" cells and $c_i = 0$ for the super sink.
Because of (4.33), different values for p will only affect cells with $l_i > p$ so that only values of $p = \{1, 2, \ldots, \max_{i \in I} l_i\}$ are useful. For this case study, we set $p = 2$ since a large amount of cells is one- or two-laned ($l_i = \{1, 2\}$). For cells with four lanes, setting $p = 2$ will provide advantages in evacuation organization, see Figure 4.13 and 4.14.

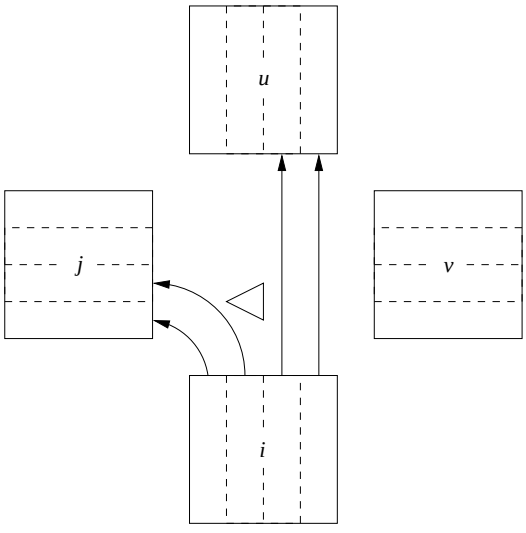

Figure 4.13: Possible Routing at Intersection for $p = 2$

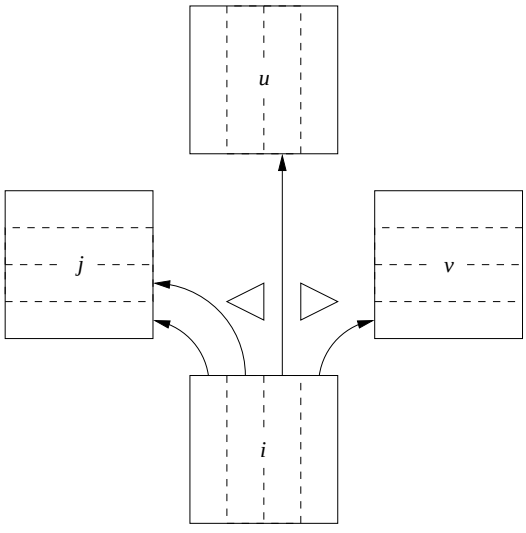

Figure 4.14: Possible Routing at Intersection for $p = 3$

By limiting $p = 2$ in Figure 4.13 evacuation organization is easier since the traffic from cell i has to be splitted up only once in the middle of the street. For $p = 3$ – see Figure 4.14 –

traffic from cell i has to be splitted up twice which is more difficult to organize compared to $p = 2$. In addition, the network in our case study has four-way intersections at maximum so that extremely diverging traffic flows as shown in Figure 4.14 would result in situations where intersections are blocked for all other adjacent cells. It is important to notice that there is no "wrong" value for p. In fact, p should be recognized as a design variable which can be chosen by the decision maker to influence the design of the evacuation plan. However, we found out that setting $p = 1$ may result in some computational issues, e.g. long computation time or no feasible solution.
The procedure stops if $\left|(\sum_{t\in T} y_{i,|I|,t} - e_i)\right| / e_i < \lambda$ for all $i \in I_S$ or no further improvement could be achieved within a given number (ρ) of succeeding iterations. We set $\lambda = 0.10$ and $\rho = 10$.
Due to the large network size and high problem complexity, we solved the ExCTEPM by a straight-forward two stage heuristic:

1. Step:
   (a) Relax constraint (4.23).
   (b) Remove the term $+(E_i - \sum_{\tau=1}^{t} b_{i\tau})$ from (4.2) and (4.4).
   (c) Reduce (4.36) only to traffic crossing conflicts.
   (d) Solve remaining problem to a maximum mipgap of 1.0% and save φ_{ij} and ϵ_{ij} values.
2. Step:
   (a) Restore constraint (4.23).
   (b) Restore the term $+(E_i - \sum_{\tau=1}^{t} b_{i\tau})$ for (4.2) and (4.4).
   (c) Solve remaining problem with φ_{ij} and ϵ_{ij} values from step 1 as parameters.

The concept of using multiple cell sizes helps to reduce the number of cells. However, constraint (4.23) leads much longer computation times compared to case of using only single cell sizes. Therefore, we relax this constraint in the first step. This simplifies the network to cells with only single size. Please remember that a road network with only one cell size and $o_j = 0.35$ would result in a network of 245 cells (236 street cells, 8 exit cells and one super sink) instead of 107 cells (98 street cells, 8 exit cells and one super sink) when multiple cell sizes are used. A network of 245 cells would be very time consuming to be solved compared to the network of multiple cell sizes, but only 107 cells. Of course, constraint (4.23) will be restored in the second step. We calculate $|T|$ analogue to the numerical example, i.e. $|T| = (8750/144) \cdot 1.5 \approx 91$.
The results of the second step (i.e. φ_{ij}, ϵ_{ij}, η_{ij}) are passed to the SUMO traffic simulation.

4.3.3 Simulation Basics

The ExCTEPM minimizes total danger for all evacuees during the planning horizon. In order to adopt this objective as a performance measure for the results of the microscopic traffic simulation, we used the following approach: Imagine a solution where the fraction of rescued evacuees at a particular point of time (within total evacuation time T_e) can be described by a curve $g(t)$ which is illustrated in Figure 4.15.

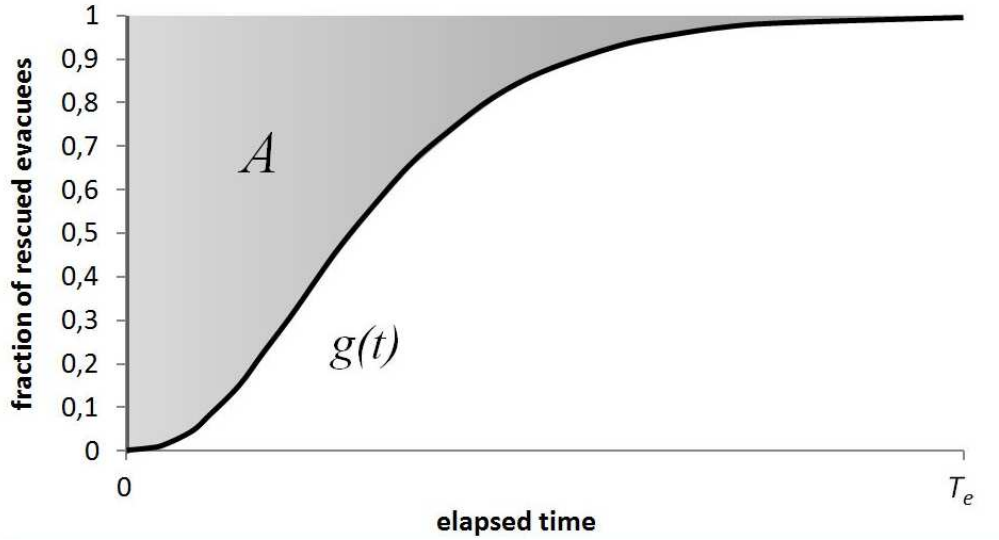

Figure 4.15: Performance Measure

The grey shaded area in Figure 4.15 (Area A) is an indicator of the quality of a solution, because its size depends on the number of rescued evacuees over time, described by the curve $g(t)$. According to the formulation of the objective function of the ExCTEPM, we additionally weight the number of rescued evacuees at a period t with the amount of elapsed time. The size of this area can be calculated using equation (4.70):

$$A = \int_0^{T_e} (1 - g(t)) \cdot t \; dt \tag{4.70}$$

We approximated (4.70) by the discretization $A = \sum_{t=0}^{T_e}((\sum_{i \in I} E_i) - g_t) \cdot t$ with g_t as the number of rescued evacuees in period t.
In order to simplify the comparison between different solutions, we scaled all areas A, all total evacuation times (T_e) and the occupation time difference between the earliest and latest exit (R_t) by dividing them by the corresponding values of the initial solution of the simulation-based optimization procedure. As a result, area size A, total evacuation time T_e as well as time range R_t of this solution will be exactly 1. We use SUMO 0.11.1 for all microscopic traffic simulations.

4.3.4 Performance

As a point of reference, we will use the initial solution of the procedure (Iteration 0) as a benchmark for our computational study. In particular, the occupation time difference between the earliest and latest exit R_t (originally $R_t = 504s$), the total evacuation time T_e (originally $T_e = 1,346s$) as well as the size of area A (originally $A = 1.637 \cdot 10^9$) were scaled to one. The results of the simulation-based optimization procedure are stated in Table 4.12 and 4.13.

The results of the simulation-based optimization procedure are pleasing in many ways. First of all, the initial solution of the ExCTEPM (without any feedback from simulation results) shows nice results in the microscopic SUMO Traffic Simulation. Although occupation times for all exits vary quite strong, total evacuation time is relatively low.

Iteration	E_1	E_2	E_3	E_4	E_5	E_6	E_7	E_8
0	1,333s	1,016s	930s	913s	948s	842s	1,327s	**1,346s**
1	1,084s	1,084s	1,067s	1,027s	1,239s	1,276s	**1,566s**	1,117s
2	1,119s	1,046s	1,079s	1,090s	**1,246s**	1,161s	1,148s	1,109s
3	**1,283s**	1,204s	1,021s	1,034s	1,057s	971s	1,132s	1,176s
4	1,093s	1,011s	1,027s	1,059s	**1,279s**	1,150s	1,234s	1,162s
5	1,189s	1,159s	1,110s	**1,190s**	1,045s	1,039s	1,109s	1,074s

Table 4.12: Exit Occupation Times for each Iteration

Iteration	R_t	T_e	A	Computation Time	Event at the End of Iteration
0	1.000	1.000	1.000	4,318s	Reallocation
1	1.069	1.163	1.137	454s	Restore (4.36)
2	0.397	0.926	0.955	218s	Reallocation
3	0.619	0.953	0.974	212s	Reallocation
4	0.532	0.950	0.972	191s	Reallocation
5	0.300	0.884	0.938	164s	STOP

Table 4.13: Performance of the Simulation-based Optimization Procedure

Computation time is much longer compared to succeeding iterations, because no major traffic routing decisions are preassigned in this iteration. As no major blocking of traffic streams on junctions exist, the reallocation model was applied. The evaluation of iteration 1 results in worsening of all key figures, in detail R_t increases by 6.9%, total evacuation time by 16.3% and the performance measure by 13.7%. This deterioration is mainly caused by massive traffic blocking directly in front of a four-lane exit, leading to strong congestions during the evacuation. This observation demonstrates that traffic touching conflicts also need to be considered in evacuation planning. Due to the determination of many heavily occupied cell connections, computation time drops siginificantly compared to iteration 0. In the following iteration, routing decisions from iteration 1 were adopted and supplemented by the re-establishment of (4.36) for the congested exit cell in iteration 1. This modification results in significantly better results, i.e. the best solution up to now. All key figures reach a new top mark, especially R_t could be improved by 60.3%. During the next iterations, the reallocation model was applied multiple times, finally resulting in a new best solution in iteration 5. Here, all key figures could be improved again, compared to the incumbent solution in iteration 2. R_t reduces to 30.0% of the initial value, total evacuation time to 88.4% and the performance measure to 93.8%. After iteration 5, the procedure stops since the reallocation of vehicles would result in adjustments lower than 10.0% of the original allocation. The simulation with SUMO took between 11 and 14 seconds in each iteration. A graphical representation of the number of rescueed evacuees over time can be found in Figure 4.16. We refused to display the charts of every iteration since the results of iteration 3 and iteration 4 are similar to iteration 2.
The initial solution of the ExCTEPM performs quite well in terms of R_t, T_e and A. On the other hand, these results also indicate that traffic touching conflicts should be considered in the model formulation. However, the reallocation model helps to enhance the initial solution and to lower total evacuation time by more than 11%.

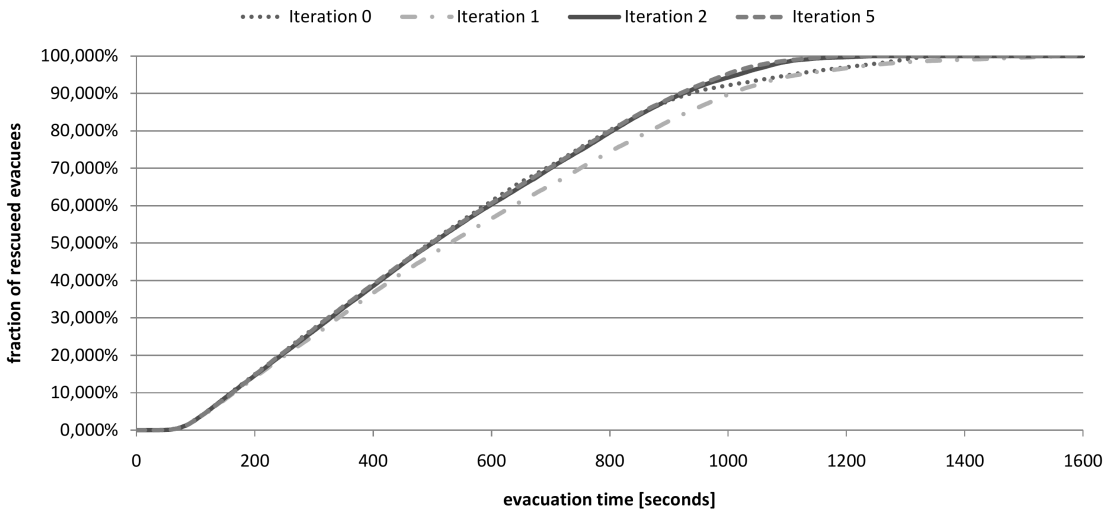

Figure 4.16: Number of rescued evacuees over time

Chapter 5

Heuristic Solution Procedures

Since the ExCTEPM is a deterministic optimization model, it can not cover stochastic aspects or uncertainty in general. Moreover, the realism of traffic illustration in the ExCTEPM is considerably lower than in microscopic traffic simulations. However, in Chapter 3 and Chapter 4 we showed, that the results of the (Ex)CTEPM work fine as input data for succeeding microscopic traffic simulation software which includes more realistic traffic behavior mechanisms. We also demonstrated the potential of the ExCTEPM since it is a very versatile approach capable of generating high quality evacuation plans which are applicable to real-world evacuation problems.
Nevertheless, the preceding chapter also demonstrates that the ExCTEPM is hardly applicable to larger real-world scenarios because of large computation times even for moderately sized instances. Although a simple heuristic solution procedure was applied, computational effort and computational requirements were still high. Taking a closer look on the problem complexity, we observe that the ExCTEPM contains a path constrained network flow problem which is known to be NP–complete, see Garey and Johnson (1979). Thus, the problem described in the ExCTEPM also belongs to the class of NP-complete problems so that finding optimal solutions for larger instances will be a difficult task.
To overcome these difficulties, we will present two heuristic procedures for solving the ExCTEPM in this chapter, namely a shortest-path based heuristic as well as a static version of the ExCTEPM. The latter shows some similarities to the original formulation of the ExCTEPM, especially in its basic concepts, i.e. usage of cells, consideration of lanes, etc. However, this approach is simpler since it lacks the dynamic character of the ExCTEPM. In a computational study we will demonstrate the effectiveness of our approach in nine real-world scenarios of different road network size, population and risk distribution, respectively. The following contents are based on the work of Kimms and Maassen (2010a).

5.1 Extended Cell-Transmission-Based Evacuation Planning

For the sake of self-containedness of this chapter, we first recapitulate the notation and model formulation of the ExCTEPM in the following. In its presented form, the model (5.1) – (5.27) is identical to the model (4.1) – (4.8), (4.11) – (4.16), (4.23) and (4.25) – (4.36) in Chapter 4. Thus, the explanation of the objective function and constraints is exactly the same as discussed before.

5.1.1 Notation

Sets and parameters:

$T = \{1, \ldots, \lvert T \rvert\}$	index set of periods (where $\lvert T \rvert$ is the index of the last period of the planning horizon)
$N = \{1, \ldots, \lvert N \rvert\}$	index set of different cell size multipliers (where $\lvert N \rvert$ denotes the maximum cell size)
$I = \{1, \ldots, \lvert I \rvert\}$	index set of cells
I_n	index set of cells of cell size n ($\bigcup_{n \in N} I_n = I$)
$\lvert I \rvert$	index of super sink
I_S	index set of sink cells ($I_S = \{i \in I : \beta_{i,\lvert I \rvert} = 1\}$)
c_{it}	danger of being at cell i in period t ($c_{it} \geq 0$)
β_{ij}	$= \beta_{ji} = 1$, if a traffic flow from cell i to cell j (and vice versa) can be established (0, otherwise)
N_{it}	maximum vehicle capacity of cell i (on all lanes) in period t
E_i	number of vehicles starting their evacuation in cell i (derived from population in cell i)
Q_{it}	maximum number of in- and outflowing vehicles (on all lanes) per period into / from cell i in period t
l_i	number of lanes in cell i
n_i	size of cell i
p	maximum number of outgoing traffic streams
x_{i1}	number of vehicles en route at cell i at the end of period 1, i.e. before the evacuation starts

Decision Variables:

z_{it}	number of vehicles residing, leaving or waiting in cell i in period t
x_{it}	number of residing vehicles at cell i at the end of period t
y_{ijt}	number of vehicles leaving section i in period t and reaching section j in period $t + 1$
b_{it}	number of vehicles starting their evacuation at cell i in period t
φ_{ij}	$= 1$, if and only if a connection from cell i to cell j will be used by evacuation traffic
ϵ_{ij}	number of lanes used by an evacuation traffic stream from cell i to cell j

Given this notation the ExCTEPM can be formulated as follows:

5.1.2 Model Formulation

$$\min \sum_{i\in I}\sum_{t\in T} c_{it}\cdot z_{it} \tag{5.1}$$

subject to

$$z_{it} = x_{it} + \sum_{j\in I} y_{ijt} + (E_i - \sum_{\tau=1}^{t} b_{i\tau}) \qquad i\in I\ ;\ t\in T \tag{5.2}$$

$$x_{it} = b_{it} + x_{i,t-1} + \sum_{j\in I} y_{ji,t-1} - \sum_{j\in I} y_{ijt} \qquad i\in I\ ;\ t=2,\ldots,|T| \tag{5.3}$$

$$\sum_{j\in I}\sum_{\tau=1}^{t} y_{ij\tau} \le \sum_{j\in I}\sum_{\tau=1}^{\max(t-n_i,1)} y_{ji\tau} + \sum_{\tau=1}^{\max(t-\lceil n_i/2\rceil+1,1)} b_{i\tau} + x_{i1} \qquad i\in I : n_i\ge 2\ ;\ t=2,\ldots,|T| \tag{5.4}$$

$$z_{it} \le N_{it} + (E_i - \sum_{\tau=1}^{t} b_{i\tau}) \qquad i\in I\ ;\ t\in T \tag{5.5}$$

$$x_{it} \le N_{it} \qquad i\in I\ ;\ t\in T \tag{5.6}$$

$$\sum_{t\in T} b_{it} = E_i \qquad i\in I \tag{5.7}$$

$$x_{|I|,|T|} = \sum_{i\in I}(E_i + x_{i1}) \tag{5.8}$$

$$\sum_{i\in I} y_{ijt} \le (N_{jt} - x_{jt}) \qquad j\in I\ ;\ t\in T \tag{5.9}$$

$$y_{ijt} \le N_{it}\cdot\beta_{ij} \qquad i,j\in I\ ;\ t\in T \tag{5.10}$$

$$y_{ijt} \le \frac{Q_{jt}}{l_j}\cdot\epsilon_{ij} \qquad i,j\in I\ ;\ t\in T \tag{5.11}$$

$$y_{ijt} \le \frac{Q_{it}}{l_i}\cdot\epsilon_{ij} \qquad i,j\in I\ ;\ t\in T \tag{5.12}$$

$$\sum_{i\in I}\varphi_{ij} \le l_j \qquad j\in I \tag{5.13}$$

$$\sum_{j\in I}\varphi_{ij} \le p \qquad i\in I \tag{5.14}$$

$$\varphi_{ij} + \varphi_{jk} \le 1 \qquad i,j,k\in I\ :\beta_{ij}=1\ ;\beta_{ik}=1 \tag{5.15}$$

$$\varphi_{ij} \le \beta_{ij} \qquad i,j\in I \tag{5.16}$$

$$\epsilon_{ij} \le \varphi_{ij}\cdot\min\{l_i,l_j\} \qquad i,j\in I \tag{5.17}$$

$$\sum_{i\in I}\epsilon_{ij} \le l_j \qquad j\in I \tag{5.18}$$

$$\sum_{j\in I}\epsilon_{ij} \le l_i \qquad i\in I \tag{5.19}$$

$$\varphi_{ij} + \varphi_{ji} + \varphi_{uv} + \varphi_{vu} \le 1 \qquad i,j,u,v\in I : \beta_{ij}=\beta_{iu}=\beta_{iv}=\beta_{ju}=\beta_{jv}=\beta_{uv}=1 \tag{5.20}$$

$$z_{it}, x_{it}, b_{it} \ge 0 \qquad i\in I\ ;\ t\in T \tag{5.21}$$

$$y_{ijt} \geq 0 \qquad i,j \in I\,;\; t \in T \qquad (5.22)$$
$$\epsilon_{ij} \in \mathbb{N}_0 \qquad i,j \in I \qquad (5.23)$$
$$\varphi_{ij} \in \{0,1\} \qquad i,j \in I \qquad (5.24)$$
$$x_{i1} = 0 \qquad i \in I \qquad (5.25)$$
$$b_{i1} = 0 \qquad i \in I \qquad (5.26)$$
$$y_{ij1} = 0 \qquad i \in I\,;\; j \in I \qquad (5.27)$$

5.2 Heuristic Approaches

In order to transfer high quality solutions of the ExCTEPM to large-scale instances, heuristic procedures with relatively low memory requirements and short computation times are needed. In this section, we introduce a shortest-path based heuristic as well as an iterative heuristic based on a static version of the ExCTEPM, called static ExCTEPM.
Efficient solution procedures for the system optimum dynamic traffic assignment model in the seminal work of Ziliaskopoulos (2000) are presented in Shen et al. (2007) and Zheng and Chiu (2011). Shen et al. (2007) develop a dynamic network simplex method that is supplemented by a point-queue model. Zheng and Chiu (2011) show that the proposed problem is equivalent to the earliest arrival flow and can be efficiently solved by a network flow algorithm for the earliest arrival flow on a time-expanded network.
However, since the ExCTEPM is a different optimization problem, we prefer an other approach: In our opinion, the major difficulty in solving the ExCTEPM is to determine in which direction vehicles should drive and where merging and diverging processes take place. If the driving direction (in terms of φ_{ij}) is fixed, the allocation of lanes (in terms of ϵ_{ij}) can be regarded as a "fine-adjustment". Hence, finding almost optimal values for φ_{ij} is the most demanding task when solving the ExCTEPM and this is what both heuristics do. The shortest-path heuristic determines φ_{ij} values on the basis of the most frequently used cell connections, whereas the static ExCTEPM heuristic computes φ_{ij} values in such a way that the maximum occupation time of all cell connections will be minimized. The results of both heuristics – i.e. values for φ_{ij} – are then used as input parameters for the original ExCTEPM which dramatically reduces computation time since a large number of integer variables are fixed.

5.2.1 Basics

When it comes to design of heuristic solution procedures, fundamental characteristics of problem instances have to be taken into account. Evacuations are often caused by natural disasters like floods or earthquakes or by human-caused threats like fire, chemical accidents or terror attacks, respectively. All these events have in common that they appear as single (local) events and that the measure of risk decreases with increasing distance. Hence, we can argue that in the case of an evacuation there is a highly endangered emergency planning zone (EPZ_0) in the center of the threat (with very high measure of risk) which actually raises the need for evacuation. Furthermore, the highly endangered EPZ (EPZ_0) is surrounded by "regular" EPZs ($EPZ_1, EPZ_2, \ldots$, with (different) lower levels of risk) which also have to be evacuated. Figure 5.1 illustrates these relations for a threat (e.g. disarming a large unexploded bomb) in the center of an urban area with one highly endangered EPZ and two less endangered EPZs.

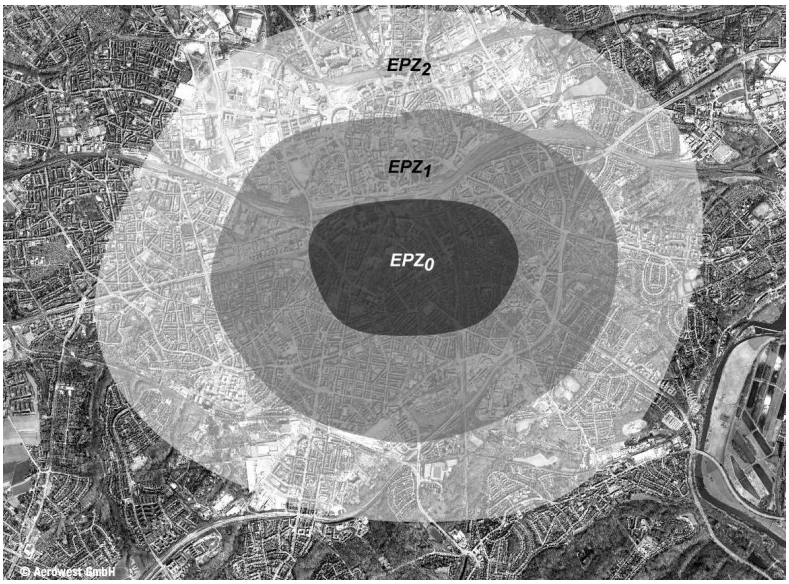

Figure 5.1: Possible Locations of Emergency Planning Zones (EPZ_h)

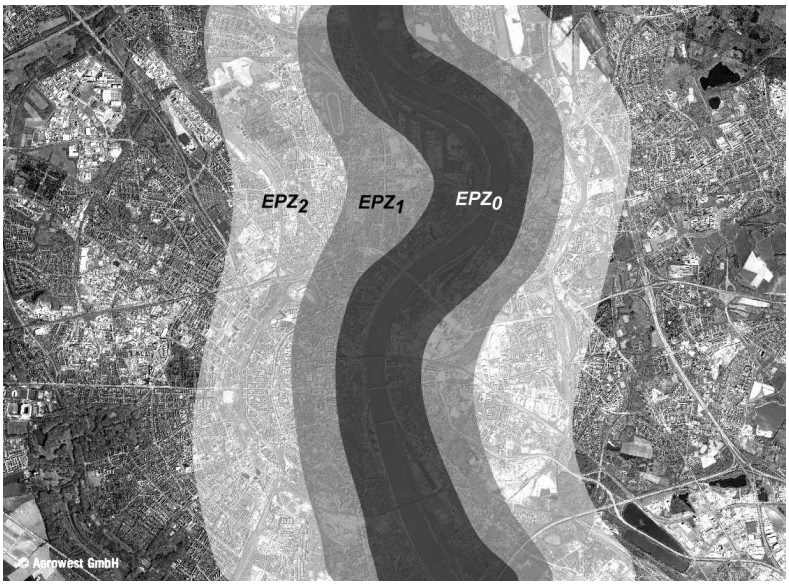

Figure 5.2: Other Possible Locations of Emergency Planning Zones (EPZ_h)

Formally, the sets $EPZ_0, EPZ_1, EPZ_2, \ldots$ define a partition of the index set I, i.e. $EPZ_h \cap EPZ_{h'} = \emptyset$ for $h \neq h'$ and $\bigcup_h EPZ_h = I$. Let H denote the index set of the EPZs so that $|H|$ is the number of emergency planning zones. For ease of understanding, we will denote the parameter c_{it} as $c_{it}^{EPZ_h}$ to emphasize that cell i is located inside the EPZ h. Three topics need special attention here. Firstly, we assume that the measure of risk significantly varies with the distance to the center of risk. In detail, we imply that

$$c_{it}^{EPZ_h} >> c_{jt}^{EPZ_{h+1}} \qquad h = 0, \ldots, |H| - 1 \ ; \ i \in EPZ_h \ ; \ j \in EPZ_{h+1} \ ; \ t \in T \tag{5.28}$$

holds since almost every threat has "critical" distances which relate to certain levels of risk. Additionally, we assume that the measure of risk within an EPZ is the same for every cell (e.g. $c_{it}^{EPZ_h} = c_{jt}^{EPZ_h}$ for all $h = 0, 1, 2, \ldots; i, j \in EPZ_h; t \in T$) and that $|I| \in EPZ_{|H|}$.

Secondly, we have to point out that c_{it} must be interpreted as a control variable for the decision maker. In Section 4.1.1, we already discussed that e.g. c_{it} might be related to the concentration of hazardous materials in the air, but c_{it} also allows the decision maker to "control" the solution of the ExCTEPM taking practical experiences into account. For example, the decision maker may share the opinion that a certain street segment should be used less by evacuating vehicles – i.e. higher values for c_{it} – because the road surface is in worse condition compared to alternative street segments. Similarities to this approach can be found in multicriteria optimization, where the weights of different (partially interfering) objectives also represent a control variable for the decision maker.
Thirdly, it has to be noticed that the shape of the most endangered EPZ and the regular EPZs do not have to be ring-shaped or uniform in general. In fact, the shape may depend on several aspects, e.g. the kind of threat as well as meteorological, topographical, demographical or political concerns. Interested readers can find more detailed information on how to determine emergency planning zones in Golding and Kasperson (1988) and Sorensen et al. (1992). In Figure 5.1, the threat (e.g. a large unexploded bomb) is localized on a single spot and risk is uniformly distributed around the place of discovery since all surrounding buildings have the same level of protection against a possible bomb explosion. In the case of a city with a large river and an upcoming flood, the shape of the EPZs may look like displayed in Figure 5.2. Of course, the floodwater would first hit the area next to the river. Therefore, this area can be declared as the most endangered EPZ (EPZ_0). The measure of risk decreases with increasing distance to the river so that EPZ_1 and EPZ_2 can be specified as shown in Figure 5.2. The shape of the EPZs can also take irregular forms, e.g. in the case of a Tsunami heading towards a city on a mountained area, different levels of altitude may define the EPZs.

5.2.2 Shortest-Path based ExCTEPM

In the literature, shortest-path based approaches are likely to be used when dealing with traffic routing / traffic assignment or evacuation problems, e.g. Chen and Feng (2000), Karbowicz and Macgregor Smith (1984), Stepanov and MacGregor Smith (2009), Wang and Cheng (2006), Yamada (1996). Furthermore, shortest-path algorithms are explored very well (see Ahuja et al. (1993) and Fu et al. (2006) for reviews) and by now, state-of-the-art shortest-path algorithms are capable of handling very large networks as can be seen in Peyer et al. (2009) and Xu et al. (2007).
Since the calculation of shortest paths can be done easily, the main problem for a shortest-path based heuristic is how to convert the knowledge of shortest paths into an evacuation plan. For our purposes, shortest paths are expressed by a row of $i \rightarrow j$ pairs, e.g. if the shortest path from cell 1 (starting cell) to the cell 20 (super sink) is 1→7→13→19→20 the connections from 1→7, 7→13, 13→19, 19→20 are used. To determine shortest paths, our shortest-path algorithm (a standard optimization model for shortest paths applications) uses $d_{ij} = (c_i \cdot n_i + c_j \cdot n_j)/(l_i + l_j)$ as weights for $i \rightarrow j$ pairs. After the computation of all shortest paths (one shortest path per cell), a new parameter w_{ij} is computed by adding the number of vehicles using the connection from cell i to cell j on their shortest paths. In the following, the parameter w_{ij} will be used in an optimization model to determine, which connections from cell i to cell j should be used in an evacuation plan.

Additional Parameters:

Y = a large number, e.g. $\sum_{i \in I} E_i$

Additional Variables:

η_{ij} = number of vehicles using the connection from cell i to cell j

$$\max \sum_{i \in I} \sum_{j \in I} w_{ij} \cdot \varphi_{ij} \tag{5.29}$$

subject to (5.13)–(5.16), (5.20), (5.24) and

$$\sum_{i \in I} \eta_{ij} + E_j = \sum_{k \in I} \eta_{jk} \qquad j = 1, \ldots, |I| - 1 \tag{5.30}$$

$$\sum_{i \in I} \eta_{i,|I|} = \sum_{i \in I} E_i \tag{5.31}$$

$$\eta_{ij} \leq \varphi_{ij} \cdot Y \qquad i, j \in I \tag{5.32}$$

$$\varphi_{ij} + \varphi_{ji} \leq 1 \qquad i, j \in I \tag{5.33}$$

$$\eta_{ij} \geq 0 \qquad i, j \in I \tag{5.34}$$

The objective function (5.29) maximizes the number of vehicles using (at least parts of) their shortest paths. A standard vehicle flow equation is stated in (5.30). Equation (5.31) ensures that all vehicles will be evacuated and (5.32) restricts traffic flow (in terms of η_{ij}) to those connections from cell i to cell j which will be used in the evacuation plan. In addition to vehicle flow constraints in the ExCTEPM, constraint (5.33) is needed to avoid situations where traffic is routed in opposite directions between two cells. The domain of the new decision variables is defined in (5.34).
One major weakness of this approach is the fact that the shortest path for each cell is calculated independent of the shortest paths from other cells. On the one hand, traffic capacities are taken into account by including l_i in the computation of w_{ij}. On the other hand, the relation between the number of vehicles traveling from cell i to cell j and the number of periods, which will be necessary to cope with the generated traffic volume in these cells, is completely disregarded. Due to the nature of this approach, it is not able to take the number of periods – a connection from cell i to cell j will be occupied due to a certain traffic volume – into account. The computational study in Section 5.3 will illustrate that this fact will tremendously affect solution quality, for Scenarios 1–6: $\varnothing gap = 88.9\%$.

A possible shortest-path based heuristic for solving the ExCTEPM can be designed in the following manner:

1. Step: Calculate a shortest path from each cell i ($i = 1, \ldots, |I| - 1$) to super sink $|I|$. Result: w_{ij} values.

2. Step: Solve the MIP (5.13)–(5.16), (5.20), (5.24) and (5.29) – (5.34) with w_{ij} as parameter. Result: Values for φ_{ij} for all $i, j \in I$.

3. Step: Use φ_{ij} values as input parameters for the ExCTEPM.

Please note that we will not address the details of the computation of shortest paths in this work, we refer to Ahuja et al. (1993) for further details. For our purposes, we use a straightforward implementation of the shortest path problem in terms of a simple linear optimization model which can be found in standard math programming text books. This optimization model has been used in a standalone procedure coded in AMPL (see *http://www.ampl.com*) to generate all shortest paths.

5.2.3 Static ExCTEPM

The minimization of risk for evacuees generally relates to the minimization of the occupation of the street network. The occupation of the street network can be expressed by the number of periods it is used and the number of periods a certain connection between to cells is used can be computed by (5.35).

$$\frac{\eta_{ij}}{\min(\frac{Q_i}{l_i}, \frac{Q_j}{l_j}) \cdot \epsilon_{ij}} = M_{ij} \qquad i, j \in I \tag{5.35}$$

where η_{ij} is the total number of vehicles using the connection $i \rightarrow j$ (i.e. $\eta_{ij} = \sum_t y_{ijt}$) and M_{ij} is the amount of time (measured in periods) this connection will be used under maximum traffic flow. Additionally, we assume that road capacities don't change within the planning horizon, so that $Q_{it} \rightarrow Q_i$ and $Q_{jt} \rightarrow Q_j$. In the original formulation of the ExCTEPM, there was no need for the variable M_{ij}, since the number of periods a certain connection is used could be derived from y_{ijt}. Unfortunately, η_{ij}, ϵ_{ij} as well as M_{ij} are not known in advance since these values are the result of the optimization.
The objective (5.1) minimizes total risk for all evacuees in the complete planning horizon. However, when the results of the ExCTEPM were evaluated in a traffic simulation, it turned out that the occupancy rates of exits may be unbalanced, so that a reallocation approach to balance occupancy rates was discussed and successfully applied in the preceding chapter. The basic idea of this approach is to reallocate evacuees from highly occupied exits to less occupied exits in order to minimize total evacuation time and to maximize the number of escaped evacuees at each point of time in the planning horizon, whereby worsening of the objective value will be accepted. Here, we will adopt this idea, but instead of just balancing exit occupancy rates, we will consider every $i \rightarrow j$ connection. The occupancy rate of a specific $i \rightarrow j$ connection can be calculated by (5.35). For the case of minimizing maximum occupancy rates of all $i \rightarrow j$ connections, (5.35) can be transformed into (5.36) because $\epsilon_{ij} \in \mathbb{N}_0$:

$$\frac{\eta_{ij}}{\min(\frac{Q_i}{l_i}, \frac{Q_j}{l_j})} \leq M \cdot \epsilon_{ij} \qquad i, j \in I \tag{5.36}$$

where M_{ij} is substituted by M. By choosing the value of M, traffic flow can be controlled as the following simple example illustrates, see Figure 5.3.

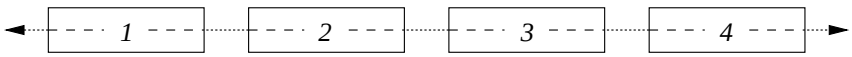

Figure 5.3: Basic Idea of Static ExCTEPM Heuristic

We assume that the population is 50 vehicles in cell 2 and 50 vehicles in cell 3. The maximum flow capacity on all lanes is 10 vehicles per period for every cell. If $M \leq 10$

holds, all vehicles may travel to cell 1 (or cell 4) in order to escape. This solution would be feasible since exactly 10 (the upper limit of M) periods (100 vehicles / 10 vehicles per period) are needed between cell 1 and 2 as well as cell 2 and 3. Otherwise, if $M \leq 5$ holds, the only feasible routing consists of 50 vehicles traveling from cell 2 to cell 1 and 50 vehicles traveling from cell 3 to cell 4. The former solution would not be feasible for $M \leq 5$. It is easy to notice, that evacuation time decreases to 50% and that connections are uniformly occupied in the complete evacuation network.
Based on these thoughts, the Static ExCTEPM can be defined as follows:

$$\min M \tag{5.37}$$

subject to (5.13)–(5.20), (5.23), (5.24), (5.36) and

$$\sum_{i \in I} \eta_{ij} + E_j = \sum_{k \in I} \eta_{jk} \qquad j = 1, \ldots, |I| - 1 \tag{5.38}$$

$$\sum_{i \in I} E_i = \sum_{i \in I} \eta_{i,|I|} \tag{5.39}$$

$$\eta_{ij} \leq \epsilon_{ij} \cdot Y \qquad i, j \in I \tag{5.40}$$

$$\varphi_{ij} + \varphi_{ji} \leq 1 \qquad i, j \in I \tag{5.41}$$

$$\epsilon_{i,|I|} = l_i \qquad i \in I : \beta_{i,|I|} = 1 \tag{5.42}$$

$$M \geq 0 \tag{5.43}$$

$$\eta_{ij} \geq 0 \qquad i, j \in I \tag{5.44}$$

The objective (5.37) in combination with (5.36) minimizes maximum usage time of all $i \rightarrow j$ connections. Equation (5.38) is a simplified static version of flow balance equation (5.3). (5.39) ensures that all vehicles will leave the evacuation network and (5.40) restricts traffic flows only to those $i \rightarrow j$ connections where at least one lane is established. Constraint (5.41) avoids traffic flows in opposite directions between two cells and (5.42) is a preprocessing constraint as it fixes the number of established lanes from exit cells to the super sink to the maximum number of lanes. (5.43) as well as (5.44) specify the domain of η_{ij} and M, respectively. It has to be noticed that this optimization problem is non-linear due to constraint (5.36).

Since the objective just consists of a single variable, the optimization (= minimization) process can be done by a binary search algorithm, see Davis (1969). The main advantage of this procedure is the transformation of the non-linear optimization problem (5.13) – (5.20), (5.23), (5.24), (5.36) – (5.44) to the linear constraint satisfaction problem (5.13) – (5.20), (5.23), (5.24), (5.36), (5.38) – (5.44), since M can be defined as a parameter.

1. Solve Static ExCTEPM:
   (a) Set a lower bound $LB = 1$, set an upper bound $UB = |T|$, set a test value $\lambda = (LB + UB)/2$, set a stopping criterion, e.g. $\mu_1 = 0.01$ and $\mu_2 = 0.5$.
   (b) Set $M = \lambda$ and solve the constraint satisfaction problem (5.13) – (5.20), (5.23), (5.24), (5.36), (5.38) – (5.44).
   (c) If a solution exists: set $UB = \lambda$.

(d) If no solution exists: set $LB = \lambda$.

(e) set $\lambda = (LB + UB)/2$.

(f) Go back to Step (b) if $1-(LB/UB) > \mu_1$ and $UB-LB > \mu_2$, otherwise STOP.

The binary search algorithm iteratively cuts the (remaining) search space into halves until one of the stopping criterions $1 - (LB/UB) \leq \mu_1$ or $UB - LB \leq \mu_2$ is met. The number of required iterations depends on the values of $|T|$, μ_1 and μ_2.
As discussed at the beginning of Section 5.2 the purpose of the static ExCTEPM heuristic is to generate values for all φ_{ij} variables since these variables mainly determine the evacuation plan. At this point, is must be clear that the outcome of the static ExCTEPM model – i.e. values for all φ_{ij} variables – is only intended to be used as input parameters for the original ExCTEPM. Hence, solutions computed on the basis of the static ExCTEPM heuristic are always solutions of the original (dynamic) ExCTEPM which was supplemented by prespecified (= fixed) values for all φ_{ij} variables.

As explained earlier in Section 5.2.1, the measure of risk usually relates to the distance to the center of risk. In the case of an evacuation with one highly endangered EPZ and several regular EPZs, highly endangered areas (i.e. the most endangered EPZ) need to be evacuated with higher priority since the risk of residing in the most endangered EPZ is much higher than in regular EPZs or safe zones (see (5.28)). This relation also holds between different EPZs so that more endangered areas have to be evacuated with higher priority than less endangered areas in general. These considerations can be implemented in the existing static ExCTEPM procedure by defining a set of EPZs $h = 0, \ldots, |H|$, composed of the most endangered EPZ and regular EPZs. Each cell in the evacuation network belongs to exactly one EPZ h. Additionally, we assume that $c_{it:i\in h} >> c_{it:i\in h+1}$ for all $h = 0, \ldots, |H| - 1$ holds so that cells within EPZ_0 take the highest c_{it} values of all cells in the evacuation network. Again, we assume that $|I| \in EPZ_{|H|}$.
It has to be mentioned that in the case of $|H| > 1$, there exist $|H|$ "copies" of constraint (5.36). Each copy h of (5.36) covers all cells i within EPZ_0,...,EPZ_h. Moreover, each copy is also characterized by a unique M_h. If instances with multiple levels of risk are solved, all M_h values are optimized successively by the binary search algorithm, starting with M_0. Here, it is important that a calculated value for M_h will still be present in the calculation of all succeeding computations (e.g. M_{h+1}, M_{h+2},...). This proceeding ensures that already computed M_h values for highly endangered areas will be kept for succeeding computations. Thus, all M_h values are considered in every iteration of the algorithm. For a specific EPZ h, all values $M_{h'}$ (with $h' = 0, \ldots, h-1$) have already been minimized by the binary search and all values $M_{h''}$ (with $h'' = h+1, \ldots, |H|$) are still set to $M_{h''} = |T|$.
The previously introduced algorithm can be extended as stated below:

1. Set $h = 0$.

2. Solve Static ExCTEPM:

   (a) Set a lower bound for EPZ h $LB_h = 1$, set an upper bound for EPZ h $UB_h = |T|$, set a test value $\lambda = (LB_h + UB_h)/2$, set $M_{h'} = |T|$ for all $h' = h, \ldots, |H|$, set a stopping criterion, e.g. $\mu_1 = 0.01$ and $\mu_2 = 0.5$.

   (b) Set $M_h = \lambda$ and solve the constraint satisfaction problem (5.13) – (5.20), (5.23), (5.24), (5.36), (5.38) – (5.44).

   (c) If a solution exists: set $UB_h = \lambda$.

(d) If no solution exists: set $LB_h = \lambda$.

(e) set $\lambda = (LB_h + UB_h)/2$.

(f) Go back to Step (b) if $1 - (LB_h/UB_h) > \mu_1$ and $UB_h - LB_h > \mu_2$, otherwise set $M_h = UB_h$ and go to Step 3/4.

3. *Fix all routing decisions (φ_{ij} values) for all cells i inside EPZs $0, \ldots, h$.*

4. Set $h = h + 1$.

5. Go back to Step 2 if $h < |H| + 1$, otherwise STOP.

The third step represents a slightly modified version of the original static ExCTEPM heuristic. In its standard form, traffic routing – in terms of φ_{ij} values – for all cells inside EPZs $0, \ldots, h$ is not fixed and has to be determined anew in each iteration h. (Please note that there is a difference between the fixation φ_{ij}-values and the fixation of M_h-values, because φ_{ij} determines the traffic routing and M_h the maximum occupation of cell connections within an EPZ h.) This fact may lead to computational issues for large networks (e.g. $|I| > 300$) if tight bounds exist for already computed EPZs h – in terms of preferably low values for $M_0, \ldots, M_{h-1}$. Therefore, we added the third step, which fixes traffic routing decision in terms of φ_{ij} for already computed EPZs. As this proceeding might affect solution quality negatively due to reduced solution space for succeeding computations of M_h values, it will only be applied for larger networks, i.e. Scenarios 8 and 9.
The assignment of a cell i to a EPZ h is raised by the parameter c_{it}. In detail, we assume that each EPZ is characterized by a predetermined measure of risk interval $[\underline{c}_{ht}, \overline{c}_{ht}]$ so that all cells $i \in I : \underline{c}_{ht} \leq c_{it} \leq \overline{c}_{ht}$ are part of EPZ h.
It has to be noticed that for the case of a Tsunami heading towards a city in a mountain area, EPZs defined in respect to the altitude may lead to incoherent EPZs. However, our approach can also be applied to such problems.

5.3 Computational Study

In order to prove effectiveness of our heuristic solution approaches, evacuation plans for nine large real-world evacuation scenarios will be computed in this section. The shortest-path based ExCTEPM as well as the static ExCTEPM heuristic were written in AMPL. Runtime requirements are denoted as "solvetime" in subsequent tables and are determined as the wall clock seconds. It turns out that CPLEX (see *http://www-01.ibm.com/software/integration/optimization/cplex-optimizer*) and GUROBI (see *http://www.gurobi.com*) perform better in the case of the static ExCTEPM, if an objective function is added to the (constraint satisfaction) model, although this objective function or the objective function value have absolutely no relevance for the constraint satisfaction problem or the procedure itself. For this purpose, we use $\min \sum_{i \in I} \sum_{j \in I} \eta_{ij} \cdot d_{ij}$ with $d_{ij} = ((c_i \cdot n_i) + (c_j \cdot n_j))/(l_i + l_j)$. Furthermore we will demonstrate a simple approach to compute lower bounds, which will help to evaluate solution quality if the optimum solution is unknown. We also tested the performance of different commercial state-of-the-art solvers, i.e. CPLEX 10.0.0 and GUROBI 3.0.1. It should be noticed that GUROBI runs on two cores of the CPU whereas CPLEX uses only one core, leading to a theoretical advantage of 50% in computation time for GUROBI. All tests were run on a computer using an Intel X9100 (3.06 Ghz), 8 GB of memory and Windows Vista (64-bit).

5.3.1 Basics

All real-world test scenarios take place in the city of Duisburg, Germany. This city is located in the western part of the Ruhr area and it can be regarded as a typical urban area because of high population density and the existence of an urban road system. The first six instances (Scenarios 1–6) are limited to the district of Neudorf, which can be found in the East of Duisburg. The last three instances (Scenarios 7–9) cover a larger area of Duisburg, namely the districts of Neudorf, Duissern, Hochfeld, Dellviertel and the old town. In detail, scenarios differ from each other in terms of network size, population size, distribution of risk as well as the number of EPZs, see Table 5.1 with NL as total network length, Veh. as total population (number of vehicles) in all cells and #Cells as the number of cells in the evacuation network including one supersink (without population). Values in brackets represent the number of vehicles starting in the corresponding cells.

Scenario	NL	Veh.	#Cells	#Cells EPZ_0	#Cells EPZ_1	#Cells EPZ_2
1	23 km	8,750	107	106 (8,750)	-	-
2	23 km	13,102	107	106 (13,102)	-	-
3	23 km	8,750	107	13 (1,407)	93 (7,343)	-
4	23 km	8,750	107	22 (2,500)	84 (6,250)	-
5	23 km	8,750	107	4 (486)	9 (921)	93 (7,343)
6	23 km	8,750	107	7 (655)	11 (1,396)	88 (6,699)
7	83 km	25,856	339	338 (25,856)	-	-
8	83 km	25,856	339	54 (6,270)	284 (19,586)	-
9	83 km	25,856	339	16 (1,340)	46 (4,414)	276 (20,102)

Table 5.1: Characteristics of Scenarios 1 – 9

The remaining parameters were set to the following values. We use the cell size optimization approach from Section 4.1.4 to determine cell sizes (and flow capacities (Q_i)) for all scenarios:

- Scenarios 1,2,7: $c_{it}^{EPZ_0} = 10^2 \cdot t$
- Scenarios 3,4,8: $c_{it}^{EPZ_0} = 10^4 \cdot t$, $c_{it}^{EPZ_1} = 10^2 \cdot t$
- Scenarios 5,6,9: $c_{it}^{EPZ_0} = 10^6 \cdot t$, $c_{it}^{EPZ_1} = 10^4 \cdot t$, $c_{it}^{EPZ_2} = 10^2 \cdot t$
- Scenarios 1–9: $c_{|I|,t} = 0 \cdot t$
- $p = 2$
- Scenarios 1–6: $Q_i = l_i \cdot 6$ for cells with 50 km/h and 30 km/h driving speed.

- Scenarios 7–9: $Q_i = l_i \cdot 5$ for cells with 50 km/h, 30 km/h and 100 km/h driving speed.
- Values for $|T|$ are calculated by dividing the total number of vehicles by the outflow capacities of all cells leading to the super sink, e.g. $8750/144 = 60.76$ for the case of Scenario 1. Afterwards this value is multiplied by 1.5, e.g. $60.76 \cdot 1.5 \approx 91$. It has to be noticed that the factor 1.5 might be too low in some cases, normally leading to no feasible solution, but in some rare cases also to feasible solutions with minor degradations of the objective function value. In our computational study, we increase the factor by steps of 0.5, leading to the factors 2, 2.5, 3, 3.5 and so on. On the other hand, these large factors might increase the planning horizon to levels where computational limits in terms of memory are reached. In such cases, we reduce the factors in steps of 0.05 until a solution can be obtained.

Additionally, we compute the number of constraints and variables for each scenario with AMPL to illustrate the dimensions of these instances. We set $|T| = 91$ for Scenarios 1,3–6 and $|T| = 136$ for Scenario 2. These values are calculated using the standard factor of 1.5 as discussed above.
For the computation of the number of constraints and variables in Scenarios 7–9, we set $|T| = 132$. Originally, $|T|$ for Scenarios 7–9 should have been set to $|T| = 141$ using again a factor of 1.5. Due to computational limits we were not able to compute the number of constraints and variables for Scenarios 7–9 using more than 132 periods representing a factor of 1.4. However, these numbers may also provide a sufficient estimation of problem size. Please note that this limitation has absolutely no relevance for the computational study since we are solving the ExCTEPM using φ_{ij} (and ϵ_{ij}) as parameters. The number of constraints and variables for each scenario can be found in Table 5.2. We also add the number of variables and constraints which were eliminated by AMPL's presolve.

Sc.	$\|T\|$	After AMPL's Presolve			Eliminated by AMPL's Presolve		Before AMPL's Presolve	
		#Constraints	#Variables					
			#Integer	#Linear	#Const.	#Var.	#Const.	#Var.
1	91	141,118	1,044	74,973	84,894	23,594	226,012	99,611
2	136	210,778	1,044	112,593	113,514	23,909	324,292	137,546
3	91	141,118	1,044	74,973	84,894	23,594	226,012	99,611
4	91	141,118	1,044	74,973	84,894	23,594	226,012	99,611
5	91	141,118	1,044	74,973	84,894	23,594	226,012	99,611
6	91	141,118	1,044	74,973	84,894	23,594	226,012	99,611
7	132	624,393	3,164	332,517	517,796	241,717	1,142,189	577,398
8	132	624,393	3,164	332,517	517,796	241,717	1,142,189	577,398
9	132	624,393	3,164	332,517	517,796	241,717	1,142,189	577,398

Table 5.2: #Constraints and #Variables in Scenarios 1–9

The relative gap for every solution is computed by the following equation:

$$gap = \frac{Sol - Sol_{best}}{Sol_{best}} \cdot 100 \tag{5.45}$$

where Sol_{best} is the objective function value of the best known feasible solution of the ExCTEPM from our experiments and Sol is the the objective function value of the solution of the ExCTEPM to be examined. This definition will lead to values of 0.0 for the best

known solution, to values of $gap \geq 0$ for feasible solutions and to values of $gap \leq 0$ for lower bounds. In order to scale all results to percent-values, multiplication by the factor 100 is included.
All solutions generated by our heuristics were evaluated using the original ExCTEPM with a slightly extended objective function, i.e. $\min \sum_{i \in I} \sum_{t \in T} c_{it} \cdot z_{it} + 10^{-5} \cdot \sum_{i,j \in I} \sum_{t \in T} y_{ijt}$ and $-10^{-6} \cdot \sum_{t \in T} x_{|I|,t}$. The first additional term ensures that no unnecessary vehicle movements occur, which might be the case if two adjacent cells share the same level of danger. The second additional term ensures that vehicles are not evacuating later than necessary. During our computational tests it also turned out that the second term helps to decrease computation time of the ExCTEPM significantly. Both heuristics define an evacuation plan by setting all φ_{ij} values for all $i, j \in I$. The precise evacuation flows (expressed by y_{ijt}) and the objective values are calculated in the original ExCTEPM with φ_{ij} as parameters. If multiple cell sizes are used, the computation of the final solution in Scenarios 1–6 is carried out by two steps. In the first step, constraint (5.4) will be relaxed and the remaining problem will be solved to a maximum mipgap of 0.1% using φ_{ij} values as parameters. The second step now uses the (integer) values of φ_{ij} (from the shortest-path or static ExCTEPM heuristic) and ϵ_{ij} (from the first step) as parameters to solve the original model formulation of the ExCTEPM including constraint (5.4). The computation time for the second step is very short, since all former integer variables are now fixed: Hence, the remaining problem becomes an LP. The second step can be missed, if only single cell sizes are used since constraint (5.4) would not exist in this case.
During our computational study, it turned out that the solutions obtained by the shortest-path based heuristic are not competitive compared to the solutions of the static ExCTEPM. Thus, we only tested the static ExCTEPM for Scenarios 7–9. Moreover, we also compare the results of using the static ExCTEPM in its original formulation and the modified formulation which fixes routing decisions of previously computed EPZs. The final solutions are computed in only one step which uses φ_{ij} and ϵ_{ij} values from the results of the (modified) static ExCTEPM as parameters. This step corresponds to the second step of the solution procedure for Scenarios 1–6 since only an LP has to be solved.

5.3.2 Computing Lower Bounds

Results of Section 5.3.4 will show that the original formulation of the ExCTEPM cannot be applied to large real-world instances. Thus, there clearly is a need for lower bounds in order to evaluate quality of the solutions generated by the shortest-path based ExCTEPM and the static ExCTEPM. For our purposes, we use the original model formulation of the ExCTEPM, but a simplified network. In detail, we replace every EPZ h and the super sink $|I|$ in the original evacuation network by exactly one cell i' leading to a network with $|H| + 1$ cells. All required parameters can be derived from the original network:

- The number of vehicles evacuating from a cell i' (representing EPZ_h) in the simplified network can be derived from the original network with $E_{i'} = \sum_{i \in EPZ_h} E_i$.

- The number of lanes connecting two cells i' and j' in the simplified network (representing EPZ_h and EPZ_{h+1}) can be determined manually by simply allocating as many lanes as possible from each cell at the outer border of EPZ h to lanes of cells at the inner border of the surrounding EPZ $h + 1$. A mathematical formulation would correspond to the following optimization model where $\epsilon_{i'j'}$ is the number of allocated lanes between EPZ h and EPZ g.

$$\epsilon_{i'j'} = \max \sum_{i \in EPZ_h} \sum_{j \in EPZ_g} \beta_{ij} \cdot \epsilon_{ij} \tag{5.46}$$

subject to

$$\sum_{j \in EPZ_g} \epsilon_{ij} \leq l_i \qquad i \in EPZ_h \tag{5.47}$$

$$\sum_{i \in EPZ_h} \epsilon_{ij} \leq l_j \qquad j \in EPZ_g \tag{5.48}$$

$$\epsilon_{ij} \in \mathbb{N}_0 \qquad i \in EPZ_h; j \in EPZ_g \tag{5.49}$$

- $\beta_{i'j'} = 1$, if two cell i' and j' in the simplified network (representing EPZ_h and EPZ_g in the original network) adjoin to each other, 0 otherwise. E.g. $\beta_{i'j'}$ matrix for Figure 5.1 looks like stated below:

$\beta_{i'j'}$	1 (EPZ_0)	2 (EPZ_1)	3 (EPZ_2)	4 (Safe Area)
1 (EPZ_0)	-	1	0	0
2 (EPZ_1)	1	-	1	0
3 (EPZ_2)	0	1	-	1
4 (Safe Area)	0	0	1	-

Table 5.3: $\beta_{i'j'}$ Values for the simplified network

As our tests include evacuation networks with three EPZs at maximum, the largest networks for computing lower bounds consist of four cells. Such dimensions can be handled easily with the original ExCTEPM model formulation.

5.3.3 Medium Urban Road Network (Scenarios 1–6)

The district of Neudorf is characterized by a street network with a total length of approximately 23 kilometers. Based on information from 2006, there are around 26,000 residents living in Neudorf. The street network can be modeled with 107 cells. For all computational tests using the static ExCTEPM, we set $\mu_1 = 0.01$ and $\mu_2 = 0.5$. In order to bound computation time of the static ExCTEPM, we limit the number of explored nodes to 75,000 and set a time limit of 1800 seconds per iteration. Based upon the information we gain from the lower bound solution, we could fine-adjust LB and UB to closer values which would help to lower computation time. Since the first iterations of solving the static ExCTEPM are solved extremely quickly, we resign these adjustments at this point. For the computation of the objective function value of the ExCTEPM (with parameters from the static ExCTEPM heuristic) as well as a starting point for the static ExCTEPM heuristic, we use $|T| = 91$ for Scenarios 1,3–6 and $|T| = 136$ for Scenario 2, each representing a factor of 1.5. The settings for $|T|$ to compute the objective function value of the ExCTEPM on the basis of the results from the shortest-path heuristic had to be set higher, i.e. $|T| = 182$ (factor 3.0) for Scenario 1 and Scenario 4, $|T| = 273/255$ (factor 3.0/2.8) for Scenario 2, $|T| = 152$ (factor 2.5) for Scenario 3 and Scenario 5 as well as $|T| = 213$ (factor 3.5) for Scenario 6. The computation of all shortest paths for the shortest-path based heuristic took about 47 seconds (+/- 0.6 seconds) in each scenario. The complete network is displayed in Figure 5.4.

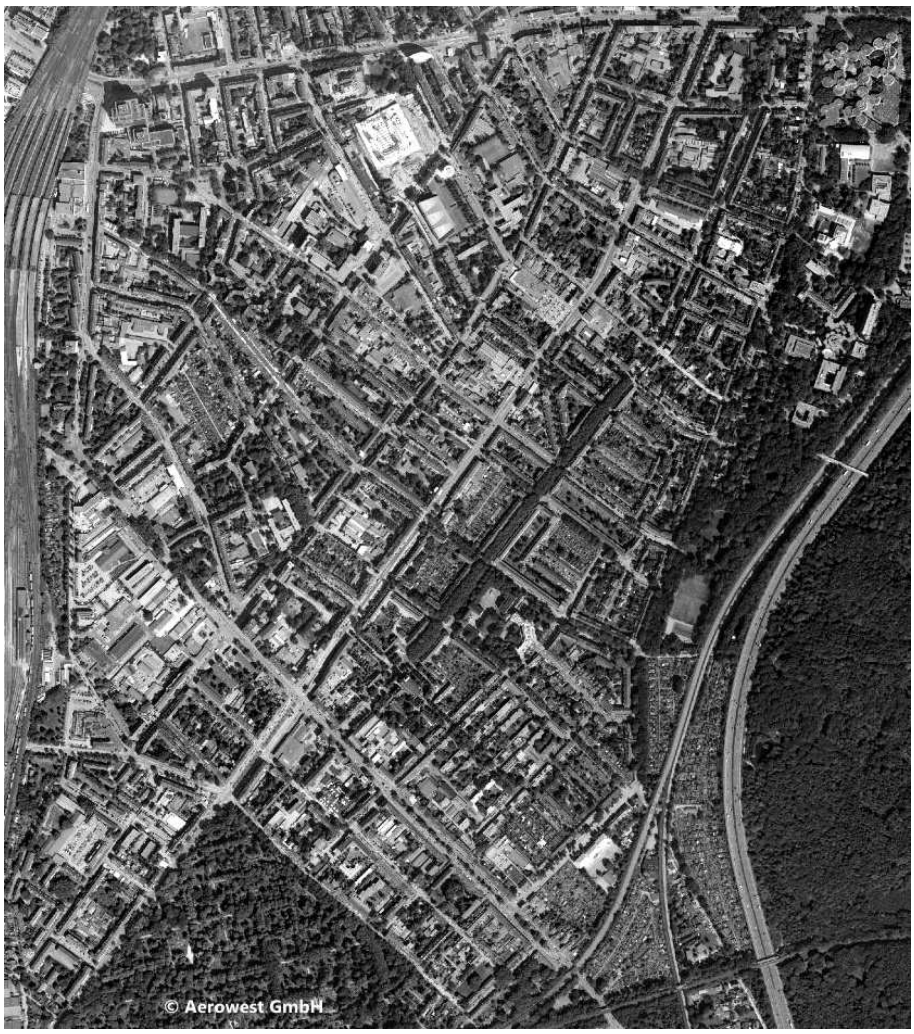

Figure 5.4: Medium Urban Road Network (Neudorf)

5.3.3.1 Scenario 1

Scenario 1 can be interpreted as a standard scenario since no special risk distribution is applied. In detail, the network is uniformly endangered, i.e. there is exactly one EPZ, see Figure C.1. This case may represent a preventative evacuation.

	gap [%]	solvetime [s]
Static ExCTEPM (CPLEX)	0.07	360
Static ExCTEPM (GUROBI)	0.00	209
Shortest Path ExCTEPM	99.52	693
LB	-13.12	< 1
LB ExCTEPM (CPLEX)	-9.15	-
ExCTEPM (CPLEX)	0.000	$> 21,600 (+7,200)$

Table 5.4: Scenario 1 Results

It can be easily recognized that the static ExCTEPM performs much better than the shortest-path based heuristic. In fact, the static ExCTEPM delivers very good solutions ($gap < 10\%$) with both software packages, but with an advantage for GUROBI in terms of computation time. The original ExCTEPM was not able to find a feasible solution within 6 hours (21,600 seconds) of computation time, so that the solution obtained by the static ExCTEPM was used as a starting point. After another 2 hours (7,200 seconds) of computation time, CPLEX was not able to improve the solution. Our lower bound solution is outperformed by the lower bound obtained by CPLEX after 2 hours of computation time. Figure 5.5 displays the solution for a small piece of the network in Scenario 1. Stops at the end of some arrows indicate barriers that can not be passed by vehicles.

Figure 5.5: Solution Example

As the graphical representation of solutions always look similar to Figure 5.5, we renounce to provide suchlike figures for other scenarios. Interested readers find a detailed graphical representation of an evacuation plan for Duisburg - Neudorf in Kimms and Maassen (2011b). We also decide only to use the reference solution of our heuristics as a starting point for the computation of the EXCTEPM since the computation of the EXCTEPM seems to be not very promising if no feasible solution can be found within 6 hours of computation time.

5.3.3.2 Scenario 2

Scenario 2 is very similar to Scenario 1 since risk is again distributed uniformly, see Figure C.2. However, population size in Scenario 2 is 50% higher than in Scenario 1.

	gap [%]	solvetime [s]
Static ExCTEPM (CPLEX)	0.00	1,546
Static ExCTEPM (GUROBI)	0.15	1,050
Shortest Path ExCTEPM	100.38	1,090
LB	-11.32	< 1
LB ExCTEPM (CPLEX)	-	-
ExCTEPM (CPLEX)	0.000	$> 7,200$

Table 5.5: Scenario 2 Results

The results show some similarities to Scenario 1: Again, the static ExCTEPM outperforms the shortest-path based heuristic. The static ExCTEPM with CPLEX results in a slightly better solution compared to GUROBI. The ExCTEPM was not able to enhance the solution generated by our heuristic. Furthermore, CPLEX was not able to compute a lower bound within 2 hours of computation time when the EXCTEPM was solved.

5.3.3.3 Scenario 3

This scenario is the first to include different levels of risk within the evacuation network. In detail, there is a center of risk in the center of the network surrounded by a lower endangered area, see Figure C.3. Due to the increased number of EPZs, more iterations are required when the static ExCTEPM is applied.

	gap [%]	solvetime [s]
Static ExCTEPM (CPLEX)	0.00	933
Static ExCTEPM (GUROBI)	4.59	271
Shortest Path ExCTEPM	79.36	478
LB	-31.34	< 1
LB ExCTEPM (CPLEX)	-20.20	-
ExCTEPM (CPLEX)	0.000	$> 7,200$

Table 5.6: Scenario 3 Results

The shortest-path heuristic shows again much worse results compared to the static ExCTEPM. Furthermore, GUROBI and CPLEX deliver different solutions when the static ExCTEPM is used. Although GUROBI achieves slightly lower values for M_h, the solution worsens about 5% compared to the static ExCTEPM computed by CPLEX. This fact shows that reaching the lowest feasible M_h values is no guarantee for obtaining the best solution. Again, the original ExCTEPM was not able to enhance the solution obtained by

the static ExCTEPM and our lower bound performs worse than the lower bound of the EXCTEPM after two hours of computation.

5.3.3.4 Scenario 4

This scenario also consists of two EPZs, but in contrast to Scenario 3, the center of risk is located in the north-western part of Neudorf, see Figure C.4. Additionally, EPZ_0 is much larger in terms of residents and the number of cells compared to Scenario 3. Hence, occupancy rate of exits might not be totally balanced since some exits are located nearby the more endangered area EPZ_0.

	gap [%]	solvetime [s]
Static ExCTEPM (CPLEX)	0.00	1,106
Static ExCTEPM (GUROBI)	10.44	386
Shortest Path ExCTEPM	145.51	629
LB	-53.47	< 1
LB ExCTEPM (CPLEX)	-30.98	-
ExCTEPM (CPLEX)	0.000	$> 7,200$

Table 5.7: Scenario 4 Results

The results of Scenario 4 are interesting in many ways. Firstly, the shortest-path based ExCTEPM performs extremely worse in comparison to Scenarios 1–3. Secondly, the gap between the best known solution and the best lower bound is larger than in all scenarios before. This might be caused by locating EPZ_0 on the edge of the network. The static ExCTEPM with GUROBI again obtains lower M_h values, but again the solution is about 10% inferior compared to the static ExCTEPM with CPLEX.

5.3.3.5 Scenario 5

Scenario 5 is the first scenario which includes three EPZs, see Figure C.5. Analogous to Scenario 3, the most endangered EPZ (EPZ_0) is situated in the center of the network, surrounded by a small EPZ_1. The number of residents and cells affected by a high measure of risk is the same as in Scenario 3.

	gap [%]	solvetime [s]
Static ExCTEPM (CPLEX)	0.92	757
Static ExCTEPM (GUROBI)	0.00	676
Shortest Path ExCTEPM	74.50	414
LB	-32.29	< 1
LB ExCTEPM (CPLEX)	-2.21	-
ExCTEPM (CPLEX)	0.000	$> 7,200$

Table 5.8: Scenario 5 Results

Results of Scenario 5 are surprising in several points. Firstly, the gap between the solution of the shortest-path based ExCTEPM is much lower than in Scenario 4. Secondly, the gap between the best known solution and the best lower bound is 2.21% which proves that the static ExCTEPM obtained a near-optimal solution. Thirdly, the ExCTEPM lower bound performs much better than our lower bound solution. In summary, it seems that it is easier to compute a high quality solution (and to prove quality) for this instance than for all previously discussed scenarios.

5.3.3.6 Scenario 6

Scenario 6 is the consequential continuation of the previously introduced scenarios. Similar to Scenario 5, three EPZs are taken into account, but here the center of risk is located in the south-western part of the network, see Figure C.6.

	gap [%]	solvetime [s]
Static ExCTEPM (CPLEX)	0.00	3,339
Static ExCTEPM (GUROBI)	0.20	606
Shortest Path ExCTEPM	34.34	966
LB	-52.36	< 1
LB ExCTEPM (CPLEX)	-41.02	-
ExCTEPM (CPLEX)	0.000	$> 7,200$

Table 5.9: Scenario 6 Results

The performance of the lower bounds, especially the lower bound computed by the ExCTEPM, show some analogies to Scenario 4, which is also characterized by a center of risk located on the edge of the evacuation network. This fact may lead to different or unbalanced occupancy rates of exits. Additionally, GUROBI shows advantages in proving feasibility / infeasibility during the computation of the static ExCTEPM. Furthermore, the ExCTEPM was not able to enhance the solution generated by the static ExCTEPM within 2 hours of computation, respectively.

5.3.4 Large Urban Road Network (Scenarios 7–9)

Around 77,000 residents are living in the districts of Neudorf, Duissern, Hochfeld, Dellviertel and the old town. The street network can be described by 339 cells of different cell sizes representing a total network length of approximately 83 kilometers. Again, we set $\mu_1 = 0.01$ and $\mu_2 = 0.5$. Additionally, we set the node limit of the B&B Tree to 75,000 nodes and we define a time limit of 1,800 seconds per iteration when the static ExCTEPM is solved. We set $|T| = 141$ (factor 1.5) for the static ExCTEPM in Scenarios 7 and 8. Due to computational limits, we have to lower this value for the computation of the solution the ExCTEPM, i.e. we set $|T| = 136$ (factor 1.45). The static ExCTEPM heuristic in Scenario 9 was conducted using $|T| = 188$ (factor 2.0).
Due to the fact that the shortest-path based ExCTEPM is outperformed by the static ExCTEPM in Scenarios 1 – 6, we decided not to apply the shortest-path based ExCTEPM, but only to use the static ExCTEPM heuristic for Scenarios 7-9. In contrast to Scenarios 1–6, we also derive lower bounds for the binary search algorithm from our lower bound computation of the ExCTEPM. For Scenarios 7 and 8, we were able to compute the objective values of the ExCTEPM using φ_{ij} and ϵ_{ij} as parameters. However, in Scenario 9, memory requirements were too high because of larger values for $|T|$ so that no objective values could be computed for this scenario. To give an idea of the solution quality we compare the M_h values of the static ExCTEPM heuristic to those values from our lower bound. Moreover, we apply the modified static ExCTEPM heuristic – which fixes traffic routing for all EPZs h with already computed M_h-values – for the first time. Network details can be extracted from Figure 5.6.

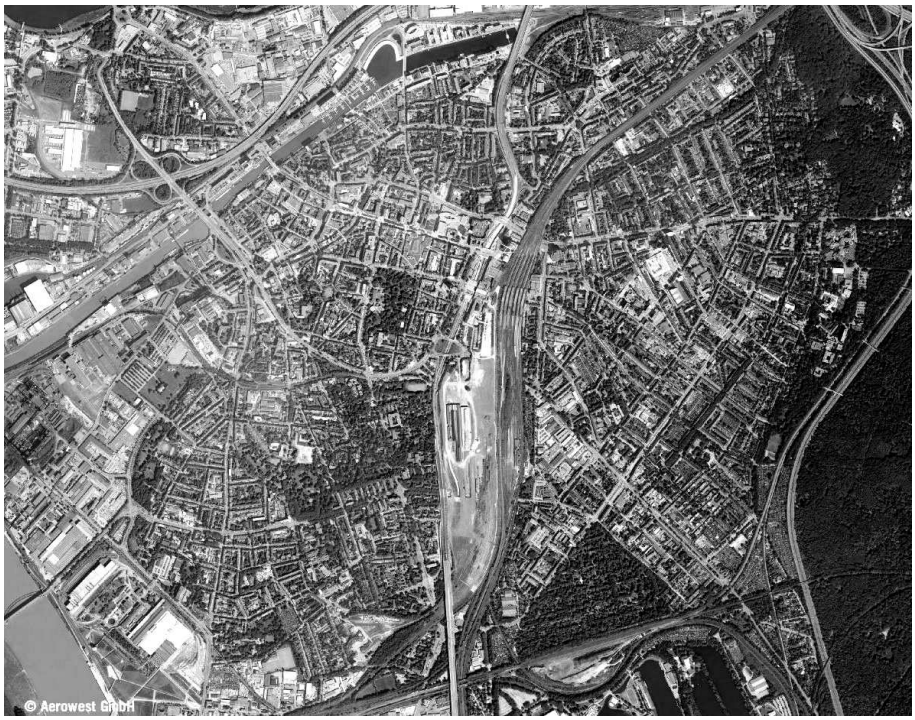

Figure 5.6: Large Urban Road Network (Duisburg)

5.3.4.1 Scenario 7

This scenario consists of only one EPZ leading to uniformly distributed risk in the complete network, see Figure C.7. The lower bound helps to reduce the number of iterations due to improved initial values for LB in the binary search algorithm, see Section 5.3.4.

	gap [%]	solvetime [s]
Static ExCTEPM (GUROBI)	0.00	313
LB	-24.89	< 1

Table 5.10: Scenario 7 Results

The static ExCTEPM (computed with GUROBI) finishes after about 313 seconds with a very promising solution. Here, the solution time is relatively short compared to Scenarios 1 and 2 because we additionally use ϵ_{ij} values (beside φ_{ij} values) as input parameters so that only an LP has to be solved after running the binary search algorithm. The gap between the best known solution and our lower bound is larger compared to Scenario 1. We do not apply CPLEX to this problem in order to keep computation time as low as possible. The difference between the M_0-values from the lower bound and from the heuristic solution is small, see Table 5.13.

5.3.4.2 Scenario 8

Analogous to Scenarios 3 and 4, this scenario also includes two EPZs. The center of risk is situated in the south-western part of the network, right in the middle of the district Hochfeld, see Figure C.8.
Although there is not much difference between the static ExCTEPM and the modified static ExCTEPM in solution quality, differences in computation time are quite larger.

	gap [%]	solvetime [s]
mod. Static ExCTEPM (GUROBI)	0.00	536
Static ExCTEPM (GUROBI)	3.77	4,629
LB	-48.15	< 1

Table 5.11: Scenario 8 Results

Since the modification of the static ExCTEPM is effective only after the "first" EPZ, values for M_0 are the same. The gap between the lower bound and the best known solution is relatively large compared to the results in Scenarios 1–6. This rising might be caused by the significantly increased network size.

5.3.4.3 Scenario 9

This scenario is the most complex scenario in the computational study due to the large network size and the existence of three EPZs. The center of risk is located in the north-eastern part of the network, touching the districts Neudorf and Duissern, see Figure C.9.

	LB	static ExCTEPM	mod. static ExCTEPM
M_0	13	20.52 (+57.8%)	20.52 (+57.8%)
M_1	30	65.18 (+117.3%)	59.63 (+98.8%)
M_2	95	167.66 (+76.5%)	173.47 (+82.6%)

Table 5.12: Scenario 9 Results

The results from the static ExCTEPM and the modified static ExCTEPM differ significantly in computation time and values for M_h. In detail, computation time for the modified static ExCTEPM (static ExCTEPM) was 60.1 seconds (3,111 seconds). This shows that the modification can have tremendous effects on solution quality (in terms of M_h values) and computation time. This scenario also shows benefits and weaknesses of the modified static ExCTEPM. On the one hand, the value for M_1 is lower compared to the standard static ExCTEPM although the M_0 values are the same. This illustrates that the fixation of traffic routing decisions in a previous step may lead to lower M_h values in the succeeding computations due to easier finding of feasible solutions. On the other hand, the modified static ExCTEPM achieves a higher value for M_2, which might be the result of already fixed traffic routing decisions reducing the search space compared to the standard static ExCTEPM. As already mentioned in the discussion of Scenarios 4 and 6, the situation of the center of risk on the edge of the network may affect the number of vehicles using the nearby located exits. This may lead to unbalanced occupancy rates that are not covered in the computation of the lower bound values for M_h.

5.3.5 Summary

The performance of the shortest-path based ExCTEPM is disappointing for every scenario, except Scenario 6. In contrast, the static EXTEPM outperforms the shortest-path based ExCTEPM in every scenario. Furthermore, the static ExCTEPM obtains very good or even near optimal (Scenario 5) solutions in less computational time. If the same two step solution procedure used in Scenarios 1-6 would have been applied to Scenarios 7–9, computation times would have been a lot longer. However, using φ_{ij} and ϵ_{ij} values as parameters, computation times for Scenarios 7 and 8 could be lowered significantly since ϵ_{ij} values were already determined. Attempts to apply the ExCTEPM to Scenario 9 fail

because of too high memory requirements.
We also compare the ratio between the lower bound and the static ExCTEPM (GUROBI) values for M_h with the ratio of these values in selected scenarios, see Table 5.13.

		Lower Bound	(mod.) static ExCTEPM
Scenario 1	M_0	61	64.28 (+5.4%)
Scenario 7	M_0	95	103.63 (+9.1%)
Scenario 4	M_0	18	28.77 (+59.8%)
	M_1	61	76.23 (+25.0%)
Scenario 8	M_0	44	54.61 (+24.1%)
	M_1	95	109.38 (+15.1%)
Scenario 6	M_0	7	15.06 (+115.1%)
	M_1	13	35.10 (+170.0%)
	M_2	61	79.75 (+30.7%)
Scenario 9	M_0	13	20.52 (+57.8%)
	M_1	30	59.63 (+98.8%))
	M_2	95	173.47 (+82.6%)

Table 5.13: Comparison between Scenarios (1 $\Leftrightarrow$ 7), (4 $\Leftrightarrow$ 8), (6 $\Leftrightarrow$ 9)

We choose Scenario 1 (for comparison with Scenario 7), Scenario 4 (compared with Scenario 8) and Scenario 6 (compared with Scenario 9) since the number and location of EPZs are comparable. The relative differences are quite small, see Table 5.13.
The introduced method to deduce lower bounds on the basis of a simplification of the original evacuation network turns out to work well, especially when only one EPZ exists. For more than one EPZ, our lower bound is clearly outperformed by the lower bound from the ExCTEPM. However, even for very large networks, this lower bound can be computed with very little computational effort and helps to evaluate solution quality.

Chapter 6

Evacuation Planning with Rescue Teams

The basic ideas of the Cell-Transmission-Model (CTM) by Daganzo (1994) were used in in the previous chapters for evacuation planning in urban areas. However, no approach considers the assignment of rescue teams which will be needed in case of fire fighting, bomb disposal or evacuating public buildings like hospitals. In evacuation scenarios, traffic capacities are limited and have to be used as efficiently as possible to reduce danger for the population. Rescue teams usually have to enter the network in opposite driving direction to evacuating vehicles so that difficulties in traffic routing are unavoidable.
To the best of our knowledge, the assignment of rescue teams in the scope of evacuation planning is only discussed in Xie and Turnquist (2009) and Bretschneider (2011) up to now. Xie and Turnquist (2009) present a (static) lane-based discrete network design model which is combined with a stochastic traffic flow equilibrium framework. Due to its bi-level structure and its combinatorial characteristics, this problem is non-convex. Therefore, the authors develop a Lagrangian-based Tabu Search Heuristic which is preceded by a shortest path heuristic to determine the rescue team routes. A similar problem can be found in Bretschneider (2011). The author considers the problem of finding routes for shuttle buses within an evacuation. Since crossing conflicts can not always be avoided when shuttle buses are implemented, penalties for crossing conflicts are introduced.
In this chapter, we will introduce an extension for the ExCTEPM which allows to integrate rescue team (contra-)flow into evacuation planning simultaneously. Two types of (in- and outflowing) traffic participants (evacuating vehicles and rescue teams) will be considered. On the basis of this model, we will integrate the assignment of rescue teams in a flexible framework and reoptimize evacuation planning taking the rescue team route determination into account. Due to the dynamic nature of our model, we will be able to generate time-dependent schedules for rescue teams, to coordinate evacuation traffic and rescue traffic simultaneously, to find optimal (i.e. least disruptive) routes for the rescue teams and to reoptimize evacuation traffic routing under consideration of rescue team routes.
Another possible optimization approach might consist of “Bi-level programming” where the shortest travel time of rescue team vehicles to destination cells will be determined under the condition that total danger for evacuees will be minimized. Suchlike approaches are reasonable in this context, but we will not get back to this approach in this work.
We present a three-staged heuristic procedure which is able to solve real world cases with up to 8750 vehicles within reasonable time. This chapter is based on the work of Kimms and Maassen (2010b). To ensure self-containedness of this chapter, we will repeat some already introduced constraints and explanations. This procedure should also help

to enhance readability since a large number of constraints will be utilized.

6.1 Integrating Rescue Team Traffic

Some disasters may include the need for routing rescue teams to the origin of danger in order to limit even more danger for the population. However, the assignment of rescue teams in evacuation scenarios is not trivial since the following questions have to be answered:

1. Where are rescue teams positioned?
2. Which route(s) will rescue teams use?
3. When will the route(s) be reserved for rescue teams?
4. How can street or lane closures be organized?

We want to discuss these questions briefly. Rescue teams can be located inside or outside the considered urban street network which needs to be evacuated. Large urban areas usually take advantage of an own fire department so that for example small or medium fire fighting operations can be carried out by the local fire department. In the case of larger fires or threats that exceed the capabilities of a local fire department in terms of the number of fire fighters or special-trained experts (e.g. bomb disposal expert), additional rescue teams outside the considered network must be called. Depending on the dimension of the incident, external rescue teams have to choose one or more network entrance(s) under consideration of evacuation traffic and distance to the operational area. Thus, the number of required routes for rescue teams and the determination of the routes themselves depend to the capacity and position of demanded (special-trained) rescue teams.
In this chapter, we will focus on scenarios where rescue teams "just" have to arrive at the origin of danger at a predefined point of time at the latest. Here, street sections must be reserved for rescue team traffic before rescue team traffic occurs. For safety reasons, there should also be at least some time buffer between rescue team and evacuation traffic. Suchlike scenarios additionally offer the ability to open originally closed streets for evacuation traffic after rescue teams passed these streets, but again, there should be a time buffer included.
The amount of rescue team vehicles is relatively low compared to the number of evacuating vehicles. Thus, it actually should be sufficient to reserve only a single lane for rescue team traffic. However, this would also lead to several problems. Firstly, evacuees may not accept the need to reserve some lanes for rescue traffic. Instead, they may think that these lanes (although closed for evacuation traffic) represent a faster way to escape leading to accidents with rescue teams at worst. Secondly, routing rescue teams through a multi-lane street network is even more complex than routing through streets. Especially turning moves need special attention to avoid traffic crossing conflicts at junctions. Thus, we decided to reserve whole street sections for rescue team traffic to avoid the last-mentioned difficulties.

6.2 ExCTEPM with Rescue Teams

Since the presented model in this chapter mainly bases on the discussed ExCTEPM, a large portion of the notation is identical. However, new parameters and decision variables are needed to cover rescue teams so that we will first introduce the complete notation. Afterwards, the complete model formulation will be presented. Due to the increased complexity of the model formulation, we will provide explanations in close proximity.

6.2.1 Notation

Sets:

- Let $I = \{1, \ldots, |I|\}$ be the index set of cells in the evacuation network, where $|I|$ is a super sink for evacuation traffic. This set can be classified by relevance for rescue teams, network exits and cell size.
- We denote I_R ($I_R \subset I$) as the index set of destination cells for rescue teams, i.e. the set of cells with a positive demand for rescue teams.
- The subset I_S ($I_S \subset I$) is the index set of "exit-cells" including all cells connected to the super sink $|I|$ ($I_S = \{i \in I : \beta_{i,|I|} = 1\}$).
- The cell size of a cell can be integer multiples of a "standard" cell size, where $N = \{1, \ldots, |N|\}$ is the index set of (integer) cell size multipliers. Hence, a cell of size n can be passed in at least n periods and I_n is the index set of cells of cell size n.
- The parameter n_i indicates the size of cell i. More detailed explanations can be found in Section 4.1.1.
- Furthermore, the index set of periods is $T = \{1, \ldots, |T|\}$, where $|T|$ is the index of the last period.

Parameters: Each cell i ($i \in I$) can be described by several characteristics, namely

- the danger of being at cell i in period t c_{it} ($c_{it} \geq 0$),
- the maximum vehicle capacity on all lanes N_{it},
- the number of vehicles E_i starting their evacuation in cell i,
- the maximum number of in- and outflowing vehicles on all lanes per period into/from cell i in period t Q_{it},
- the number of lanes l_i,
- the number of rescue team vehicles P_i which are positioned in cell i and
- the minimum demand of rescue team vehicles in cell i D_i.

In addition, there are also some non-cell-specific parameters:

- β_{ij} ($= \beta_{ji} = 1$) denotes that cell i and cell j are connected so that a traffic flow from cell i to cell j (and vice versa) can be established, $\beta_{ij}(= \beta_{ji}) = 0$ otherwise.
- Time buffers – measured in number of periods – between the occurance of rescue team traffic and succeeding evacuation traffic (evacuation traffic and succeeding rescue team traffic) are captured in δ^+ (δ^-).
- t_r is a specific predetermined period in the planning horizon, where rescue team vehicles must have arrived at destination cells at the latest.
- $\hat{t}_i$ is necessary to consider traveling times of externally positioned rescue teams, where $\hat{t}_i + 1$ is the first period where rescue teams may travel from the super sink to a network entrance cell i ($i \in I_S$).

Decision Variables: When we consider a cell in a certain period, the following actions may take place. Residents start their evacuation, vehicles en route reside in this cell (e.g. due to congestion) or vehicles leave / enter this cell. These processes are captured in the following decision variables:

- The number of vehicles starting their evacuation at cell i in period t is b_{it}.
- x_{it} is the number of residing vehicles in cell i at the end of period t.
- y_{ijt} denotes the number of vehicles leaving cell i in period t and reaching cell j in period $t+1$. Please note that it is sufficient to consider only those flow variables y_{ijt} (and y^r_{ijt}) where $\beta_{ij} = 1$ holds.
- z_{it} covers these values by including all residing, leaving and waiting vehicles in cell i in period t.

In terms of rescue team integration into evacuation planning, we decided to use a cell-based integration of rescue traffic instead of lane-based integration due to the reasons annotated in Section 6.1. Hence, a cell i in period t can either be used by evacuation traffic or rescue team traffic, but not simultaneously. Therefore, we introduce two new binary decision variables, namely

- σ_{it} denotes whether a cell i in period t can be used for evacuation traffic ($\sigma_{it} = 0$) or rescue traffic ($\sigma_{it} = 1$).
- r_{ijt} is 1, if and only if rescue team traffic flows from cell i to cell j in period t, otherwise 0.

The final evacuation plan can be derived from φ_{ij} ($\varphi_{ij} \in \{0, 1\}$) and ϵ_{ij} ($\epsilon_{ij} \in \mathbb{N}_0$), where

- φ_{ij} is 1, if evacuation traffic flows from cell i to cell j, 0 otherwise.
- ϵ_{ij} represents the number of lanes between cell i and cell j used for evacuation traffic.

The assignment of rescue teams in the context of CTM-based evacuation planning can be regarded as the interlocking of two interdependent CTM-based traffic routing problems. Therefore, the decision variables for rescue team traffic, namely x^r_{it}, y^r_{ijt}, b^r_{it}, φ^r_{ij} and ϵ^r_{ij} can be defined referring to the already known decision variables for evacuation traffic. The final assignment plan for rescue teams can be derived from these variables.

6.2.2 Model Formulation

Based on the introduced sets, parameters and decision variables, the mixed integer linear optimization model for Cell-Transmission-based evacuation planning with rescue teams can be formulated as follows:

$$\min \sum_{i \in I} \sum_{t \in T} c_{it} \cdot z_{it} \tag{6.1}$$

The objective function (6.1) minimizes the number of vehicles exposed by a certain level of danger c_{it} in a period t and at a certain cell i. In detail, vehicles are more endangered for larger values for c_i and t. In Addition to (6.1), numerous constraints are needed:

$$z_{it} = x_{it} + \sum_{j \in I} y_{ijt} + (E_i - \sum_{\tau=1}^{t} b_{i\tau}) \qquad i \in I\ ;\ t \in T \tag{6.2}$$

$$x_{it} = b_{it} + x_{i,t-1} + \sum_{j \in I} y_{ji,t-1} - \sum_{j \in I} y_{ijt} \qquad i \in I\ ;\ t = 2, \ldots, |T| \tag{6.3}$$

Equation (6.2) ensures that all vehicles residing, leaving or waiting in cell i are involved in the objective function. (6.3) is a standard vehicle flow constraint, whereas the number of residing vehicles at the end of period t equals the number of vehicles starting their evacuation in period t plus the number of residing vehicles in cell i at the end of period $t-1$ plus the number of inflowing vehicles reaching cell i in period t minus the number of outflowing vehicles leaving cell i, respectively. This definition also holds for rescue team traffic with the corresponding decision variables, see (6.4).

$$x^r_{it} = b^r_{it} + x^r_{i,t-1} + \sum_{j \in I} y^r_{ji,t-1} - \sum_{j \in I} y^r_{ijt} \qquad i \in I\ ;\ t = 2, \ldots, |T| \tag{6.4}$$

Figure 6.1 outlines constraints (6.3) and (6.4) for a single cell with two lanes:

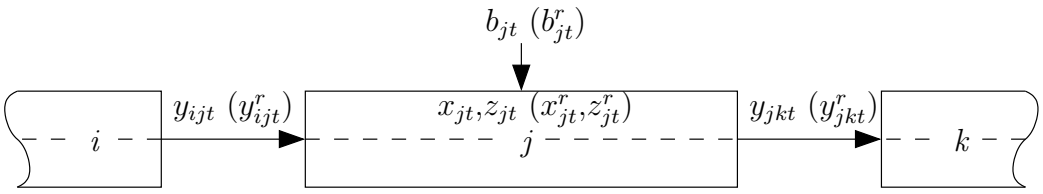

Figure 6.1: Graphical Illustration of (6.3) and (6.4)

If cells of size $n \geq 2$ are used, additional constraints are needed to capture travel times of at least n periods for a cell of size n, see constraints (6.5) and (6.6).

$$\sum_{j \in I} \sum_{\tau=1}^{t} y_{ij\tau} \leq \sum_{j \in I} \sum_{\tau=1}^{\max(t-n_i,1)} y_{ji\tau} + \sum_{\tau=1}^{\max(t-\lceil n_i/2 \rceil+1,1)} b_{i\tau} + x_{i1} \quad i \in I : n_i \geq 2\ ;\ t = 2, \ldots, |T| \tag{6.5}$$

Constraint (6.5) limits the cumulated number of vehicles leaving a cell i between period 1 and period t to the cumulated number of vehicles entering the cell between period 1 and period $t - n_i$ plus the vehicles starting their evacuation between period 1 and period $t - \lceil n_i/2 \rceil + 1$ plus the initial street occupation in terms of x_{i1}, whereas n_i is the size of cell i. This constraint ensures that vehicles starting their evacuation in other cells need at least n periods to pass this cell. Residents in cell i start their evacuation in the "center" of the cell if the term $t - \lceil n_i/2 \rceil + 1$ is used. However, this approach allows to modify the "starting point" as desired by the decision maker. Because of (6.3), this constraint only needs to be defined for cells i of size $n_i \geq 2$. Of course, all these assumptions and restrictions also apply to rescue team traffic, see (6.6).

$$\sum_{j\in I}\sum_{\tau=1}^{t} y^r_{ij\tau} \leq \sum_{j\in I}\sum_{\tau=1}^{\max(t-n_i,1)} y^r_{ji\tau} + \sum_{\tau=1}^{\max(t-\lceil n_i/2\rceil+1,1)} b^r_{i\tau} + x^r_{i1} \quad i \in I : n_i \geq 2\ ;\ t = 2,\ldots,|T| \tag{6.6}$$

As every street section has only limited capacities for vehicles, corresponding constraints are necessary:

$$z_{it} \leq N_{it} + (E_i - \sum_{\tau=1}^{t} b_{i\tau}) \qquad i \in I\ ;\ t \in T \tag{6.7}$$

$$x_{it} \leq N_{it} \qquad i \in I\ ;\ t \in T \tag{6.8}$$

Constraint (6.7) ensures that the number of vehicles (incl. all vehicles that have not left their homes, yet) in a cell i during a period t does not exceed the maximum capacity of this cell plus the number of vehicles which have not entered the network so far. Similar to (6.7), constraint (6.8) (and (6.9) for rescue team traffic) force the number of evacuation (or rescue team vehicles) in cell i at the end of period t to be lower than the maximum capacity of this cell.

$$x^r_{it} \leq N_{it} \qquad i \in I\ ;\ t \in T \tag{6.9}$$

As discussed in Section 6.1, the position of rescue teams and the demand for rescue teams have to be considered in the model formulation.

$$x^r_{it} \geq D_i \qquad i \in I_R\ ;\ t \in t_r,\ldots,|T| \tag{6.10}$$

$$\sum_{t\in T} b^r_{it} \leq P_i \qquad i \in I \tag{6.11}$$

Constraint (6.10) guarantees that the demand for rescue teams in a cell i will be met until a prespecified period in the planning horizon (t_r) to the end of the planning horizon. The position of rescue teams is captured in (6.11). This constraint limits the number of departing rescue team vehicles to the available rescue team vehicles in cell i.
In the context of evacuation planning, it has to be ensured that all endangered persons will leave their homes, see (6.12). Equation (6.13) secures that all evacuees will arrive at safe destinations (i.e. the super sink $|I|$), where x_{i1} represents an initial occupation of street sections before the evacuation starts, e.g. due to rush hour traffic. However, we assume in the following that no initial traffic in terms of x_{i1} exists, see (6.54).

$$\sum_{t\in T} b_{it} = E_i \qquad i \in I \tag{6.12}$$

$$x_{|I|,|T|} = \sum_{i\in I}(E_i + x_{i1}) \tag{6.13}$$

The number of (evacuation or rescue team) vehicles leaving cell i and entering cell j in a period t is limited in several ways:

$$\sum_{i\in I} y_{ijt} \leq (N_{jt} - x_{jt}) \qquad j \in I\ ;\ t \in T \tag{6.14}$$

$$y_{ijt} \leq \frac{Q_{jt}}{l_j} \cdot \epsilon_{ij} \qquad i,j \in I \ ; \ t \in T \tag{6.15}$$

$$y_{ijt} \leq \frac{Q_{it}}{l_i} \cdot \epsilon_{ij} \qquad i,j \in I \ ; \ t \in T \tag{6.16}$$

$$y_{ijt} \leq N_{it} \cdot \beta_{ij} \qquad i,j \in I \ ; \ t \in T \tag{6.17}$$

(6.14) limits the number of cell-changing vehicles to the space in the destination cell j, which is currently not occupied by residing vehicles. Moreover, constraints (6.15) and (6.16) ensure that the number of cell-changing vehicles does not exceed the in- or outflow capacities of the origin or destination cell. Constraint (6.17) additionally limits traffic flow per period to N_{it} and existing connections. These explanations also apply to cell-changing rescue team vehicles, see (6.18)– (6.21).

$$\sum_{i \in I} y^r_{ijt} \leq (N_{jt} - x^r_{jt}) \qquad j \in I \ ; \ t \in T \tag{6.18}$$

$$y^r_{ijt} \leq \frac{Q_{jt}}{l_j} \cdot \epsilon^r_{ij} \qquad i,j \in I \ ; \ t \in T \tag{6.19}$$

$$y^r_{ijt} \leq \frac{Q_{it}}{l_i} \cdot \epsilon^r_{ij} \qquad i,j \in I \ ; \ t \in T \tag{6.20}$$

$$y^r_{ijt} \leq N_{it} \cdot \beta_{ij} \qquad i,j \in I \ ; \ t \in T \tag{6.21}$$

During the introduction of all sets, parameters and decision variables at the beginning of this section, we already discussed how to integrate rescue team traffic into evacuation planning. We decided to implement a cell-based integration of rescue teams instead of a lane-based integration and to add time buffers between rescue team and evacuation traffic. By doing so, we aim to increase safety and to avoid accidents between evacuating vehicles and rescue teams vehicles since evacuation traffic routes and rescue traffic routes may cross or touch each other. (M' is a large number.)

$$\sum_{j \in I} \sum_{\tau = g(t)}^{t} y^r_{ij\tau} + \sum_{j \in I} \sum_{\tau = g(t)}^{t} y^r_{ji\tau} + \sum_{\tau = g(t)}^{t} x^r_{i\tau} \leq \sigma_{it} \cdot M' \qquad i = 1, \ldots, |I| - 1 \ ; \ t \in T \tag{6.22}$$

$$\sum_{j \in I} \sum_{\tau = g^r(t)}^{t} y_{ij\tau} + \sum_{j \in I} \sum_{\tau = g^r(t)}^{t} y_{ji\tau} + \sum_{\tau = g^r(t)}^{t} x_{i\tau} \leq (1 - \sigma_{it}) \cdot M' \quad i = 1, \ldots, |I| - 1 \ ; \ t \in T \tag{6.23}$$

Constraints (6.22) and (6.23) assure that cells can either be used for evacuation traffic or rescue team traffic. Additionally, these constraints make sure that time buffers δ^+ (δ^-) will be considered. The functions $g(t)$ and $g^r(t)$ are defined as $g(t) = \max(1, t - \delta^+)$ and $g^r(t) = \max(1, t - \delta^-)$. Since interactions of (6.22) and (6.23) are more complex, a simple example consisting of 12 periods with $\delta^+ = 2$, $\delta^- = 3$ and $\sigma_{it} = 1$ for $t = 6, \ldots, 9$ ($\sigma_{it} = 0$, otherwise) will be studied. For this purpose, we rewrite (6.22) and (6.23), respectively, as

$$\sum_{\tau = g(t)}^{t} LHS^{(6.22)}_{\tau} \leq \sigma_{it} \cdot M' \qquad i = 1, \ldots, |I| - 1 \ ; \ t \in T \tag{6.24}$$

$$\sum_{\tau=g^r(t)}^{t} LHS_{\tau}^{(6.23)} \leq (1-\sigma_{it}) \cdot M' \qquad i = 1,\ldots,|I|-1 \ ; \ t \in T \tag{6.25}$$

where

$$LHS_{\tau}^{(6.22)} = \sum_{j \in I} y_{ij\tau}^{r} + \sum_{j \in I} y_{ji\tau}^{r} + x_{i\tau}^{r} \tag{6.26}$$

$$LHS_{\tau}^{(6.23)} = \sum_{j \in I} y_{ij\tau} + \sum_{j \in I} y_{ji\tau} + x_{i\tau} \tag{6.27}$$

Given this, Table 6.1 provides insight into which decision variables must be equal to zero and which ones may have a positive value.

For $\sigma_{it} = 0$ in period 1,2,10,11,12, rescue traffic is prohibited by (6.22) and evacuation traffic is allowed by (6.23). In period 6 and 7 with $\sigma_{it} = 1$, rescue traffic is possible due to (6.22), but evacuation traffic is forbidden because of (6.23). The transition area between evacuation traffic and rescue team traffic (and vice versa) can be found in period 3,4,5,8,9 with $\sigma_{it} = 0$ for $t = 3,4,5$ and $\sigma_{it} = 1$ for $t = 8,9$. This transition is caused by δ^- prohibiting evacuation traffic in period 3,4,5 because of $\sigma_{i,6} = 1$ and δ^+ prohibiting rescue team traffic in period 8 and 9 due to $\sigma_{i,10} = 0$. In general we can say that evacuation traffic will not flow in a period t' with $\sigma_{i,t'} = 1$ and the last δ^- periods before a consecutive row of $\sigma_{it} = 1$ starts.

Evacuation Traffic has also to be blocked at intersections, when rescue team traffic passes this intersection. We use the constraints (6.28) and (6.29) to ensure that rescue team traffic and evacuation traffic not use the same junction at the same time, also considering the time buffers δ^+ and δ^-.

$$y_{ijt}^{r} \leq r_{ijt} \cdot M' \qquad i,j \ \in I \ ; \ t \in T \tag{6.28}$$

$$\sum_{\tau=\max(1,t-\delta^-)}^{\min(|T|,t+\delta^+)} y_{uw\tau} \leq (1-r_{ijt}) \cdot M' \qquad i,j,u,w \in I; \ t \in T : \beta_{ij} = \beta_{iu} = \beta_{iw} = \beta_{ju} = \beta_{jw} = \beta_{uw} = 1 \tag{6.29}$$

According to Section 4.1.2, logical constraints are needed to describe relations between structural decision variables and to guarantee real-world-applicability:

$$\varphi_{ij} \leq \beta_{ij} \qquad i,j \in I \tag{6.30}$$

$$\epsilon_{ij} \leq \varphi_{ij} \cdot \min\{l_i, l_j\} \qquad i,j \in I \tag{6.31}$$

Constraint (6.30) secures that vehicles can flow from cell i to cell j if, and only if a connection in terms of $\beta_{ij} = 1$ between these cells exist. Furthermore, the number of lanes which will be used for evacuation flow between cell i and cell j is limited by φ_{ij} and the minimum number of lanes regarding cell i and cell j, see (6.31).

So far, evacuation plans may lead to odd situations which are not applicable in real world. Imagine a small part of a network with traffic flows as shown in Figure 3.5. In this case, the

t	τ	σ_{it}	$LHS_\tau^{(6.22)}$	$LHS_\tau^{(6.23)}$	
1	1	0	≤ 0	$\leq M'$	
2	1	0	≤ 0	$\leq M'$	Evacuation Traffic
2	2	0	≤ 0	$\leq M'$	
3	1	0	≤ 0	$\leq M'$	
3	2	0	≤ 0	$\leq M'$	
3	3	0	≤ 0	$\leq M'$	
4	1	0	$-$	$\leq M'$	
4	2	0	≤ 0	$\leq M'$	
4	3	0	≤ 0	$\leq M'$	δ^-
4	4	0	≤ 0	$\leq M'$	
5	2	0	$-$	$\leq M'$	
5	3	0	≤ 0	$\leq M'$	
5	4	0	≤ 0	$\leq M'$	
5	5	0	≤ 0	$\leq M'$	
6	**3**	1	$-$	≤ 0	
6	**4**	1	$\leq M'$	≤ 0	
6	**5**	1	$\leq M'$	≤ 0	
6	6	1	$\leq M'$	≤ 0	Rescue Team Traffic
7	4	1	$-$	≤ 0	
7	5	1	$\leq M'$	≤ 0	
7	6	1	$\leq M'$	≤ 0	
7	7	1	$\leq M'$	≤ 0	
8	5	1	$-$	≤ 0	
8	6	1	$\leq M'$	≤ 0	
8	7	1	$\leq M'$	≤ 0	
8	8	1	$\leq M'$	≤ 0	δ^+
9	6	1	$-$	≤ 0	
9	7	1	$\leq M'$	≤ 0	
9	8	1	$\leq M'$	≤ 0	
9	9	1	$\leq M'$	≤ 0	
10	7	0	$-$	$\leq M'$	
10	**8**	0	≤ 0	$\leq M'$	
10	**9**	0	≤ 0	$\leq M'$	
10	10	0	≤ 0	$\leq M'$	
11	8	0	$-$	$\leq M'$	
11	9	0	≤ 0	$\leq M'$	Evacuation Traffic
11	10	0	≤ 0	$\leq M'$	
11	11	0	≤ 0	$\leq M'$	
12	9	0	$-$	$\leq M'$	
12	10	0	≤ 0	$\leq M'$	
12	11	0	≤ 0	$\leq M'$	
12	12	0	≤ 0	$\leq M'$	

Table 6.1: Example of (6.22) and (6.23) for a cell i with $\sigma_{it} = 1$ for $t = 6, \ldots, 9$ ($\sigma_{it} = 0$, otherwise), $\delta^+ = 2$ and $\delta^- = 3$

ExCTEPM tries to circumvent the bottleneck from cell i to cell k by creating an additional traffic flow from cell i to cell j finally reaching cell k. Such situations are undesired in real world applications as they imply vehicles to turn over in cell j. However, suchlike situations are forbidden by (6.32) as traffic flows from cell j to cell k (dashed line) can not be established if traffic flows from cell i to cell j and connections between cell i, j and k in terms of $\beta_{ij} = \beta_{ik} = 1$ exist.

$$\varphi_{ij} + \varphi_{jk} \leq 1 \qquad i,j,k \in I \ : \beta_{ij} = \beta_{ik} = 1 \tag{6.32}$$

Of course, all constraints (6.30) – (6.32) also hold for rescue team traffic so that these constraints can be adopted and slightly modified to match rescue team traffic, see (6.33) – (6.35).

$$\varphi^r_{ij} \leq \beta_{ij} \qquad i,j \in I \tag{6.33}$$
$$\epsilon^r_{ij} \leq \varphi^r_{ij} \cdot \min\{l_i, l_j\} \qquad i,j \in I \tag{6.34}$$
$$\varphi^r_{ij} + \varphi^r_{jk} \leq 1 \qquad i,j,k \in I \ : \beta_{ij} = \beta_{ik} = 1 \tag{6.35}$$

Evacuation plans should be designed in respect to traffic safety and practicability. Therefore, in Section 4.1.2, we developed so-called "traffic flow limitation" constraints, see (6.36) – (6.39).

$$\sum_{i \in I} \varphi_{ij} \leq l_j \qquad j \in I \tag{6.36}$$
$$\sum_{j \in I} \varphi_{ij} \leq p \qquad i \in I \tag{6.37}$$
$$\sum_{i \in I} \epsilon_{ij} \leq l_j \qquad j \in I \tag{6.38}$$
$$\sum_{j \in I} \epsilon_{ij} \leq l_i \qquad i \in I \tag{6.39}$$

Constraint (6.36) limits the number of ingoing traffic streams from other cells to cell j to the number of lanes in cell j. By doing so, merging processes at junctions are not appearing. The number of outgoing traffic streams from cell i to other cells is limited to a value p, see (6.37). Again, we decided to set $p = 2$ in our computational studies, see Section 4.3.2. Finally, the number of lanes used for ingoing (6.38) and outgoing (6.39) traffic flows are limited to the number of lanes in the destination or origin cell, leading to further reductions of nonessential merging and diverging processes. In contrast to (6.30) – (6.32) where all constraints are adopted to rescue team traffic, only (6.38) and (6.39) will be transfered to rescue team traffic at this point (see (6.40) and (6.41)) as rescue team traffic is expected to show none or only few merging and diverging processes.

$$\sum_{i \in I} \epsilon^r_{ij} \leq l_j \qquad j \in I \tag{6.40}$$
$$\sum_{j \in I} \epsilon^r_{ij} \leq l_i \qquad i \in I \tag{6.41}$$

These constraints help to guide traffic through the network in a less conflictual and safer way since merging processes at junctions will be avoided. However, as discussed in Section 4.1.3, there might exist some real-world scenarios where no feasible solution exist when these constraints are applied, e.g. imagine a four-way junction with four one-lane streets, three of them are deadlocks. If traffic from these three (deadlock) streets is flowing towards the junction and these three independent traffic streams must be merged into the non-deadlock street, it is easy to see that that kind of merging processes are forbidden by (6.36). In such cases, we suggest to relax these constraints ((6.36), (6.38)) and to add the constraint $\sum_{i \in I} y_{ijt} \leq Q_{jt}$ for all cells $j \in I$ and periods $t \in T$ where (6.36) and (6.38) have been relaxed. The relaxation of (6.36) and (6.38) ensures feasible solutions and the new constraint assures that traffic flow capacities are not exceeded. Since suchlike infeasibilities are usually caused by traffic-merging constraints, rescue team traffic are usually not affected by these observations due to the lack of merging processes. As we will see in the Section 6.4, constraints (6.36) and (6.38) will be relaxed only for one single instance.

One major concern in terms of traffic safety and real-world-applicability are traffic crossing or traffic touching conflicts at junctions. For four cells i, j, u, v at a junction as displayed in Figure 4.5, it has to be ensured that no traffic crossing or traffic touching conflicts regarding evacuation traffic and rescue team traffic exist.

$$\varphi_{ij} + \varphi_{ji} + \varphi_{uv} + \varphi_{vu} \leq 1 \qquad i,j,u,v \in I : \beta_{ij} = \beta_{iu} = \beta_{iv} = \beta_{ju} = \beta_{jv} = \beta_{uv} = 1 \tag{6.42}$$

This constraint also holds for rescue team traffic, so that (6.43) can be formulated.

$$\varphi^r_{ij} + \varphi^r_{ji} + \varphi^r_{uv} + \varphi^r_{vu} \leq 1 \qquad i,j,u,v \in I : \beta_{ij} = \beta_{iu} = \beta_{iv} = \beta_{ju} = \beta_{jv} = \beta_{uv} = 1 \tag{6.43}$$

Finally, (6.44) – (6.53) define the domain of all decision variables.

$$\epsilon_{ij} \in \mathbb{N}_0 \qquad i,j \in I \tag{6.44}$$
$$\varphi_{ij} \in \{0,1\} \qquad i,j \in I \tag{6.45}$$
$$z_{it}, x_{it}, b_{it} \geq 0 \qquad i \in I\,;\ t \in T \tag{6.46}$$
$$y_{ijt} \geq 0 \qquad i,j \in I\,;\ t \in T \tag{6.47}$$

$$\epsilon^r_{ij} \in \mathbb{N}_0 \qquad i,j \in I \tag{6.48}$$
$$\varphi^r_{ij} \in \{0,1\} \qquad i,j \in I \tag{6.49}$$
$$x^r_{it}, b^r_{it} \geq 0 \qquad i \in I\,;\ t \in T \tag{6.50}$$
$$y^r_{ijt} \geq 0 \qquad i,j \in I\,;\ t \in T \tag{6.51}$$
$$r_{ijt} \in \{0,1\} \qquad i,j \in I\,;\ t \in T \tag{6.52}$$
$$\sigma_{it} \in \{0,1\} \qquad i \in I\,;\ t \in T \tag{6.53}$$

To assure that no vehicle movements occur before the evacuation starts – i.e. in period $t = 1$, boundary conditions (6.54)–(6.56) fix the corresponding decision variables to zero.

$$x_{i1} = 0 \qquad i \in I \tag{6.54}$$
$$b_{i1} = 0 \qquad i \in I \tag{6.55}$$
$$y_{ij1} = 0 \qquad i \in I \ ; \ j \in I \tag{6.56}$$

Of course, also rescue team traffic must be forbidden for period $t = 1$, see (6.57)–(6.59)

$$x^r_{i1} = 0 \qquad i \in I \tag{6.57}$$
$$b^r_{i1} = 0 \qquad i \in I \tag{6.58}$$
$$y^r_{ij1} = 0 \qquad i \in I \ ; \ j \in I \tag{6.59}$$

Enhancements: As discussed in Section 6.1, rescue teams may be positioned outside the endangered network so that these rescue teams have to enter the network through a cell i ($i \in I_S$). These cells also represent exits for evacuation flow so that one major decision in evacuation planning with rescue teams is to determine which cell $i \in I_S$ should be used as an rescue team entrance. However, the availability of rescue teams may vary in terms of earliest arrival time at a certain entrance cell and in terms of rescue team vehicle capacity.

$$\sum_{t=1}^{\hat{t}_i} y^r_{|I|,it} = 0 \qquad i \in I_S \tag{6.60}$$
$$\sum_{t \in T} y^r_{|I|,jt} \leq P'_j \qquad j \in I_S \tag{6.61}$$

Constraint (6.60) prevents all rescue team flows from the super sink $|I|$ to a certain network entrance cell $i \in I_S$ until a period $\hat{t}_i$ ($\hat{t}_i \geq 1$) with $\hat{t}_i + 1$ as the first period where rescue teams may travel to the network entrance cell i ($i \in I_S$). Limited vehicle capacities in terms of P'_j for outside positioned rescue teams are covered in (6.61).

6.3 Heuristic Solution Approach

We already discussed at the beginning of Chapter 5 that the original formulation of the ExCTEPM contains a path constrained network flow problem which is known to be NP-complete, see Garey and Johnson (1979). Thus, finding optimal solutions for larger instances will be a difficult task. Since the considered problem in this chapter can be regarded as an enhanced ExCTEPM, a three-staged heuristic approach for solving the evacuation planning problem with integrated rescue team traffic will be presented in this section. This approach utilizes the "static ExCTEPM" heuristic, introduced in Chapter 5 which is facilitated by a shortest-path based heuristic to determine rescue team routes.

6.3.1 Basic Ideas

Frequent appearances of similar constraints for evacuation traffic and rescue team traffic indicate that the present optimization problem consists of two interlocking CTM-based routing problems. Firstly, evacuation planning for the complete network and secondly rescue team route determination. Based upon these essential thoughts, we develop a three-step heuristic procedure, which works in the following manner:

Step 1: Generate an evacuation plan for the complete network without rescue team traffic by the static ExCTEPM heuristic, see Section 5.2.3.

Step 2: Determine rescue team route(s) by a shortest-path(s) based heuristic taking the results from Step 1 into account.

Step 3: Generate an evacuation plan for the complete network with rescue team traffic by a modified static ExCTEPM heuristic.

It should be noticed that our heuristic focuses on problems, where rescue team traffic just have to arrive at a given set of cells in the network.

6.3.2 Step 1 – Evacuation Planning

This step contains the creation of an evacuation plan regardless of demand for rescue teams and rescue team traffic. This problem has been studied in Chapter 5 and a fast heuristic procedure named "static ExCTEPM" has been introduced. We will adopt this approach here in its original form. The basic idea of the static ExCTEPM heuristic is to transform the dynamic Cell-Transmission-based problem into a static Cell-based network flow problem. In detail, we drop the dimension of time and introduce a new variable η_{ij} to denote the total number of vehicles using the connection from cell i to cell j. Hence, we do not care about how many vehicles travel from one cell to another cell in a certain period, but how many vehicles travel from one cell to another cell at all. By doing so, the model formulation can be simplified and the number of decision variables and constraints reduces significantly, because only traffic routing constraints and variables are needed. As the resulting static optimization problem contains nonlinearities, a binary search algorithm is applied, where the subproblem in each iteration is linear.

The static cell-based constraint satisfaction problem can be formulated as stated below, where η_{ij} denotes the total number of vehicles traveling from cell i to cell j (i.e. $\eta_{ij} =$

$\sum_{t \in T} y_{ijt}$ for $i, j \in I$) and M is the maximum amount of time (measured in periods), a connection between two cells is used.

Find M and η_{ij}

subject to (6.30) – (6.32), (6.36) – (6.39), (6.42), (6.44), (6.45) and

$$\frac{\eta_{ij}}{\min(\frac{Q_i}{l_i}, \frac{Q_j}{l_j})} \leq M \cdot \epsilon_{ij} \qquad i, j \in I \tag{6.62}$$

$$\sum_{i \in I} \eta_{ij} + E_j = \sum_{k \in I} \eta_{jk} \qquad j = 1, \ldots, |I| - 1 \tag{6.63}$$

$$\sum_{i \in I} E_i = \sum_{i \in I} \eta_{i,|I|} \tag{6.64}$$

$$\eta_{ij} \leq \epsilon_{ij} \cdot Y \qquad i, j \in I \tag{6.65}$$

$$\varphi_{ij} + \varphi_{ji} \leq 1 \qquad i, j \in I \tag{6.66}$$

$$\epsilon_{i,|I|} = l_i \qquad i \in I : \beta_{i,|I|} = 1 \tag{6.67}$$

$$M \geq 0 \tag{6.68}$$

$$\eta_{ij} \geq 0 \qquad i, j \in I \tag{6.69}$$

Constraint (6.62) calculates the number of periods, a connection from cell i to cell j is used and ensures that no connection is occupied longer than M periods. (6.63) is a simplified version of the vehicle flow equation (6.3) in the original model formulation and (6.64) guarantees that all vehicles leave the evacuation network and arrive at the super sink $|I|$. (6.65) restricts traffic flows only to those connections from cell i to cell j where at least one lane is established, whereas Y is a large number, e.g. $Y = \sum_{i \in I} E_i$. Moreover, constraint (6.66) avoids traffic flows in opposite directions between two cells. (6.67) is a preprocessing constraint as it fixes the number of established lanes from exit cells to the super sink to the maximum number of lanes. The domain of the decision variables is defined in (6.68) and (6.69).
Normally, the objective function should be formulated as $\min M$, but this implies that M is a decision variable resulting in non-linearities in constraint (6.62). We overcome this issue by defining M formally as a parameter, which will be minimized using a binary search algorithm. This algorithm is already stated in Section 5.2.3.

During our computational tests, it turned out that the computation time can be lowered by adding an objective function to the (constraint satisfaction) model, although this objective function or the objective function value have absolutely no relevance for the constraint satisfaction problem or the procedure itself. We use $\min \sum_{i \in I} \sum_{j \in I} \eta_{ij} \cdot d_{ij}$ with $d_{ij} = ((c_i \cdot n_i) + (c_j \cdot n_j))/(l_i + l_j)$.
In some evacuation scenarios, it may happen that the level of danger (i.e. c_{it}) varies within the network. In Section 5.2.1, we provide an extensive discussion on how to determine Evacuation Planning Zones (EPZ) on the basis of different levels of danger and how the knowledge of these zones can be implemented in the Static ExCTEPM heuristic. The basic idea is that the binary search algorithm will be executed multiple times, each time for a specific set of cells, whereas subsequent sets of cells always include the preceding set(s). By doing so, a unique M_h value can be computed for each EPZ_h. For the sake of simplicity, we refer to Section 5.2.3 at this point.

The solution obtained from the static ExCTEPM – i.e. values for φ_{ij} – will be used as parameters for the original model formulation of the ExCTEPM ((6.1) – (6.3), (6.5), (6.7), (6.8), (6.12), (6.13), (6.14) – (6.17), (6.30) – (6.32), (6.36) – (6.39), (6.42), (6.44) – (6.47), (6.54)–(6.56)) to generate a feasible evacuation plan. It has to be mentioned that the (remaining simplified) ExCTEPM with φ_{ij} as parameters can be solved much faster since a large number of integer variables are fixed. Afterwards, optimal values of decision variables from the solved ExCTEPM were taken and passed to the next step (Step 2) in terms of $\hat{y}_{it}$. This parameter is defined as $\hat{y}_{it} = \sum_{j \in I} \sum_{\tau=t}^{|T|} (y_{ij\tau} + y_{ji\tau}) \cdot n_i$ for all $i \in I; t \in T$ capturing all vehicles using cell i in period t and all succeeding periods.

6.3.3 Step 2 – Rescue Team Route Determination

This step determines rescue team route(s) with respect to the evacuation plan created in Step 1. We already demonstrate in Table 6.1 that evacuation traffic flow in cell i in period t is prohibited for $\sigma_{it} = 1$. However, evacuation traffic is also prohibited in δ^- periods before so that a new binary auxiliary decision variable σ'_{it} is introduced to cover all periods where evacuation traffic is forbidden. The corresponding optimization model can be formulated as follows:

$$\min \sum_{i=1}^{|I|-1} \sum_{t=1}^{|T|} \sigma'_{it} \cdot \hat{y}_{it} \cdot c_i + \sum_{\substack{i,j,u,w=1,\ldots,|I|-1: \\ j,u,w \in J_i, \\ \varphi^{rp}_{ij} = \varphi_{uw} = 1}} \sum_{t=1}^{|T|} \sigma'_{it} \cdot \hat{y}_{ut} \cdot c_u \tag{6.70}$$

subject to (6.4), (6.6), (6.9), (6.10), (6.11), (6.18) – (6.21), (6.22), (6.28), (6.33) – (6.35), (6.40), (6.41), (6.43), (6.48) – (6.53), (6.57) – (6.59), (6.60), (6.61) and

$$\sigma'_{it} \cdot (\delta^- + 1) \geq \sum_{\tau=t}^{t+\delta^-} \sigma_{i\tau} \qquad i \in 1, \ldots, |I| - 1 \; ; \; t \in T \tag{6.71}$$

The objective function (6.70) minimizes the weighted disruption of evacuation traffic. The first term covers all cells directly affected by rescue traffic and the second term includes all cells indirectly concerned by rescue traffic because of traffic crossing or traffic touching conflicts at junctions. Please note that the second term is defined only at junctions (implied by the set J_i, i.e. at least four cells adjacent to the same junction so that $\beta_{ij} = \beta_{iu} = \beta_{iw} = \beta_{ju} = \beta_{jw} = \beta_{uw} = 1$ holds), where a rescue team traffic stream (in terms of φ^{rp}_{ij}, see below for explanation of φ^{rp}_{ij}) crosses or touches an evacuation traffic stream (in terms of φ_{uw}). We added the term $+10^{-5} \cdot \sum_{i \in I} \sum_{t=1}^{|T|} (\sigma_{it} + \sigma'_{it})$ to the objective function since the model may set some σ_{it} or σ'_{it} values to 1 if $\hat{y}_{it} = 0$, although this would not be necessary due to constraint (6.22) and maybe disadvantageous in the successive steps of the heuristic. (6.71) calculates all periods, where no evacuation traffic is possible due to the assignment of rescue team traffic and the time buffers before and after the occurance of rescue team traffic.

The main difficulty with solving this optimization problem is the large number of binary decision variables primarily caused by σ_{it} and r_{ijt}. We already know in advance that many of these σ_{it} and r_{ijt} values will be 0 after optimization since rescue team traffic will be integrated in a way interfering with evacuation traffic as little as possible. Thus, our approach for solving this optimization problem is as follows:

1. Rescue Team Route Determination:
   (a) Set a bound $\Omega = \infty$, set counter $\kappa = 0$, let ω be the objective value of (6.70), let $P = \{\emptyset\}$, let γ be the number of iterations without solution improvements before terminating.
   (b) Calculate (new) routing $\phi \notin P$ from the super sink $|I|$ to all cells $i \in I_R$ with $D_i \geq 1$. Result: φ_{ij}^{rp} and η_{ij}^{rp} values.
   (c) Solve Rescue Team Route Determination with φ_{ij}^{rp} and η_{ij}^{rp} values as parameters and additional constraints (6.86)–(6.91).
   (d) If $\omega < \Omega$, set $\Omega = \omega$, set $\kappa = 0$, otherwise set $\kappa = \kappa + 1$.
   (e) Add current rescue team routing ϕ to P.
   (f) Go back to step (b) if $\kappa < \gamma$, otherwise STOP.

The calculation of the shortest path(s) in step (b) is conducted by a simple network flow model using the following notation.

Parameters:

d_{ij} "weight" of using the connection from cell i to cell j, $d_{ij} = \sum_{t=1}^{|T|}(\hat{y}_{it} + \hat{y}_{jt})$

Decision variables:

φ_{ij}^{rp} =1, if and only if a connection from cell i to cell j is used as a rescue team route, otherwise 0
η_{ij}^{rp} total number of rescue team vehicles traveling from cell i to cell j
v_i auxiliary value of cell i to avoid cycles

Based on this notation, the mixed integer linear optimization model for determining route(s) for rescue teams can be stated as follows:

$$\min \sum_{i \in I} \sum_{j \in I} \varphi_{ij}^{rp} \cdot d_{ij} \tag{6.72}$$

subject to

$$\sum_{i \in I} \eta_{ij}^{rp} + P_j - D_j = \sum_{k \in I} \eta_{jk}^{rp} \qquad j \in I \tag{6.73}$$

$$\eta_{ij}^{rp} \leq \varphi_{ij}^{rp} \cdot Y \qquad i, j \in I \tag{6.74}$$

$$\varphi_{ij}^{rp} \leq \eta_{ij}^{rp} \qquad i, j \in I \tag{6.75}$$

$$\varphi_{ij}^{rp} \leq \beta_{ij} \qquad i, j \in I \tag{6.76}$$

$$\varphi_{ij}^{rp} + \varphi_{jk}^{rp} \leq 1 \qquad i, j, k \in I : \beta_{ij} = \beta_{ik} = 1 \tag{6.77}$$

$$\varphi_{ij}^{rp} + \varphi_{ji}^{rp} + \varphi_{uv}^{rp} + \varphi_{vu}^{rp} \leq 1 \qquad i, j, u, v \in I : \beta_{ij} = \beta_{iu} = \beta_{iv} = \beta_{ju} = \beta_{jv} = \beta_{uv} = 1 \tag{6.78}$$

$$\sum_{j \in I} \varphi_{ij}^{rp} \leq l_i \qquad i \in I \tag{6.79}$$

$$\sum_{i \in I} \varphi_{ij}^{rp} \leq l_j \qquad j \in I \tag{6.80}$$

$$v_{|I|} = 1 \tag{6.81}$$

$$v_j + |I| \geq v_i + 1 + (|I| \cdot \varphi_{ij}^{rp}) \qquad i, j \in I : i \neq j \tag{6.82}$$

$$\varphi_{ij}^{rp} \in \{0, 1\} \qquad i, j \in I \tag{6.83}$$

$$v_i \geq 0 \qquad i \in I \tag{6.84}$$

$$\eta_{ij}^{rp} \geq 0 \qquad i, j \in I \tag{6.85}$$

The objective function (6.72) minimizes the potential interfering of rescue team traffic with evacuation traffic. A standard vehicle flow equation is stated in (6.73). Constraints (6.74) and (6.75) ensure that $\varphi_{ij}^{rp} = 0$ if $\eta_{ij}^{rp} = 0$, $\varphi_{ij}^{rp} \geq 1$ if $\eta_{ij}^{rp} \geq 1$ and vice versa. Furthermore, constraint (6.76) restricts rescue team traffic only to existing connections from a cell i to a cell j. The constraints (6.77) and (6.78) correspond to (6.35) and (6.43) in the original model formulation. In order to assure that constraint (6.40) and (6.41) will be met, slightly modified versions of these constraints are stated in (6.79) and (6.80). Cycles in rescue team routes will be avoided by constraint (6.81) and (6.82). The domain of the decision variables is stated in (6.83) – (6.85).

$$\sigma_{it} = 0 \qquad i \in I \ ; \ t = 1, \dots |T| \ : \ \sum_{j \in I} \varphi_{ij}^{rp} + \varphi_{ji}^{rp} = 0 \tag{6.86}$$

$$\sigma'_{it} \leq \sigma_{it} \qquad i \in I \ ; \ t = 1, \dots |T| \ : \ \sum_{j \in I} \varphi_{ij}^{rp} + \varphi_{ji}^{rp} = 0 \tag{6.87}$$

$$\varphi_{ij}^{r} \leq \varphi_{ij}^{rp} \qquad i, j \in I \tag{6.88}$$

$$\epsilon_{ij}^{r} \leq \varphi_{ij}^{rp} \cdot \min(l_i, l_j) \qquad i, j \in I \tag{6.89}$$

$$r_{ijt} = 0 \qquad i, j \in I \ ; \ t = 1, \dots |T| : \varphi_{ij}^{rp} = 0 \tag{6.90}$$

$$\sum_{t=1}^{|T|} y_{ijt}^{r} = \eta_{ij}^{rp} \qquad i, j \in I \tag{6.91}$$

The constraints (6.86)–(6.91) have a preprocessing character since these constraints fix many integer variables to zero. In detail, (6.86) and (6.87) fix σ_{it} and σ'_{it} to zero, if cell i is not part of the shortest path(s) in terms of φ_{ij}^{rp} and φ_{ji}^{rp}. Afterwards, constraints (6.88) and (6.89) also fix the corresponding φ_{ij}^{r} and ϵ_{ij}^{r} variables to zero, if the connection from cell i to cell j is not part of the rescue team route(s) in terms of φ_{ij}^{rp}. Equation (6.90) fixes r_{ijt} values to zero, when cell i and cell j are not part of the rescue team traffic route(s) and (6.91) ensures that rescue teams will use exactly the route that is intended to be used by the shortest path(s) calculations.
Some aspects need special attention here: Firstly, it is sufficient to consider the periods from $1, \dots, t_r + \delta^+$ since all σ_{it} values with $t > t_r + \delta^+$ can be set to 0 or 1 depending on the route determination before t_r. Please note that the preprocessing constraints (6.86)–(6.91) should be defined for the same planning horizon as the decision variables to ensure that as much variables as possible will be fixed by these constraints. Secondly, adding the (preprocessing) constraints (6.86)–(6.91) as well as reducing the planning horizon to $1, \dots, t_r + \delta^+$ lead to massive reductions in problem size, computational effort and solving time.

6.3.4 Step 3 – Evacuation and Rescue Team Planning

The integrated evacuation and rescue team planning utilizes information gained from Step 1 and Step 2 resulting in an evacuation planning problem with restricted routing options

due to rescue team traffic. We assume that the evacuation plan in Step 1 (without rescue teams) shows considerable accordance with the final evacuation plan in Step 3 (with rescue teams). Now, the task is to route traffic differently, when conflicts between evacuation traffic (from Step 1) and rescue team traffic (from Step 2) exist. In detail we create two new parameters, namely $\tilde{\sigma_i}$ and $\tilde{r_{ij}}$. $\tilde{\sigma_i}$ represents the number of periods, where evacuation traffic in a cell i in Step 1 is not possible due rescue team traffic and the parameter $\tilde{r_{ij}}$ denotes the number of periods during the complete planning horizon, where a junction is blocked for evacuation traffic due to rescue team traffic. These parameters are calculated as follows:

1. Compute $\tilde{\sigma_i}$
   (a) Set $i = 0$, $\tilde{\sigma_i} = 0$ for all $i \in I$
   (b) Let $i = i + 1$, $t = 0$
   (c) Let $t = t + 1$
   (d) Let $\tilde{\sigma_i} = \tilde{\sigma_i} + 1$, if $\hat{y}_{it} > 0$ and $\sigma'_{it} > 0$
   (e) Go back to step (c), if $t < |T|$, otherwise proceed to step (f)
   (f) Go back to step (b), if $i < |I| - 1$, otherwise STOP.

$$\tilde{r_{ij}} = \sum_{t \in 1,\ldots,|T|} r_{ijt} + \delta^+ + \delta^- \qquad i,j \in 1,\ldots,|I|-1 : \sum_{t \in 1,\ldots,|T|} r_{ijt} > 0 \tag{6.92}$$

These parameters are necessary because our static ExCTEPM heuristic for solving Step 3 of the heuristic procedure can be regarded as a static optimization problem which also needs "static" (i.e. not time dependent) parameters as an input. Since σ'_{it} and r_{ijt} depend on a period t, new parameters were introduced. On the basis of these new parameters, we can formulate a modified static ExCTEPM heuristic as follows:

Find M and η_{ij}

subject to (6.30) – (6.32), (6.36) – (6.39), (6.42), (6.44), (6.45), (6.63) – (6.69) and

$$\frac{\eta_{ij}}{\min(\frac{Q_i}{l_i}, \frac{Q_j}{l_j})} \leq \max(0, M - \max(\tilde{\sigma_i}, \tilde{\sigma_j})) \cdot \epsilon_{ij} \qquad i,j \in I \tag{6.93}$$

$$\frac{\eta_{ij}}{\min(\frac{Q_i}{l_i}, \frac{Q_j}{l_j})} \leq \max(0, M - \tilde{r_{uw}}) \cdot \epsilon_{ij} \qquad i,j,u,w \in I : \beta_{ij} = \beta_{iu} = \beta_{iw} = \beta_{ju} = \beta_{jw} = \beta_{uw} = 1 \tag{6.94}$$

$$\frac{\eta_{ij}}{\min(\frac{Q_i}{l_i}, \frac{Q_j}{l_j})} \leq (t_r - \tilde{\sigma_i}) \cdot \epsilon_{ij} \qquad i \in I_R \; ; \; j \in I \tag{6.95}$$

This constraint satisfaction problem is formulated similar to Step 1 with two major differences in (6.93), (6.94) and (6.95). Analogue to (6.62), (6.93) again calculates the number of periods a connection from cell i to cell j is used and that no connection is occupied more than $M - \max(\tilde{\sigma_i}, \tilde{\sigma_j})$ periods. Here, we take into account that a connection from cell i to cell j can not be used like in Step 1, if evacuation traffic is interfered by rescue team traffic in terms of $\tilde{\sigma_i}$ and $\tilde{\sigma_j}$. Hence, we reduce the vehicle flow capacity of a connection from cell i to cell j by the maximum number of periods evacuation traffic will

not be possible due to rescue team traffic in cell i and cell j. Constraint (6.94) takes into account that junctions can also not be used as before, if rescue team traffic uses this junction. Moreover, all cells with positive demand for rescue teams – i.e. i $\in I_R$ – must be evacuated after $t_r - \tilde{\sigma}_i$ periods at the latest since these cells are closed for evacuation traffic till the end of the planning horizon, see (6.95). Again, we added the same objective function to the (constraint satisfaction) model as in Step 1, i.e. $\min \sum_{i \in I} \sum_{j \in I} \eta_{ij} \cdot d_{ij}$ with $d_{ij} = ((c_i \cdot n_i) + (c_j \cdot n_j))/(l_i + l_j)$.
Finally, the resulting φ_{ij} values as well as values for all φ^r_{ij}, σ_{it} and r_{ijt} variables from Step 2 are passed to the original model formulation presented in Section 6.2, see (6.1) – (6.61).
The complete heuristic procedure is illustrated in Figure 6.2 and a few aspects need more attention. The computation of the ExCTEPM in Step 1 and the ExCTEPM with Rescue Team Traffic in Step 3 is conducted in two steps, if multiple cell sizes are used. In the first step, we use the values of φ_{ij} in Step 1 of the heuristic (and additionally φ^r_{ij}, σ_{it} and r_{ijt} in Step 3 of the heuristic) as parameters and relax the constraints for multiple cell sizes, namely (6.5) in Step 1 as well as (6.5) and (6.6) in Step 3. We then solve the remaining model with ϵ_{ij} and ϵ^r_{ij} as integer variables to a maximum mipgap of 0.1%. In the second step, we use the previously determined values for ϵ_{ij} and ϵ^r_{ij} as parameters, restore constraint (6.5) and (6.6) and solve the remaining LP. If only a single cell size is used, the second step can be omitted. Another discussion point is that the heuristic may not generate feasible solutions straightaway, especially in the case of sparse networks with long deadlockstreets. Therefore, we add a loop after Step 3 of the heuristic to ensure feasibility.

6.3.5 Numerical Example

We will illustrate the complete procedure for a small example: The considered network consists of 12 cells (plus the super sink in cell 13) of the same cell size with three exits. Two-lane cells are cells 1-5 as well as 9-12 and four-lance cells are cells 6-8. Cells 6 and 9 are located in the highly endangered zone. Both cells have a demand for two rescue team vehicles each. We set $c_{it} = c_i \cdot t$ with $c_i = 10^4$ for cells within the most endangered zone, $c_i = 10^2$ for all remaining cells and $c_i = 0$ for the super sink. The number of vehicles starting is not important to be known precisely. We have chosen it randomly between 10 and 100. In total this example resulted in 786 vehicles. Rescue team traffic is not limited in terms of (6.60) and (6.61). Moreover, we assume that flow and vehicle capacities are constant over time.
The solutions for each step obtained by our heuristic procedure for this sample are presented in Figures 6.3 – 6.5. In the first step, only evacuation traffic is considered. The solid arrows represent evacuation flows and the numbers in brackets indicate in which periods the corresponding connection is occupied. Here, it is easy to see that the occupancy rate of all exits is almost identical since all exits are used the same number of periods. On the basis of these evacuation flows, rescue teams are assigned in Step 2, indicated by non-solid arrows. In this step, rescue team traffic is scheduled as late as possible ($t_r = 13$) using a two-lane cell (instead of a four-lane cell, e.g. cell 8) in order to affect evacuation flow as little as possible. In the last step, a new evacuation plan is designed taking rescue team traffic into account. Since cell 12 is not available for evacuation traffic in periods 9–12, other exits have to compensate this loss of capacity. Therefore, more vehicles are escaping through cell 1 and cell 8 leading to reasonable changes in the evacuation plan compared to Step 1.

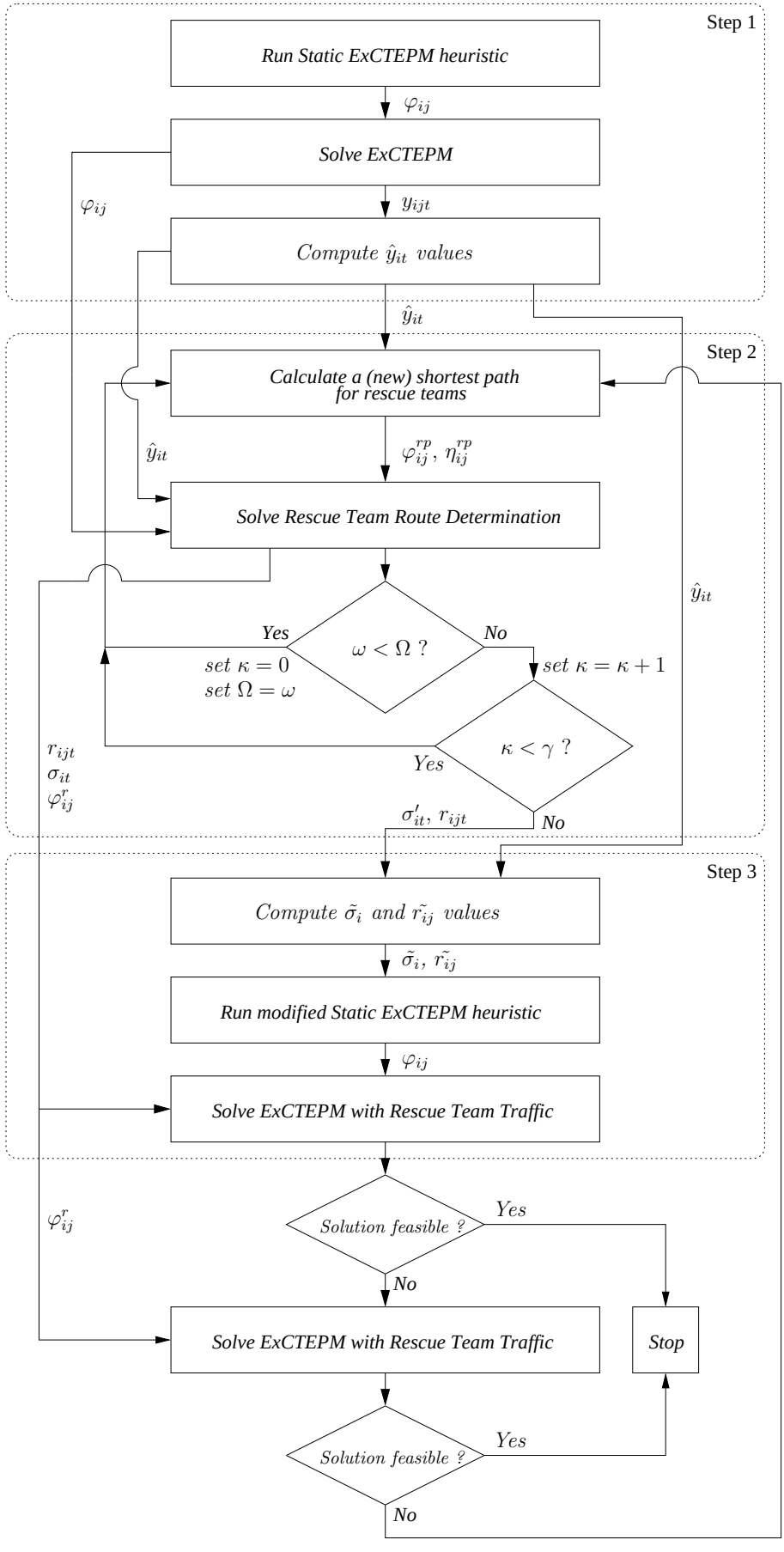

Figure 6.2: Heuristic Procedure and Information Exchange

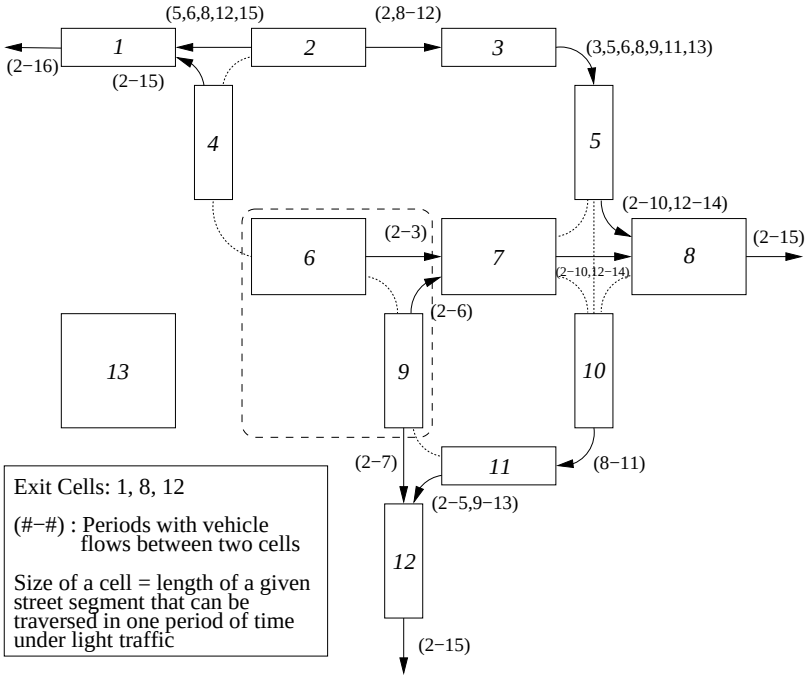

Figure 6.3: Example Network with Solution from Step 1

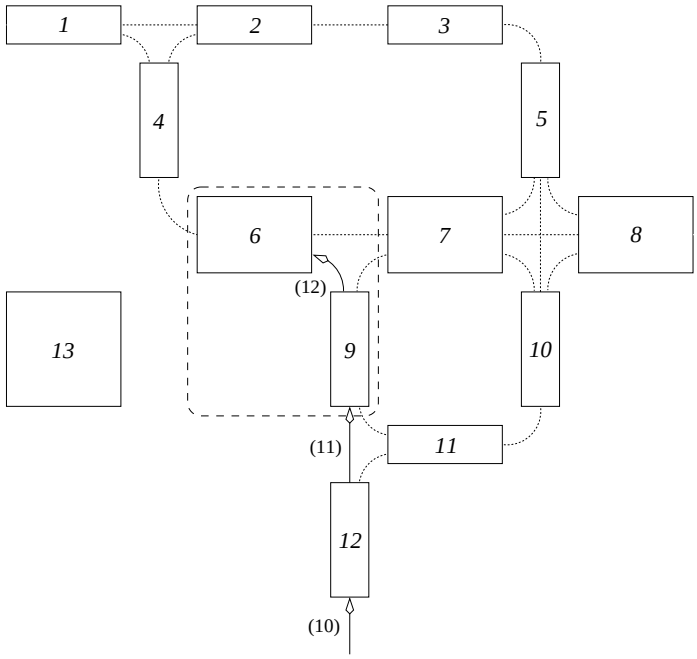

Figure 6.4: Example Network with Solution from Step 2

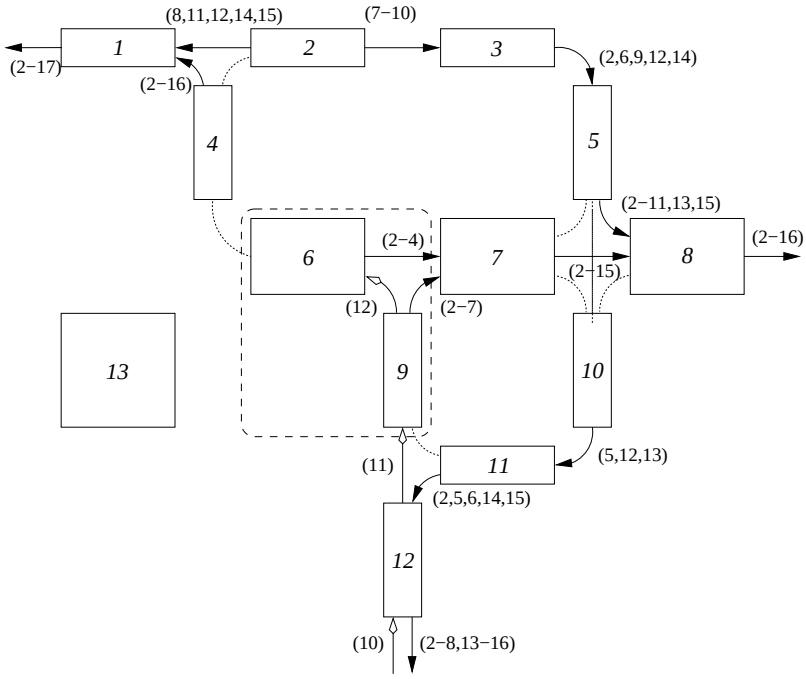

Figure 6.5: Example Network with Solution from Step 3

6.4 Computational Study

Our computational experiments are comprised of three parts. The first part uses small examples which can be solved optimally. Moreover, we illustrate the sensitivity of the objective function (6.1) to wrong decisions in a simple network. The second part deals with the application of our heuristic approach to the same network introduced in the first part. Thirdly, we will illustrate applicability of our approach for larger instances, which can not be solved optimally due to computational limits. All tests were run on a computer using an Intel X9100 (3.06 Ghz), 8 GB of memory and Windows Vista (64-bit). All optimization models and procedures were coded in AMPL (see *http://www.ampl.com*) using the GUROBI 3.0.1 solver (see *http://www.gurobi.com*).

6.4.1 Sensitivity of the Objective Function

Our small test network consists of 44 cells (plus the super sink) of the same size including five exits (1, 10, 16, 38, 44). The number of lanes per cell can be derived from the shape of the cells, whereas slim (wide) cells consist of two (four) lanes. The number of evacuating vehicles per cell is a random number between 10 and 90 leading to a total number of 2,111 vehicles. The most endangered zone ranges over cells 18, 22, 26, 27, 28, 31, 32 (box with broken line). Again, we set $c_{it} = c_i \cdot t$ with $c_i = 10^4$ for cells within the most endangered zone, $c_i = 10^2$ for all remaining cells and $c_i = 0$ for the super sink. Cells 22 and 27 have a positive rescue team demand and no capacity limits for rescue teams exist. Again, we assume that flow and vehicle capacities are constant over time. We set $|T| = 35$ and $t_r = 13$. We apply no rescue team traffic limitations in terms of (6.60) and (6.61). The optimum solution for this network with 100% population is displayed in Figure 6.6.

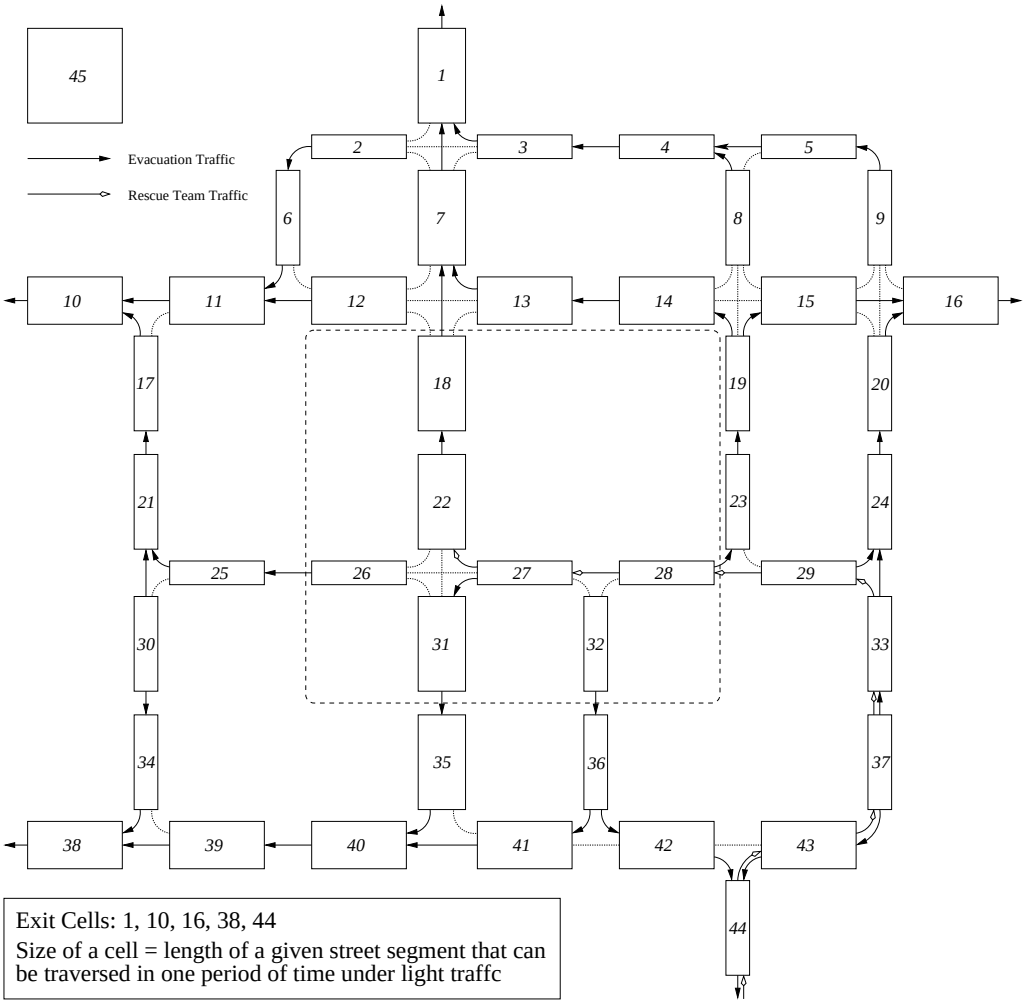

Figure 6.6: Test Network with Optimum Solution for 100% Population

In order to investigate sensitivity of the objective function (6.1) to wrong decisions, we calculate the optimum solution for this instance and add one, two or three decisions which disagree with the optimum solution. If non-optimal decisions were fixed in the optimization process, the objective values increases, leading to a positive gap. Here, we want to show that the evacuation planning with rescue teams problem reacts sensible to deviations from the optimum solution. Results are shown in Table 6.2, 6.3 and 6.4.

The relative gap for every solution is computed by the following equation:

$$gap = \frac{Sol - Sol_{best}}{Sol_{best}} \cdot 100 \tag{6.96}$$

where Sol_{best} is the objective function value of the best known feasible solution from our experiments and Sol is the objective function value of the solution to be examined. This definition will lead to values of 0.0 for the best known solution, to values of $gap > 0$ for feasible solutions and to values of $gap < 0$ for lower bounds. In order to scale all results to percent-values, a multiplication with the factor 100 is included.

	Decisions	100 % Population Gap	75% Population Gap	50% Population Gap
1	$\varphi_{13,7} = 0$	1.3%	0.9%	0.2%
2	$\varphi_{5,4} = 0$	0.5%	0.6%	0.2%
3	$\varphi_{40,39} = 0$	9.7%	8.1%	5.0%
4	$\varphi_{9,5} = 0$	0.5%	0.6%	0.2%
5	$\varphi_{32,36} = 0$	17.5%	20.6%	26.1%
6	$\varphi_{35,40} = 0$	8.8%	7.5%	4.6%
7	$\varphi_{18,7} = 0$	1.5%	0.9%	0.2%
8	$\varphi_{31,35} = 0$	13.1%	15.3%	16.2%
9	$\varphi_{24,20} = 0$	1.8%	2.3%	0.4%
10	$\varphi_{4,3} = 0$	3.8%	2.9%	0.7%
	Max	17.5%	20.6%	26.1%
	Min	0.5%	0.6%	0.2%
	$\oslash$	5.8%	6.0%	5.4%

Table 6.2: Results for One Wrong Decision and Different Populations

	Decisions	100 % Population Gap	75% Population Gap	50% Population Gap
1	$\varphi_{13,7} = 0$ $\varphi_{6,2} = 0$	1.5%	1.4%	0.2%
2	$\varphi_{5,4} = 0$ $\varphi_{34,38} = 0$	0.9%	0.8%	1.3%
3	$\varphi_{40,39} = 0$ $\varphi_{13,7} = 0$	10.6%	9.1%	5.4%
4	$\varphi_{9,5} = 0$ $\varphi_{23,19} = 0$	12.4%	14.8%	12.1%
5	$\varphi_{32,36} = 0$ $\varphi_{28,23} = 0$	18.2%	21.1%	26.3%
6	$\varphi_{35,40} = 0$ $\varphi_{12,11} = 0$	11.1%	8.8%	4.9%
7	$\varphi_{18,7} = 0$ $\varphi_{33,24} = 0$	1.6%	1.1%	0.2%
8	$\varphi_{31,35} = 0$ $\varphi_{19,15} = 0$	14.6%	15.7%	16.6%
9	$\varphi_{24,20} = 0$ $\varphi_{33,37} = 0$	15.6%	17.6%	14.2%
10	$\varphi_{4,3} = 0$ $\varphi_{30,21} = 0$	4.5%	3.5%	0.9%
	Max	18.2%	21.1%	26.3%
	Min	0.9%	0.8%	0.2%
	$\oslash$	9.1%	9.4%	8.2%

Table 6.3: Results for Two Wrong Decision and Different Populations

	Decisions	100 % Population Gap	75% Population Gap	50% Population Gap
1	$\varphi_{13,7} = 0$ $\varphi_{6,2}$=0 $\varphi_{36,41}$=0	3.7%	3.3%	1.4%
2	$\varphi_{5,4} = 0$ $\varphi_{34,38} = 0$ $\varphi_{26,25} = 0$	6.1%	5.6%	7.2%
3	$\varphi_{40,39} = 0$ $\varphi_{13,7} = 0$ $\varphi_{29,24} = 0$	19.7%	20.6%	16.6%
4	$\varphi_{9,5} = 0$ $\varphi_{23,19} = 0$ $\varphi_{25,21} = 0$	16.6%	17.7%	13.7%
5	$\varphi_{32,36} = 0$ $\varphi_{28,23} = 0$ $\varphi_{30,21} = 0$	19.1%	21.4%	26.3%
6	$\varphi_{35,40} = 0$ $\varphi_{12,11} = 0$ $\varphi_{6,11} = 0$	13.6%	11.1%	7.4%
7	$\varphi_{18,7} = 0$ $\varphi_{33,24} = 0$ $\varphi_{30,21} = 0$	2.7%	1.8%	0.4%
8	$\varphi_{31,35} = 0$ $\varphi_{19,15} = 0$ $\varphi_{37,43} = 0$	16.2%	16.3%	16.9%
9	$\varphi_{24,20} = 0$ $\varphi_{33,37} = 0$ $\varphi_{9,5} = 0$	17.4%	19.4%	15.5%
10	$\varphi_{4,3} = 0$ $\varphi_{30,21} = 0$ $\varphi_{35,40} = 0$	12.8%	10.8%	7.4%
	Max	19.7%	21.4%	26.3%
	Min	2.7%	1.8%	0.4%
	⊘	12.8%	12.8%	11.3%

Table 6.4: Results for Three Wrong Decision and Different Populations

As a result, it is obvious that even minor deviations from the optimum solution may lead to significantly worse results. In the case of only one wrong decision, the objective function value degrades by only 0.2% at best and 26.1% at worst. It is also worth noticing that the average worsening of the objective function value is almost the same for all populations. In the case of two and three wrong decisions, maximum, minimum and average degradation of the objective function value further increases, whereas the influence of the population size stays the same, see Tables 6.3 and 6.4. The degradation of the objective function value peaks in one case with 50% population and three wrong decisions with a worsening of 26.3%. Thus, we can assume that the development of heuristic approaches for solving this problem is very difficult due to the sensitivity of the objective function to wrong decisions.

6.4.2 Application of the Heuristic Approach

In this section, we will apply our heuristic procedure to a small sample network and to two larger real world networks. During our computational tests, we found out that adding special terms to the objective function speed up the computational process significantly. In detail, we added the terms $+10^{-5} \cdot \sum_{i,j \in I} \sum_{t \in T} y_{ijt}$ and $-10^{-6} \cdot \sum_{t \in T} x_{|I|,t}$ to the objective function of the ExCTEPM in Step 1 of the heuristic, the term $+10^{-5} \cdot \sum_{i,j \in I} \sum_{t \in T} y^r_{ijt}$ to the objective function of Rescue Team Route Determination in Step 2 of the heuristic and $+10^{-5} \cdot \sum_{i,j \in I} \sum_{t \in T} (y_{ijt} + y^r_{ijt})$ as well as $-10^{-6} \cdot \sum_{t \in T} x_{|I|,t}$ to the objective function of the ExCTEPM with Rescue Team Traffic in Step 3 of the heuristic as well as the objective function of the original model formulation (see (6.1) – (6.61)). The first term always avoids unnecessary vehicle movements which may occur if two adjacent cell share the same level of danger. The second term forces vehicles to enter the super sink not later than necessary which may occur in cases where exit cells share the same level of danger as the super sink. However, the second term also tends to reduce computation time by cutting redundant solutions off. We also apply a time limit of 180 seconds for step (b) and (c) in Step 2 of the heuristic, which was not met during the complete computational study. Each iteration of the binary search algorithm in Step 1 and Step 3 of the heuristic has been terminated after the exploration of 75,000 nodes of the branch & bound tree.

6.4.2.1 Small Sample Network

In the first part of this section, we already illustrated that minor deviations from the optimum solution may lead to degradation of the objective value by large two-digit percentages. However, we will apply our heuristic presented in Section 6.3 to this relatively small network in order to show that this heuristic is able to generate high quality solutions regarding the majority of routing decisions. The results from our heuristic approach are displayed in Table 6.5:

	Optimum Solution		Heuristic Solution	
	Gap	solvetime [s]	Gap	solvetime [s]
100% Pop.	0.0%	450	2.6%	223
75% Pop.	0.0%	413	0.9%	100
50% Pop.	0.0%	192	1.9%	51

Table 6.5: Results of Heuristic Procedure for Sample Network

Solution quality and runtime of our heuristic approach for these three specific instances are very good. Compared to Tables 6.2, 6.3, 6.4, degradation of the objective function value is very low (2.6% for 100% Population, 0.9% for 75% Population, 1.9% for 50% Population, calculated with (6.96)), which implies that no major mis-routings take place. The most time demanding step for the instances with 50% and 75% population is the determination of rescue team path(s), consuming approx. 93% / 85% of total computation time for 75% / 50% population cases. The instance with 100% population is the only instance in the computational study, where no feasible solution could be found in the first run. Instead, we had to solve the ExCTEPM with rescue team traffic using only φ^r_{ij} as a parameter, but not φ_{ij}, σ_{it} and r_{ijt}.

6.4.2.2 Larger (Real World) Networks

The original model formulation for Cell-Transmission-based Evacuation Planning with Rescue Teams is very demanding in terms of memory requirements and computing time due to the large number of integer variables and constraints. In this regard, our heuristic approach gains significant advantages since the main problem is decomposed into smaller subproblems (evacuation planning, assignment of rescue teams and evacuation planning with rescue teams) whereas each subproblem is solved with by a combination of tailor-made heuristics and standard software. Thus, our approach can be adopted to even larger instances, delivering feasible solutions in short time. In the following, we will illustrate the adaptability of our approach for two real-world scenarios, namely the districts of Neudorf and Wanheimer Ort in the city of Duisburg, Germany. Both districts are displayed in Figure 6.7 and 6.8:

Figure 6.7: Duisburg - Neudorf

The data set for Neudorf is "Scenario 3" taken from Section 5.3 and supplemented by rescue team specific parameters, i.e. D_i, P_i, $\delta^+ = 1$, $\delta^- = 1$, $|T| = 91$ and $t_r = 25$.

Figure 6.8: Duisburg - Wanheimer Ort

Again, we apply no rescue team traffic limitations in terms of (6.60) and (6.61) and flow and vehicle capacities are constant over time. Based on up to date information, there are about 26,000 residents living in Neudorf leading to 8,750 vehicles, if three residents will use one vehicle on average. The considered network consists of 106 cells plus the super sink. The most endangered area is located in the center of the network, including a total of 13 cells, whereas four cells have a demand of 3 rescue teams vehicles each. Analogue to previous networks, we set $c_{it} = c_i \cdot t$ with $c_i = 10^4$ for cells within the most endangered zone, $c_i = 10^2$ for all remaining cells and $c_i = 0$ for the super sink. Rescue teams may enter the network through eight exit cells. On average, approximately 83 vehicles are starting their evacuation in each cell taking the super sink not into account.
The district Wanheimer Ort corresponds to a network of 134 cells including seven exit cells and a super sink. In Wanheimer Ort, 15,650 residents live, so that approx. 5,257 vehicles will be used for evacuation. The most endangered zone is located in the center of the network, affecting a total of 3 cells. The values for c_{it} are defined in the same manner as in all previous networks, setting $c_{it} = c_i \cdot t$ with $c_i = 10^4$ for cells within the most endangered zone, $c_i = 10^2$ for all remaining cells and $c_i = 0$ for the super sink. The average number of starting vehicles per cell is approximately 40 excluding the super sink. Moreover, the district Wanheimer Ort is characterized by a large number of one-lane streets leading to computational problems (no feasible solution) due to (6.36) and (6.38), see the discussion in Section 6.2. Therefore, we relax both constraints for all cells $j \in I$ with $l_j = 1$ in the model formulation of the ExCTEPM as well as the heuristic procedures

in Step 1 and Step 3 and add the new constraint $\sum_{i \in I} y_{ijt} \leq Q_{jt}$ for all cells $j \in I$ with $l_j = 1$ in the model formulation of the ExCTEPM in Step 1 and Step 3. Rescue team specific parameters were set to: $\delta^+ = 2$, $\delta^- = 2$, $|T| = 94$ and $t_r = 35$. Analogue to Neudorf, rescue team traffic limitations in terms of (6.60) and (6.61) were not applied and we assume that flow and vehicle capacities are constant over time. The results for both real-world instances are displayed in Table 6.6:

	Neudorf		Wanheimer Ort	
	Obj. Val.	solvetime [s]	Obj. Val.	solvetime [s]
LB_{ET}	1388240000	–	423971000	–
ET (Step 1)	1819560000	269	449379000	383
ET+RT (Steps 1–3)	1799610000	990	467010000	1,523

Table 6.6: Results of Heuristic Procedure for Neudorf and Wanheimer Ort

Using the best known feasible solutions for evacuation traffic (ET) as benchmarks, the solutions obtained by our heuristic approach for evacuation planning with rescue team traffic (ET+RT) are very good. In detail, the objective function value worsens by -1.1% (Neudorf) and 3.9% (Wanheimer Ort) in relation to the (heuristically computeted) objective function values for evacuation traffic. The negative gap for Neudorf exists due to a surprising improvement of the objective value although rescue team traffic has been considered. In comparison to the best known lower bound for the evacuation planning problem without rescue team traffic (LB_{ET}), results are also very promising since the degradation of the objective function value compared to the lower bound is 29.6% (Neudorf) and 10.2% (Wanheimer Ort), respectively.
Runtime for the first instance (Neudorf) splits in approximately 27% for Step 1, 17% for Step 2 and 56% for Step 3. An explanation for this might be found in the modified / additional constraint (6.93)–(6.95) for the static ExCTEPM heuristic in Step 3 or the enhanced model formulation of the ExCTEPM compared to Step 1. Step 2 runs relatively quick due to the smaller network size compared to Wanheimer Ort. In the second instance (Wanheimer Ort), Step 2 consumes approx. 62% of total compuatation time, whereby Step 1 and Step 2 need relatively less time compared to Neudorf although network size increases. This speed-up might be caused by the relaxation of constraint (6.36) and (6.38) for all cells j with $l_j = 1$.
Another interesting point is the route choice for rescue teams. In Neudorf, rescue teams use a relatively low frequented exit in the south-western part of Neudorf as the entrance and the chosen path leads directly to the center of danger without any detours. For the case of Wanheimer Ort, rescue teams choose also a low frequented exit in the eastern part of Wanheimer Ort, but the route through the network is not as straight as in the first instance. In particular, rescue teams mainly use small side streets and accept a longer access route in order to leave traffic on a highly occupied street – that would represent the shortest path from this exit – untouched.

Chapter 7

Evacuation Planning with Vehicles and Pedestrians

During an evacuation, all available flow capacities should be taken into account in the planning process. However, most of the literature dealing with evacuation planning problems from urban areas considers only one traffic mode, e.g. evacuation by vehicle. This assumption is reasonable since people evacuating from a large urban area usually want to take their valuables along with them and they need something to transport it, i.e. their vehicles. However, when it comes to evacuation of urban areas, at least two individual traffic modes can be taken into account, namely evacuation by vehicle and evacuation by foot in order to lower evacuation time and total danger for the evacuees. Furthermore, if evacuation is performed only by vehicles, it is often assumed that all evacuees can escape using a sufficient number of vehicles. This assumption probably holds for most inhabited areas in industrial countries, but there might also exist other scenarios where at least some evacuees have to escape by foot due to an insufficient number of vehicles. On the other hand, evacuating by foot might lead to improvements in terms of faster evacuation, because people living at the brink of the endangered area may escape faster, if they are not entering the (congested) road network, but escaping by foot, taking their valuables by themselves. Such situations might also lead to lower evacuation times for vehicles, since the road network capacities are less occupied.

To the best of our knowledge, only Sinuany-Stern and Stern (1993) covered the topic of evacuating people by car and by foot within an integrated simulation approach. They used several route choice mechanisms to determine routing decision en route. Among other aspects, they investigated the influence of different route selection mechanisms, the influence of "friction" between pedestrians and vehicles as well as different population sizes, but not the effects of integrating the mode choice.

In this chapter, we will include the mode choice (by vehicle, by foot) into an integrated evacuation planning optimization approach and discuss some universal properties. Again, we use the ExCTEPM introduced in Chapter 4 as a basis. This chapter bases on the work of Kimms and Maassen (2011a). Similar to Chapter 6, where we recapitulate the notation and model formulation of the ExCTEPM for the sake of readability, we will again display the used notation, but in a more compact tabularly form.

7.1 Integrating Pedestrian Flows

We already discussed that flow capacities should be used as efficiently as possible in the case of an evacuation in order to minimize danger for affected people. If we consider an additional mode choice (evacuation by foot), previously unused flow capacities can now be used. On the other side, the evacuation planning problem becomes more complex since more interactions between pedestrians and other pedestrians as well pedestrians and vehicles must be considered. In the following, we will first discuss how sidewalks can be implemented into a cell-based evacuation planning approach. Subsequently, conflicts between pedestrians and pedestrians/vehicles will be covered.

7.1.1 Sidewalk Modeling

The Cell-Transmission approach by Daganzo is intended to be used for vehicle traffic only. Now, we adopt the basic ideas of this approach to additionally model pedestrian traffic. If we only take vehicles within a cell-transmission-based framework into account, a street network can be transformed in a cell-based network as shown in Figure 7.1.

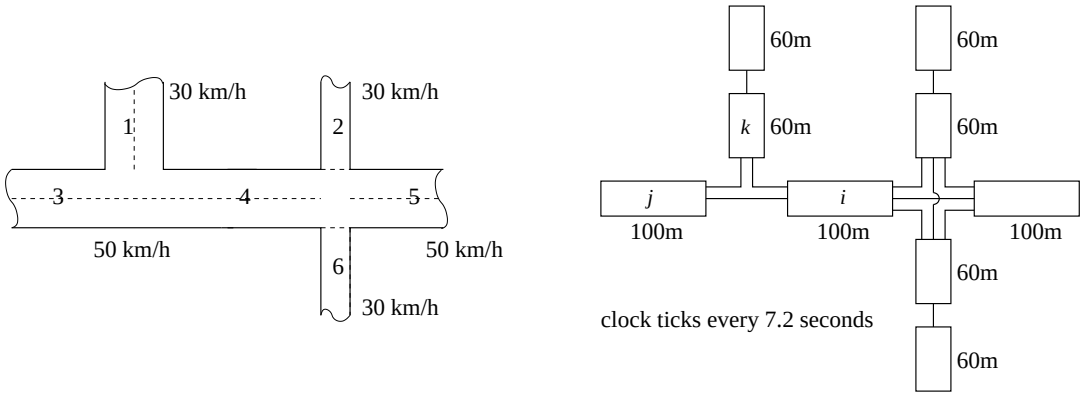

Figure 7.1: Cell Based Network Representation for Streets only

To cover pedestrian flows, the cell-based network must be modified . Therefore, we add two “sidewalk” cells as placeholders to every “street” cell as displayed in Figure 7.2.

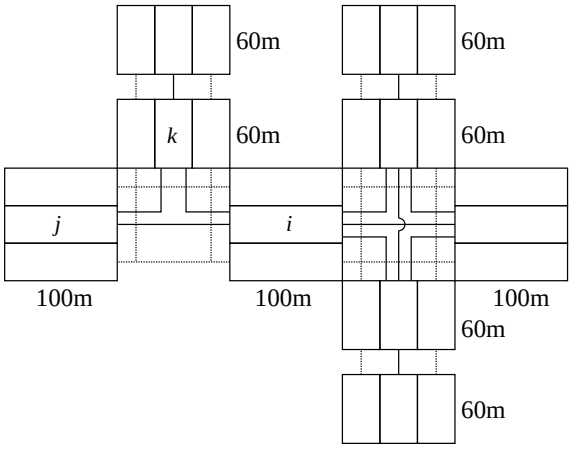

Figure 7.2: Cell Based Network Representation for Streets and Sidewalks

Solid lines represent possible vehicle flows and the dotted lines display only basic pedestrian flows for the sake of simplicity. A detailed illustration of possible pedestrian flows can be found in Figure 7.9 and 7.10.
The introduction of sidewalk cells significantly increases the number of required cells to model a network with streets and sidewalks. However, this modification is necessary in order to capture the potential crossing conflicts between vehicle and pedestrian traffic at junctions.
Another important aspect is the different movement speed of vehicles and pedestrians. While vehicle move with different driving speeds (in light traffic) in respect to the road infrastructure (e.g. 30km/h on narrow streets, 50km/h on urban streets and 100km/h on highways), pedestrians have a much slower and more constant (free-flowing) walking speed of approximately 5km/h. Therefore, the number of sidewalk cells is much higher than the number of street cells. For example, a narrow street with a vehicle driving speed of 30km/h (=8.33m/s) combined with a period length of 9 seconds can be described by a cell with a length of ($8.33m/s \cdot 9s =$) 75m. Pedestrians with a walking speed of 5km/h, will need 54 seconds to pass a distance of 75m which corresponds to 6 periods. Hence, the sidewalk must be modeled by six cells in order to cover the lower movement speed of pedestrians. Please note that the size of sidewalk cells is always the same on streets with different vehicle driving speeds (e.g. 50km/h or 30km/h), because the size of sidewalk cells only depends on the walking speed of pedestrians. In this case, each sidewalk cell would be 12.5m meters long. Figure 7.3 illustrates these relations. Cell 1 is a street cell for vehicles and cells 2-13 are sidewalk cells for pedestrians.

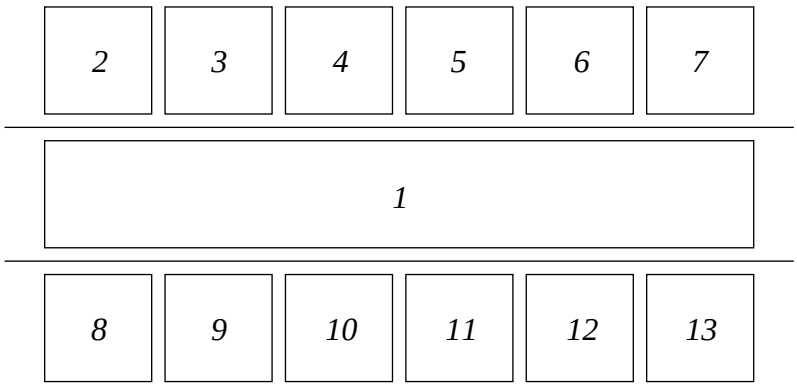

Figure 7.3: Relation between Cells for Vehicles and Pedestrians for One Cell Size

It is apparent that the number of cells rapidly increases when street *and* sidewalk cells should be considered. For the case of streets with a driving speed of 50km/h, each sidewalk must be modeled by 10 cells to capture the relations between the movement speeds (50km/h vs. 5km/h → 10:1) adequately. We discussed a comparable problem when we introduced the concept of multiple cell sizes, see Section 4.1.1. The purpose of using multiple cell sizes is to merge two or more cells on a single street with no junctions into just one cell in order to reduce the number of cells required to describe a given network. This approach fits perfectly to the issue of having a large amount of sidewalk cells in a row without junctions, because sidewalk cells on streets with a driving speed of 50km/h (30km/h) can be modeled as a single cell of size $n = 10$ ($n = 6$), see Figure 7.4.

Again, Cell 1 denotes the street cell which is now surrounded by only two sidewalk cells

Figure 7.4: Relation between Cells for Vehicles and Pedestrians for Multiple Cell Sizes

2 and 3 of size $n = 10$ for vehicles driving at 50km/h and $n = 6$ for vehicles driving at 30km/h. By doing so, network size of an "only-vehicles" network increases by the factor 3 when sidewalk cells are considered since every street cell will be surrounded by two sidewalk cells of larger size.
However, the concept of multiple cell sizes is primarily designed for streets with relatively simple traffic flows in one or two directions. When sidewalks are considered, more (pedestrian) flows within a section (including one street and two pedestrian cells) are possible, see Figure 7.5. Again, the center cell is a street cell, surrounded by two sidewalk cells above and below.

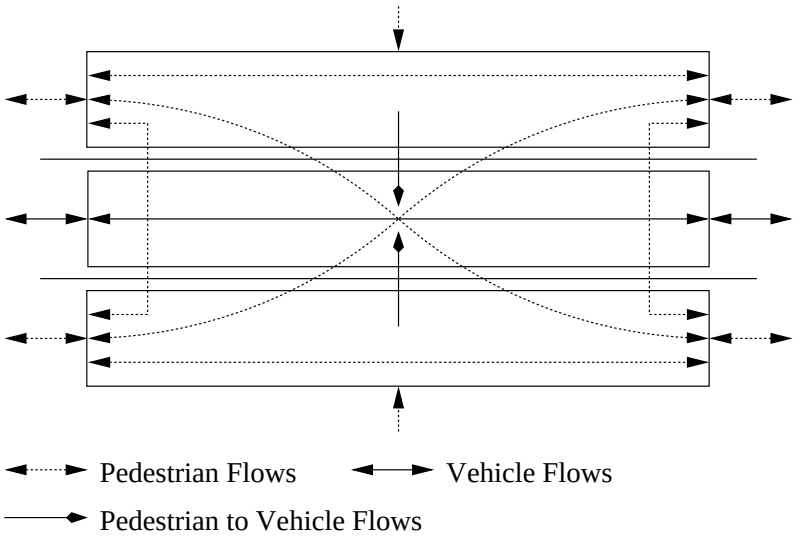

Figure 7.5: Possible Vehicle and Pedestrian Flows on a Street Section

It is easy to see that the ability to cross a street, to change the sidewalk and to switch to vehicles results in more possible flows compared to the street, on which flows are more simple. When these pedestrian flows should be included in evacuation planning, the concept of using only one cell (of larger size) to model a sidewalk reaches its limits since we do not see any implementation where these pedestrian flows can be implemented adequately. For example, we have to differentiate between three possible destination cells when pedestrians enter a sidewalk cell. All of these three destinations can be reached within different time horizons, i.e. for the case shown in Figure 7.3 two periods if pedestrians only change the side of the street and proceed in the same direction where they came from, six peri-

ods if pedestrians walk the complete sidewalk and seven periods if pedestrians walk the complete sidewalk and change the side of the street (one period for crossing the street). Moreover, these movements are direction-dependent, i.e. we have to differentiate between movements where pedestrians proceed to a new destination cell and movements where pedestrians return to the original street section where the they originally came from, but only on the other side of the street. These issues get even more complex when residents starting their evacuation have to be considered. Concluding, the usage of only one cell to model a sidewalk is not an appropriate approach to capture (complex) pedestrian flows.
Hence, if all pedestrian flows illustrated in Figure 7.5 should be considered and crossing the street should be possible all over the street, we have to model sidewalk cells as cells of size $n = 1$. Unfortunately, this approach results in a large number of cells, even for small networks, e.g. a street network modeled by 10 street cells of size $n = 1$, each with a driving speed of 50km/h results in a network with 210 cells, where each street cell is surrounded by 20 sidewalk cells. Of course, street cells with a driving speed of 30km/h require the adding of "only" 12 cells, but the effect stays generally the same. Depending on the driving speeds within the network, the number of cells required to include pedestrian traffic thus increases by the factor 12-20.
As already explained, pedestrians may change the side of the street at different segments, for example at the very beginning of the sidewalk, the very end of the sidewalk or somewhere in between. Additionally, residents may decide to change the sidewalk as soon as they leave their homes so that street crossing may take place over the complete street length. These alternatives are illustrated in Figure 7.6 for street with a driving speed of 30km/h.

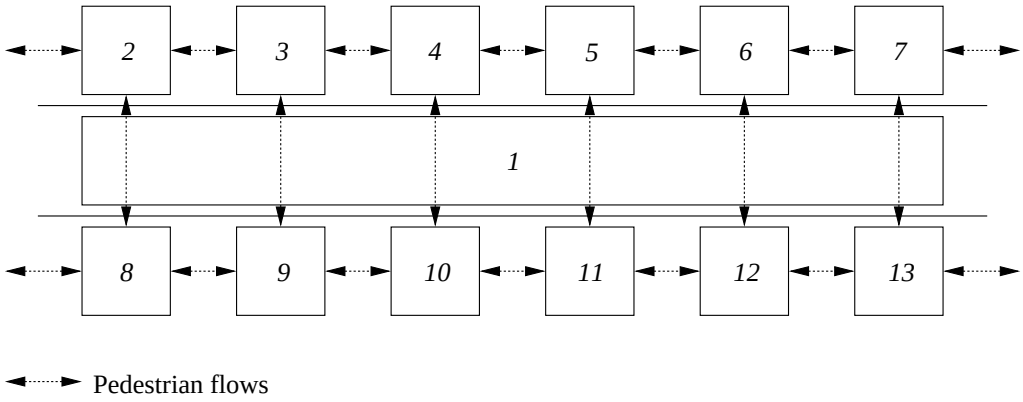

Figure 7.6: Pedestrian Flows within a Street Section for One Cell Size

Using the representation in Figure 7.6, all pedestrian flows illustrated in Figure 7.5 are implemented correctly. If pedestrians enter the street section via cell 2, they will need two periods to leave the street section via cell 8, six periods the leave the street section via cell 7 and seven periods to leave the street section via cell 13. In the latter case, it is obvious that different paths can be used, e.g. $2 \rightarrow 3 \rightarrow 4 \rightarrow 5 \rightarrow 6 \rightarrow 7 \rightarrow 13$, $2 \rightarrow 3 \rightarrow 4 \rightarrow 5 \rightarrow 6 \rightarrow 12 \rightarrow 13$, $2 \rightarrow 3 \rightarrow 4 \rightarrow 5 \rightarrow 11 \rightarrow 12 \rightarrow 13$ etc.. However, these paths are highly redundant since the number of periods to get from cell 2 to cell 13 is always the same. Additionally, we can assume that danger for evacuees is uniformly distributed within a street section so that it makes nearly no difference, which path pedestrians take. Thus, for the sake of simplicity, we assume that changing the side of the street is only possible between the outer pedestrian cells of a street section, see Figure 7.7.

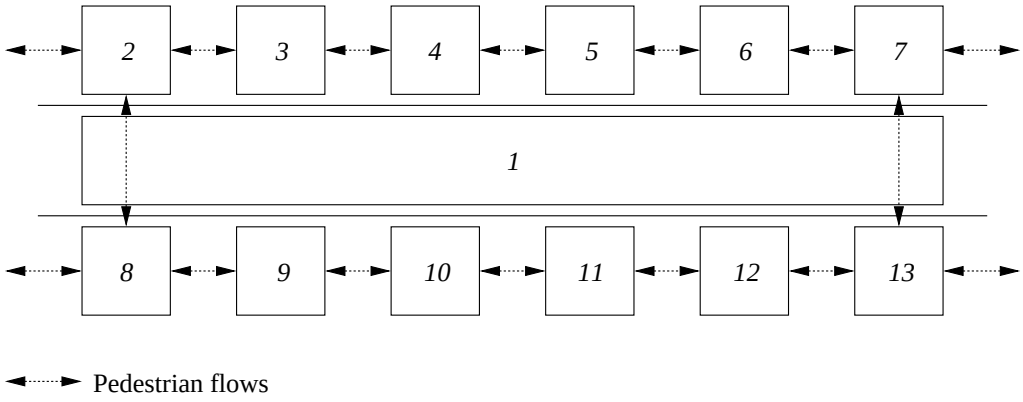

Figure 7.7: Reduced Pedestrian Flows within a Street Section for One Cell Size

If we now take a closer look at the cells 3–6 and 9–12, we observe that these cells can be merged into one larger cell without major interferences. In detail, these larger cells do not allow any street crossing so that pedestrian flows within these larger cells are much simpler than before. It should be noted that always 3 three cells are needed to describe one sidewalk, independent of the driving speed on the street. e.g. the size of the large sidewalk cell is $n = 8$ on streets with 50km/h driving speed and $n = 4$ on streets with 30km/h driving speed. In combination with two surrounding (sidewalk) cells, each of size $n = 1$ the original "length" of $n = 10$ and $n = 6$ can be ensured, respectively. Figure 7.8 illustrates these relations.

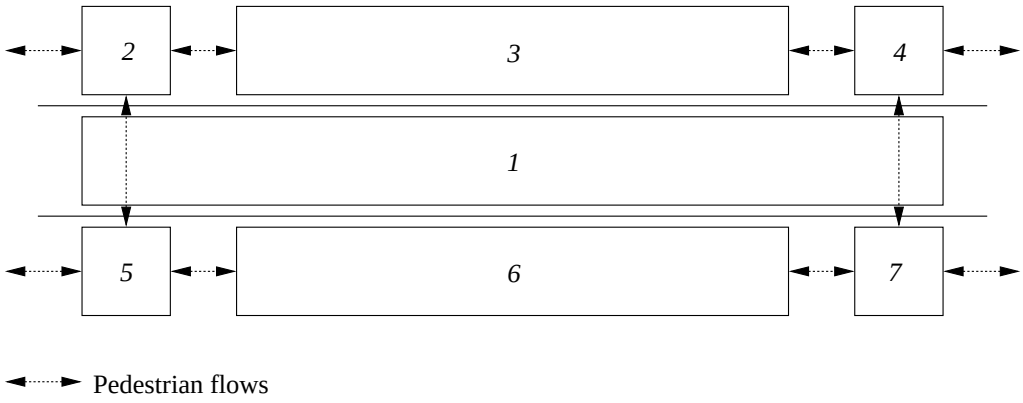

Figure 7.8: Reduced Pedestrian Flows within a Street Section for Multiple Cell Sizes

As the approach illustrated in Figure 7.8 combines a relatively low number of additional cells with sufficient flexibility for pedestrians flows, we will use this approach in the following.

7.1.2 Crossing Conflicts

The integration of pedestrian flows into evacuation planning with vehicles result in a large number of potential crossing conflicts at junctions. However, to ensure a widely unobstructed evacuation process these crossing conflicts must be avoided. For the case of a junction with three entrances/exits, we identify 15 potential crossing conflicts between

vehicles and pedestrians as well as pedestrians and other pedestrians, see Figure 7.9. Although danger for crossing pedestrian flows is much lower than for crossing vehicle flows, we also want to avoid suchlike conflicts for pedestrians to ensure uninterrupted pedestrian flows.

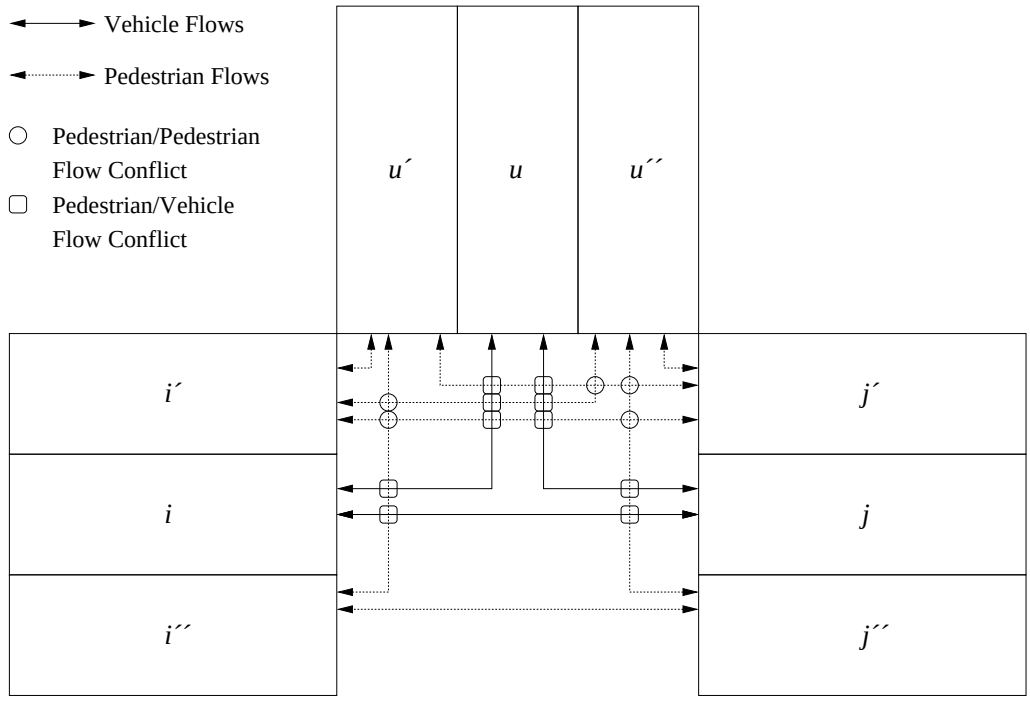

Figure 7.9: Crossing Conflicts at a t-junction

Figure 7.9 illustrates potential vehicle and pedestrians movements as well as crossing conflicts on a t-junction. We assume that pedestrian flows are not allowed to cross junctions diagonally. Instead, only movements as illustrated in Figure 7.9 are possible, if no conflict with vehicle flows exists. In total, there are 10 crossing conflicts between vehicles and pedestrians as well as 5 crossing conflicts between pedestrians and other pedestrians.
For the case of a junction with four entrances/exits, the number of potential crossing conflicts increases to 56, divided into 36 crossing conflicts between vehicles and pedestrians as well as 20 crossing conflicts between pedestrians and other pedestrians, see Figure 7.10.

Figure 7.10 displays potential pedestrian movements within a four-way junction. Again, we assume that pedestrians are not allowed to cross junctions diagonally. A four-way junction also includes a crossing conflict between vehicles in the center of the junction, marked by a cross in Figure 7.10.
For junctions with five or more entrances/exits, crossing conflicts can be constructed analogously to three and four-way junctions. However, for the sake of simplicity, we refer only to three and four-way junctions in this work.
Please recall that pedestrians are allowed to change the sidewalk of the street, if pedestrian flows and vehicle flows are not conflicting. This assumption allows that pedestrians can theoretically reach every sidewalk in the network without major detours.

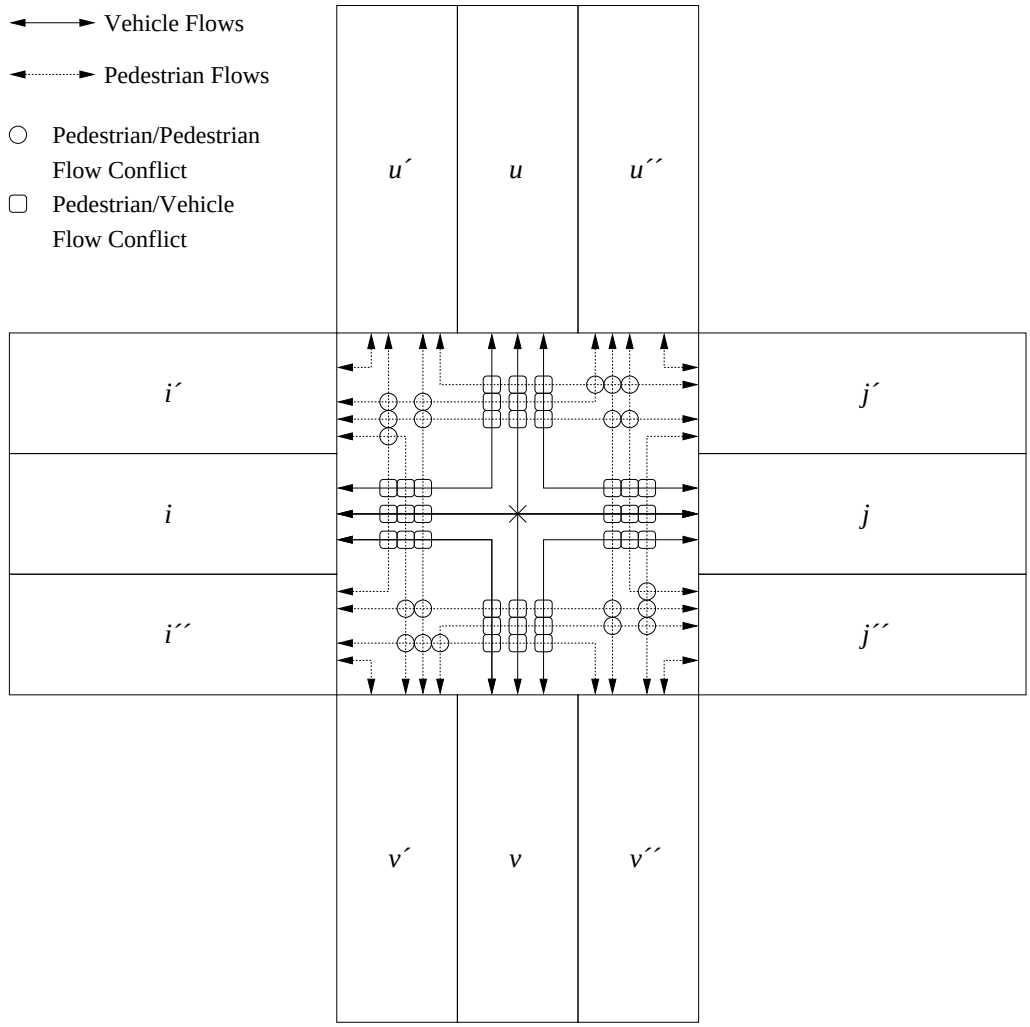

Figure 7.10: Crossing Conflicts at a four-way junction

7.2 ExCTEPM with Pedestrians

Since our integrated approach for evacuation planning with vehicles and pedestrians mainly bases on the ExCTEPM, we name our approach "ExCTEPM with pedestrians" or use the acronym "ExCTEPMP". In order to capture pedestrian traffic, intersections and connections between cells must be considered more in detail. Moreover, we have to introduce a large number of new variables to cover pedestrian flows and the changeover from pedestrian to vehicle traffic. We use the following notation.

7.2.1 Notation

Parameters:

$T = \{1, \ldots, \lvert T \rvert\}$	Index set of periods (where $\lvert T \rvert$ is the index of the last period of the planning horizon)
$I = \{1, \ldots, \lvert I \rvert\}$	Index set of cells with the following differentiation: $\lvert I \rvert - 1$: super sink for vehicles (from street cells) $\lvert I \rvert$: super sink for pedestrians (from sidewalk cells) I_v : street cells (for vehicles) including super sink $\lvert I \rvert - 1$ I_p : sidewalk cells (for pedestrians) including super sink $\lvert I \rvert$
$S = \{1, \ldots, \lvert S \rvert\}$	Index set of intersections
c_{it}	danger of being at cell i in period t ($c_{it} \geq 0$)
β_{ij}	$= \beta_{ji} = 1$, if a traffic flow from cell i to cell j (and vice versa) can be established, 0 otherwise (no mode switch)
β^c_{ij}	$= \beta^c_{ji} = 1$, if cell i and cell j belong to the same street section and a traffic flow can be established, 0 otherwise (mode switch possible)
β^s_{is}	if cell i is connected to intersection s
N_{it}	maximum vehicle / pedestrian capacity of (street/sidewalk) cell i on all "lanes" in period t
E_i	number of evacuees starting their evacuation in cell i
E^p_i	number of evacuees in cell i forced to escape by foot
Q_{it}	maximum number of in- and outflowing vehicles / pedestrians on all "lanes" into / from (street/sidewalk) cell i in period t
l_i	number of "lanes" in (street/sidewalk) cell i
p	maximum number of outflowing evacuation traffic streams
x_{i1}	number of vehicles at cell i before the evacuation starts
x^p_{i1}	number of pedestrians at cell i before the evacuation starts
a	maximum number of evacuees per vehicle
n_i	size of (pedestrian) cell i

Decision Variables:

z_{it}	number of vehicles residing, leaving or waiting in cell i in period t
z^p_{it}	number of evacuating pedestrians residing, leaving or waiting in cell i in period t
x_{it}	number of residing vehicles at cell i at the end of period t
x^p_{it}	number of residing pedestrians at cell i at the end of period t
y_{ijt}	number of evacuating vehicles leaving (street) cell i in period t and reaching (street) cell j
y^p_{ijt}	number of pedestrians leaving (sidewalk) cell i in period t and reaching (sidewalk) cell j
y^{cp}_{ijt}	number of pedestrians leaving (sidewalk) cell i in period t and reaching (street) cell j in a vehicle
y^{cv}_{ijt}	number of vehicles starting evacuation in (street) cell j in period t coming from (sidewalk) cell i as pedestrians
b^p_{it}	number of pedestrians starting evacuation at cell i in period t
φ_{ij}	$= 1$, if vehicles drive from cell i to cell j, 0 otherwise
φ^p_{ij}	$= 1$, if pedestrians move from cell i to cell j, 0 otherwise
ϵ_{ij}	number of used lanes between cell i and cell j for vehicles
ϵ^p_{ij}	number of used lanes between cell i and cell j for pedestrians

7.2.2 Model Formulation

Based on this notation, we can formulate the ExCTEPM with pedestrians as follows:

$$\min \sum_{i \in I_v} \sum_{t \in T} c_{it} \cdot z_{it} \cdot a + \sum_{i \in I_p} \sum_{t \in T} c_{it} \cdot z^p_{it} \tag{7.1}$$

subject to

$$z_{it} = x_{it} + \sum_{j \in I_v} y_{ijt} \qquad i \in I_v \ ; \ t \in T \tag{7.2}$$

$$z^p_{it} = x^p_{it} + \sum_{j \in I_p} y^p_{ijt} + \sum_{\substack{j \in I_v: \\ \beta^c_{ij}=1}} y^{cp}_{ijt} + (E_i - \sum_{\tau=1}^{t} b^p_{i\tau}) \qquad i \in I_p \ ; \ t \in T \tag{7.3}$$

$$x_{it} = x_{i,t-1} + \sum_{j \in I_v} y_{ji,t-1} - \sum_{j \in I_v} y_{ijt} + \sum_{\substack{j \in I_p: \\ \beta^c_{ji}=1}} y^{cv}_{ji,t-1} \qquad i \in I_v \ ; \ t = 2, \ldots, |T| \tag{7.4}$$

$$x^p_{it} = b^p_{it} + x^p_{i,t-1} + \sum_{j \in I_p} y^p_{ji,t-1} - \sum_{j \in I_p} y^p_{ijt} - \sum_{\substack{j \in I_v: \\ \beta^c_{ij}=1}} y^{cp}_{ijt} \qquad i \in I_p \ ; \ t = 2, \ldots, |T| \tag{7.5}$$

$$\begin{aligned} \sum_{j \in I_p} \sum_{\tau=1}^{t} y^p_{ij\tau} \leq \sum_{j \in I_p} \sum_{\tau=1}^{\max(t-n_i,1)} y^p_{ji\tau} + \sum_{\tau=1}^{\max(t-\lceil n_i/2 \rceil+1,1)} b^p_{i\tau} \\ - \sum_{\substack{k \in I_v: \\ \beta^c_{ik}=1}} \sum_{\tau=1}^{\max(t-\lceil n_i/2 \rceil+1,1)} y^{cp}_{ik\tau} + x^p_{i1} \qquad i \in I_p : n_i \geq 2 \ ; \ t \in 2, \ldots, |T| \end{aligned} \tag{7.6}$$

$$y^{cv}_{ijt} \cdot a \geq y^{cp}_{ijt} \qquad i \in I_p \ ; \ j \in I_v : \beta^c_{ij} = 1 \ ; \ t \in T \tag{7.7}$$

$$z_{it} \leq N_{it} \qquad i \in I_v \ ; \ t \in T \tag{7.8}$$

$$z^p_{it} \leq N_{it} + (E_i - \sum_{\tau=1}^{t} b^p_{i\tau}) \qquad i \in I_p \ ; \ t \in T \tag{7.9}$$

$$x_{it} \leq N_{it} \qquad i \in I_v \ ; \ t \in T \tag{7.10}$$

$$x^p_{it} \leq N_{it} \qquad i \in I_p \ ; \ t \in T \tag{7.11}$$

$$\sum_{t \in T} b^p_{it} = E_i \qquad i \in I_p \tag{7.12}$$

$$\sum_{i \in I_p} \sum_{j \in I_v : \beta^c_{ij=1}} \sum_{t \in T} y^{cv}_{ijt} + \sum_{i \in I_v} x_{i1} = x_{|I|-1,|T|} \tag{7.13}$$

$$\sum_{i \in I_p} (E_i - \sum_{j \in I_v : \beta^c_{ij=1}} \sum_{t \in T} y^{cp}_{ijt} + x^p_{i1}) = x_{|I|,|T|} \tag{7.14}$$

$$\sum_{i \in I_v} y_{ijt} \leq (N_{jt} - x_{jt}) \qquad j \in I_v \ ; \ t \in T \tag{7.15}$$

$$\sum_{i \in I_p} y^p_{ijt} \leq (N_{jt} - x^p_{jt}) \qquad j \in I_p \ ; \ t \in T \tag{7.16}$$

$$y_{ijt} \leq N_{it} \cdot \beta_{ij} \qquad i,j \in I_v \ ; \ t \in T \qquad (7.17)$$

$$y^p_{ijt} \leq N_{it} \cdot \beta_{ij} \qquad i,j \in I_p \ ; \ t \in T \qquad (7.18)$$

$$y_{ijt} \leq \frac{Q_{jt}}{l_j} \cdot \epsilon_{ij} \qquad i,j \in I_v \ ; \ t \in T \qquad (7.19)$$

$$y_{ijt} \leq \frac{Q_{it}}{l_i} \cdot \epsilon_{ij} \qquad i,j \in I_v \ ; \ t \in T \qquad (7.20)$$

$$y^p_{ijt} \leq \frac{Q_{jt}}{l_j} \cdot \epsilon^p_{ij} \qquad i,j \in I_p \ ; \ t \in T \qquad (7.21)$$

$$y^p_{ijt} \leq \frac{Q_{it}}{l_i} \cdot \epsilon^p_{ij} \qquad i,j \in I_p \ ; \ t \in T \qquad (7.22)$$

$$\sum_{j \in I_v : \beta^c_{ij} = 1} y^{cp}_{ijt} \leq b^p_{it} \qquad i \in I_p \ ; \ t \in T \qquad (7.23)$$

$$\sum_{j \in I_v : \beta^c_{ij} = 1} \sum_{t \in T} y^{cp}_{ijt} \leq E_i - E^p_i \qquad i \in I_p \qquad (7.24)$$

$$\varphi_{ij} + \varphi_{jk} \leq 1 \qquad i,j,k \in I_v : \beta_{ij} = \beta_{ik} = 1 \qquad (7.25)$$

$$\varphi^p_{ij} + \varphi^p_{jk} \leq 1 + \beta^c_{ij} + \beta^c_{jk} \qquad i,j,k \in I_p \ ; \ s \in S : \beta^s_{is} = \beta^s_{js} = \beta^s_{ks} = 1 \qquad (7.26)$$

$$\varphi_{ij} \leq \beta_{ij} \qquad i,j \in I_v \qquad (7.27)$$

$$\varphi^p_{ij} \leq \beta_{ij} \qquad i,j \in I_p \qquad (7.28)$$

$$\epsilon_{ij} \leq \varphi_{ij} \cdot \min\{l_i, l_j\} \qquad i,j \in I_v \qquad (7.29)$$

$$\epsilon^p_{ij} \leq \varphi^p_{ij} \cdot \min\{l_i, l_j\} \qquad i,j \in I_p \qquad (7.30)$$

$$\sum_{i \in I_v} \varphi_{ij} \leq l_j \qquad j \in I_v \qquad (7.31)$$

$$\sum_{j \in I_v} \varphi_{ij} \leq p \qquad i \in I_v \qquad (7.32)$$

$$\sum_{i \in I_v} \epsilon_{ij} \leq l_j \qquad j \in I_v \qquad (7.33)$$

$$\sum_{j \in I_v} \epsilon_{ij} \leq l_i \qquad i \in I_v \qquad (7.34)$$

$$\sum_{i \in I_p} y^p_{ijt} \leq Q_{jt} \qquad j \in I_p \ ; \ t \in T \qquad (7.35)$$

$$\sum_{j \in I_p} y^p_{ijt} \leq Q_{it} \qquad i \in I_p \ ; \ t \in T \qquad (7.36)$$

$$\varphi_{ij} + \varphi_{ji} + \varphi_{uv} + \varphi_{vu} \leq 1 \qquad i,j,u,v \in I_v : \beta_{ij} = \beta_{iu} = \beta_{iv} = \beta_{ju} = \beta_{jv} = \beta_{uv} = 1 \qquad (7.37)$$

$$\varphi_{ij} + \varphi_{ji} + \varphi^p_{uv} + \varphi^p_{vu} \leq 1 \qquad \text{for all } i \to j \ (i,j \in I_v) \text{ crossing } u \to v \ (u,v \in I_p) \qquad (7.38)$$

$$\varphi^p_{ij} + \varphi^p_{ji} + \varphi^p_{uv} + \varphi^p_{vu} \leq 1 \qquad \text{for all } i \to j \ (i,j \in I_p) \text{ crossing } u \to v \ (u,v \in I_p) \qquad (7.39)$$

$$\varphi_{vu} + \varphi_{uv} + \varphi^p_{ij} + \varphi^p_{ji} \leq 1 \qquad i,j,k,l \in I_p \ ; \ u,v \in I_v : \beta^c_{ij} = \beta^c_{kl} = \beta_{ik} = \beta_{jl} = 1 \ \beta^c_{ik} = \beta^c_{jl} = 0 \ \beta^c_{iu} = \beta^c_{ju} = \beta^c_{kv} = \beta^c_{lv} = 1 \tag{7.40}$$

$$\epsilon_{ij} \in \mathbb{N}_0 \qquad i,j \in I_v \tag{7.41}$$

$$\epsilon^p_{ij} \in \mathbb{N}_0 \qquad i,j \in I_p \tag{7.42}$$

$$\varphi_{ij} \in \{0,1\} \qquad i,j \in I_v \tag{7.43}$$

$$\varphi^p_{ij} \in \{0,1\} \qquad i,j \in I_p \tag{7.44}$$

$$z_{it}, x_{it} \geq 0 \qquad i \in I_v \ ; \ t \in T \tag{7.45}$$

$$z^p_{it}, x^p_{it}, b^p_{it} \geq 0 \qquad i \in I_p \ ; \ t \in T \tag{7.46}$$

$$y_{ijt} \geq 0 \qquad i,j \in I_v \ ; \ t \in T \tag{7.47}$$

$$y^p_{ijt} \geq 0 \qquad i,j \in I_p \ ; \ t \in T \tag{7.48}$$

$$y^{cp}_{ijt} \geq 0 \qquad i \in I_p \ ; \ j \in I_v : \beta^c_{ij} = 1 \ ; \ t \in T \tag{7.49}$$

$$y^{cv}_{ijt} \in \mathbb{N}_0 \qquad i \in I_p \ ; \ j \in I_v : \beta^c_{ij} = 1 \ ; \ t \in T \tag{7.50}$$

$$x_{i1} = 0 \qquad i \in I_v \tag{7.51}$$

$$y_{ij1} = 0 \qquad i,j \in I_v \tag{7.52}$$

$$x^p_{i1} = 0 \qquad i \in I_p \tag{7.53}$$

$$b^p_{i1} = 0 \qquad i \in I_p \tag{7.54}$$

$$y^p_{ij1} = 0 \qquad i,j \in I_p \tag{7.55}$$

$$y^{cp}_{ij1} = 0 \qquad i \in I_p \ ; \ j \in I_v : \beta^c_{ij} = 1 \tag{7.56}$$

$$y^{cv}_{ij1} = 0 \qquad i \in I_p \ ; \ j \in I_v : \beta^c_{ij} = 1 \tag{7.57}$$

The objective function (7.1) minimizes total danger for all evacuees leaving the endangered area by vehicle (first term) and by foot (second term) during the planning horizon. Please note that vehicles are always additionally weighted with the parameter a, regardless of the number of evacuees inside a vehicle. Since unoccupied seats within a vehicle represent capacities which can be used without additional costs, vehicles starting from a specific cell i usually will be loaded with the maximum number of evacuees in an optimum solution, if the number of seats equals the number of evacuees starting in cell i. However, there are also situations where not every seat in a vehicle is used, e.g. if $E_i \bmod a > 0$ holds and all residents are escaping by vehicle. In such cases, vehicles will be loaded in respect to the remaining number of evacuees. Moreover, we added some additional terms to the objective function to improve readability of the solution and computation time. Firstly, we added $+10^{-5} \cdot \sum_{i,j \in I_v} \sum_{t \in T} y_{ijt}$ as well as $+10^{-5} \cdot \sum_{i,j \in I_p} \sum_{t \in T} y^p_{ijt}$ to the objective function in order to avoid unnecessary vehicle and pedestrian movements, which may occur if two adjacent cells share the same level of danger. Secondly, we added the term $-10^{-6} \cdot \sum_{t \in T} (x_{|I|-1,t} + x^p_{|I|,t})$ to ensure that vehicles escape the network as fast as possible. However, it turned out that the second term also helps to reduce computation time for our examples. Equation (7.2) and (7.3) calculate the number of vehicles and pedestrians in danger in cell i in period t. Please note that equation (7.3) also includes the number of

evacuees which have not left their homes until a given period t. (7.4) and (7.5) represent vehicle and pedestrian flow equations. In detail, the number of residing vehicles in a cell i at the end of period t is equal to the number of residing vehicles from a period before plus the number of incoming vehicles minus the number of outgoing vehicles plus the number of evacuees starting the evacuation by car in period $t-1$. For pedestrians, the number of residing pedestrians in cell i at the end of period t is equal to the number of residents starting their evacuation in period t plus the number of residing pedestrians from a period before plus the number of incoming pedestrians minus the number of outgoing pedestrians minus the number of pedestrians switching to their vehicles. It should be mentioned that the decision to evacuate by vehicle is non-reversal, i.e. evacuees which have entered their cars once have to escape by car. To cover multiple cell sizes for pedestrians, constraint (7.6) limits the number of outgoing pedestrians in regard to incoming pedestrians and cell size. In detail, the total number of outgoing pedestrians till a period t is lower or equal to the total number of pedestrians which have entered the cell not later than $t-n_i$ periods before plus the total number of residents starting their evacuation not later than $t-\lceil n_i/2 \rceil+1$ periods before (denoting approx. the "middle" of a cell) which have decided not to escape by car plus the initial number of pedestrians in this cell. To ensure that the number of starting vehicles provide enough space for all residents which have decided to evacuate by vehicle constraint (7.7) is needed. Since every additional vehicle leads to increased "cost" in the objective function, only as many vehicles as absolutely necessary will be created in the model.
Constraints (7.8)–(7.11) represent capacity limits for the number of vehicles/pedestrians in cell i in period t. The equations (7.12)–(7.14) ensure that all evacuees will leave their homes and reach a safe place (i.e. one of the super sinks) within the planning horizon.
Moreover, the number of vehicles traveling from cell i to cell j have to be restricted in several ways, see constraints (7.15)–(7.22). In detail, the number of cell changing vehicles must not exceed free space in the destination cell ((7.15) and (7.16)), the maximum vehicle capacity of a cell ((7.17) and (7.18)) as well as the vehicle flow capacities of allocated lanes ((7.19)–(7.22)).
It must also be assured that only residents in a certain cell may start their evacuation by car, see (7.23). Otherwise it would be possible to begin the evacuation by foot, walking a few streets and finally switching to a vehicle in a non-origin cell to finish the evacuation. As already explained at the beginning of this chapter, there may exist some scenarios, where the number of evacuees exceeds the number of available seats in vehicles so that some evacuees have to escape by foot. Suchlike situations are captured by constraint (7.24), where at least E_i^p evacuees are forced to escape by foot. In order to avoid odd situations between three cells like displayed in Figure 3.5, constraints (7.25) (for vehicles) and (7.26) (for pedestrians) are needed. The application of (7.26) for pedestrians also requires the introduction of a set of intersections to determine where suchlike situations between sidewalk cells may exist. In detail, every intersection with more than two entrances / exits is part of S. Moreover, to allow crossing a street in front of an intersection if no conflict with another pedestrian or vehicle flow exists, the term $+\beta_{ij}^c + \beta_{jk}^c$ is added to (7.26).
The constraints (7.27)–(7.30) prohibit vehicle/pedestrian flow and lane allocations only to those cell combinations, where a direct connection in terms of β_{ij} exists. In order to guide traffic in a little or almost non-conflicting way, we already introduced traffic flow limitation constraints, see (7.31)–(7.34). These constraints assure that there will be no merging processes at junctions so that traffic can flow undisturbed through junctions, which are normally a very critical place in traffic planning. We apply these constraints only to vehicle traffic since movement speeds of pedestrians are much lower so that merg-

ing processes at junctions will be possible. It has to be mentioned that there may exist some situations, where no feasible solution due to (7.31) and (7.33) exists, e.g. imagine a t-junction with three one lane streets, two being a deadlock and one not being a deadlock. The only feasible solution consists of vehicles traveling from the deadlock streets to the non-deadlock street. However, suchlike situations are forbidden by (7.31) and (7.33), so that these constraints have to be relaxed. To ensure that traffic flow capabilities will be met, the constraint $\sum_{i \in I_v} y^p_{ijt} \leq Q_{jt}$ must be added in such situations. Since there are no counterparts of constraints (7.31)–(7.34) for pedestrians, similar constraints have to be added for pedestrian traffic to assure adequate in- and outflow, see (7.35) and (7.36).
As already displayed in Figure 7.9 and 7.10 there are several crossing conflicts between vehicle flows and other vehicle flows, vehicle flows and pedestrian flows as well as pedestrian flows and other pedestrian flows. Traffic crossing and traffic touching conflicts between vehicles at junctions can be avoided relatively simple by constraint (7.37). Crossing conflicts between pedestrians and vehicles as well as pedestrians and pedestrians (as discussed in Section 7.1.2) are illustrated in constraints (7.38) and (7.39).
Constraint (7.40) ensures that there will be no conflicts between vehicles and pedestrians crossing a street. Figure 7.11 illustrates these relations for a simple case with two consecutive located cells, each consisting of one street and several sidewalk cells.

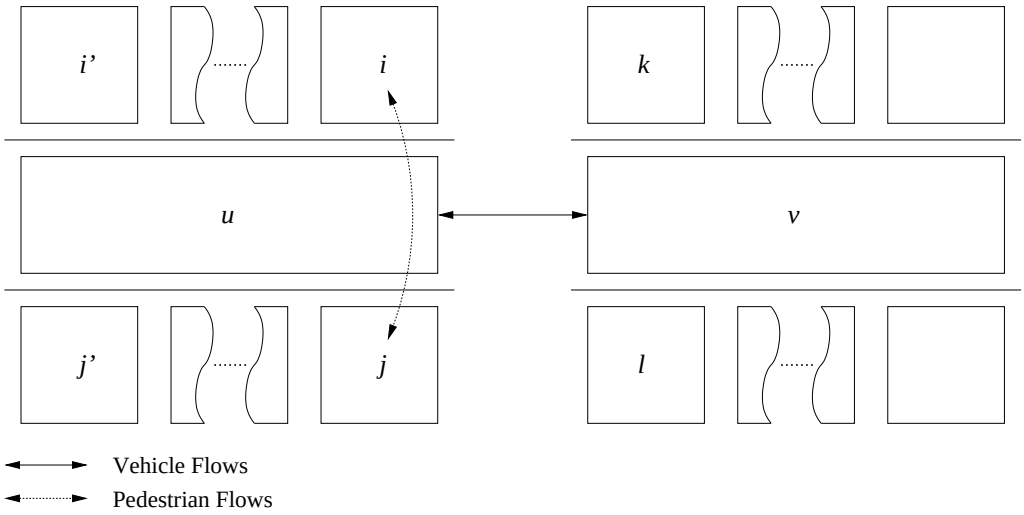

Figure 7.11: Street Crossing and Vehicle Flows

Here, constraint (7.40) makes sure that no pedestrians are allowed to cross the street from cell i to cell j (or vice versa), if a vehicle flow from cell u to cell v (or vice versa) exists. However, if vehicles are leaving cell u only in direction of cell v, pedestrians are allowed to cross the street at a different place, i.e. from cell i' to cell j' (or vice versa). Of course, this constraint also holds for junctions.
Finally, (7.41)–(7.50) define the domain of the decision variables. Please note that it is sufficient to consider only those flow variables y_{ijt} and y^p_{ijt} where $\beta_{ij} = 1$ holds and those flow variables y^{cp}_{ijt} and y^{cv}_{ijt} where $\beta^c_{ij} = 1$ holds, respectively. In contrast to all previously used version of the ExCTEPM, the new flow variable y^{cv}_{ijt} will be defined as an integer variable to ensure integrality for the number of starting vehicles. To ensure that no vehicle or pedestrian movements occur before the evacuation starts – i.e. period 1 –, boundary conditions (7.51) – (7.57) set all relevant decision variables to zero in the first period.

7.3 Numerical Examples

In this section, we illustrate the functionality of the optimization model for two artificial instances. Moreover, we apply some basic thoughts concerning evacuation planning with vehicles and pedestrians to a real-world instance. We implemented the optimization model in AMPL (*http://www.ampl.com/*) and solved it using the GUROBI 3.0.1 solver (*http://gurobi.com/*). All experiments were conducted on a computer using an Intel X9100 (3.06 Ghz), 8 GB of memory and Windows Vista (64-bit).

7.3.1 Artificial Network Examples

To demonstrate the functionality of our integrated optimization model, we prepared two artificial networks of different size. We set the length of a street cell with a driving speed of 50 km/h to 125m. According to this, street cells with a driving speed of 30 km/h are 75m and (standard) sidewalk cells are 12.5m long. The population is distributed randomly between 10 and 20 residents for each (standard) sidewalk cell. Sidewalk cells of larger size are inhabited by a proportional larger number of residents. Moreover, we assume that all evacuees can escape by vehicle, if desired. The danger in terms of c_{it} is also distributed uniformly with $c_{it} = c_i \cdot t$ with $c_i = 100$ for all cells within the network and $c_i = 0$ for both super sinks. Flow and vehicle/pedestrian capacities are constant over time.
The first network consists of only two sections (50 km/h driving speed), leading to two street cells and a total of 12 sidewalk cells. Evacuees can escape through cell 1, 2, 3, 6, 11 and 14. The topology of the network is displayed in Figure 7.12.

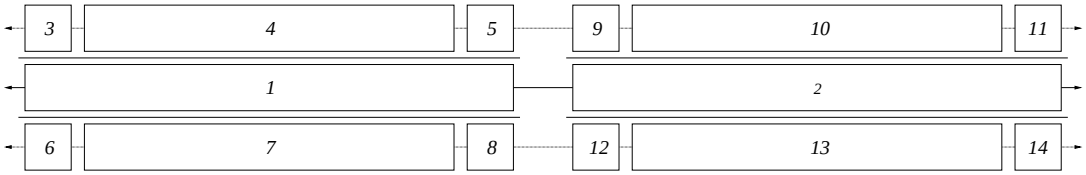

Figure 7.12: Topology of Test Network 1

We computed the optimum solutions for this network setting $a = 1, 3, 5$. The computation times are 0.2 seconds ($a = 1$), 27 seconds ($a = 3$)and 1.8 seconds ($a = 5$). We set $|T| = 20$. The solution using $a = 3$ is shown in Figure 7.13. The arrows indicate pedestrian and vehicle flows. If a pedestrian cell is connected to a street cell, these evacuees switch to vehicles and escape using the street network. In this case (Figure 7.13), most pedestrians switch to vehicles, especially in the center of the network (i.e. cell 4, 5, 7, 8, 9, 10, 12, 13). However, some evacuees located at the brink of the network (i.e. cell 3, 6, 11, 12 and partially cell 4, 7, 10 and 13) evacuate by foot. This observation corresponds to the common sense, because the incentive to escape by foot decreases with increasing distance to the safe zone.

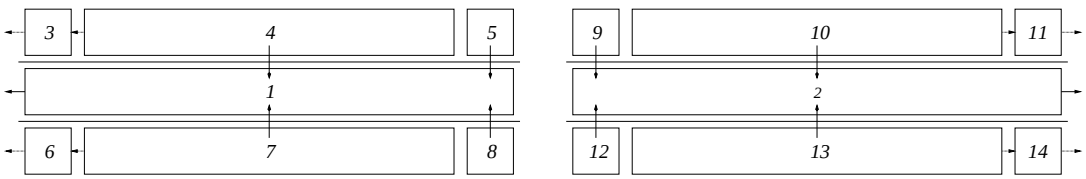

Figure 7.13: Solution of Test Network 1 for $a = 3$

The second artificial network consists of four street segments, three of them with a driving speed of 50 km/h and one segment with a driving speed of 30 km/h. Again, we use random numbers between 10 and 20 to generate the population for a standard sidewalk cell. Moreover, we increased $|T|$ to $|T| = 30$ and set $a = 1, 3, 5$. The network topology is shown in Figure 7.14.

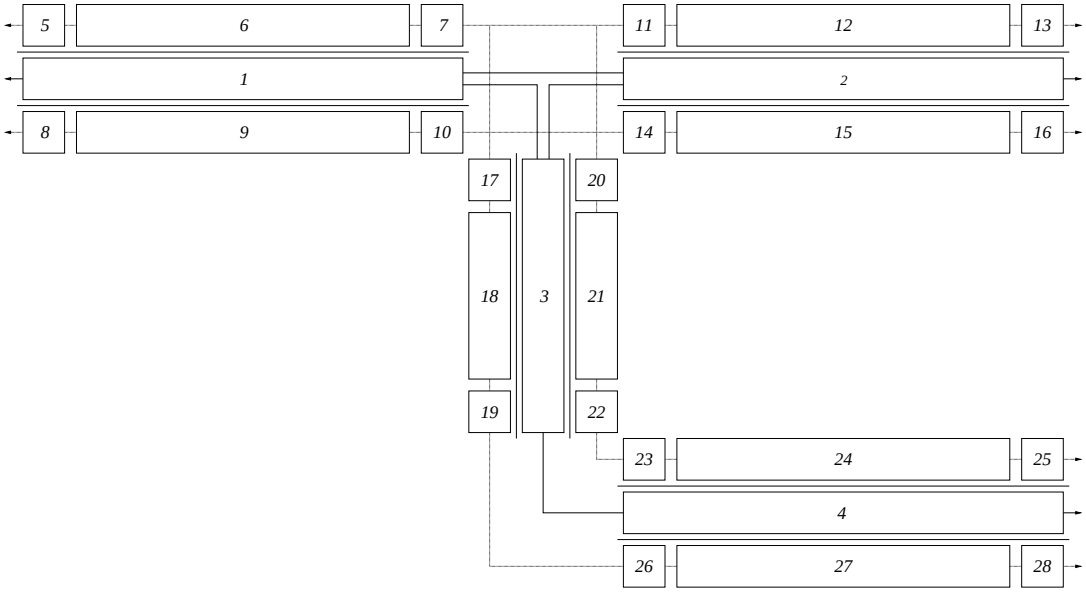

Figure 7.14: Topology of Test Network 2

Although this network is only slightly larger than the first network, GUROBI has an issue with proving optimality of a solution for $a = 3$ and $a = 5$. We set a time limit of two hours for the computation, but the solver made only very little progress after the first few minutes. For example, for $a = 3$ GUROBI gets stuck at a mipgap of 0.34% after 175 seconds, which could not be enhanced within the remaining computation time. For $a = 5$, the solver starts with a promising mipgap of 1.95% after 16 seconds of computation time and shows little progress within the first hour of computation, finally reaching a mipgap of 1.53% after 3,710 seconds. This gap could not be further improved within the time limit. Hence, there might exists some effects which significantly slow down the computation process. The computational progress for $a = 3$ and $a = 5$ is displayed in Figure 7.15.

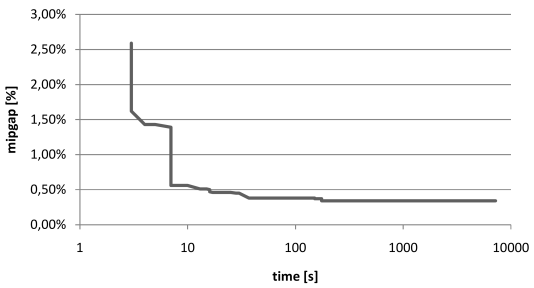

(a) $a = 3$

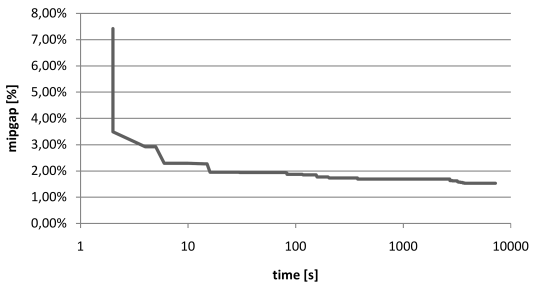

(b) $a = 5$

Figure 7.15: Computational Progress for Second Test Network

Since the aim of this chapter is to provide an integrated approach for evacuation planning with vehicles and pedestrians we will not discuss potential explanations for these observations at this point. The best known solution of the second test network for $a = 5$ is illustrated in Figure 7.16. Again, the same observations as in Figure 7.13 can be found. Cells located in the center of the network are almost completely evacuated by vehicle, whereas evacuation by foot can mainly be found in the adjacencies of the safe zone. It should be noticed that very few pedestrians are using the path $21 \rightarrow 22 \rightarrow 23$ ($\rightarrow 24 \rightarrow 25 \rightarrow |I|$) which might be caused by the remaining mipgap of 1.53% after two hours of computation time.

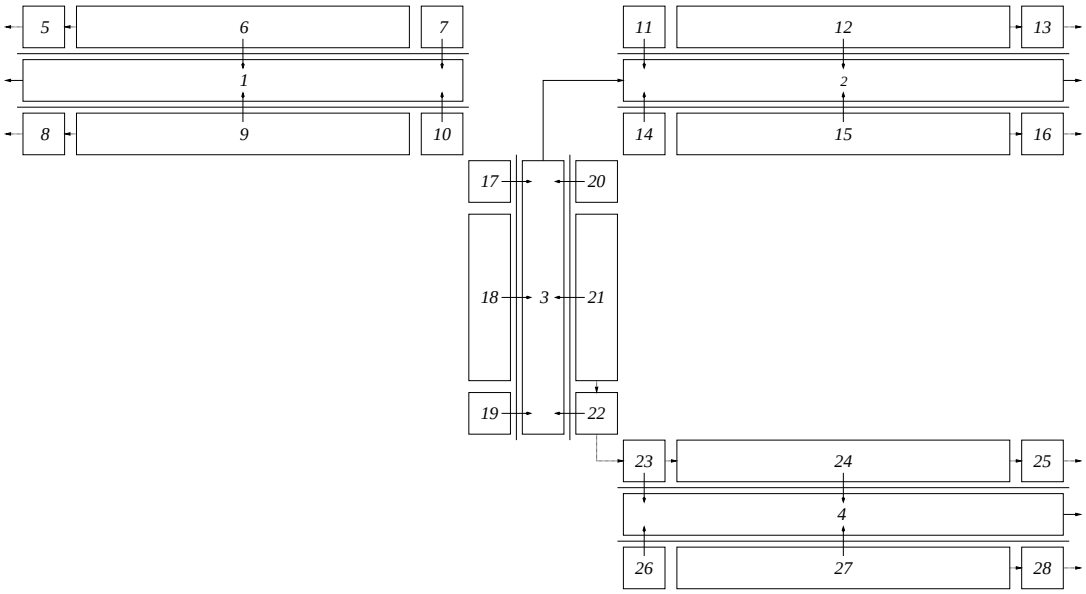

Figure 7.16: Solution of Test Network 2 for $a = 5$

7.3.2 Considerations for a Real-World Network Example

When evacuations are performed using only one mode, e.g. evacuation by vehicle, the total evacuation time can be regarded as an upper bound for the maximum reasonable walking time of evacuees. As an example the evacuation of the district Neudorf in the city of Duisburg finishes after about 70 periods in the ExCTEPM. Thus, there is no incentive for evacuees to evacuate by foot, if the walking time utilizing the shortest path from their homes to the nearest exit is larger than 70 periods. If we further imagine that residents living nearby an exit will escape by foot, total evacuation time will be reduced because of decreasing traffic volume on streets. Thus, the number of potential evacuations by foot decreases even further, because the total evacuation time may drop e.g. to 50 periods, making evacuation by foot even more unattractive for residents not living nearby an exit. Another problem covers the possibility that the shortest path to an exit may be not usable due to crossing vehicle flows so that time-wasting detours must be accepted, finally leading to further reductions in potential evacuations by foot.
Figure 7.17 illustrates these thoughts for total evacuation times of approximately 70 periods (lighter area) and 50 periods (darker area). The black line delimits the endangered zone and the numbers refer to the eight existing exits. We assume that residents evacuating by foot can take the shortest path to exits. It is easy to recognize that residents

living in the center of the endangered zone have no incentive to evacuate by foot since the walking time – even using the shortest path – would be larger than the evacuation time by car on (congested) streets.

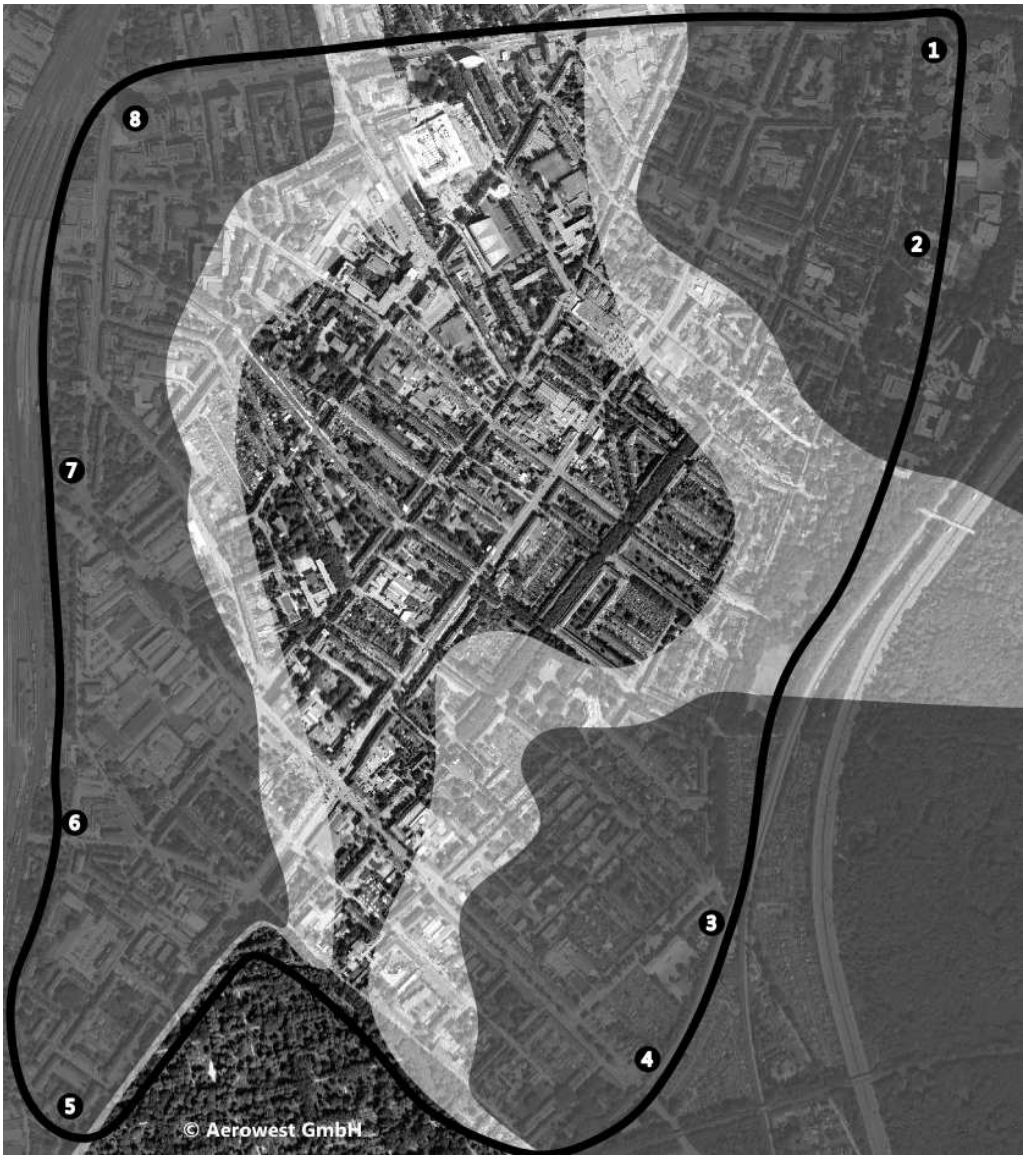

Figure 7.17: Potential Evacuation by Foot in Duisburg Neudorf

Chapter 8

Conclusions and Future Research

Evacuation Planning always is a challenging task, especially when methods of operations research are used since a large number of important interactions have to be considered and the resulting optimization problems become very complex even for small instances leading to enormous computational effort for solving these instances. This work presents various evacuation planning optimization models with extensions for integrating rescue team traffic and pedestrian traffic. Moreover, we provide heuristic procedures for generating high quality solutions within reasonable time even for large real world scenarios and we combined the output of our optimization models with microscopic traffic simulations to achieve a better estimation of the evacuation process itself under more realistic circumstances.
The basis for all evacuation planning models in this work is the Cell-Transmission-Model by Daganzo (1994) and Daganzo (1995). We adopted the basic ideas of this model, which was originally intended to be used for traffic simulation, but not for optimization purposes. The basic concept of the CTM is to represent a street section by a number of equal sized cells, whereas the size of a cell corresponds to the distance a vehicle can travel in one period of time under light traffic. Under consideration of traffic flow and vehicle capacities of cells, the vehicles move from cell to cell representing the traffic flow over time. During this work, these ideas were extended to meet additional requirements (see traffic flow limitations in the ExCTEPM in Chapter 4) and applied to new circumstances (see rescue team traffic in Chapter 6 and pedestrian traffic in Chapter 7).

Before evacuation plans can be computed, decisions regarding the selection of street segments in a real-world road network and the conversion of a given road network into a cell-based network to take advantage of the Cell-Transmission approach have to be made. Large urban areas consists of an large number of segments, if all dead-end streets and side streets are taken into account. However, for evacuation planning, not all of these segments carry large amounts of traffic so that we consider only arterials and major streets.
The choice of the cell size has two effects. On the one hand, cells should be as large as possible to keep the number of cells (and periods of time) at a manageable level. Please note that larger cells automatically correspond to longer time periods by definition of the size of a cell. On the other hand, cells should be as small as possible to match the lengths of the street sections in a given road network adequately. We face this trade-off by minimizing the number of cells under consideration of a given maximum deviation, see Section 4.1.4. This approach allows to contrast the corresponding number of cells with different levels of accuracy in network representation and to settle for the best compromise for the decision maker.

Most of the evacuation planning models in this work assume that all endangered persons have access to vehicles to escape, either as a driver or as a passenger. The only exception is the simultaneous evacuation planning for vehicles and pedestrians in Chapter 7, where the number of persons, which have to evacuate by foot because of too few vehicles are considered explicitly. Although the solutions of the presented evacuation planning models provide detailed information on how an evacuation plan for a given instance should look like, the practical implementation also requires the positioning of traffic flow guiding facilities (e.g. barricades) and police forces. Since the data acquisition before the computation and the computation itself also requires some time, evacuation plans on the basis of the evacuation planning models in this work should be computed for different scenarios in advance so that an adequate evacuation plan is instantly available when the decision to evacuate has been made.

The CTEPM represents the basis for all succeeding optimization models in this work. We use the fundamental idea of Daganzo (1994) and Daganzo (1995) to model the street network with cells of a given size, where vehicles move from cell to cell under consideration of traffic flow capacities. Since the CTEPM is an LP, it can be solved efficiently within a few minutes even for larger instances, see Chapter 3. However, the CTEPM does not provide any traffic routing limitations which would be reasonable in real world applications such as the avoidance of traffic crossing and traffic touching conflicts as well as limiting merging processes to abet smooth traffic flows. The solution from the CTEPM has been evaluated in a real world case for a densely populated district in Duisburg, Germany. This evaluation also includes a sensitivity analysis to capture effects like different departure patterns, different population sizes and the existence of initial traffic at the beginning of the evacuation.
The ExCTEPM takes advantage of the basic principle of the CTEPM, but addresses several weaknesses of the CTEPM, see Chapter 4: Firstly, the CTEPM captures only flows of vehicles on the complete street segment, but not lane-dependent, even if merging or diverging process take place. Thus, the solutions from the CTEPM might lead to situations, where a non-integer number of lanes should be assigned between two cells, which is difficult to apply in real-world situations. Secondly, the CTEPM does not avoid traffic crossing or traffic touching conflicts at all, leading to potentially dangerous situations at junctions. Thirdly, traffic routing during an evacuation should be as simple as possible since the evacuees are already frightened above-average. This can be obtained by limiting merging and diverging processes according to the characteristics of the street segments. The ExCTEPM also allows to use cells of different size, which leads to large reductions in the number of required cells to describe a given network.
Since evacuations may take place due to a dangerous event inside the endangered network, rescue teams should enter the network to prevent the origin of danger from causing even more risk to the population. The flow of rescue teams is contrarily oriented to the evacuation flow so that a large number of potential conflicts exists. These conflicts need to be considered when rescue team routes and evacuation routes will be determined. In Chapter 6, we introduced a new version of the ExCTEPM to capture evacuation traffic and rescue team traffic simultaneously. To keep conflicts between evacuation and rescue team traffic low, a temporal reservation of complete street segments for rescue team traffic was introduced. By doing so, conflicts between evacuation traffic and rescue team traffic could be avoided completely, since a street segment is used either by evacuation traffic or by rescue team traffic.

Although there is a large number of vehicles in urban areas, there might exist scenarios, where at least some evacuees have to escape by foot. For suchlike evacuation problems, we developed the ExCTEPMP to cover pedestrian and vehicle flows simultaneously, see Chapter 7. The consideration of pedestrian traffic requires to model sidewalk cells and to cope with more complex routing options compared to vehicle-only traffic since pedestrians are allowed to change the side of the street at street segments and at junctions. Now, each intersection is characterized by several crossing conflicts between vehicles/pedestrians and pedestrians which need to be avoided to ensure smooth vehicle and pedestrian flows.

The realistic illustration of traffic is a very difficult task since traffic dynamics are very complex by nature. Today, the best approximation of traffic can be obtained by microscopic traffic simulations since these approaches take advantage of state-of-the-art models to describe interdependencies between traffic participants at a high level of detail. The attempt to apply the same level of detail and realism in traffic illustration to an optimization approach will very likely result in almost unsolvable problems. However, traffic simulations are a very good chance to evaluate evacuation plans under more realistic circumstances. Moreover, the results gained from traffic simulations can be very helpful in the optimization phase to generate evacuations plans which show better performance in the simulation runs. Suchlike simulation-based optimization approaches are often used for complex and non-deterministic problems, see Chapter 2. We developed a simulation-based optimization approach using the SUMO Traffic Simulation and applied this approach to a real world case, where several performance measures (total evacuation time, number of evacuated persons at a certain period and exit occupation time) could be enhanced considerably.

Small instances of each evacuation planning model could be solved with standard software in short time. However, real-world evacuation often affect a large area so that heuristic approaches are needed to generate useful solutions for large instances within an appropriate time horizon. Since the CTEPM is an LP due to the real-valued domains of all decision variables, it can be solved for larger networks within minutes. However, the integration of traffic flow limitations and the explicit consideration of lanes in the ExCTEPM result in the need for integer and binary variables so that the simplex algorithm was not sufficient any more. Instead, IP-methods are necessary to compute optimum (integer) solutions. However, due to the introduction of integer variables, the optimization problems became very hard to solve so that specialized heuristic procedures were necessary. Therefore, we developed two heuristics for the ExCTEPM – see Chapter 5 –, namely a shortest path based routing and the static ExCTEPM. The static ExCTEPM clearly outperforms the shortest path based heuristic in solution quality in several real-world scenarios while staying within reasonable computation times. The comparison of both heuristics also illustrated that feasible solutions are no guarantee for high quality objective function values. Instead, the objective function seems to be very sensitive to deviations from the optimum solution.
This assumption also holds for the evacuation planning with rescue teams, see Chapter 6. A sensitivity analysis concerning the impact of deviations from the optimum evacuation and rescue team routing demonstrated that degradations of the objective function value within two digits percentages are not uncommon. Since the problem of routing evacuation and rescue team traffic simultaneously can be regarded as even more complex than the ExCTEPM, a three-staged solution procedure on the basis of the static ExCTEPM heuristic was developed. The heuristic first generates an evacuation plan for evacuation traffic only. Afterwards, rescue teams are integrated into the evacuation traffic in such a

way that affects evacuation traffic as less as possible. The last step reorganizes the evacuation traffic in respect to fixed rescue team traffic routes. This heuristic shows promising performance for three artificial and two real-world instances, both in solution quality and computation time.

Future Research

Although the presented optimization and simulation models cover essential aspects of evacuation, some issues are not considered at all. The following aspects represent disregards of the presented work and should be interpreted as a motivation for potential future work.

At first, people driving behavior in stressful situations like evacuations may be different compared to average situations. For example, mentally demanding situations result in more aggressiveness leading to decreased headways to put pressure on other drivers ahead, see Tu et al. (2010). Since the driving behavior is essential for realistic traffic illustration, these effects should not be underrated.

Another aspect covers the will of evacuees to consolidate with family members and to evacuate together, see Murray-Tuite and Mahmassani (2003) and Murray-Tuite and Mahmassani (2004). Suchlike assumptions have tremendous effects on evacuation routing and total evacuation time since people eventually move towards the danger instead of away from it.

Moreover, we simplified the process of entering the network in our optimization models by assuming that (flows of) vehicles can enter the network at every time as long as the given constraints are met, e.g. sufficient free space in a cell. In reality, the network entering process is more time consuming and arrestive since people have to back out of a parking space, to wait until enough free space is available and to accelerate to the desired driving speed. Here, other cars may even have to slow down when an additional vehicle enters the network.

Two main aspects that determine the routing in an evacuation plan are the supply in terms of flow capacities (represented by network topology) and the demand in terms of evacuees (represented by population distribution). While the flow capacities change very slow over time, e.g. by adding new lanes to streets, the distribution of the population strongly changes within the time of day. Therefore, it is very difficult to forecast the population distribution at a given time and therefore to calculate evacuation plans matching the current distribution. The same argumentation also holds for preparation times. Large buildings (e.g. hospitals or nursing homes) take much longer to be evacuated than an average town house, simply because ill, injured or old people are not able to take care of themselves.

In this work, we assume that all vehicles are homogeneous in terms of vehicle length, number of passengers and driving behavior. By considering a heterogeneous fleet of vehicles with different passenger loadings and vehicle lengths, a more realistic traffic representation could be obtained, especially in the traffic simulation. An increased diversity of traffic participants in terms of including different traffic modes – e.g. vehicles, pedestrians, train, bus, metro – would also contribute to a more realistic evacuation reproduction.

Beside these new aspects, future work may also cover the development of an integrated optimization model to cover evacuation traffic, rescue team traffic and pedestrians simultaneously. Since the resulting model will be very complex and hard to solve, new heuristic approaches also need to be designed.

Appendix A

Appendix: Centre for Research on the Epidemiology of Disasters – Emergency Events Database – Trends

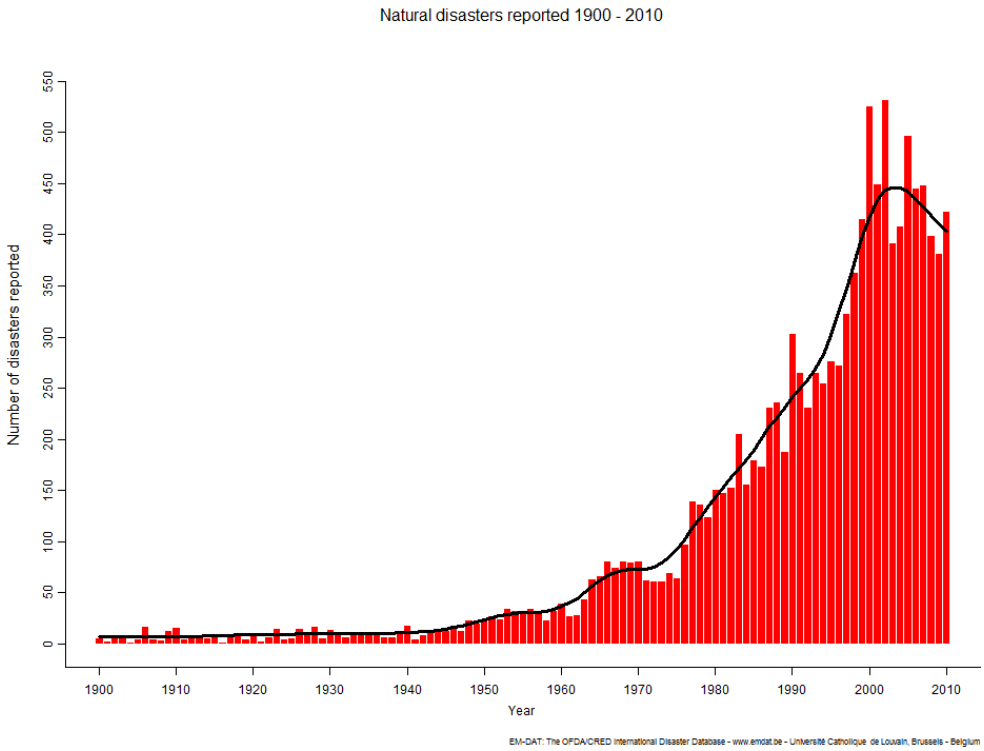

Figure A.1: Natural Disasters Reported 1900 - 2010

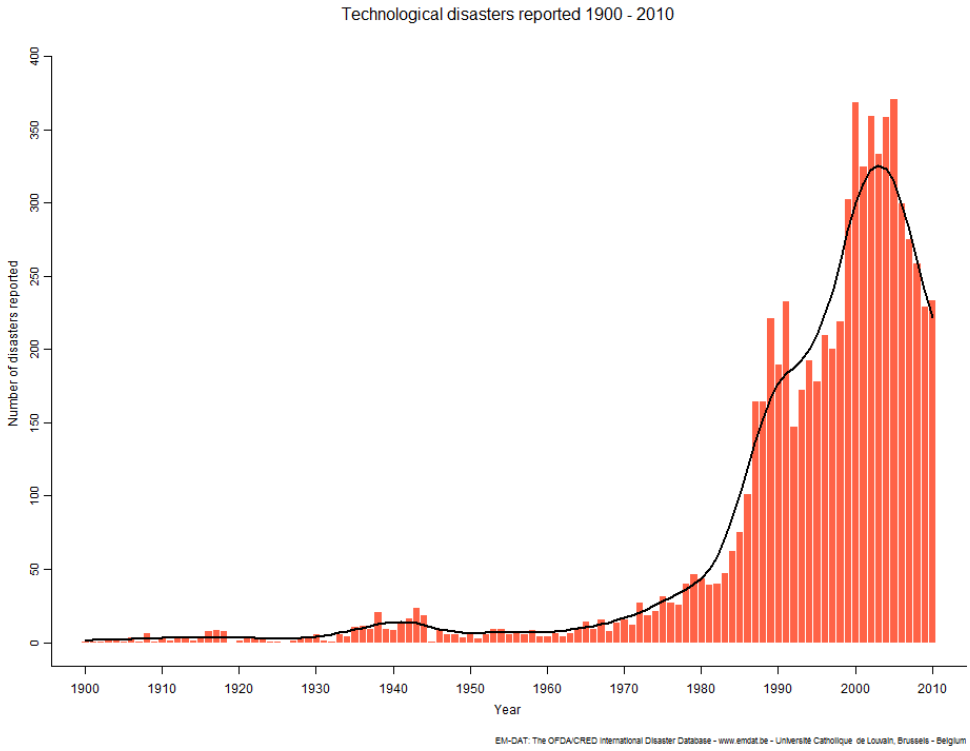

Figure A.2: Technological Disasters Reported 1900 - 2010

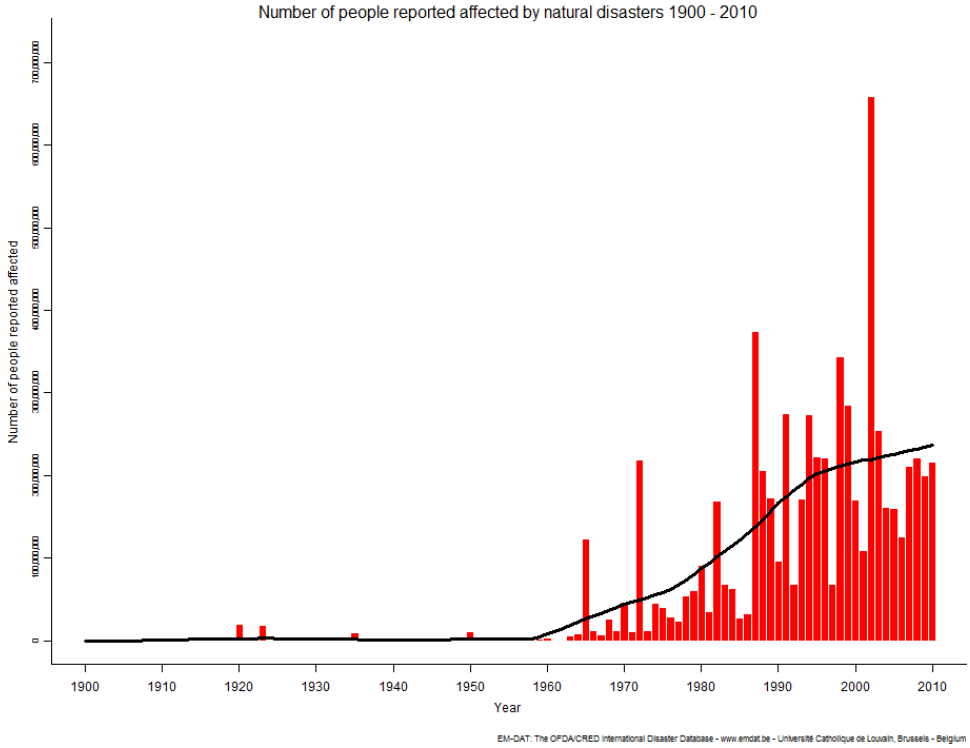

Figure A.3: Number of People Reported Affected by Natural Disasters 1900 - 2010

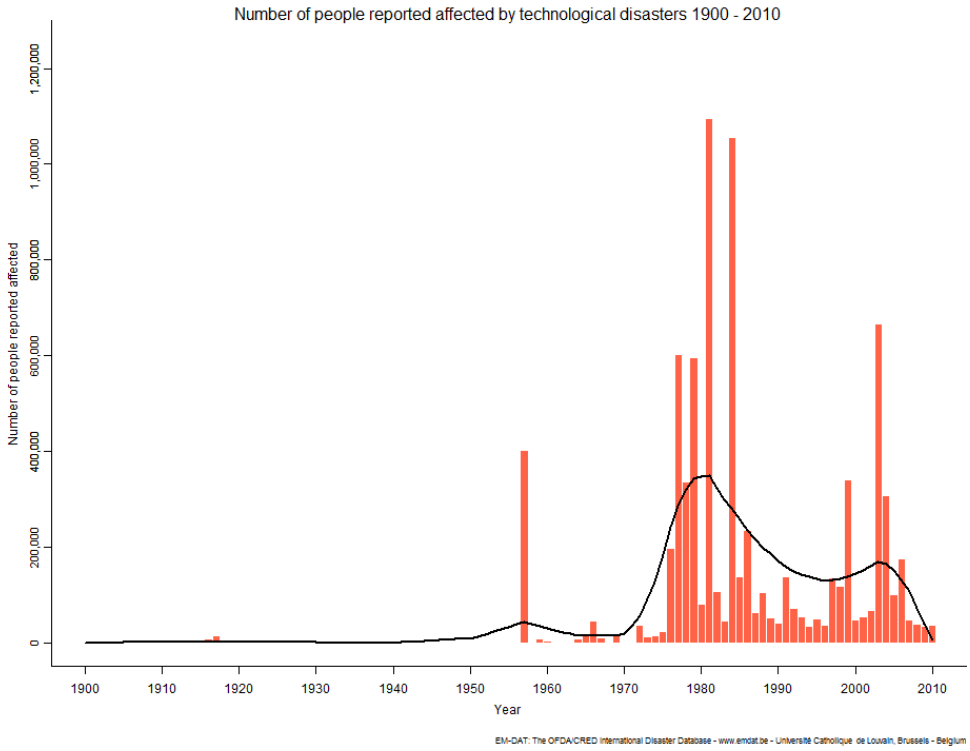

Figure A.4: Number of People Reported Affected by Technological Disasters 1900 - 2010

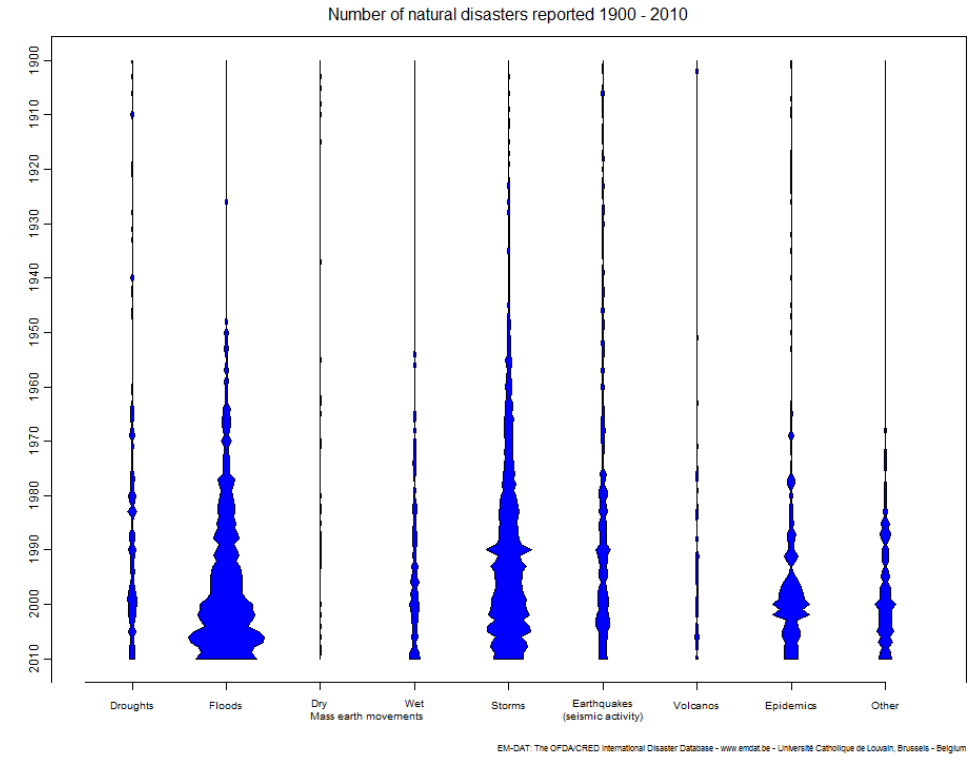

Figure A.5: Number of Natural Disasters Reported 1900 - 2010

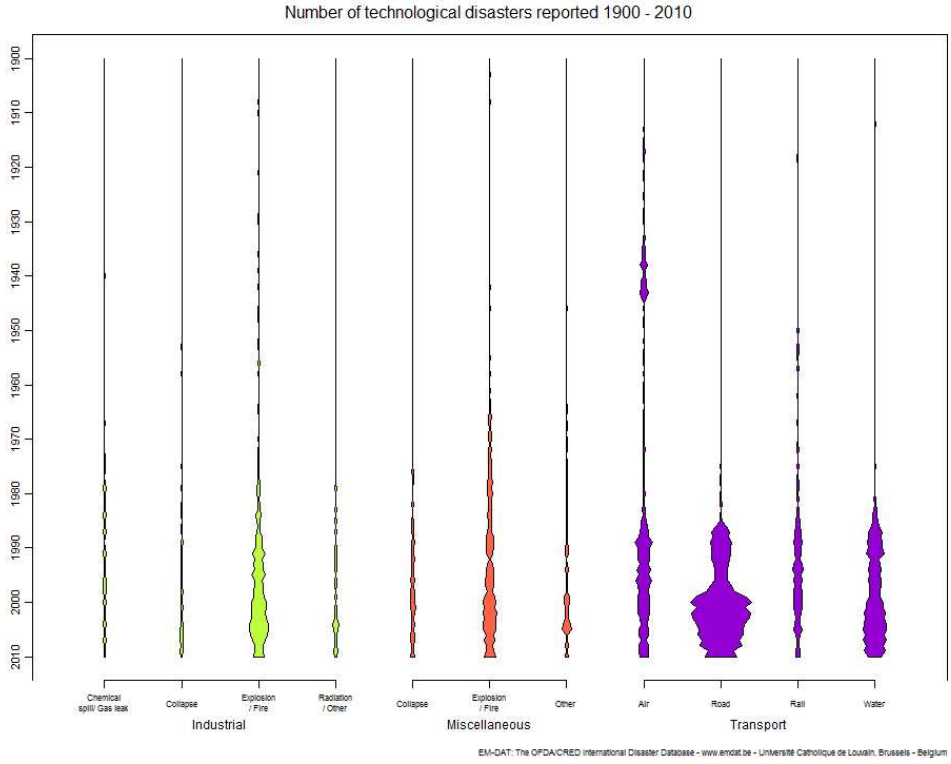

Figure A.6: Number of Technological Disasters Reported 1900 - 2010

Appendix B

Appendix: SUMO Model of the Duisburg–Neudorf Case

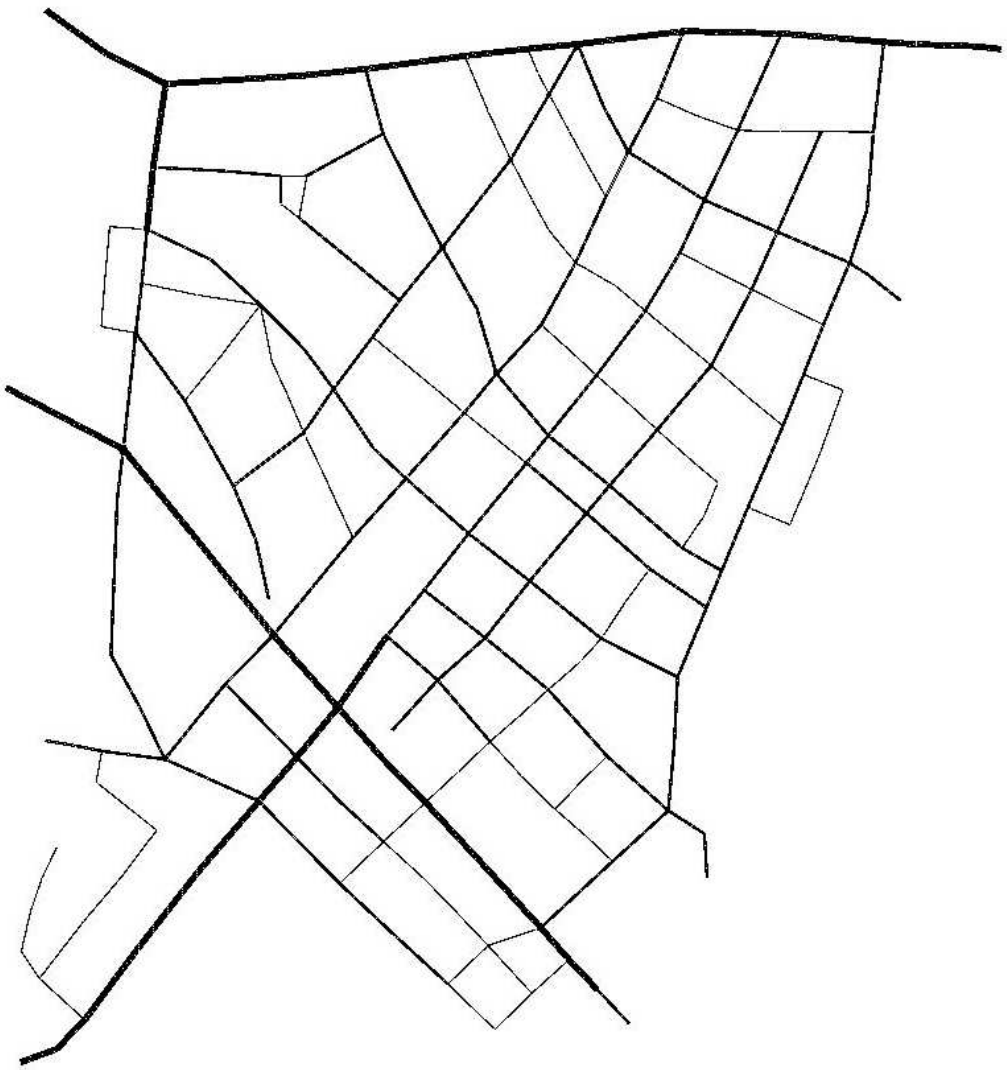

Figure B.1: An Illustration of the Duisburg–Neudorf Simulation Model

Appendix C

Appendix: Scenario Overview for Heuristic Solution Procedures

The darker the color of the EPZ the higher the danger in this EPZ.

Figure C.1: Scenario 1

Figure C.2: Scenario 2

Figure C.3: Scenario 3

Figure C.4: Scenario 4

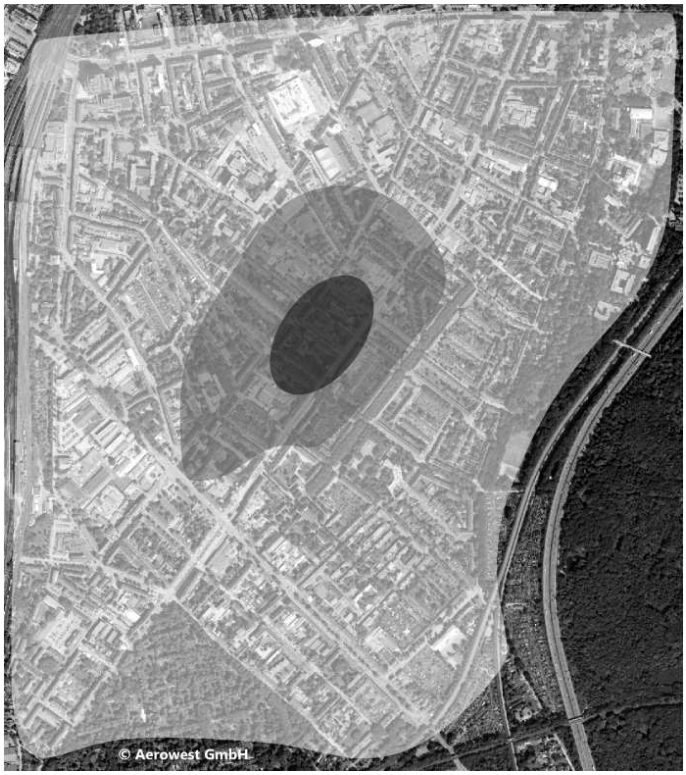

Figure C.5: Scenario 5

Figure C.6: Scenario 6

Figure C.7: Scenario 7

Figure C.8: Scenario 8

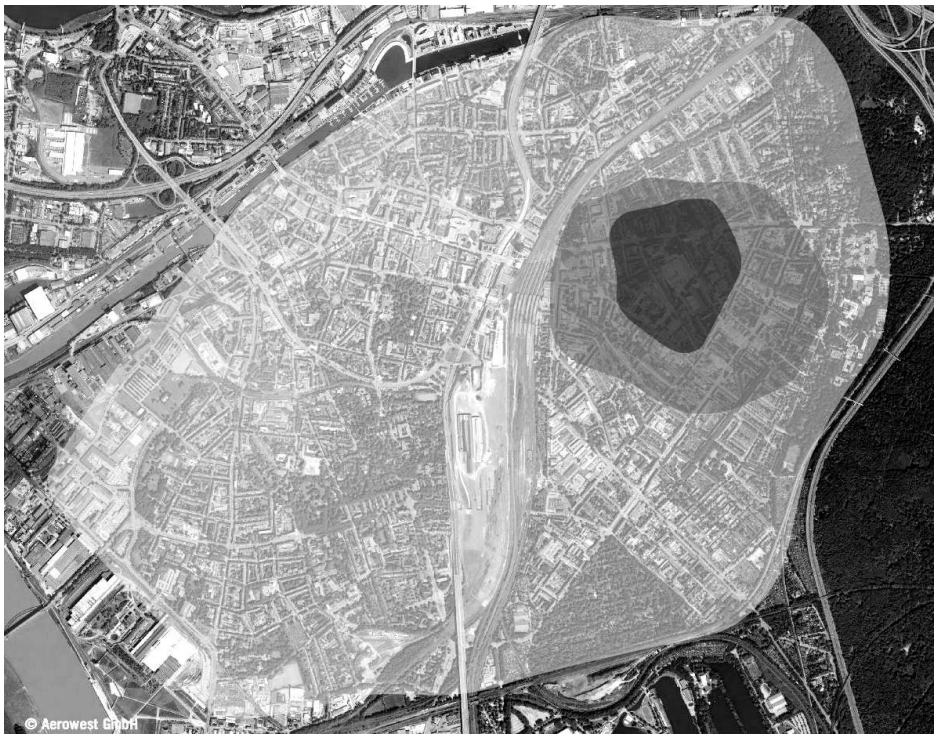

Figure C.9: Scenario 9

Bibliography

Ahmed, M. A. and Alkhamis, T. M., (2002), Simulation-based Optimization using Simulated Annealing with Ranking and Selection, *Computers & Operations Research*, **29** (4), pp. 387–402.

Ahuja, R. K., Magnanti, T. L., and Orlin, J. B., (1993), *Network Flows: Theory, Algorithms, and Applications*, Prentice Hall, New Jersey.

Alrefaei, M. H. and Alawneh, A. J., (2005), Solution Quality of Random Search Methods for Discrete Stochastic Optimization, *Mathematics and Computers in Simulation*, **68** (2), pp. 115–125.

Andradóttir, S., (1996), A Global Search Method for Discrete Stochastic Optimization, *SIAM Journal on Optimization*, **6** (2), pp. 513–530.

Andreas, A. K. and Smith, J. C., (2009), Decomposition Algorithms for the Design of a Nonsimultaneous Capacitated Evacuation Tree Network, *Networks*, **53** (2), pp. 91–103.

April, J., Glover, F., Kelly, J. P., and Laguna, M., (2003), Practical Introduction to Simulation Optimization, in: Chick, S., Sánchez, P. J., Ferrin, D., and Morrice, D. J., eds., *Proceedings of the 2003 Winter Simulation Conference*.

Bish, D. R., (2011), Planning for a Bus-based Evacuation, *OR Spectrum*, **33** (3), pp. 629–654.

Bretschneider, S., (2011), Mathematical Models for Evacuation Planning in Urban Areas, PhD Thesis, University of Duisburg–Essen.

Bretschneider, S. and Kimms, A., (2011), A Basic Mathematical Model for Evacuation Planning in Urban Areas, *Transportation Research Part A: Policy and Practice*, **45** (6), pp. 523–539.

Bretschneider, S. and Kimms, A., (2012), Pattern-Based Evacuation Planning for Urban Areas, *European Journal of Operational Research*, **216** (1), pp. 57–69.

Burstedde, C., Klauck, K., Schadschneider, A., and Zittartz, J., (2001), Simulation of Pedestrian Dynamics Using a Two Dimensional Cellular Automaton, *Physica A: Statistical Mechanics and its Applications*, **295** (3-4), pp. 507–525.

Chakraborty, J. and Armstrong, M. P., (1995), Using Geographic Plume Analysis to assess Community Vulnerability to Hazardous Accidents, *Computers, Environment and Urban Systems*, **19** (5-6), pp. 341–356.

Chen, H. K. and Feng, G., (2000), Heuristics for the Stochastic/Dynamic User-Optimal Route Choice Problem, *European Journal of Operational Research*, **126** (1), pp. 13–30.

Chen, X. and Zhan, F., (2008), Agent-based Modeling and Simulation of Urban Evacuation: Relative Effectiveness of Simultaneous and Staged Evacuation Strategies, *Journal of the Operational Research Society*, **59**, pp. 25–33.

Chiu, Y. C., Zheng, H., Villalobos, J., and Gautam, B., (2007), Modeling No-Notice Mass Evacuation Using a Dynamic Traffic Flow Optimization Model, *IIE Transactions*, **39** (1), pp. 83–94.

Cova, T. J. and Johnson, J. P., (2003), A Network Flow Model for Lane-Based Evacuation Routing, *Transportation Research Part A: Policy and Practice*, **37** (7), pp. 579–604.

Daganzo, C. F., (1994), The Cell Transmission Model: A Dynamic Representation of Highway Traffic Consistent with the Hydrodynamic Theory, *Transportation Research Part B: Methodological*, **28** (4), pp. 269–287.

Daganzo, C. F., (1995), The Cell Transmission Model, Part II: Network Traffic, *Transportation Research Part B: Methodological*, **29** (2), pp. 79–93.

Davis, C. H., (1969), The Binary Search Algorithm, *American Documentation*, **20** (2), p. 167.

Dijkstra, E. W., (1959), A Note on Two Problems in Connexion with Graphs, *Numerische Mathematik*, **1** (1), pp. 269–271.

Domschke, W. and Drexl, A., (2005), *Einführung in Operations Research*, 6 ed., Springer, Berlin.

Eppstein, D., (1999), Finding the k Shortest Paths, *SIAM Journal on Computing*, **28** (2), pp. 652–673.

Fang, Z., Zong, X., Li, Q., Li, Q., and Xiong, S., (2011), Hierarchical Multi-objective Evacuation Routing in Stadium using Ant Colony Optimization Approach, *Journal of Transport Geography*, **19** (3), pp. 443–451.

FEMA, (1996), Guide for All-Hazard Emergency Operations Planning, United States Federal Emergency Management Agency, USA.

Fu, L., Sun, D., and Rilett, L. R., (2006), Heuristic Shortest Path Algorithms for Transportation Applications: State of the Art, *Computers & Operations Research*, **33** (1), pp. 3324–3343.

Fu, M. C., (2002), Optimization for Simulation: Theory vs. Practice, *INFORMS Journal on Computing*, **14** (3), pp. 192–215.

Fu, M. C., Chen, C.-H., and Shi, L., (2008), Some Topics for Simulation Optimization, in: Mason, S. J., Hill, R. R., Mönch, L., Rose, O., Jefferson, T., and Fowler, J. W., eds., *Proceedings of the 2008 Winter Simulation Conference*, pp. 27–38.

Garey, M. R. and Johnson, D. S., (1979), *Computers and Intractability — A Guide to the Theory of NP–Completeness*, Freeman, New York.

Georgiadou, P. S., Papazoglou, I. A., Kiranoudis, C. T., and Markatos, N. C., (2007), Modeling Emergency Evacuation for Major Hazard Industrial Sites, *Reliability Engineering & System Safety*, **92** (10), pp. 1388–1402.

Golding, D. and Kasperson, R. E., (1988), Emergency Planning and Nuclear Power: Looking to the Next Accident, *Land Use Policy*, **5** (1), pp. 19–36.

Gosavi, A., (2003), *Simulation-Based Optimization: Parametric Optimization Techniques and Reinforcement Learning*, Kluwer Academic Publishers Group, Dordrecht.

Graf, M. and Kimms, A., (2011), An Option-based Revenue Management Procedure for Strategic Airline Alliances, *European Journal of Operational Research*, **215** (2), pp. 459–469.

Guo, R. Y. and Huang, H. J., (2008), A Mobile Lattice Gas Model for Simulating Pedestrian Evacuation, *Physica A: Statistical Mechanics and its Applications*, **387** (2-3), pp. 580–586.

Gwynne, S., Galea, E. R., Owen, M., Lawrence, P. J., and Filippidis, L., (1999), A Review of the Methodologies Used in the Computer Simulation of Evacuation from the Built Environment, *Building and Environment*, **34** (6), pp. 741–749.

Hamacher, H. W. and Tjandra, S. A., (2001), Mathematical Modeling of Evacuation Problems: A State of Art, Berichte des Frauenhofer ITWM, Nr. 24.

Han, L. D., Yuan, F., Chin, S., and Hwang, H., (2006), Global Optimization of Emergency Evacuation Assignments, *Interfaces*, **36** (6), pp. 502–513.

Helbing, D. and Molnár, P., (1995), Social Force Model for Pedestrian Dynamics, *Physical Review E*, **51** (5), pp. 4282–4286.

Jaluria, Y., (2009), Simulation-based Optimization of Thermal Systems, *Applied Thermal Engineering*, **29** (7), pp. 1346–1355.

Jia, H., Ordóñez, F., and Dessouky, M. M., (2007), Solution Approaches for Facility Location of Medical Supplies for Large-scale Emergencies, *Computers and Industrial Engineering*, **52** (2), pp. 257–276.

Jung, J. Y., Blau, G., Pekny, J. F., Reklaitis, G. V., and Eversdyk, D., (2004), A Simulation Based Optimization Approach to Supply Chain Management under Demand Uncertainty, *Computers & Chemical Engineering*, **28** (10), pp. 2087–2106.

Kalafatas, G. and Peeta, S., (2009), Planning for Evacuation: Insights from an Efficient Network Design Model, *Journal of Infrastructure Systems*, **15** (21), pp. 21–30.

Karbowicz, C. J. and Macgregor Smith, J., (1984), A k-Shortest Paths Routing Heuristic for Stochastic Network Evacuation Models, *Engineering Optimization*, **7** (4), pp. 253–280.

Kim, S. and Shekhar, S., (2008), Contraflow Transportation Network Reconfiguration for Evacuation Route Planning, *IEEE Transactions on Knowledge and Data Engineering*, **20** (8), pp. 1115–1129.

Kimms, A. and Maassen, K.-C., (2009), Extended Cell-Transmission-Based Evacuation Planning in Urban Areas, Working Paper, University of Duisburg - Essen.

Kimms, A. and Maassen, K.-C., (2010a), A Fast Heuristic Approach for Large Scale Cell-Transmission-Based Evacuation Planning, Working Paper, University of Duisburg - Essen.

Kimms, A. and Maassen, K.-C., (2010b), Cell-Transmission-Based Evacuation Planning with Rescue Teams, Working Paper, University of Duisburg - Essen.

Kimms, A. and Maassen, K.-C., (2011a), Cell-Transmission-Based Evacuation Planning with Vehicles and Pedestrians, Working Paper, University of Duisburg - Essen.

Kimms, A. and Maassen, K.-C., (2011b), Optimization and Simulation of Traffic Flows in the Case of Evacuating Urban Areas, *OR Spectrum*, **33** (3), pp. 571–593.

Kimms, A., Maassen, K.-C., and Pottbäcker, S., (2011), Guiding Traffic in the Case of Big Events with Spot Checks on Traffic and Additional Parking Space Requirements, *Central European Journal of Operations Research, to appear.*

Kirchner, A. and Schadschneider, A., (2002), Simulation of Evacuation Processes using a Bionics-inspired Cellular Automaton Model for Pedestrian Dynamics, *Physica A: Statistical Mechanics and its Applications*, **312** (1-2), pp. 260–276.

Kongsomsaksakul, S., Yang, C., and Chen, A., (2005), Shelter Location-allocation Model for Flood Evacuation Planning, *Journal of the Eastern Asia Society for Transportation Studies*, **6**, pp. 4237–4252.

Krajzewicz, D., (2009), Kombination von taktischen und strategischen Einflüssen in einer mikroskopischen Verkehrsflusssimulation, Fahrermodellierung in Wissenschaft und Wirtschaft, 2. Berliner Fachtagung für Fahrermodellierung, Verein Deutscher Ingenieure [Fortschritt-Berichte VDI / 22]: Fortschritt-Berichte / VDI ; Nr. 28 : Reihe 22, Mensch-Maschine-Systeme (28). VDI-Verlag.

Krauß, S., (1998), Microscopic Modeling of Traffic Flow: Investigation of Collision Free Vehicle Dynamics, PhD Thesis, University of Cologne, Hauptabteilung Mobilität und Systemtechnik des DLR Köln.

Krauß, S., Wagner, P., and Gawron, C., (1997), Metastable States in a Microscopic Model of Traffic Flow, *Physical Review E*, **55** (5), pp. 5597–5602.

Lahmar, M., Assavapokee, T., and Ardekani, S. A., (2006), A Dynamic Transportation Planning Support System for Hurricane Evacuation, 2006 IEEE Intelligent Transportation Systems Conference: Toronto, Ontario, Canada, 17-20 September 2006. Vol. 2, pp. 612-617.

Lee, D., Kim, H., Park, J.-H., and Park, B.-J., (2003), The Current Status and Future Issues in Human Evacuation from Ships, *Safety Science*, **41** (10), pp. 861–876.

Li, L., Jin, M., and Zhang, L., (2011), Sheltering Network Planning and Management with a Case in the Gulf Coast Region, *International Journal of Production Economics*, **131** (2), pp. 431–440.

Li, Y., (2009), A Simulation-based Evolutionary Approach to LNA Circuit Design Optimization, *Applied Mathematics and Computation*, **209** (1), pp. 57–67.

Lighthill, M. J. and Whitham, G. B., (1955), On kinematic waves II. A theory of traffic flow on long crowded roads, *Proceedings of the Royal Society of London. Series A, Mathematical and Physical Sciences*, **229** (1178), pp. 317–345.

Lindell, M. K., (2008), EMBLEM2: An Empirically Based Large Scale Evacuation Time Estimate Model, *Transportation Research Part A: Policy and Practice*, **42** (1), pp. 140–154.

Liu, Y., Chang, G.-L., Liu, Y., and Lai, X., (2008), Corridor-Based Emergency Evacuation System for Washington, D.C. - System Development and Case Study, *Transportation Research Record*, **2041**, pp. 58–67.

Mayer, S., (2011), Methoden und Anwendungen der simulationsbasierten Optimierung, *Wirtschaftswissenschaftliches Studium*, **40**, pp. 218–224.

Mete, H. O. and Zabinsky, Z. B., (2010), Stochastic Optimization of Medical Supply Location and Distribution in Disaster Management, *International Journal of Production Economics*, **126** (1), pp. 76–84.

Murray-Tuite, P. M. and Mahmassani, H. S., (2003), Model of Household Trip-Chain Sequencing in Emergency Evacuation, *Transportation Research Record*, **1831**, pp. 21–29.

Murray-Tuite, P. M. and Mahmassani, H. S., (2004), Transportation Network Evacuation Planning with Household Activity Interactions, *Transportation Research Record*, **1894**, pp. 150–159.

Nagel, K. and Rickert, M., (2001), Parallel implementation of the TRANSSIMS micro-simulation, *Parallel Computing*, **27** (12), pp. 1611–1639.

Nagel, K. and Schreckenberg, M., (1992), A Cellular Automaton Model for Freeway Traffic, *Journal de Physique I*, **2** (12), pp. 2221–2229.

Parisi, D. R. and Dorso, C. O., (2005), Microscopic Dynamics of Pedestrian Evacuation, *Physica A: Statistical Mechanics and its Applications*, **354**, pp. 606–618.

Peyer, S., Rautenbach, D., and Vygen, J., (2009), A Generalization of Dijkstra's Shortest Path Algorithm with Applications to VLSI Routing, *Journal of Discrete Algorithms*, **7** (4), pp. 377–390.

Richards, P. I., (1956), Shockwaves on the highway, *Operations Research*, **4** (1), pp. 42–51.

Saadatseresht, M., Mansourian, A., and Taleai, M., (2009), Evacuation Planning Using Multiobjective Evolutionary Optimization Approach, *European Journal of Operational Research*, **198** (1), pp. 305–314.

Sayyady, F. and Eksioglu, S. D., (2010), Optimizing the Use of Public Transit System during No-notice Evacuation of Urban Areas, *Computers and Industrial Engineering*, **59** (4), pp. 488–495.

Sbayti, H. and Mahmassani, H. S., (2006), Optimal Scheduling of Evacuation Operations, *Transportation Research Record*, **1964**, pp. 238–246.

Schwartz, J. D., Wang, W., and Rivera, D. E., (2006), Simulation-based Optimization of Process Control Policies for Inventory Management in Supply Chains, *Automatica*, **42** (8), pp. 1311–1320.

Sheffi, Y., Mahmassani, H., and Powell, W. B., (1982), A Transportation Network Evacuation Model, *Transportation Research Part A: General*, **16** (3), pp. 209–218.

Shen, W., Nie, Y., and Zhang, H. M., (2007), Dynamic Network Simplex Method for Designing Emergency Evacuation Plans, *Transportation Research Record*, **2022**, pp. 83–93.

Sherali, H. D., Carter, T. B., and Hobeika, A. G., (1991), A Location-allocation Model and Algorithm for Evacuation Planning under Hurricane/Flood Conditions, *Transportation Research Part B: Methodological*, **25** (6), pp. 439–452.

Sinuany-Stern, Z. and Stern, E., (1993), Simulating the Evacuation of a Small City: The Effects of Traffic Factors, *Socio-Economic Planning Sciences*, **27** (2), pp. 97–108.

Song, W., Xu, X., Wang, B.-H., and Ni, S., (2006), Simulation of Evacuation Processes using a Multi-grid Model for Pedestrian Dynamics, *Physica A: Statistical Mechanics and its Applications*, **363** (2), pp. 492–500.

Sorensen, J. H., Carnes, S. A., and Rogers, G. O., (1992), An Approach for Deriving Emergency Planning Zones for Chemical Munitions Emergencies, *Journal of Hazardous Materials*, **30** (3), pp. 223–242.

Southworth, F., (1991), Regional Evacuation Modeling: A State-of-the-Art Review, Tech. Rep. ORNL/TM-11740, ORNL Oak Ridge National Laboratory.

Stepanov, A. and MacGregor Smith, J., (2009), Multi-objective evacuation routing in transportation networks, *European Journal of Operational Research*, **198** (2), pp. 435–466.

Tu, H., Tamminga, G., Drolenga, H., de Wit, J., and van der Berg, W., (2010), Evacuation Plan of the City of Almere: Simulating the Impact of Driving Behavior on Evacuation Clearance Time, *Procedia Engineering*, **3**, pp. 67–75.

Tuydes, H. and Ziliaskopoulos, A. K., (2004), Network Re-Design to Optimize Evacuation Contraflow, Technical Report 04-4715, Proc. 83rd Ann. Meeting of the Transportation Research Board.

Tuydes, H. and Ziliaskopoulos, A. K., (2006), Tabu–Based Heuristic Approach for Optimization of Network Evacuation Contraflow, *Transportation Research Record*, **1964**, pp. 157–168.

Ukkusuri, S. V. and Waller, S. T., (2008), Linear Programming Models for the User and System Optimal Dynamic Network Design Problem: Formulations, Comparisons and Extensions, *Networks and Spatial Economics*, **8** (4), pp. 383–406.

Urbina, E. and Wolshon, B., (2003), National Review of Hurricane Evacuation Plans and Policies: A Comparison and Contrast of State Practices, *Transportation Research Part A: Policy and Practice*, **37** (3), pp. 257–275.

Varas, A., Cornejo, M. D., Mainemer, D., Toledo, B., Rogan, J., Muñoz, V., and Valdivia, J. A., (2007), Cellular Automaton Model for Evacuation Process with Obstacles, *Physica A: Statistical Mechanics and its Applications*, **382** (2), pp. 631–642.

Wang, J. and Cheng, L., (2006), Application of Auction Algorithm for Shortest Paths to Traffic Assignment, *Journal of Transportation Systems Engineering and Information Technology*, **6** (6), pp. 79–82.

Wolshon, B., (2001), "One-Way-Out": Contraflow Freeway Operation for Hurricane Evacuation, *Natural Hazards Review*, **2** (3), pp. 105–112.

Xie, C., Lin, D.-Y., and Waller, S. T., (2010), A Dynamic Evacuation Network Optimization Problem with Lane Reversal and Crossing Elimination Strategies, *Transportation Research Part E: Logistics and Transportation Review*, **46** (3), pp. 295–316.

Xie, C. and Turnquist, M. A., (2009), Integrated Evacuation Network Optimization and Emergency Vehicle Assignment, *Transportation Research Record*, **2091**, pp. 79–90.

Xie, C. and Turnquist, M. A., (2011), Lane-based Evacuation Network Optimization: An Integrated Lagrangian Relaxation and Tabu Search Approach, *Transportation Research Part C: Emerging Technologies*, **19** (1), pp. 40–63.

Xu, M. H., Liu, Y. Q., Huang, Q. L., Zhang, Y. X., and Luan, G. F., (2007), An Improved Dijkstra's Shortest Path Algorithm for Sparse Networks, *Applied Mathematics and Computation*, **185** (1), pp. 247–254.

Yamada, T., (1996), A Network Flow Approach to a City Emergency Evacuation Planning, *International Journal of Systems Science*, **27** (10), pp. 931–936.

Yazici, M. A. and Ozbay, K., (2008), Evacuation Modelling in the United States: Does the Demand Model Choice Matter?, *Transport Reviews: A Transnational Transdisciplinary Journal*, **28** (6), pp. 757–779.

Yue, H., Guan, H., Shao, C., and Zhang, X., (2011), Simulation of Pedestrian Evacuation with asymmetrical Exits Layout, *Physica A: Statistical Mechanics and its Applications*, **390** (2), pp. 198–207.

Zhang, J., Hodgson, J., and Erkut, E., (2000), Using GIS to assess the Risks of Hazardous Materials Transport in Networks, *European Journal of Operational Research*, **121** (2), pp. 316–329.

Zheng, H. and Chiu, Y.-C., (2011), A Network Flow Algorithm for the Cell-Based Single-Destination System Optimal Dynamic Traffic Assignment Problem, *Transportation Science*, **45** (1), pp. 121–137.

Zheng, X., Li, W., and Guan, C., (2010), Simulation of Evacuation Processes in a Square with a Partition Wall using a Cellular Automaton Model for Pedestrian Dynamics, *Physica A: Statistical Mechanics and its Applications*, **389** (11), pp. 2177–2188.

Zheng, X., Zhong, T., and Liu, M., (2009), Modeling Crowd Evacuation of a Building Based on Seven Methodological Approaches, *Building and Environment*, **44** (3), pp. 437–445.

Ziliaskopoulos, A. K., (2000), A Linear Programming Model for the Single Destination System Optimum Dynamic Traffic Assignment Problem, *Transportation Science*, **34** (1), pp. 37–49.

Acknowledgement

The work was done with financial support from the WestLB Stiftung Zukunft NRW. We thank AEROWEST GmbH for the written permission to use their photography of the Duisburg area in Figures 3.4, 5.1, 5.2, 5.4, 5.5, 5.6, 6.7, 6.8, 7.17 and C.1 – C.9.

Eidesstattliche Erklärung

Hiermit versichere ich, dass ich die vorliegende Dissertation selbstständig und ohne unerlaubte Hilfe angefertigt und andere als die in der Dissertation angegebenen Hilfsmittel nicht benutzt habe. Alle Stellen, die wörtlich oder sinngemäß aus anderen Schriften entnommen sind, habe ich als solche kenntlich gemacht.

Duisburg, September 2011 Klaus-Christian Maassen